Study of the Antiviral Immune Response of Zebrafish (*Danio rerio*) against the Hemorrhagic Virus SVCV

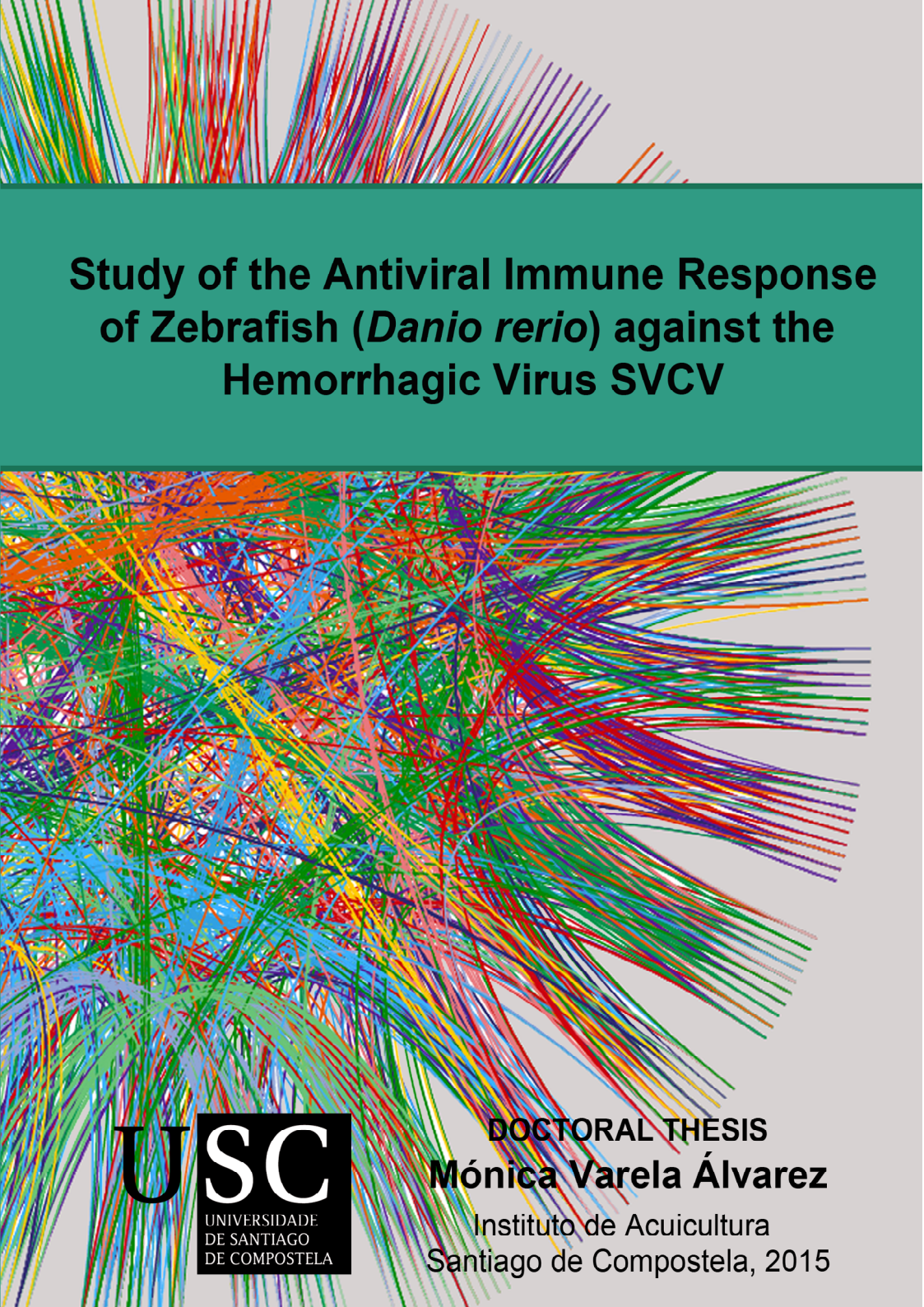

USC
UNIVERSIDADE DE SANTIAGO DE COMPOSTELA

DOCTORAL THESIS

Mónica Varela Álvarez

Instituto de Acuicultura

Santiago de Compostela, 2015

INSTITUTO DE ACUICULTURA

PROGRAMA DE DOCTORADO
INTERUNIVERSITARIO EN ACUICULTURA

STUDY OF THE ANTIVIRAL IMMUNE RESPONSE OF ZEBRAFISH (*Danio rerio*) AGAINST THE HEMORRHAGIC VIRUS SVCV

MEMORIA

que para la obtención del Título de Doctor por la Universidad de Santiago de Compostela presenta

Mónica Varela Álvarez

SANTIAGO DE COMPOSTELA, 2015

SANTIAGO DE COMPOSTELA, 2015

ANTONIO FIGUERAS HUERTA, PROFESOR DE INVESTIGACIÓN DEL CSIC, BEATRIZ NOVOA GARCÍA, INVESTIGADORA CIENTÍFICA DEL CSIC Y JESÚS LAMAS FERNÁNDEZ, PROFESOR TITULAR DE LA USC,

CERTIFICAN:

Que la presente memoria titulada "Study of the antiviral immune response of zebrafish (*Danio rerio*) against the hemorrhagic virus SVCV", que para optar al Grado de Doctor en Biología presenta Dña. MÓNICA VARELA ÁLVAREZ, ha sido realizada bajo nuestra dirección y/o tutela. Y considerando que constituye trabajo de tesis, autorizamos su presentación a la Comisión Académica correspondiente.

Y para que así conste, expedimos el presente certificado en Santiago de Compostela, a 25 de Julio de 2015.

La Doctoranda El Tutor

Fdo: Mónica Varela Álvarez Fdo: Jesús Lamas Fernández

Los Directores de la Tesis

Fdo: Antonio Figueras Huerta Fdo: Beatriz Novoa García

The work presented in this thesis has been supported by the projects:

-Spanish Ministerio de Ciencia e Innovación CSD2007-00002 (AQUAGENOMICS).

-Spanish Ministerio de Economía e Innovación (AGL2011-28921-C03)

-European structural funds (FEDER) and Spanish Ministerio de Ciencia e Innovación (CSIC08-1E-102).

-European ITN 289209 (FishForPharma).

-Predoctoral grant from the JAE Program (JAEPre_2010_0181_S1) funded by CSIC and European structural funds.

AGRADECIMIENTOS

A mis directores, Bea y Antonio, por estos años, por hacer que sea mejor y más fuerte, y sobre todo por la confianza que siempre han puesto en mí. GRACIAS.

A Suso, por darme la primera oportunidad en este "mundillo", sin ella hoy no estaría escribiendo esto.

Posiblemente tampoco estaría escribiendo esto si no fuese por ella, por Patri. Gracias por cambiar mi vida, aunque por ello una coruñesa fuese a parar a Vigo…

Al resto de becarios del grupo, a Rebe, a Fornito y a Paolo, por tantas horas compartidas en la mejor compañía. A PDR, a Rebeca y a MM, por las charlas y los buenos consejos.

A los demás miembros del grupo, en especial a Álex, por esos momentos inspiradores, las lecciones en el confocal y los ánimos en los malos momentos.

Thanks to Annemarie and her group for the 3 months I spent in Leiden. Definitely, time that marked a before and an after. Also grateful for the opportunity to continue my career as part of their group (A Annemarie y a todo su grupo por los 3 meses que pasé en Leiden. Sin duda hubo un antes y un después. Agradecida también por la oportunidad de continuar mi carrera formando parte de su grupo).

A mis compis de Lab2 del CIBUS, en especial, a Carla, por sus consejos y por "formarme para el éxito".

A todos los que me habéis soportado en los últimos años, en los momentos buenos y sobre todo en los malos. Agradecimiento especial a mis "Reinas Cotillas", a pesar de mis ausencias ellas siempre están ahí.

A mis padres y a mi hermana. Nunca podré agradeceros lo suficiente todos los años de apoyo incondicional. GRACIAS.

A mi pequeña familia. A mi BabyLeo, por acompañarme en la recta final de esta etapa aún sin saberlo y, por portarse bien y no adelantar su fecha de nacimiento. A Diego, el mejor compañero de vida, por su paciencia y comprensión (incluso los fines de semana de trabajo), por sus ánimos, su apoyo incondicional y por acompañarme en la próxima etapa ∞

Gracias!!!

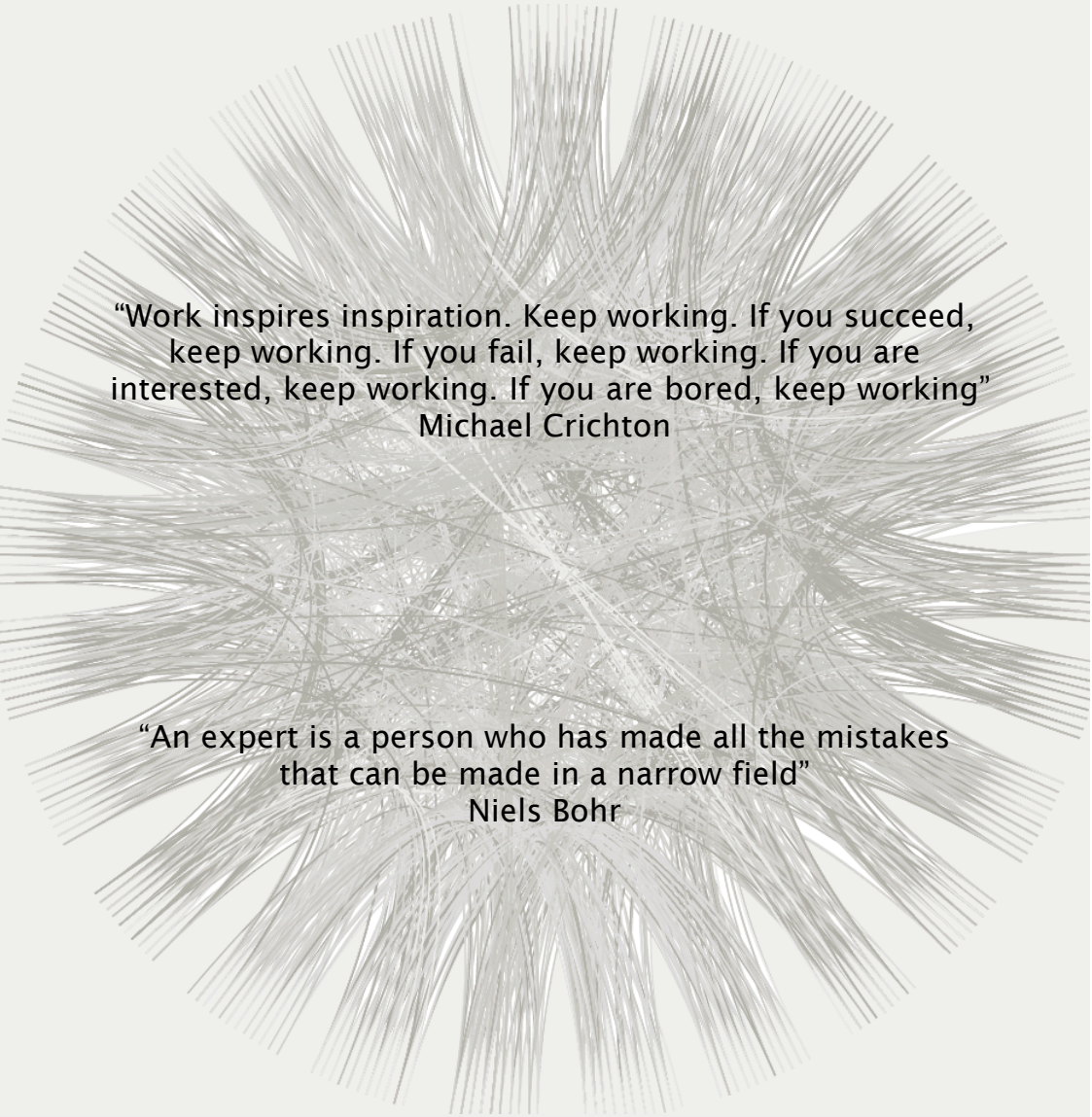

“Work inspires inspiration. Keep working. If you succeed, keep working. If you fail, keep working. If you are interested, keep working. If you are bored, keep working”
Michael Crichton

“An expert is a person who has made all the mistakes that can be made in a narrow field”
Niels Bohr

CONTENTS

LIST OF FIGURES

LIST OF TABLES

Chapter 1

General Introduction: Antiviral Innate Immune Response in Zebrafish (*Danio rerio*)

Mónica Varela, Antonio Figueras and Beatriz Novoa
Manuscript in preparation

1

1.1. Zebrafish as an infectious disease model

Zebrafish (*Danio rerio*) has been used as a model in research for more than 100 years (Sullivan and Kim, 2008). The zebrafish is an outstanding tool for embryological research, but also for genomics, genetics and immunology (Novoa and Figueras, 2012; Santoriello and Zon, 2012). Among the advantages of the use of zebrafish as an animal model we can highlight its small size, relatively rapid life cycle, ease of breeding and genetic modification, external fertilization and embryo transparency (Westerfield 2000; Nüsslein-Volhard, 2002).

The advantage of the increased use of zebrafish as a vertebrate model has facilitated the development of genomic tools. Zebrafish genome is available on-line (www.ensembl.org/Danio_rerio/Info/Index), fact that has prompted the identification and annotation of its genes. Furthermore, progress in the knowledge of the zebrafish genome has been facilitated because of the highly conserved synteny observed with the human genome (Figure 1.1). This is one advantage that encourages the use of zebrafish as a model, but so is the ease of generating mutant lines, transgenic lines and transient *in vivo* assays. Moreover, zebrafish biology allows ready access to all developmental stages, and the optical clarity of embryos and larvae allow real-time imaging of developing pathologies (Lieschke and Currie, 2007).

In recent years the use of zebrafish as a model for human diseases has stood out, with important examples such as different types of cancer (White et al., 2013; Rasighaemi et al., 2015), Alzheimer´s disease (Newman et al., 2014), obesity (Forn-Cuní et al., 2014) or cardiac disease (Bakkers, 2011), among others. In addition, zebrafish is being widely used as a tool for the study of infectious diseases and host-pathogen interactions (Novoa and Figueras, 2012; Tobin et al., 2012). Numerous bacterial, viral and

fungal models of infection have been studied taking advantage of zebrafish (Davis et al., 2002; Nelly, 2002; Van der Sar, 2003; Chao et al., 2010; Palha et al., 2013; Nguyen-Chi et al., 2014; Varela et al., 2014a).

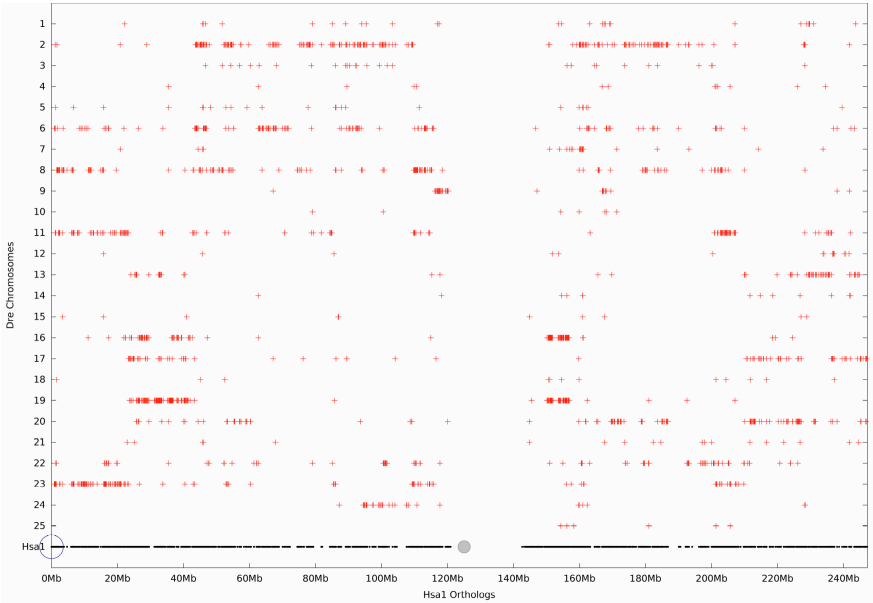

Figure 1.1. Ortholog genes in zebrafish and human genomes. Dot plot of ortholog genes of the *Danio rerio* genome and the *Homo sapiens* chromosome 1. Red crosses indicate orthologs. Derived from the Synteny Database (syntenydb.uoregon.edu/synteni_db/).

1.2. Zebrafish innate immunity

Zebrafish possesses a highly developed immune system that allows in depth study of both the basic aspects of the immunological response and its interaction with different organisms and pathogens (Novoa and Figueras 2012; Santoriello and Zon, 2012).

Innate immune responses are characteristic of all eukaryotic organisms and represent the non-specific defense against pathogens. Zebrafish innate immune response is

composed by cellular, molecular, chemical and physical components.

The principal cellular components of the zebrafish innate immune system are phagocytic macrophages and neutrophils, which are similar to those in mammals in terms of morphology, molecular signatures and functionality (Bennett et al., 2001). Other cell types, as non-specific cytotoxic cells (NCCs), considered the evolutionary precursor of mammalian NK cells, have been identified in zebrafish but their functionality needs yet to be studied (Moss et al., 2009). The existence of transgenic lines with fluorescent innate cells (Figure 1.2) and the ease of viewing, make zebrafish model one with a high potential for the study of the interactions between hos cells and pathogens. Moreover, during the first four days of development, the zebrafish exhibits no adaptive immunity markers (Traver et al., 2003). This fact makes zebrafish larvae a valuable tool for the study of the innate immunity in exclusive, as it is not until 4-6 weeks post-fertilization that adaptive immunity becomes fully functional (Lam et al., 2004).

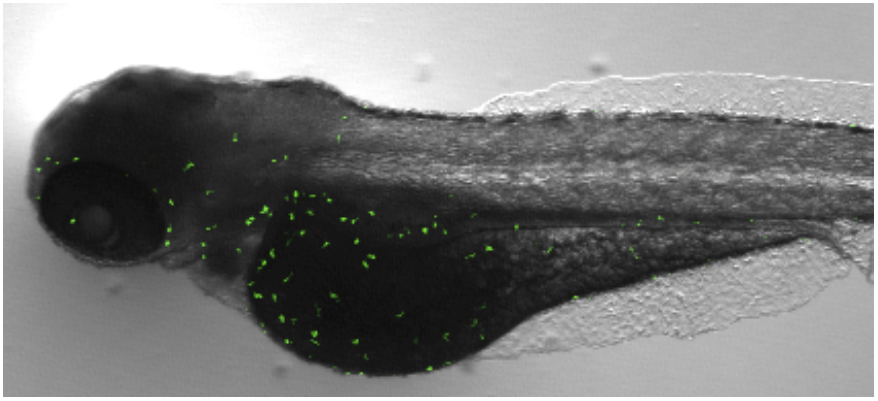

Figure 1.2. Zebrafish transgenic larvae. 5 days post-fertilization transgenic Tg(Mpx:GFP) zebrafish larvae showing fluorescent neutrophils.

Zebrafish innate immune system shows a strong degree of sequence conservation in many genes of the innate immune system. Several genes involved in the innate response, as cytokines or Toll-like receptors (TLRs), present a high sequence homology with those of mammals and current studies are focused on sequence homology and functional homology. Despite the sequence conservation, the zebrafish genome has numerous gene duplications (Figure 1.3), as in the case of perforin genes. And this fact, which supposedly represents an evolutionary advantage in aquatic organisms, more exposed to pathogens, makes zebrafish functional studies difficult to compare to those made in high vertebrates.

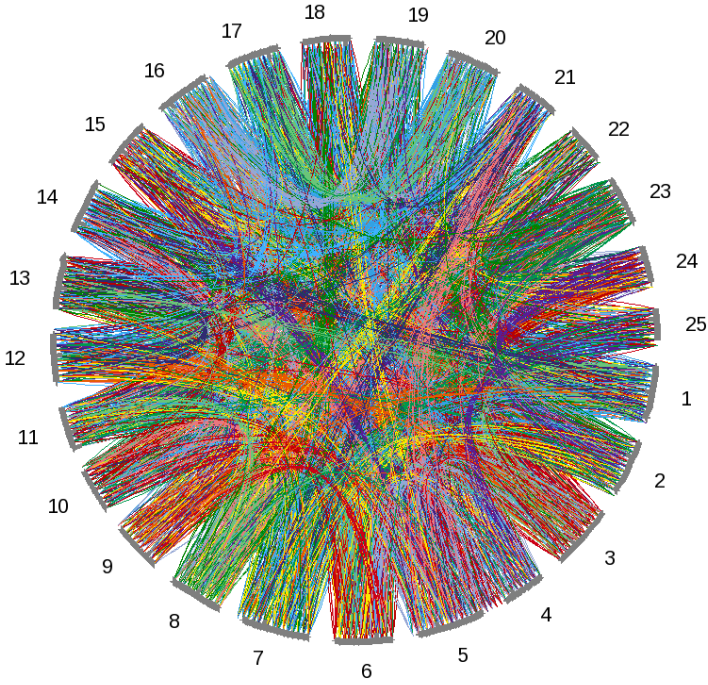

Figure 1.3. Paralog genes in zebrafish genome. Circle plot of paralog genes from the *Danio rerio* genome derived from the Synteny Database (syntenydb.uoregon.edu/synteni_db/) and using the Homo sapiens genome as outgroup.

1.3. Antiviral innate immunity

The innate immune response is essential for the survival of organisms. Innate immunity is the first line of defence against pathogens and infections (Kimbrell and Beutler, 2001).

Induction of the antiviral innate immune response depends on recognition of viral components by host. Cells of the immune system detect viruses through pattern recognition receptors (PRRs) located inside or in the cell surface. Vertebrate cells express many different PPRs and among these we found TLRs, retinoic acid-inducible gene I-like receptors (RLRs), nucleotide oligomerization domain-like receptors (NLRs, also called NACHT, LRR and PYD domain proteins) and cytosolic DNA sensors. The existence of multiple viral sensing PRRs improves the cell response and allows a quickly and effective defence. PPRs initiate antimicrobial defence mechanisms through several conserved signalling pathways (Broz and Monack, 2013). This ultimately result in the activation of genes and synthesis of molecules, including cytokines, chemokines, cell adhesion molecules, and immunoreceptors (Akira et al., 2006), which together orchestrate the early host response to infection and at the same time represent an important link to the adaptive immune response (Mogensen, 2009). PRRs detecting viral pathogens lead to the activation of transcription factors such as interferon regulatory factors (IRFs) and nuclear factor kappa beta (NFκβ) to induce the antiviral interferon and inflammatory immune responses (Wu and Chen, 2014).

The activation of IRFs induces the production of several antiviral response-related genes. The interferon (IFN) system is crucial in the fight against virus, and is capable of controlling most, if not all, virus infections in absence of adaptive immunity (Randall and Goodbourn, 2008). In acute viral infections, IFN induces IFN-stimulated genes (ISGs), which contribute to the overall effects

against a given virus (Sadler and Williams, 2008; Schoggins and Rice, 2011).

The inflammatory response initiated after recognition of virus is also important for the clearance of viral pathogens. Activation of NFκB triggers production of pro-inflammatory cytokines including interleukin-6 (IL6), interleukin-1β (IL1β) and tumor necrosis factor- α (TNFα) (Pang and Iwasaki, 2012).

1.4. Antiviral pattern recognition in zebrafish

1.4.1. TLRs

The Toll-like receptor gene family is an important group of host PRRs that recognize a multitude of pathogen-associated molecular patterns (PAMP). Multiple TLRs have been identified in the zebrafish genome as 24 putative variants of TLR family were identified (Sullivan and Kim, 2008). Although not all of the ligands specific for each receptor have been identified, it is known that many signalling molecules and pathways are conserved between zebrafish and mammals.

TLRs have been studied in zebrafish in response to bacterial and also viral stimuli. Regarding viral recognition in zebrafish, *tlr3*, *tlr7*, *tlr8a/b*, *tlr9* and *tlr22*, which is unique in fish, have been related with the response against virus (Figure 1.4). *tlr3* and *tlr22* share significant resemblance regarding cellular localization and molecular function (Pietretti and Wiegertjes, 2014) and can detect viral replication by binding to double-stranded RNA (dsRNA) or its analog poly I:C. On the other hand, *tlr7* and *tlr8* specifically recognize single-stranded RNA (ssRNA) and *tlr9* recognizes unmethylated CpG DNA present in the genomes of virus.

Zebrafish *tlr3* transcripts were up-regulated in response to infection with Snakehead Rhabdovirus (SHRV), a ssRNA virus

(Phelan et al., 2005). *tlr3* was also up-regulated during an infection with Viral Hemorrhagic Septicaemia Virus (VHSV) (Novoa et al., 2006) and during a zebrafish larvae waterborne and systemic infection with Spring Viremia of Carp Virus (SVCV), a dsRNA virus (López-Muñoz et al., 2010; Varela et al., 2014a). In spite of the fact that little is known about zebrafish *tlr22,* its modulation after poly I:C stimulation (Sundaram et al., 2012) and, during larvae waterborne and systemic infection with SVCV (López-Muñoz et al., 2010; Varela et al., 2014a) was reported. *tlr7*, *tlr8a/b* and *tlr9* were little studied in zebrafish, only the modulation of *tlr7* and *tlr8a* were confirmed against SVCV in zebrafish (Varela et al., 2014a). These genes were modulated with virus or antiviral synthetic compounds as imidazoquinolines in other fish species therefore it has been assumed a similar functionality in zebrafish (Kileng et al., 2008; Skjaeveland et al., 2008).

1.4.2. RLRs

This receptor family is composed by three members: retinoic acid-inducible gene I (RIG-I) (Nie et al., 2015), melanoma differentiation associated factor 5 (MDA5) (Zou et al., 2014) and laboratory of genetics and physiology 2 (LGP2) (Zou et al., 2009). They are cytosolic receptors of the family of DExD/H box RNA helicases with the capacity of detecting the presence of viral RNAs. In general, RIG-I preferentially bind to a short, uncapped 5´-triphosphorylated (5´-ppp) ssRNA juxtaposed to a short region of dsRNA (Hornung et al., 2006), whereas MDA5 recognizes the internal duplex structure of dsRNA (Wu et al., 2013). Both respond also to different-sized poly I:C, a synthetic form of dsRNA (Kato et al., 2008). On the other hand, LGP2 binds to dsRNA and ssRNA with higher affinity than both RIG-I and MDA5 (Moresco and Beutler, 2010). However, the function of LGP2 in virus recognition and signaling has remained controversial, as it has been suggested

both negative and positive regulatory roles for LGP2 in antiviral immune responses (Zhu et al., 2014). The RLR members RIG-I and MDA5 contain two N-terminal CARD domains, however LGP2 does not (Bruns et al., 2013). The N-terminal CARD regions are responsible for interacting with downstream signaling components, resulting in the transcriptional activation of antiviral-related genes (Yoneyama and Fujita, 2009).

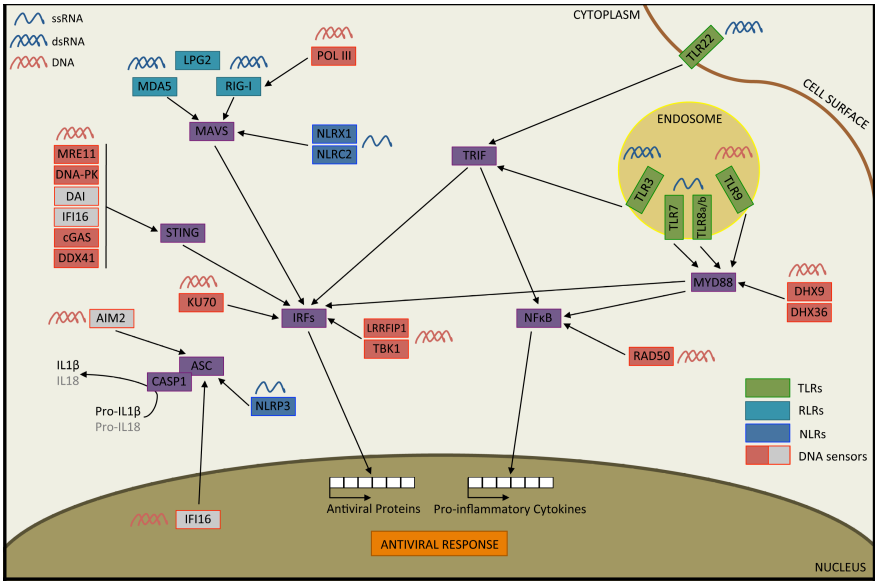

Figure 1.4. Antiviral pattern recognition in zebrafish. TLRs are represented by green squares, RLRs by light blue squares, NLRs by dark blue squares and DNA sensors by red squares. Grey squares represent non-identified genes in the genome of zebrafish.

The RLRs are crucial to the RNA virus triggered antiviral signalling pathways in mammals. In zebrafish, data are limited to a couple of studies but seems that signalling cascades activated after viral recognition by RLRs are similar to those in high vertebrates (Figure 1.4). IFN signalling pathway and inflammatory response are activated after NLRs recognize the virus. Stimulation of CARD domain of zebrafish *rig-I* significantly activates de NFκB

and IFN signaling pathways, leading to the expression of *tnfa*, *il8* and IFN-induced *mx*, *isg15* and viperin (Nie et al., 2015). Recently, Chen et al., (2015) reported that the knockdown of *rig-I* expression repressed the antiviral and inflammatory responses during an infection with nervous necrosis virus (NNV) in zebrafish. On the other hand*, mda5* was up-regulated in cell lines following the infection with SVCV (Zou et al., 2014). Moreover, the over-expression of *mda5*-spliced forms in fish cells resulted in significant induction of type I interferon promoter activity and enabled the protection of transfected cells against SVCV infection (Zou et al., 2014). Furthermore, *lgp2* plays a very important role in the production of type I IFN in fish (Hikima et al., 2012), but this gene has not yet been fully characterised in zebrafish.

1.4.3. NLRs

NLRs comprise a family of intracellular pathogen recognition receptors that can activate the innate immune system via NFκB, mitogen-activated protein kinase (MAPK), inflammasome, and IFN signaling (Lupfer and Kanneganti, 2013). NLRs comprise a large receptor family but only NLRP3, NLRC2, NLRX1 and NLRC5 have been associated with viral detection (Figure 1.4) (Kanneganti et al., 2006; Sabbah et al., 2009; Lupfer and Kanneganti, 2013). Many human viruses activate NLRP3 inflammasome, and seems that ion flux is a key feature for NLRP3 sensing of viral infection (Lupfer et al., 2015). NLRC2 induced the activation of the MAVS-IRF3-IFN pathway after the recognition of viral ssRNA (Sabbah et al., 2009). Moreover, NLRC2 appeared to be a central regulator of inflammation during viral infection, controlling both pro- and anti-inflammatory events (Lupfer and Kanneganti, 2013).

In zebrafish, many NLRs have been localized in their genome but there are no data about their implication in viral infections (Laing et al., 2008).

1.4.4. DNA sensors

Intracellular dsDNA produced during infection with pathogens such as dsDNA viruses and bacteria or from phagocytised dead cells is a potent inducer of immune responses resulting in the production of pro-inflammatory cytokines and IFNs. Multiple cytosolic DNA sensors exist, many of which operate in a cell-type specific manner (Keating et al., 2011). Many DNA sensors have been identified in recent years: TANK-binding kinase (TBK1), DNA-dependent activator of IFN-regulatory factors (DAI or ZBP-1), RNA polymerase III (RNA Pol III), AIM2, IFI16, LRRFIP1, DHX9, DHX36, DDX41, Ku70, DNA-PK, MRE11, cGAS, STING and Rad50 (Figure 1.4). Most of DNA sensors operate via STING, which can also act as a DNA sensor itself, a protein shown to have a central role in controlling altered gene induction in response to DNA *in vivo* (Dempsey and Bowie, 2015). AIM2 and IFI16 activate caspase-1-dependent maturation of the pro-inflammatory cytokines IL1β and IL18 (Sharma and Fitzgerald, 2011). Concerning zebrafish, many of these genes are located in the genome but there is not research about them. It is known that crucian carp (*Carassius auratus*) *sting* serves as a mediator for distinct fish IFN gene activation dependent on *irf3* and *irf7* (Sun et al., 2011). Moreover, *sting* over-expressing fish cells were almost fully protected against RNA virus infection with a strong inhibition of both DNA and RNA virus replication (Biacchesi et al., 2012). Furthermore, Sun et al., (2011) revealed the ability of crucian carp *tbk1* to induce IFN response. In olive flounder (*Paralichthys olivaceus*), *ddx41* functions as a cytosolic DNA sensor that is capable of inducing antiviral activity and inflammatory responses (Quynh et al., 2015).

The understanding of innate intracellular DNA sensing pathways has advanced rapidly in recent years but there are key questions that need further research, especially in the field of fish innate response.

1.5. Interferon pathway response in zebrafish

Viruses trigger the expression of IFNs. IFNs belong to class II helical cytokine family and, in mammals, can be divided into three different groups: type I (α, β, ω, ε and κ), type II (γ), and type III (λ) (Pestka et al., 2004). In zebrafish, there are two types of IFN: Type I (divided in group I, composed by *ifnφ1* and *ifnφ4*, and group II, composed by i*fnφ2* and *ifnφ3*), and Type II (composed by ifnγ1 and ifnγ2) (Stein et al., 2007; Zou et al., 2007).

The two groups of type I IFNs were found to signal via two different receptors in zebrafish (Aggad et al., 2009) and have been shown that both protect against virus (Lopez-Muñoz et al., 2009). Moreover, they induced many ISGs, some of them with a direct antiviral activity as *mx* or *pkr* (Briolat et al., 2014). Some ISGs also attract or activate cells with specialized roles in antiviral defense.

Among ISGs, a protein family called IFIT (interferon-induced proteins with tetratricopeptide repeats) has acquired some relevancy in recent years (Diamond and Farzan, 2013, Zhou et al., 2013, Fensterl and Sen, 2014; Varela et al., 2014b). This family of proteins has been characterized in zebrafish (Varela et al., 2014b), with some of its members showing antiviral properties *in vivo,* upon a viral infection with SVCV.

Type II IFNs, are typically secreted by CD4+ Th1 cells and NK cells in mammals. They can induce apoptosis, especially during viral infection, and inhibits cell proliferation (Zou and Secombes, 2011). Fish *ifnγ* induced the expression of many ISGs that also respond to type I IFNs (Martin et al., 2007; Grayfer and Belosevic,

2009), suggesting the existence of a cross-activation of the innate antiviral responses elicited by type I and type II IFNs. In zebrafish, *ifnγ1* and *ifnγ2* can be induced by SVCV in adults, not in larvae (Aggad et al., 2010).

1.6. Antiviral inflammatory response in zebrafish

The inflammatory response is a crucial innate defence mechanism. A state of inflammation is necessary for proper function of host defences, since it involves circulating immune cells and antimicrobial components of the plasma at the site of infection (van der Vaart et al., 2012). The main pro-inflammatory cytokines produced by the cellular components of the innate response in response to a virus are TNFα, IL1β, IL8 and IL6. These cytokines are necessary to promote inflammation and to promote chemotaxis of macrophages and neutrophils to the site of infection. In zebrafish, *tnfα, il1β* and *il6* was induced in larvae as a result of a systemic infection with SVCV (Varela et al., 2014a). Moreover, poly I:C stimulation induced *il6, tnfα* and *il1β* up-regulation in adult zebrafish kidney (Varela et al., 2012). VHSV also induces the expression of *tnfα* in adult zebrafish (Novoa et al., 2006).

The inflammatory response should be tightly regulated, since an imbalanced response could be harmful for the host. This happened in the case of *tnfα* and SVCV, as *tnfα* increased the susceptibility of zebrafish to SVCV (Roca et al., 2008).

In recent years, the inflammasomes have acquired great importance in the innate response to pathogens. The inflammasomes are a group of multimeric protein complexes that consist of an inflammasome sensor molecule, the adaptor protein ASC and caspase-1 (Latz et al., 2013). The activation of the inflammasomes induces de maturation and liberation of the most

studied pro-inflammatory interleukin, IL1β. This interleukin is controlled at the level of transcription, translation, maturation and secretion. It has been shown that many human viruses have the ability to activate this mechanism of defence *in vitro* (Aachoui et al., 2013; Tan and Chu, 2013). Using the zebrafish model of infection with SVCV, it has been described for the first time the possible implication of the inflammasome and the pyroptotic death of infected macrophages in the context of a whole organism during a viral infection (Varela et al., 2014a).

1.7. Zebrafish and viral infections

No naturally occurring viral infections have been characterised for zebrafish (Crim and Riley, 2012). Despite this, the use of zebrafish as a model for viral infections has increased in recent years. Most of viral studies using zebrafish were performed with fish viruses (Table 1.1). Fish viruses are able to infect and course the disease both in larvae and adult zebrafish. Thanks to these studies not only progress has been made in understanding the pathologies generated by the viruses, but also in the study of the zebrafish immune system. Remarkable progress has been made in the study of the IFN system and inflammation in zebrafish with the use of SVCV (Levraud et al., 2007; Aggad et al., 2009; Lopez-Muñoz et al., 2009; Aggad et al., 2010; Varela et al., 2014a; Varela et al., 2014b).

SVCV is an enveloped, negative sense, single stranded RNA virus of the Rhabdoviridae family. This virus has been used to perform infections in adult zebrafish (Sanders et al., 2003) but also in larvae (Levraud et al., 2007). Regarding adults, infections have been induced mostly by immersion (Sanders et al., 2003) or intraperitoneal injection (Lopez-Muñoz et al., 2009). On the other hand, in larvae, a model of viral infection by immersion (Lopez-

Muñoz et al., 2010) and by microinjection of the virus into the blood torrent to induce a systemic infection (Varela et al., 2014a) has been established. The virus induces a hemorrhagic disease in which epidermal petechial hemorrhages are characteristic.

Table 1.1. Fish viral infections studied using zebrafish.

Virus	References
Infectious hematopoietic necrosis virus (IHNV)	LaPatra et al., 2000; Wang et al., 2006; Aggad et al., 2009; Aggad et al., 2010; Ludwig et al., 2011; Briolat et al., 2014
Infectious pancreatic necrosis virus (IPNV)	LaPatra et al., 2000; Garner et al., 2003
Spring viremia of carp virus (SVCV)	Sanders et al., 2003; Wang et al., 2006; Levraud et al., 2007; Aggad et al., 2009; Lopez-Muñoz et al., 2009; Aggad et al., 2010; Lopez-Muñoz et al., 2010; Encinas et al., 2013; García-Valtanen et al., 2014; Martinez-Lopez et al., 2014; Ruyra et al., 2014; Varela et al., 2014a; Varela et al., 2014b; Li et al., 2015; Pereiro et al., 2015; Varela et al., 2015
Snakehead rhabdovirus (SHRV)	Alonso et al., 2004; Phelan et al., 2005a; Phelan et al., 2005b; Nayak et al., 2007; Gabor et al., 2013; Gabor et al., 2015
Viral hemorrhagic septicemia virus (VHSV)	Novoa et al., 2006; Dios et al., 2010; Encinas et al., 2010
Nervous necrosis virus (NNV)	Lu et al., 2008; Morick et al., 2015
Infectious spleen kidney necrosis virus (ISKNV)	Xu et al., 2008; Li et al., 2010; Xiang et al., 2010; Xiong et al., 2011; Qi and Xiang, 2015

Table 1.2. Human viral infections studied using zebrafish.

Virus	References
Herpes simplex virus (HSV-1)	Burgos et al., 2008; Antoine et al., 2014; Yakoub et al., 2014; Zou et al., 2014
Hepatitis C virus (HCV)	Ding et al., 2011; Ding et al., 2015
Chikungunya virus (CHIKV)	Palha et al., 2013; Briolat et al., 2014
Influenza A virus (IAV)	Gabor et al., 2014

In recent years several models of human viral diseases have been described in zebrafish (Table 1.2). To date only four

human viruses have been studied using zebrafish, but some as important as the hepatitis C virus (HCV) (Ding et al., 2011; Ding et al., 2015) or the influenza A virus (IAV) (Gabor et al., 2014). Given the potential of zebrafish for the study of viral diseases, it can be expected that in coming years more models of human viral diseases using zebrafish appear. This will not only contribute to greater understanding of diseases generated by viruses, but it will also boost the study of new antiviral drugs.

1.8. References

Aachoui Y, Sagulenko V, Miao EA, Stacey KJ (2013) Inflammasome-mediated pyroptotic and apoptotic cell death, and defense against infection. Curr Opin Microbiol 16:319-326.

Aggad D, Mazel M, Boudinot P, Megensen KE, Hamming OJ, Hartmann R, Kotenko S, Herbomel P, Lutfalla G, Levraud JP (2009) The two groups of zebrafish virus-induced interferons signal via distinct receptors with specific and shared chains. J Immunol 183:3924-3931.

Aggad D, Stein C, Sieger D, Mazel M, Boudinot P, Herbomel P, Levraud JP, Lutfalla G, Leptin M (2010) In vivo analysis of Ifn-ϒ1 and Ifn-ϒ2 signaling in zebrafish. J Immunol 185:6774-6782.

Akira S, Uematsu S, Takeuchi O (2006) Pathogen recognition and innate immunity. Cell 124:783-801.

Alonso M, Dim CH, Johnson MC, Pressley M, Leong JA (2004) The NV gene of snakehead rhabdovirus (SHRV) is not required for pathogenesis, and a heterologous glycoprotein can be incorporated into the SHRV envelope. J Virol 78:5875-5882.

Antoine TE, Jones KS, Dale RM, Shukla D, Tiwari V (2014) Zebrafish: modelling for herpes simplex virus infections. Zebrafish 11:17-25.

Bakkers J, 2011: Bakkers J (2011) Zebrafish as a model to study cardiac development and human cardiac disease. Cardiovasc Res 91:279-288.

Bennett CM, Kanki JP, Rhodes J, Liu TX, Paw BH, Kieran MW, Langenau DM, Delahaye-Brown A, Zon LI, Fleming MD, Look AT (2001) Myelopoiesis in the zebrafish, Danio rerio. Blood 98:643–651.

Biacchesi S, Mérour E, Lamoureux A, Bernard J, Brémont M (2012) Both STIG and MAVS fish orthologs contribute to the induction of interferon mediated by RIG-I. PLos One 7:e47737.

Briolat V, Jouneau L, Carvalho R, Palha N, Langevin C, Herbomel P, Schwartz O, Spaink HP, Levraud JP, Boudinot P (2014) Contrasted innate responses to two

viruses in zebrafish: insights into the ancestral repertoire of vertebrate IFN-stimulated genes. J Immunol 192:4328-4341.

Broz P and Monack DM (2013) Newly described pattern recognition receptors team up against intracellular pathogens. Nat Rev Immunol 13:551-565.

Bruns AM, Pollpeter D, Hadizadeh N, Myong S, Marko JF, Horvath CM. ATP hydrolysis enhances RNA recognition and antiviral signal transduction by the innate immune sensor, laboratory of genetics and physiology 2 (LGP2) J Biol Chem 288:938-946.

Burgos JS, Ripoll-Gomez J, Alfaro JM, Sastre I, Valdivieso F (2008) Zebrafish as a new model for herpes simplex virus type 1 infection. Zebrafish 5:323-333.

Chao CC, Hsu PC, Jen CF, Chen HC, Wang CH, Chan HC, Tsai PW, Tung KC, Wang CH, Lan CY, Chuang YJ (2010) Zebrafish as a Model Host for *Candida albicans* Infection. Infec Immun 78:2512-2521.

Chen HY, Liu W, Wu SY, Chiou PP, Li YH, Chen YC, Lin GH, Lu MW, Wu JL (2015) RIG-I specifically mediates group II type I IFN activation in nervous necrosis virus infected zebrafish cells. Fish Shellfish Immunol 43:427-435.

Davis JM, Clay H, Lewis JL, Ghori N, Herbomel P, Ramakrishnan L. (2002) Real-time visualization of mycobacterium-macrophage interactions leading to initiation of granuloma formation in zebrafish embryos. Immumity 17:693-702.

Dempsey A and Bowie AG (2015) Innate immune recognition of DNA: A recent history. Virology 479-480:146-152.

Diamond MS and Farzan M (2013) The broad-spectrum antiviral function of IFIT and IFITM proteins. Nat Rev Immunol 13:46-57.

Ding CB, Zhao Y, Zhang JP, Peng ZG, Song DQ, Jiang JD (2015) A zebrafish model for subgenomic hepatitis C virus replication. Int J Mol Med 35: 791-797.

Ding CB, Zhang JP, Zhao Y, Peng ZG, Song DQ, Jiang JD (2011) Zebrafish as a potential model organism for drug test against hepatitis C virus. PLoS One 6:e22921.

Dios S, Romero A, Chamorro R, Figueras A, Novoa B (2010) Effect of the temperature during antiviral immune response ontogeny in teleosts. Fish Shellfish Immunol 29:1019-1027.

Encinas P, Garcia-Valtanen P, Chinchilla B, Gomez-Casado E, Estepa A, Coll J (2013) Identification of multipath genes differentially expressed in pathway-targeted microarrays in zebrafish infected and surviving spring viremia carp virus (SVCV) suggest preventive drug candidates. PLoS One 8:e73553.

Encinas P, Rodriguez-Milla MA, Novoa B, Estepa A, Figueras A, Coll J (2010) Zebrafish fin immune responses during high mortality infections with viral haemorrhagic septicaemia rhabdovirus: A proteomic and transcriptomic approach. BMC Genomics 11:518.

Fensterl V and Sen GC (2014) Interferon-induced Ifit proteins: their role in viral pathogenesis. J Virol 89:2462-2468.

Forn-Cuní G, Varela M, Fernández-Rodríguez CM, Figueras A, Novoa B (2014) Liver immune responses to inflammatory stimuli in a diet-induced obesity model of zebrafish. J Endocrinol 224:159-170.

Gabor KA, Charette JR, Pietraszewski MJ, Wingfield DJ, Shim JS, Millard PJ, Kim CH (2015) A DN-mda5 transgenic model demonstrates that Mda5 plays an important role in snakehead rhabdovirus resistance. Dev Comp Immunol doi: 10.1016/j.dci.2015.01.006.

Gabor KA, Goody MF, Mowel WK, Breibach ME, Gratacap RL, Witten PE, Kim CH (2014) Influenza A virus infection in zebrafish recapitulates mammalian infection and sensitivity to anti-influenza drug treatment. Dis Model Mech 7:1227-1237.

Gabor KA, Stevens CR, Pietraszewski MJ, Gould TJ, Shim J, Yoder JA, Lam SH, Gong Z, Hess ST, Kim CH (2013) Super resolution microscopy reveals that caveolin-1 is required for spatial organization of CRFB1 and subsequent antiviral signalling in zebrafish. PLoS One 8:e68759.

Garcia-Valtanen P, Martinez-Lopez A, Ortega-Villaizan M, Perez L, Coll JM, Estepa A (2014) In addition to its antiviral and immunomodulatory properties,

the zebrafish β-defensin 2 (zfBD2) is a potent viral DNA vaccine molecular adjuvant. Antiviral Res 101:136-147.

Garner JN, Joshi B, Jagus R (2003) Characterization of rainbow trout and zebrafish eukaryotic initiation factor 2α and its response to endoplasmic reticulum stress and IPNV infection. Dev Comp Immunol 27:217-231.

Grayfer L and Belosevic M (2009) Molecular characterization, expression and functional analysis of goldfish (Carassius auratus) interferon gamma. Dev Comp Immunol 33:235-246.

Hikima J, Yi MK, Ohtani M, Jung CY, Kim YK, Mun JY, Kim YR, Takeyama H, Aoki T, Jung TS (2012) LGP2 expression is enhanced by interferon regulatory factor 3 in olive flounder, Paralichthys olivaceus. PLoS One 7:e51522.

Hornung V, Ellegast J, Kim S, Brzozka K, Jung A, Kato H, Poeck H, Akira S, Conzelmann KK, Schlee M, Endres S, Hartmann G (2006) 5´-Triphosphate RNA is the ligand for RIG-I. Science 314:994-997.

Kanneganti TD, Body-Malapel M, Amer A, Park JH, Whitfield J, Franchi L, Taraporewala ZF, Miller D, Patton JT, Inohara N, Nunez G (2006) Critical role for cryopyrin/Nalp3 in activation of caspase-1 in response to viral infection and double-stranded RNA. J Biol Chem 281:36560-36568.

Kato H, Takeuchi O, Mikamo-Satoh E, Hirai R, Kawai T, Matsushita K, Hiiragi A, Dermody TS, Fujita T, Akira S (2008) Length-dependent recognition of double-stranded ribonucleic acids by retinoic acid-inducible gene-I and melanoma differentiation-associated gene 5. J Exp Med 205:1601-1610.

Keating SE, Baran M, Bowie AG (2011) Cytosolic DNA sensors regulating type I interferon induction. Trends Immunol 32:574-581.

Kileng Ø, Albuquerque A, Robertsen B (2008) Induction of interferon system genes in Atlantic salmon by the imidazoquinoline S-27609, a ligand for Toll-like receptor 7. Fish Shellfish Immunol 24:514–522.

Kimbrell DA and Beutler B (2001) The evolution and genetics of innate immunity. Nat Rev Gen 2:256-267.

Laing KJ, Purcell MK, Winton JR, Hansen JD (2008) A genomic view of the NOD-like receptor family in teleost fish: identification of a novel NLR subfamily in zebrafish. BMC Evol Biol 8:42.

Lam SH, Chua HL, Gong Z, Lam TJ, Sin YM (2004) Development and maturation of the immune system in zebrafish, *Danio rerio*: a gene expression profiling, in situ hybridization and immunological study. Dev Comp Immunol 28:9-28.

LaPatra SE, Barone L, Jones GR, Zon LI (2000) Effects of infectious hematopoietic necrosis virus and infectious pancreatic necrosis virus infection on hematopoietic precursors of the zebrafish. Blood Cells Mol Dis 26:445-452.

Latz E, Xiao TS, Stutz A (2013) Activation and regulation of the inflammasomes. Nat Rev Immunol 13:397-411.

Levraud JP, Boudinot P, Colin I, Benmansour A, Peyrieras N, Herbomel P, Lutfalla G (2007) Identification of the zebrafish IFN receptor: implications for the origin of the vertebrate IFN system. J Immunol 178:4385-4394.

Li S, Guo X, Lu LF, Lu XB, Wu N, Zhang YA (2015) Regulation pattern of fish irf4 (the gene encoding IFN regulatory factor 4) by STAT6, c-Rel and IRF4. Dev Comp Immunol 51:65-73.

Li Z, Xu X, Huang L, Wu J, Lu Q, Xiang Z, Liao J, Weng S, Yu X, He J (2010) Administration of recombinant IFN1 protects zebrafish (Danio rerio) from ISKNV infection. Fish Shellfish Immunol 29:399-406.

Lieschke GJ and Currie PD (2007) Animal models of human disease: zebrafish swim into view. Nat Rev Genet 8:353-367.

Loo YM and Gale MJr (2011) Immune signaling by RIG-I-like receptors. Immunity 34:680-692.

López-Muñoz A, Roca JF, Sepulcre MP, Meseguer J, Mulero V (2010) Zebrafish larvae are unable to mount a protective antiviral response against waterbone infection by spring viremia of carp virus. Dev Comp Immunol 34:546-552.

López-Muñoz A, Roja FJ, Meseguer J, Mulero V (2009) New insights into the evolution of IFNs: zebrafish group II IFNs induce a rapid and transient expression

of IFN-dependent genes and display powerful antiviral activities. J Immunol 182:3440-3449.

Lu MW, Chao YM, Guo TC, Santi N, Evensen O, Kasani SK, Hong JR, Wu JL (2008) The interferon response is involved in nervous necrosis virus acute and persistent infection in zebrafish infection model. Mol Immunol 45:1146-1152.

Ludwig M, Palha N, Torhy C, Briolat V, Colucci-Guyon E, Brémont M, Herbomel P, Boudinot P, Levraud JP (2011) Whole-body analysis of a viral infection: vascular endothelium is a primary target of infectious hematopoietic necrosis virus in zebrafish larvae. PLoS Pathog 7:e1001269.

Lupfer C, Malik A, Kanneganti TD (2015) Inflammasome control of viral infection. Curr Opin Virol 12:38-46.

Lupfer C and Kanneganti TD (2013) The expanding role of NLRs in antiviral immunity. Immunol Rev 255:13-24.

Martin SA, Taggart JB, Seear P, Bron JE, Talbot R, Teale AJ, Sweeney GE, Hoyheim B, Houlihan DF, Tocher DR, Zou J, SEcombes CJ (2007) Interferon type I and type II responses in an Atlantic salmon (Salmo salar) SHK-1 cell line by the salmon TRAITS/SGP microarray. Physiol Genomics 32:33-44.

Martinez-Lopez A, Garcia-Valtanen P, Ortega-Villaizan M, Chico V, Gomez-Casado E, Coll JM, Estepa A (2014) VHSV G glycoprotein major determinants implicated in triggering the host type I IFN antiviral response as DNA vaccine molecular adjuvants. Vaccine 32:6012-6019.

Mogensen TH (2009) Pathogen recognition and inflammatory signalling in innate immune defences. Clin Microbiol Rev 22:240-273.

Moresco EMY and Beutler B (2010) LGP2: positive about viral sensing. Proc Natl Sci USA 107:1261-1262.

Morick D, FAigenbaum O, Smirnow M, Fellig Y, Inbal A, Kotler M (2015) Mortality caused by bath exposure of zebrafish (Danio rerio) larvae to nervous necrosis virus is limited to the fourth day postfertilization. Appl Environ Microbiol 81:3280-3287.

Moss LD, Monette MM, Jaso-Friedmann L, Leary JH, Dougan ST, Krunkosky T, Evans DL (2009) Identification of phagocytic cells, NK-like cytotoxic cell activity and the production of celular exudates in the coelomic cavity of a dult zebrafish. Dev Comp Immunol 33:1077-1087.

Nayak AS, Lage CR, Kim CH (2007) Effects of low concentrations of arsenic on the innate immune system of the zebrafish (Danio rerio). Toxicol Sci 98:118-124.

Neely MN, Pfeifer JD, Caparon M (2002) Streptococcus-zebrafish model of bacterial pathogenesis. Infect Immun 70:3904-3914.

Newman M, Ebrahimie E, Lardelli M (2014) Using the zebrafish model for Alzheimer´s disease research. Front Genet 5:189.

Nguyen-Chi et al., 2014: Nguyen-Chi M, Phan QT, Gonzalez C, Dubremetz JF, Levraud JP, Lutfalla G (2014) Transient infection of the zebrafish notochord with E. coli induces chronic inflammation. Dis Model Mech 7:871-882.

Nie L, Zhang YS, Dong WR, Xiang LX, Shao JZ (2015) Involvement of zebrafish RIG-I in NF-kB and IFN signalling pathways: insights into functional conservation of RIG-I antiviral innate immunity. Dev Comp Immunol 48:95-101.

Novoa B and Figueras A (2012) Zebrafish: model for the study of inflammation and the innate immune response to infectious diseases. Adv Exp Med Biol 946:253-275.

Novoa B, Romero A, Mulero V, Rodríguez I, Fernández I, Figueras A (2006) Zebrafish (Danio rerio) as a model for the study of vaccination against viral haemorrhagic septicaemia virus (VHSV). Vaccine 24:5806-5816.

Nüsslein-Volhard C, Dahm R (2002) Zebrafish, a practical approach. Oxford University Press, Oxford.

Palha N, Guivel-Benhassine F, Briolat V, Lutfalla G, Sourisseau M, Ellett F, Wang CH, Lieschke GJ, Herbomel P, Schwartz O, Levraud JP (2013) Real-time whole-body visualization of Chikungunya Virus infection and host interferon response in zebrafish. PLoS Pathog 9:e1003619.

Pang IK and Iwasaki A (2012) Control of antiviral immunity by pattern recognition and the microbiome. Immunol Rev 245:209-226.

Pereiro P, Varela M, Diaz-Rosales P, Romero A, Dios S, Figueras A, Novoa B (2015) Zebrafish Nk-lysins: first insights about their cellular and functional diversification. Dev Comp Immunol 51:148-159.

Pestka S, Krause CD, Walter MR (2004) Interferons, interferon-like cytokines, and their receptors. Immunol Rev 202:8-32.

Phelan PE, Pressley ME, Witten PE, Mellon MT, Blake S, Kim CH (2005a) Characterization of snakehead rhabdovirus infection in zebrafish (Danio rerio). J Virol 79:1842-1852.

Phelan PE, Mellon MT, Kim CH (2005b) Functional characterization of full-length TLR3, IRAK-4, and TRAF6 in zebrafish (Danio rerio). Mol Immunol 42:1057-1071.

Qi L and Xiang Z (2015) Molecular cloning and expression analysis of an apoptosis-associated gene Daxx from zebrafish, Danio rerio. Fish Shellfish Immunol doi: 10.1016/j.fsi.2015.03.040.

Randall RE and Goodboum S (2008) Interferons and viruses: an interplay between induction, signalling, antiviral responses and virus countermeasures. J Gen Virol 89:1-47.

Rasighaemi P, Basheer F, Liongue C, Ward AC (2015) Zebrafish as a model for leukemia an other hematopoietic disorders. J Hematol Oncol 8:29.

Ruyra A, Cano-Sarabia M, García-Valtanen P, Yero D, Gibert I, Mackenzie SA, Estepa A, Maspoch D, Roher N (2014) Targeting and stimulation of the zebrafish (Danio rerio) innate immune system with LPS/dsRNA-loaded nanoliposimes. Vaccine 32:3955-3962.

Sabbah A, Chang TH, Harnack R, Frohlich V, Tominaga K, Dube PH, Xiang Y, Bose S (2009) Activation of innate immune antiviral responses by Nod2. Nat Immunol 10:1073-1080.

Sadler AJ and Williams BR (2008) Interferon-inducible antiviral effectors. Nat Rev Immunol 8: 559-568.

Sanders GE, Batts WN, Winton JR (2003) Susceptibility of zebrafish (Danio rerio) to a model pathogen, spring viremia of carp virus. Comp Med 53:514-521.

Santoriello C, Zon LI (2012) Hooked! Modeling human disease in zebrafish. J Clin Invest 122:2337-2343.

Schoggins JW and Rice CM (2011) Interferon-stimulated genes and their antiviral effector functions. Curr Opin Virol 6:519-525.

Sharma S and Fitzgerald KA (2011) Innate immune sensing of DNA. PLos Pathog 7:e1001310.

Skjæveland I, DIliev DB, Zou J, Jorgensen T, Jorgensen JB (2008) A TLR9 homolog that is up-regulated by IFN-gamma in Atlantic salmon (*Salmo salar*). Dev Comp Immunol 32:603–607.

Stein C, Caccamo M, Laird G, Leptin M (2007) Conservation and divergence of gene families enconding components of innate immune response system in zebrafish. Genome Biol 8:R251.

Sullivan C and Kim CH (2008) Zebrafish as a model for infectious disease and immune function. Fish Shellfish Immunol 25:341-350.

Sun F, Zhang YB, Liu TK, Shi J, Wang B, (2011) Fish MITA serves as a mediator for distinct fish IFN gene activation dependent on IRF3 or IRF7. J Immunol 187:2531-2539.

Sundaram AYM, Consuegra S, Kiron V, Fernandes JMO (2012) Positive selection pressure within teleost toll-like receptors *tlr21* and *tlr22* subfamilies and their response to temperature stress and microbial components in zebrafish. Molecular Biology Reports 39:8965-8975.

Tan TY, Chu JJ (2013) Dengue virus-infected human monocytes trigger late activation of caspase-1, which mediates pro-inflammatory IL-1β secretion and pyroptosis. J Gen Virol 94:1215-1220.

Tobin DM, May RC, Wheeler RT (2012) Zebrafish: A see-through host and a fluorescent toolbox to probe host-pathogen interaction. PLoS Pathog 8:e1002349.

Traver D, Herbomel P, Patton EE, Murphey RD, Yoder JA, Litman GW, Catic A, Amemiya CT, Zon LI, Trede NS (2003) The zebrafish as a model organism to study development of the immune system. Adv Immunol 81: 253-330.

van der Sar AM, Musters RJ, van Eeden FJ, Appelmelk BJ, Vandenbroucke-Grauls CM, Bitter W (2003) Zebrafish embryos as a model host for the real time analysis of Salmonella typhimurium infections. Cell Microbiol 5: 601-611.

van der Vaart M, Spaink HP, Meijer AH (2012) Pathogen recognition and activation of the innate immune response in zebrafish. Adv Hematol 2012:159807.

Varela M, Romero A, Dios S, van der Vaart M, Figueras A, Meijer AH, Novoa B (2014a) Cellular visualization of macrophage pyroptosis and interleukin-1β release in a viral hemorrhagic infection in zebrafish larvae. J Virol 88:12026-12040.

Varela M, Diaz-Rosales P, Pereiro P, Forn-Cuní G, Costa MM, Dios S, Romero A, Figueras A, Novoa B (2014b) Interferon-induced genes of the expanded IFIT family show conserved antiviral activities in non-mammalian species. PLoS One 9:e100015.

Varela M, Forn-Cuní G, Dios S, Figueras A, Novoa B (2015) Proinflammatory caspase-a activation and antiviral state induced by a zebrafish perforin after possible cellular and functional diversification from a myeloid ancestor. J Innate Immun. DOI:10.1159/000431287.

Wang L, Wang L, Zhang HX, Zhang JH, Chen WH, Ruan XF, Xia C (2006) In vitro effects of recombinant zebrafish IFN on spring viremia of carp virus and infectious hematopoietic necrosis virus. J Interferon Cytokine Res 26:256-259.

Westerfield M (2000) The zebrafish book. A guide for the laboratory use of zebrafish (Danio rerio), 4th ed. University of Oregon Press, Eugene.

White R, Rose K, Zon L (2013) Zebrafish cancer: the state of the art and the path forward. Nat Rev Cancer 13:624-636.

Wu J and Chen ZJ (2014) Innate immune sensing and signaling of cytosolic nucleic acids. Annu Rev Immunol 32:461–488.

Wu B, Peisley A, Richards C, Yao H, Zeng X, Lin C, Chu F, Walz T, Hur S (2013) Structural basis for dsRNA recognition, filament formation, and antiviral signal activation by MDA5. Cell 152:276-789.

Xiang Z, Dong C, Qi L, Chen W, Huang L, Li Z, Xia Q, Liu D, Huang M, Weng S, He J (2010) Characteristics of the interferon regulatory factor pairs zfIRF5/7 and their stimulation expression by ISKNV infection in zebrafish (Danio rerio). Dev Comp Immunol 34:1263-1273.

Xiong XP, Dong CF, Xu X, Weng SP, Liu ZY, He JG (2011) Proteomic analysis of zebrafish (Danio rerio) infected with infectious spleen and kidney necrosis virus. Dev Comp Immunol 35:431-440.

Xu X, Zhang L, Weng S, Huang Z, Lu J, Lan D, Zhong X, Yu X, Xu A, He J (2008) A zebrafish (Danio rerio) model of infectious spleen and kidney necrosis virus (ISKNV). Virology 376:1-12.

Yakoub AM, Rawal N, Maus E, Baldwin J, Shukla D, Tiwari V (2014) Comprehensive analysis of HSV-1 entry mediated by zebrafish 3-O-Sulfotransferase isoforms: implications for the development of a zebrafish model of HSV-1 infection. J Virol 88:12915-12922.

Yoneyama M and Fujita T (2009) RNA recognition and signal transduction by RIG-I-like receptors. Immunol Rev 227:54-65.

Zhou et al., 2013: Zhou X, Michal JJ, Zhang L, Ding B, Lunney JK, Liu B, Jiang Z (2013) Interferon induced IFIT family genes in host antiviral defense. Int J Biol Sci 9:200-208.

Zhu Z, Zhang X, Wang G, Zheng H (2014) The laboratory of genetics and physiology 2: emerging insights into the controversial functions of this RIG-I-like receptor. Biomed Res Int 2014:960190.

Zou J and Secombes CJ (2011) Teleost fish interferons and their role in immunity. Dev Comp Immunol 35:1376-1387.

Zou J, Chang M, Nie P, Secombes CJ (2009) Origin and evolution of the RIG-I like RNA helicase gene family. BMC Evol Biol 9:85.

Zou J, Tafalla C, Truckle J, Secombes CJ (2007) Identification of a second group of type I IFNs in fish sheds light on IFN evolution in vertebrates. J Immunol 179:3859-3871.

Zou M, De Koninck P, Neve RL, Friedrich RW (2014) Fast gene transfer into the adult zebrafish brain by herpes simplex virus 1 (HSV-1) and electroporation: methods and optogenetic applications. Front Neural Circuits 8:41.

Zou P, Chang M, Xue N, Liu X, Li J, Fu J, Chen S, Nie P (2014) Melanoma differentiation-associated gene 5 in zebrafish provoking higher interferon-promoter activity through signalling enhacing of its shorter splicing variant. Immunology 14:192-202.

Chapter 2

Rationale and aims

Innate immunity is the organism´s first line of defence against pathogens and infections. It is characterized by pre-established, relatively unspecific and fast actions. The genes that take part in the innate immunity are fully coded in the genome and generally non-modified during the lifespan of the organism. Understand the complex mechanisms through which viruses modulate immune function should provide key information aimed to develop a range of potential targeted antiviral therapies.

The aim of this doctoral thesis is the characterisation of zebrafish antiviral response against the hemorrhagic virus spring viraemia of carp virus (SVCV), in order to know the molecules involved and deepen the knowledge of the inflammatory response caused by the pathogen (responsible cells, cell migration, genes and gene circuits involved).

The overall objective of this research is the identification of key genes in the process of defence against SVCV in zebrafish, to learn more about the pathology generated from an immunological point of view.

This thesis is structured in two sections:

Section I (Chapters 3, 4 and 5) deals with the characterisation of the expression and function of genes involved in the antiviral immune response.

Section II (Chapters 6 and 7) concerns the study of the immune and inflammatory responses caused by SVCV in zebrafish larvae.

The specific aims of this doctoral thesis are:

1) To characterise and analyse the expression of zebrafish Interferon-induced proteins with tetratricopeptide repeats (IFITs).

IFITs are involved in the protective response to viral infections, although the precise mechanism of IFITs for reducing viral proliferation is currently unknown. Exploiting the conservation of synteny between human and zebrafish genomes, we have identified 10 members of the IFIT family. The induction of these genes was examined both *in vitro* and *in vivo* after interferon (IFN) administration and SVCV challenge. The results of this study are presented in **Chapter 3** entitled **Characterisation of Interferon-Induced Genes of the Expanded IFIT Family in Zebrafish.**

2) To identify and analyse the expression of zebrafish interleukin-6 (IL6). IL6 is one of the most pleiotropic cytokines due to its importance in both innate and adaptive immune responses and other physiological processes. In this study, we identified the zebrafish *il6* homologue by investigating the synteny between the human, the fugu and the zebrafish genomes. Although zebrafish *il6* showed a low sequence homology with other IL6 sequences in other species, it presented a high structural similarity to human IL6. We also analysed *il6* expression in several different tissues, along with analysis of the expression of the genes that form the IL6 receptor complex, *il6r* and *gp130*. The results of this study are presented in **Chapter 4** entitled **Characterisation of Interleukin-6 in Zebrafish**.

3) To study the gene family evolution and the expression of zebrafish Perforins (PRFs). PRFs play a central role in the granule-dependent cell death induced by natural kiler T cells and cytotocic T lymphotyes and, participate both in defence against virus-infected and neoplastic cells and in the recognition of non-self molecules by the immune system. Little is known about fish perforin genes. We examined the zebrafish genome with the aim of increasing our knowledge about the role of perforins. We characterised 6 perforin genes in the zebrafish genome, and we

studied them at the evolutionary level in combination with expression patterns in several tissues and cell populations, both during larval development and during the course of a viral infection. The results of this study are presented in **Chapter 5** entitled **Characterisation of 6 Perforin Genes in Zebrafish.**

4) To establish the infection of zebrafish larvae with the virus SVCV as a model of hemorrhagic disease. The lack of adequate *in vivo* infection models has limited the research on viral pathogenesis and the current understanding of the underlying infection mechanisms. Most of the research regarding interactions between viruses and host cells has been performed in cell lines that might not be major targets during natural infections. We established the systemic infection of zebrafish larvae with SVCV as a model of hemorrhagic disease, with the objective of improving the knowledge of the pathology generated by this virus. The results of this study are presented in **Chapter 6** entitled **SVCV Systemic Infection in Zebrafish Larvae as a Model of Hemorrhagic Disease**.

5) To study the leukocyte dynamic and the inflammatory response during the infection of zebrafish larvae with SVCV. Host-pathogen interactions are essential for the modulation of the immune response during an infection. The presence of a pathogen alters the immune balance prevailing in a host under normal conditions causing the appearance of diseases, which lead to the death of the host if it is not able to control the infection. For the study of the inflammatory response originated by SVCV during a systemic infection in zebrafish larvae, we focused on interactions between the virus and host cells at early stages of the infection. Taking advantage of zebrafish transgenic lines and imaging techniques we identified macrophages as main target of the virus. The results of this study are presented in **Chapter 7** entitled

Leukocyte Response and Inflammation during SVCV Infection in Zebrafish Larvae.

2

Chapter 3

Characterisation of Interferon-induced Genes of the Expanded IFIT Family in Zebrafish

Published in:
-Mónica Varela, Patricia Díaz-Rosales, Patricia Pereiro, Gabriel Forn-Cuní, María M Costa, Sonia Dios, Alejandro Romero, Antonio Figueras and Beatriz Novoa. PLoS One 2014; 9(6): e100015

3.1. Introduction

Host antiviral innate immune responses begin with the detection of viruses, which triggers the induction of cellular and molecular effectors with broad antiviral activities (Kawai and Akira, 2008), including type I interferon (IFN) and hundreds of IFN-stimulated genes (ISGs), which contribute to the overall effects against a given virus (Sadler and Williams, 2008; Schoggins and Rice, 2011).

In fish, although numerous *ifn* genes have been characterized (reviewed in Zou and Secombes, 2011), their classification is controversial, as these genes are more diverse than previously thought, and their genomic structures, containing introns, are reminiscent of mammalian type III interferons (IFN-λ), although the encoded proteins are similar to type I interferons (Robertsen, 2006). Fish type I IFNs, named as interferon-phi (IFNΦ), were classified in two groups: group I (comprising IFNΦ1 and IFNΦ4) and group II (composed by IFNΦ2 and IFNΦ3) (Stein et al., 2007; Zou et al., 2007). These two groups of IFNs do not bind to the same receptor complexes in zebrafish, as was shown by Aggad et al. (2009).

Knowledge of the antiviral properties of individual ISGs is mostly limited to a few intensively studied examples, such as PKR (García et al., 2006) or MX (Martens and Howard, 2006; Haller et al., 2007). MX is a well-studied ISG in fish but our knowledge of other ISGs (e.g., Vig-1/viperin, ISG15, finTRIMs, and PKR) in fish is limited (reviewed in Verrier et al., 2011). Even in mammals, although the importance of the IFN system is clear, there is not enough information concerning the mechanism underlying the IFN-mediated inhibition of viral replication, particularly *in vivo* (Fensterl et al., 2012).

Among ISGs, a protein family called IFIT (interferon-induced proteins with tetratricopeptide repeats), which is

characterized by tetratricopeptide repeats (TPR domains), has been examined in higher vertebrates (Fensterl and Sen, 2011; Diamond and Farzan, 2013; Zhou et al., 2013). Recent studies have shown that the IFIT family is conserved in mammals, amphibians and birds, but these proteins are not present in yeast, plants or lower animals, such as fruit fly and nematodes (Zhou et al., 2013). The members of this protein family were initially named according to their molecular weights (ISG54/P54, ISG56/P56, ISG58/P58 and ISG60/P60), although currently the most relevant and recent publications have adopted the term IFIT (Zhou et al., 2013). IFIT proteins are involved in many processes in response to viral infection and other functions, such as protein-protein and protein-RNA interactions, double-stranded RNA signaling, cell migration, and proliferation (Fensterl and Sen, 2011; D´Andrea and Regan, 2003). The transcriptional induction of the IFIT family genes has been described after infection with both DNA- and RNA-viruses (Zhu and Shenk, 1997; Saha and Rangarajan, 2003; Wacher et al., 2007; Rathi et al., 2010) and after bacterial stimulation in a type I IFN-dependent manner (Berchtold et al., 2008; Ovstebo et al., 2008; Kylaniemi et al., (2009). Although their antiviral mechanisms are still poorly understood, studies have shown that IFIT genes restrict virus replication through the alteration and suppression of protein synthesis or direct binding and sequestering of viral RNA, thereby reducing their infectivity (Zhou et al., 2013).

In fish, information concerning *ifit* genes is almost non-existent. Only a few partial or unconfirmed sequences of *ifit* genes have been identified using sequencing analyses (Zhou et al., 2013; Liu et al., 2013). A formal characterization of IFIT genes and an in depth study of their regulation under different stimuli has never been done in fish.

Teleost fish offer an interesting model for the study of IFITs, not only for the clear interest in this ISG family in relation to viral

infection, which constitutes an important threat, particularly for cultured fish, but also due to the ancient separation of fish from tetrapods and the great diversity of fish species. In addition, the advantage of the increased use of zebrafish (*Danio rerio*) as an important vertebrate model for studies in developmental and biomedical research, hematopoiesis and recently, immunology, has facilitated the development of genomic tools that allow the identification of new gene families. In the present work, we describe the complete repertoire of *ifit* genes in zebrafish. Our study reveals a protein family forged through ancient duplication events, according with the results recently published (Liu et al., 2013). To further explore the antiviral properties of these IFN-stimulated genes, *in vivo* and *in vitro* experiments were conducted in zebrafish after treatment with different recombinant IFNsΦ and after viral infection. Moreover, the protective effect of three-selected zebrafish IFITs upon viral challenge was also examined *in vivo*.

3.2. Material and Methods

Sequence retrieval and analysis

The IFIT sequences were searched using the zebrafish genome assembly version Zv9 (www.ensembl.org/Daniorerio/), exploiting the conservation of synteny between the human and zebrafish genomes. The sequences were confirmed through PCR amplification using specific primers (Table S3.1) to obtain the full-length open reading frame (ORF) of each gene. The PCR products were subcloned into a pCR3.1 vector (Invitrogen) and transformed into One Shot TOP10F' competent cells (Invitrogen) for subsequent sequencing and ORF confirmation.

The identity and similarity analysis between the zebrafish, human and mouse IFIT sequences was performed using MatGAT (Campanella et al., 2003). The TPR distribution was analyzed using TPRpred (http://tprpred.tuebingen.mpg.de/) (Karpenahalli et al., 2007), and the theoretical isoelectric point (pI) and the calculated molecular weight were determined using ExPaSy tools (http://us.expasy.org/tools). The 3D-structure of zebrafish IFITs was predicted using the I-TASSER server (Roy et al., 2010), selecting the model with the best C-score, and viewed through PyMOL (http://www.pymol.org). The Template Modeling Score (TM-score), a measure of structural similarity between two proteins, was also analyzed to identify structural analogs with known crystal architecture in the Protein Data Bank (PDB; http://www.rcsb.org/pdb/).

Phylogenetic tree and analysis of Darwinian selection

IFIT-family protein sequences were retrieved from the NCBI Protein, Uniprot and Ensembl databases based on annotation. The sequences were subsequently complemented using a blastp search for homologs in different databases. The initial sequence alignment was performed using the MAFFT online server following an E-INS-i strategy (Katoh et al., 2005). The resulting alignment was pruned using Gblocks 0.91b (Talavera and Castresana, 2007) and subsequently analyzed using ProtTest 3.2 (Darriba et al., 2011) to determine the best-fit amino acid replacement model using the Akaike Information Criterion (AIC) (Akaike, 1974), specified to estimate the maximum likelihood gene tree using PhyML 3.0 (Guindon et al., 2010). The nodal confidence was calculated using the aLRT method (Anisimova and Gascuel, 2006). Edition and representation of the obtained tree was performed in FigTree v1.3.1 (http://tree.bio.ed.ac.uk/software/figtree/).

An estimation of the rates of synonymous (silent) and nonsynonymous (amino-acid-changing) substitutions was performed to identify a positive Darwinian selection in the zebrafish IFIT family using the PAML package version 4 (Yang, 2007). The maximum-likelihood (ML) approach was implemented in the CODEML program to determine the ω value among zebrafish IFITs.

Animals

Wild type adult zebrafish (*Danio rerio*) were grown in our experimental facilities according to established protocols (Westerfield, 2000; Nusslein-Volhard and Dahm, 2002) (also see http://zfin.org/zf_info/zfbook/zfbk.html). Fish care and the challenge experiments were conducted according the CSIC National Committee on Bioethics under approval number 07_09032012.

Cell cultures and viral infection

Fibroblastic like cell line, ZF4, derived from 1-day-old zebrafish embryos (ATCC CRL-2050) (Driever and Rangini, 1993) were cultured in Dulbecco's modified Eagle's medium (D/MEM/F12, Gibco) supplemented with 100 µg/mL of primocin (InvivoGen) and 10% fetal bovine serum (FBS) at 26°C. Human HEK-293 cells (ATCC CRL-1573) (Graham et al., 1977) were grown in Eagle's Minimum Essential Medium (Gibco) supplemented with 100 µg/mL primocin (InvivoGen), 1X non-essential amino acids (Gibco), 1 mM sodium pyruvate (Gibco) and 10% FBS. The cells were incubated in a 5% CO_2 atmosphere at 37°C. Kidney cell suspensions were obtained from adult fish sacrificed using anaesthesia in ice. Kidneys were homogenized through a 100-µm

mesh, and the mixture was adjusted to the required concentration (1.5×10^6 cells/ml) in Leibovitz L-15 medium (Gibco) supplemented with 100 µg/mL of Primocin (InvivoGen) and 2% FBS and maintained at 26°C. For the *in vitro* stimulations, the cells were seeded into 24-well plates at 1 ml per well.

The rhabdovirus, spring viraemia of carp virus (SVCV isolate 56/70) was used in these experiments. Experimental infections were performed at 22°C, and the viral titer was calculated as previously described (Reed and Muench, 1938).

RNA Extraction and Gene Expression

Total RNA isolation was performed using the Maxwell 16 LEV Simply RNA Tissue Kit (Promega, Madison, WI, USA) according to the manufacturer's instructions. cDNA was obtained from 1 µg of total RNA using the SuperScript III First-Strand Synthesis Supermix (Invitrogen). Specific qPCR primers were designed (Table S3.1) using the *Primer3* program (Rozen and Skaletsky, 2000), and the primer efficiency was evaluated (Pfalffl, 2001). A previously described (Díaz-Rosales et al., 2012) cDNA template was used for real-time PCR amplification, with 40 cycles and a 60°C annealing temperature. All reactions were performed with several biological replicates and using technical triplicates. The relative expression levels of the genes were normalized to the expression of 18S ribosomal RNA (McCurley and Callard, 2008), as a housekeeping gene control (primers specified in Table S3.1), following the Pfaffl method (Pfalffl, 2001).

Production of zebrafish recombinant IFNsΦ

Zebrafish *ifnφ1*, *ifnφ2* and *ifnφ3* (GenBank accession numbers: NM_207640, NC_007114 and NC_007114, respectively)

expression constructs in the pcDNA3.1/V5-His backbone were kindly provided by Dr. Mulero (University of Murcia, Spain). Recombinant IFNsΦ were produced by transfection of 6 µg the plasmids into HEK-293 cells at 70–80% confluence using the X-tremeGENE HP DNA Transfection Reagent (Roche) according to the manufacturer's instructions. Forty-eight hours after transfection, the supernatants were collected and stored at −80°C until further use.

Antiviral activity of IFIT genes in zebrafish

Three selected *ifit* genes (12b, 13a and 17a) were amplified using touchdown PCR (primers in Table S3.1), and the PCR products were cloned using the pcDNA 3.1/V5-His TOPO TA Expression Kit (Invitrogen). One Shot TOP10F competent cells (Invitrogen) were transformed to generate the plasmid constructs. Plasmid purifications were conducted using the PureLink HiPure Plasmid Midiprep Kit (Invitrogen). The recombinant plasmids were microinjected into one-cell stage zebrafish embryos with a glass microneedle using Narishige MN-151 micromanipulator and Narishige IM-30 microinjector. In each experiment, a total of 240 embryos were divided into 6 groups of 40 eggs (4 replicates of 10 embryos) and each batch was microinjected with the following treatments diluted in PBS: pcDNA 3.1-Ifit12b, pcDNA 3.1-Ifit13a, pcDNA 3.1-Ifit17a, pcDNA 3.1-empty, and PBS. An additional untreated group was included to control the egg quality and survival. The quantity of plasmid inoculated into each embryo was 100 pg/egg in a final volume of 2 nL. Three days after plasmid administration, the larvae were microinjected in the duct of Cuvier with 2 nL of a SVCV suspension at a final concentration of 10^3 $TCID_{50}$/ml. The mortalities due to the viral infection were registered for 3 days after infection before an independently feeding and therefore before an ethical approval is required (EU

directive 2010_63) (Belanger et al., 2010). Fish condition was controlled three times a day. The viral transcription in IFIT-injected larvae was quantified through qPCR using specific primers for the N gene of the SVCV at 9 hours after the infection. The relative expression of the N gene was normalized to the expression of 18S ribosomal RNA (primers specified in Table S3.1).

Statistical analysis

The results were expressed as the means ± standard error. The significant differences were determined using Students t-test. The data from the in vivo antiviral activity of IFITs was analyzed using one-way analysis of variance (ANOVA) followed by Tukeýs multiple comparison test.

3.3. Results

Defining the complete repertoire of IFIT genes in zebrafish

Using a zebrafish genome-wide blast search, we detected a high degree of synteny between the human chromosome 10 (region q23.31) and the zebrafish chromosomes 17 and 12 (Figure 3.1A). Our analysis confirmed the presence of five and three IFIT genes on zebrafish chromosomes 12 and 17, respectively. Moreover, another two genes were identified as similar to *ifit* genes (one gene on chromosome 5 and the other gene on chromosome 13).

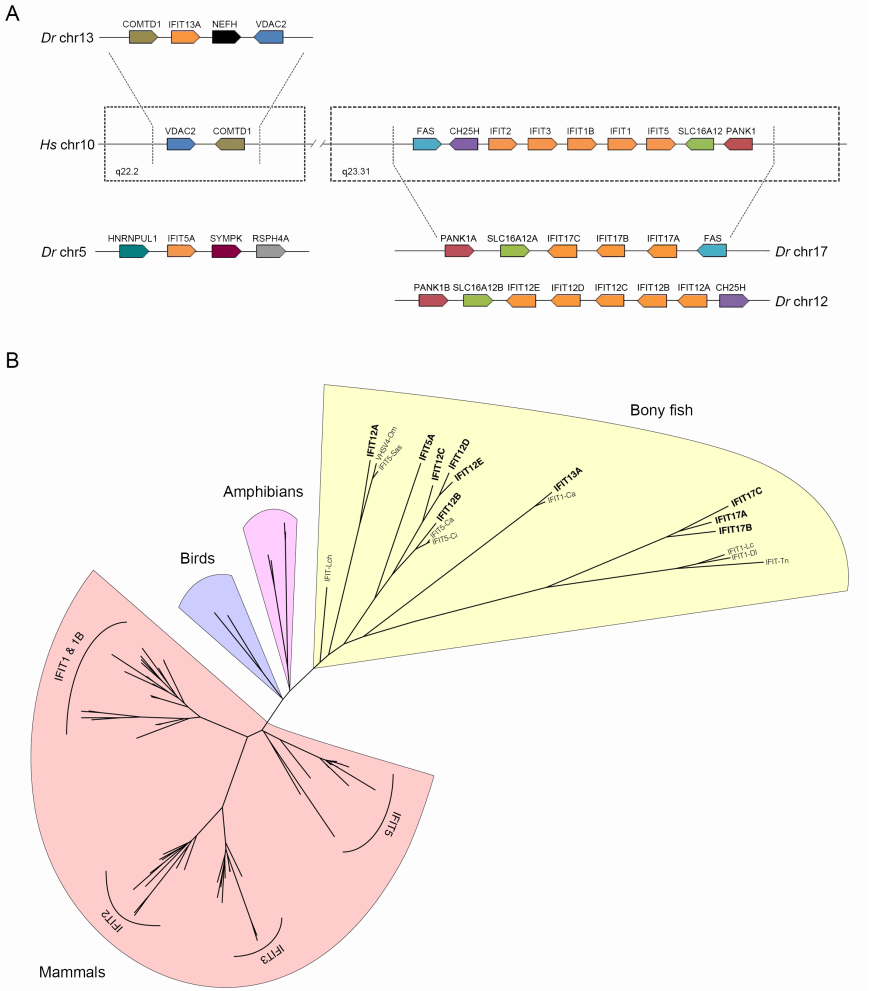

Figure 3.1. Synteny and phylogenetic analysis. A. Comparative gene location of IFIT sequences between human chromosome 10 and zebrafish chromosomes 5, 12, 13 and 17. The genes flanking the IFIT cluster, located at the q23.31 region of human chromosome 10, showed a high degree of synteny with the zebrafish chromosomes 17 and 12. Moreover, the genes surrounding zebrafish IFIT 13 were located on the same human chromosome but in the q22.2 region. An IFIT sequence was also present on zebrafish chromosome 5. B. Phylogenetic relationship between the IFIT proteins from bony fish and similar proteins described in other vertebrates, such as amphibians, birds and mammals. Lch: *Latimeria chalumnae*; Om: *Oncorhynchus mykiss*; Sas: *Salmo salar*; Ca: *Carassius auratus*; Ci: *Ctenopharyngodon idella*; Lc: *Larimichthys crocea*; Dl: *Dicentrarchus labrax*; Tn: *Tetraodon nigroviridis*.

The zebrafish *ifit* sequences were named according to their chromosomal position: *ifit5a* (ENSDARG00000088069), *ifit12a* (ENSDARG00000008098), *ifit12b* (ENSDARG00000007467), *ifit12c* (ENSDARG00000090537), *ifit12d* (not identified in the Ensembl database), *ifit12e* (ENSDARG00000090977), *ifit13a* (ENSDARG00000057173), *ifit17a* (ENSDARG00000071012), *ifit17b* (ENSDARG00000043584) and *ifit17c* (ENSDARG00000056976). In order to confirm the *ifit* sequences, we designed specific primers to amplify and sequence the 10 zebrafish *ifit* genes (primers in Table S3.1). The confirmed full-length ORFs were submitted to GenBank under accession numbers KF418356–KF418365.

The block of human IFIT genes and the pseudogene IFIT1B (IFIT-1, 1B, 2, 3 and 5) is flanked downstream by the SLC16A12 (solute carrier family 16, member 12) and PANK1 (pantothenate kinase 1) genes. These genes are also present on zebrafish chromosomes 17 and 12 but are situated upstream of the IFIT region (Figure 3.1A). The FAS (TNF receptor superfamily, member 6) and CH25H (cholesterol 25-hydroxylase) genes are located upstream of the human IFIT cluster and showed sub-partitioning in zebrafish. Thus, FAS is located on chromosome 17 and CH25H is located on chromosome 12, and both genes have an inverted orientation at the 3' region of the IFIT genes (Figure 3.1A). The q22.2 region of human chromosome 10 also showed homology with zebrafish chromosome 13. One IFIT-related gene (*ifit13a*) was identified between the COMTD1 (catechol-O-methyltransferase domain containing 1) gene at the 5' end and the NEFH (neurofilament, heavy polypeptide) and VDAC2 (voltage-dependent anion channel 2) genes at the 3' end of this chromosome. In this case, synteny was not conserved because there were no IFIT genes between the VDAC2 and COMTD1 genes in human chromosome 10 (Figure 3.1A). Moreover, another IFIT gene was identified on chromosome

5, but it was not possible to identify a conserved region between both species (Figure 3.1A).

Phylogenetic tree and analysis of Darwinian selection

Data mining for IFIT protein sequences retrieved 77 different sequences, 60 of which belonged to mammalian species, 2 bird species, 6 amphibian species and 9 fish species (Table S3.2). We used these sequences to construct a phylogenetic tree, revealing a clear separation of the IFIT sequences among the analyzed taxonomical classes (Figure 3.1B). The tree topology categorized the mammalian IFIT sequences into four main branches, IFIT1/1B, IFIT2, IFIT3 and IFIT5 homology groups, with great confidence values; however, the phylogenetic relationship among non-mammalian IFIT sequences was not clear, potentially reflecting the minor representation of these sequences in the entire analysis. For example, the evolutionary relationship of the different IFIT genes across fish species was not confidently resolved, although some sequences were orthologous. However, an interesting pattern emerged, branching the zebrafish IFIT sequences belonging to the same chromosome.

We estimated the dN/dS ratios (ω) among the zebrafish IFIT sequences to quantify the selection pressure acting on IFITs genes and determined that the genes located on chromosome 17 underwent positive Darwinian selection (ω>1). The dN/dS ratio observed between IFIT17A and IFIT17B was 1.2928, whereas this value was higher between IFITs 17B and 17C (ω = 1.4667) and between IFITs 17A and 17C (ω = 1.5130). The IFIT genes located on chromosomes 5, 12 and 13 were not subjected to this evolutionary mechanism, obtaining ω values lower than 1.

Sequencing analysis and structure domains

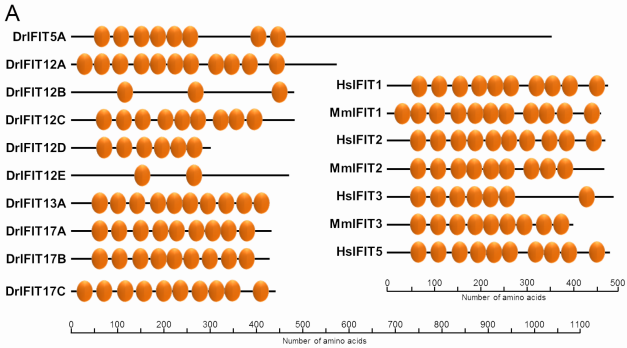

B

Number of amino acids	Calculated MW (kDa)	Theoretical pI
1038	120.29	6.70
474	54.34	8.20
482	56.38	6.69
483	55.65	6.10
302	34.92	5.00
471	54.40	6.02
429	50.08	8.75
433	50.41	6.70
429	50.03	6.85
442	51.46	6.06

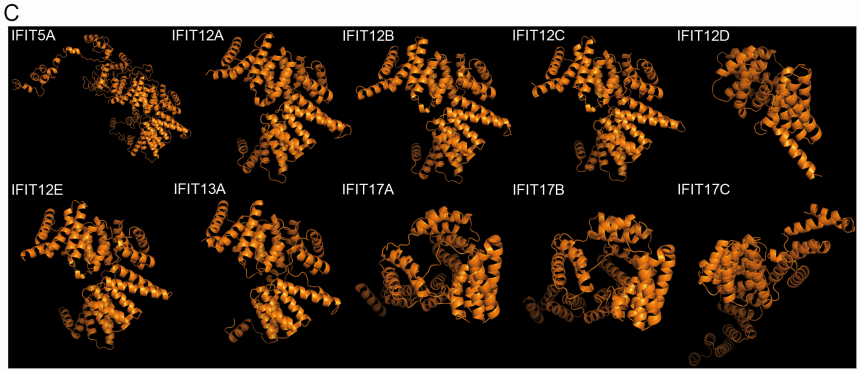

Figure 3.2. Sequence analysis and structural domain of the zebrafish IFITs. A. Tetratricopeptide repeat (TPR) motifs on the 10 IFIT proteins present in zebrafish. Orthologous proteins from human and mouse are shown for comparative purposes. B. Length, calculated molecular weight (kDa) and theoretical pI of the different zebrafish IFITs. C. 3D-structure of zebrafish IFITs, predicted using I-TASSER server, selecting the model with the best C-score and viewed using PyMOL.

The study of the domain structure revealed the presence of the characteristic TPR motifs in all the analyzed sequences (Figure 3.2A), but the number of these repeats was variable, ranging from two up to eleven repetitions. However, we also observed variability in the number and position of these characteristic domains in the four human genes and in the three IFITs described in mice (Figure 3.2A). The values of identity and similarity between zebrafish and human and murine proteins were lower than 37%

and 62%, respectively (Table S3.3). The number of amino acids varied between 302 and 483 residues for all sequences, except for isoform 5A, which presented a total of 1038 amino acids. Thus, differences in calculated molecular weights were also observed, whereas most of the proteins presented molecular weights ranging from 50–56 kDa, the 12D isoform was 34.92 kDa and IFIT5A was 120.29 kDa (Figure 3.2B). Regarding the theoretical isoelectric point (pI), the isoforms located on chromosomes 5, 12 and 17 presented values lower than 7.0, except 12A, whose pI value was 8.20. IFIT13A also showed a more basic pI value of 8.75 (Figure 3.2B).

We also examined the tridimensional structure of the IFITs and identified three different structural models (Figure 3.2C). The TM-scores observed for zebrafish IFITs revealed that human IFIT5 was the main analog protein for IFIT5A (TM-score = 0.448), IFIT12A (TM-score = 0.981), IFIT12B (TM-score = 0.966), IFIT 12C (TM-score = 0.951), IFIT12D (TM-score = 0.950), IFIT12E (TM-score = 0.969) and IFIT13A (TM-score = 0.952). However, human ISG54 or IFIT2 was the best analog for IFIT17A (TM-score = 0.947) and IFIT17B (TM-score = 0.943), and interestingly, the superhelical TPR-repeat domain of O-linked GlcNAc transferase was the template for the construction of the IFIT 17C 3D-structure (TM-score = 0.813).

Constitutive and tissue-specific expression of IFIT genes

The analysis of 8 different adult zebrafish tissues revealed a higher basal expression of *ifit* genes on chromosome 12, being *ifit12c* the gene with the largest presence in the whole of the tissues analyzed (spleen, kidney, gill, caudal fin and head). Interestingly, *ifits* with low expression in most of the tissues, showed significantly higher expression in the intestine (*12a*, *17a*, *17b*) or muscle (*13a*, *17c*) (Figure 3.3A).

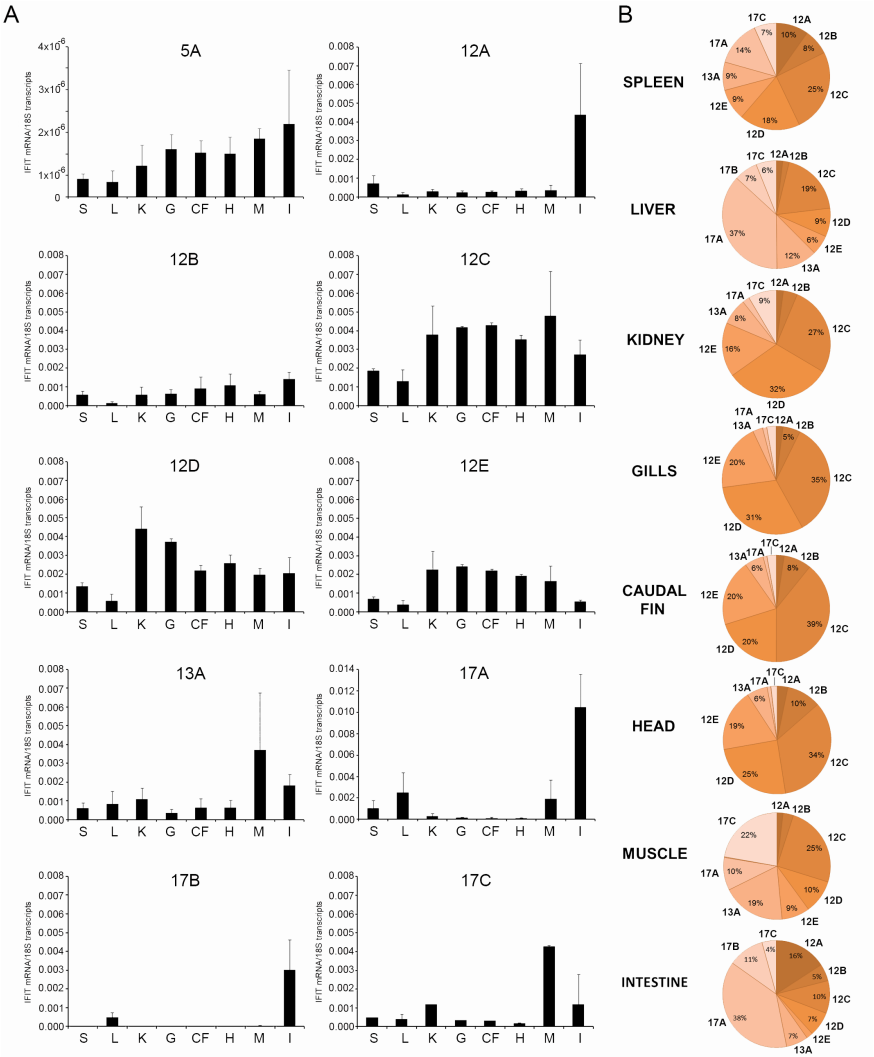

Figure 3.3. Tissue-specific expression of zebrafish *ifit* genes. A. Constitutive expression of IFIT genes in tissues of adult zebrafish (S: Spleen; L: Liver; K: Kidney; G: Gill; CF: Caudal fin; H: Head; M: Muscle; I: Intestine). For basal expression of each IFIT form, tissues were sampled and pooled, yielding a total of 4 pools of 5 fish per organ. The relative expression level of each gene, normalized to the expression level of the 18 S ribosomal RNA gene in the same tissue, was expressed as arbitrary units. The graphs represent the mean ± standard error of 4 independent samples. B. Relative proportion of the IFIT transcripts in different zebrafish tissues.

Regarding to the relative proportion of the *ifit* genes in the analyzed tissues, whereas in spleen, kidney, muscle, intestine and liver all the *ifits* were present, in gills *ifits* from chromosome 12 were predominant (Figure 3.3B).

The constitutive expression of *ifit* genes was also analyzed in ZF4 and kidney primary cells (Figure S3.1). ZF4 cells presented higher expression levels than kidney primary cell cultures. In addition, *ifits* from zebrafish chromosome 12 showed a higher basal expression in both cell types than those from chromosomes 5, 13 or 17, except for isoform *12b*, which showed lower expression in ZF4 cells.

Interferons induce the expression of *ifit* genes *in vitro*

First, we determined whether three selected zebrafish interferons (IFNΦ1, IFNΦ2 and IFNΦ3) induced the expression of zebrafish IFITs. Therefore, we analyzed the biological activity of recombinant zebrafish IFNsΦ. The activity of supernatant from HEK-293 cells transfected with plasmids containing IFNs sequences was first confirmed by a decrease in the viral titer of SVCV and the induction of *mxab* (isoforms a and b) expression in ZF4 and kidney primary cell culture, as shown in the Figure S3.2A and S3.2B.

The treatment of ZF4 cells and kidney cell cultures with interferons induced changes in the expression of *ifit* genes. Overall, the results showed higher expression values for all *ifit* genes in kidney cells than in ZF4 cells (Figure 3.4A and 3.4B). As expected, these results suggest a role of IFNs in the induction of zebrafish *ifits*. Moreover, the fact that *ifits* basal expression was higher in ZF4 than in primary cell cultures and that these cells showed a higher response to IFNs suggest a cell-specific response or mechanism.

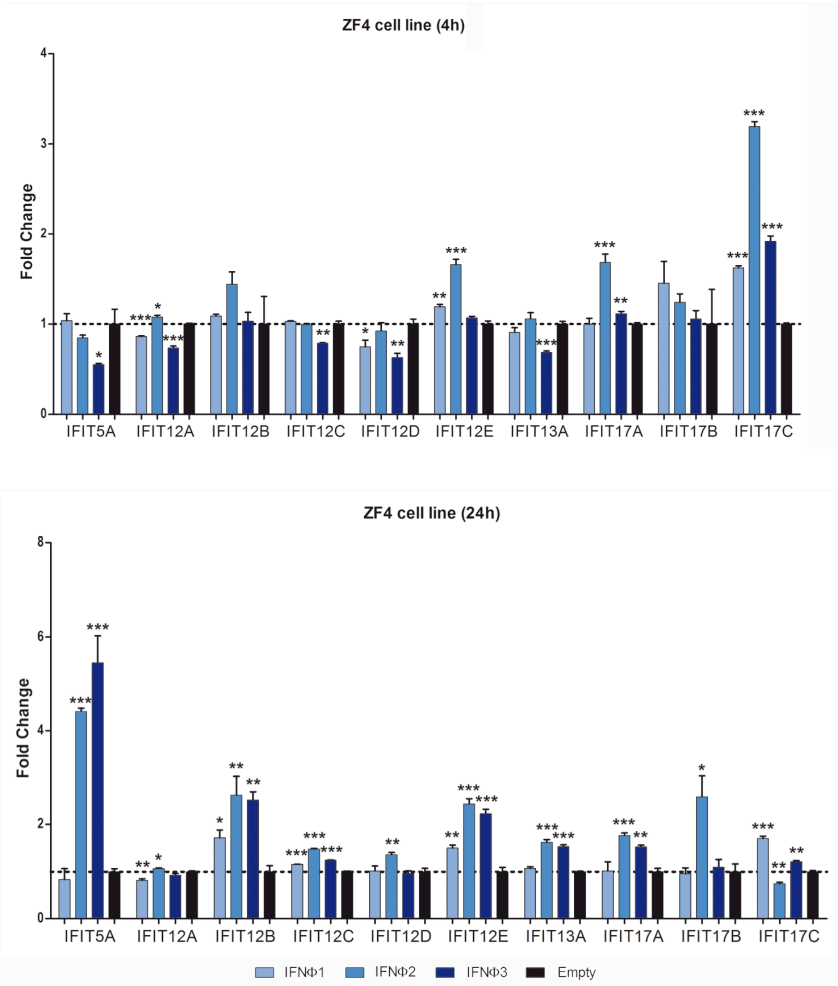

Figure 3.4. *In vitro* effect of IFNs on *ifits* expression in ZF4 cells. Expression levels of *ifit* genes in ZF4 cells after 4 and 24 hours of stimulation with supernatants from transfected HEK-293 cells with plasmids containing sequences for zf-IFNΦ1, zf-IFNΦ2 and zf-IFNΦ3. After 4 and 24 hours of stimulation, RNA was extracted and the cDNA was synthesized. Analysis of the gene expression was performed through real-time PCR, using 18S ribosomal RNA as a housekeeping gene. The expression level of each gene was expressed as fold-change with respect to the empty plasmid group. The data are represented as the mean ± standard error of three independent samples. Significant differences among cells transfected with IFNΦ plasmids and empty plasmid were displayed as ***(0.0001<p<0.001), **(0.001<p<0.01) or *(0.01<p<0.05).

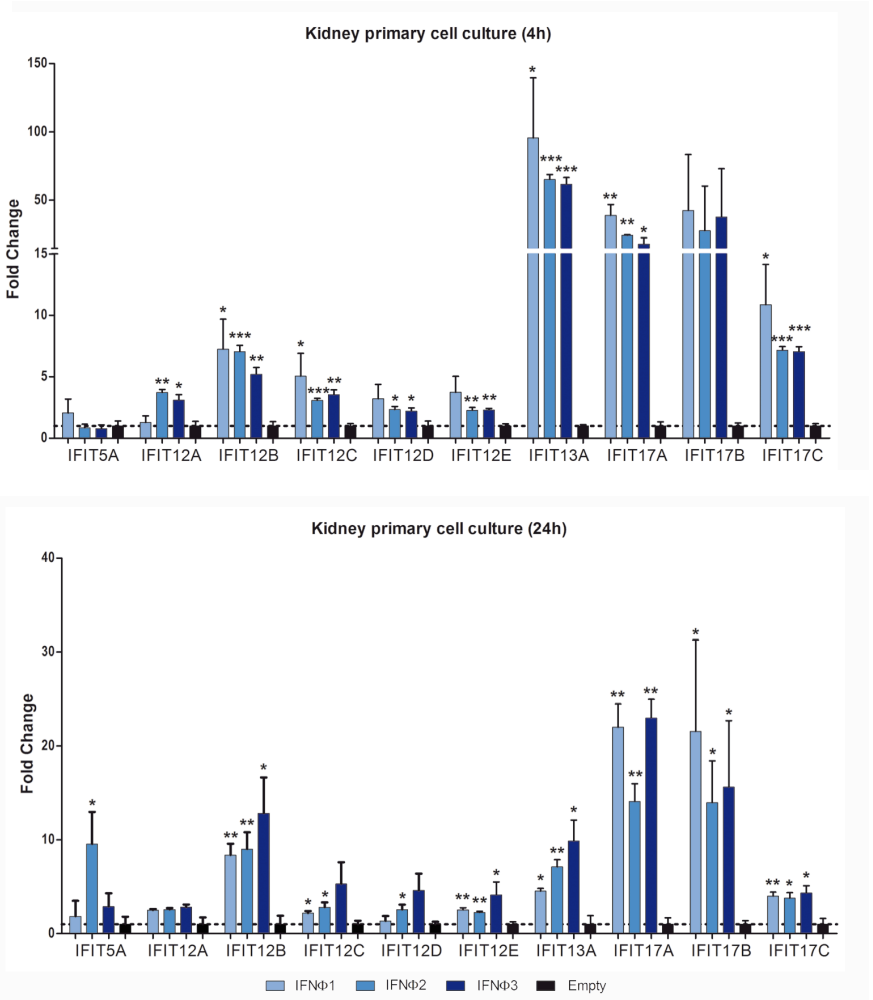

Figure 3.5. In vitro effect on IFNs on *ifits* expression in kidney primary cell cultures. Kidney primary cell cultures after 4 and 24 hours of stimulation with supernatants from transfected HEK-293 cells with plasmids containing sequences for zf-IFNΦ1, zf-IFNΦ2 and zf-IFNΦ3. After 4 and 24 hours of stimulation, RNA was extracted and the cDNA was synthesized. Analysis of the gene expression was performed through real-time PCR, using 18 S ribosomal RNA as a housekeeping gene. The expression level of each gene was expressed as fold-change with respect to the empty plasmid group. The data are represented as the mean ± standard error of three independent samples. Significant differences among cells transfected with IFNΦ plasmids and empty plasmid were displayed as ***(0.0001<p<0.001), **(0.001<p<0.01) or *(0.01<p<0.05).

In ZF4 cells, treatment with IFNs after 4 hours did not induce high levels of *ifits* expression, with the exception of *ifit17c*, which was significantly induced, regardless of the IFNΦ used. Interestingly, a significant down-regulation of isoforms *5a*, *12a*, *12c*, *12d* and *13a* was observed in cells treated with the IFNΦ3 (Figure 3.4). A higher number of isoforms was significantly induced at 24 hours compared with the results observed at 4 hours, and the *ifit* on chromosome 5 was the most induced through IFNΦ2 and IFNΦ3. The *ifits* on chromosome 12 (*12b*, *12c* and *12e*) were significantly induced, regardless of the IFNΦ used (Figure 3.4).

In primary cell culture, the *ifit* genes located on chromosomes 13 and 17 were more induced than those on chromosomes 5 and 12, and isoform *13a* showed the strongest induction at 4 hours (Figure 3.5). Regarding the effect of the different IFNsΦ, most of the *ifits* on chromosomes 12 and 13 were induced through IFNΦ2 and IFNΦ3 at 4 hours (Figure 3.5). Thus, in primary cell culture, only *ifit12b*, *ifit12c*, *ifit13a*, *ifit17a* and *ifit17c* were significantly induced through IFNΦ1 after 4 hours, whereas, after 24 hours, the significant induction of *12b*, *12c*, *12e*, *13a*, *17a*, *17b* and *17c* was observed.

Modulation of *ifits* expression upon viral challenge

Once we determined that zebrafish IFITs were modulated through interferons and showed different tissue expression profiles, we evaluated the effect of an *in vitro* viral infection on the expression of *ifits* in ZF4 and kidney primary cells. Surprisingly, SVCV did not modify the expression of the different *ifits* (with the exception of *ifit5a* in ZF4 and *ifit12b* in kidney cells that showed a slight expression increase) (Figure 3.6A). To determine whether this effect was induced through a direct effect of the virus on *ifits* expression or if the virus was affecting the interferon signaling

cascade, we measured the expression levels of *ifnφ1*, *2* and *3* and the interferon-induced protein *mxab* after *in vitro* infection. The results showed that *ifnφ1*, *2* and *3* and *mxab* were not induced in either ZF4 or kidney cells through a 24 hours *in vitro* infection (Figure 3.6B).

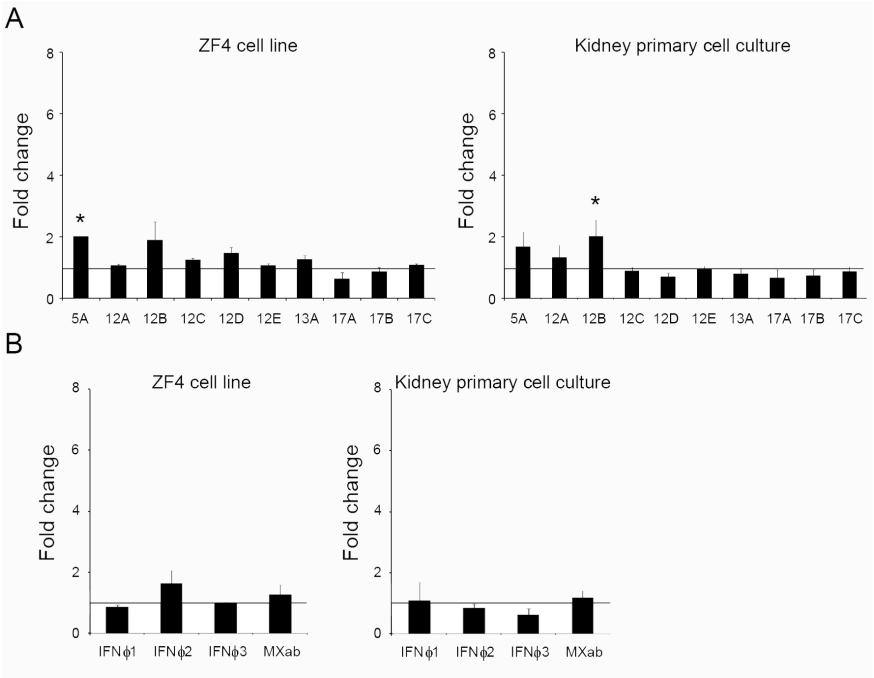

Figure 3.6. *In vitro* effect of viral infection in ZF4 cells and kidney primary cell cultures. A. Expression of *ifit* genes in ZF4 cells and kidney primary cell culture at 24 hours after infection with SVCV. B. *mxab* and *ifnφ1, 2* and *3* expression in ZF4 cells and kidney primary cell culture at 24 hours after infection with SVCV. After 24 hours of stimulation, the RNA was extracted, and the cDNA was synthesized. The analysis of gene expression was performed through real-time PCR, using 18 S ribosomal RNA as housekeeping gene. The expression level of each gene was expressed as fold-change with respect to the control group, non-infected cells. The data are shown as the mean ± error of three independent biological samples. Significant differences among infected and uninfected group were displayed as ***(0.0001<p<0.001), **(0.001<p<0.01) or *(0.01<p<0.05).

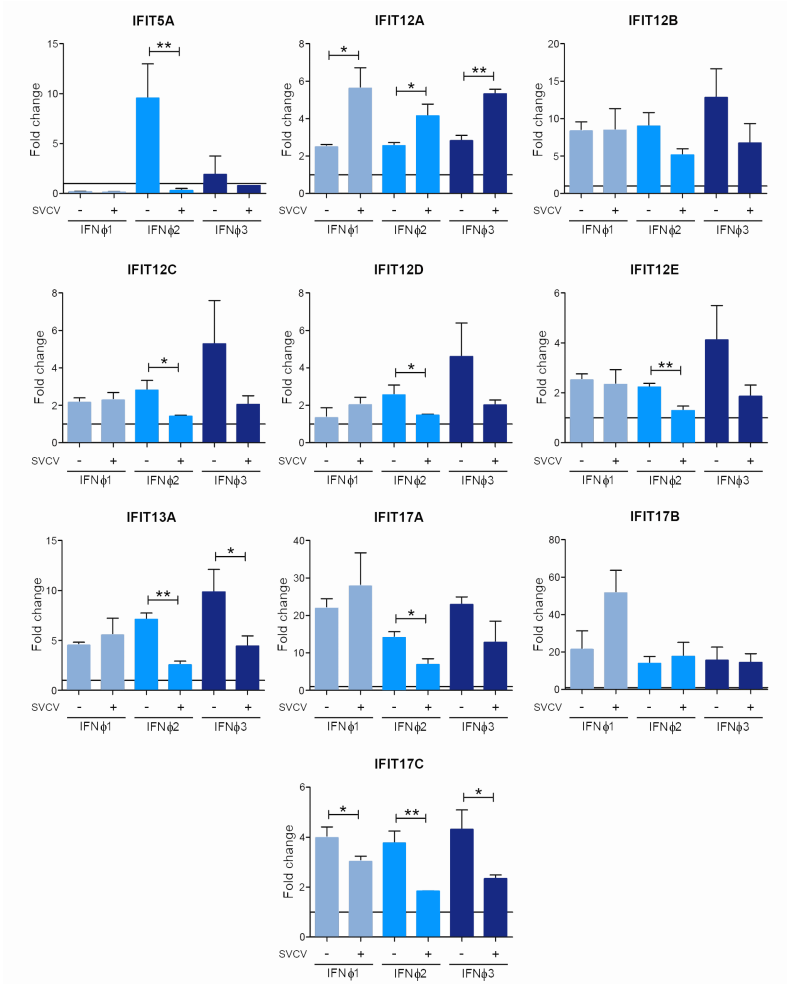

Figure 3.7. ***In vitro*** **effect of viral infection and IFN treatment in kidney primary cell cultures.** Expression level of *ifit* genes in kidney primary cell cultures after 24 hours of stimulation with supernatants from transfected HEK-293 cells with plasmids containing sequences for zf-IFNΦ1, zf-IFNΦ2 and zf-IFNΦ3 in combination with SVCV. After 24 hours of stimulation, the RNA was extracted, and the cDNA synthesized. The effect of the virus infection on the expression of IFITs induced by the different IFNs was represented as a fold-change with respect to the group stimulated with supernatant from cells transfected with the empty plasmid. The data are represented as the mean ± standard error of three independent samples. The asterisks denote significant differences between infected and non-infected groups. Significant differences were displayed as ***(0.0001<p<0.001), **(0.001<p<0.01) or *(0.01<p<0.05).

Next, we determined whether the IFNΦ-induced expression of *ifit* genes was also modulated through viral infection. Thus, the effect of the virus on kidney primary cells treated with the recombinant IFNsΦ was analyzed at 24 hours after infection (Figure 3.7). In general, the virus reduced the expression of interferon-induced *ifits*. However, the expression induced through recombinant IFNΦ1 did not show this clear decrease, and in the case of isoforms *12a*, an increment in expression was observed after viral infection. In addition, isoform *12a* was the only gene that experienced an up-modulation after stimulation with the three recombinant IFNsΦ and the infection with the virus (Figure 3.7).

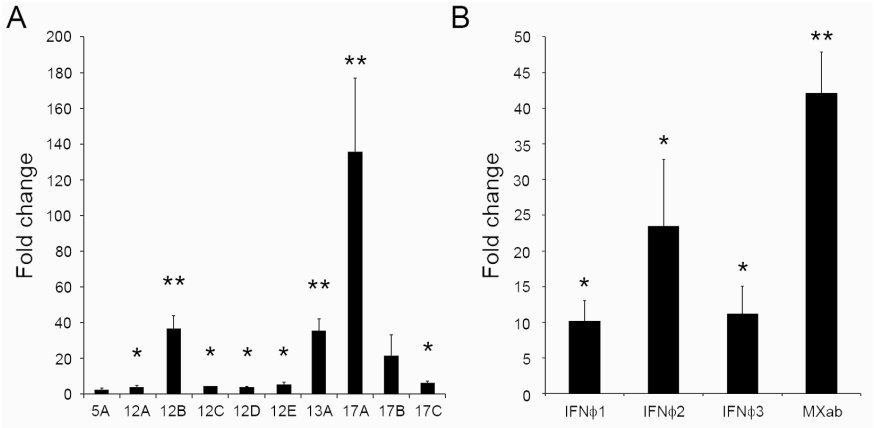

Figure 3.8. *In vivo* effect of viral infection on *ifns, mxab* and *ifit* genes expression in kidney. A. Expression of *ifit* genes in kidney cells from adult zebrafish at 24 hours after infection with SVCV. B. Expression of *ifns* and *mxab* in kidney cells from adult zebrafish at 24 hours after infection with SVCV. Adult individuals were injected intraperitoneally with 10 µl of SVCV (2.7×10^6 $TCID_{50}$/ml). RNA was isolated from head kidney cells, 24 hours post-infection. cDNA was obtained, and real-time PCR was performed using 18 S ribosomal RNA as a housekeeping gene. The expression level of each gene was expressed as fold-change with respect to the levels detected in the control group (injected with culture medium). The data are shown as the mean ± standard error of three individuals. The asterisks denote statistically significant differences with respect to the control group. Significant differences were displayed as ***(0.0001<p<0.001), **(0.001<p<0.01) or *(0.01<p<0.05).

To determine whether the trend of down-modulation of IFN-induced genes through SVCV infection also occurred *in vivo*, we examined *ifit* genes expression in kidney cells from adult animals injected with the virus. In this case, all the *ifits* showed an increase in expression after 24 hours (the increased expression of *5a* and *17b* were not statistically significant), and *17a* showed the highest fold change (Figure 3.8A). As expected, an up-regulation of all analyzed *ifnφs* was observed, being the expression of *ifnφ2* the highest detected. The interferon inducible gene *mxab* showed a statistically significant increase of 40 fold after the stimulation with SVCV (Figure 3.8B). These results denoted the different response to the virus after an *in vitro* or *in vivo* infection.

Evaluation of antiviral activity of *ifit* genes in zebrafish larvae

Next, we analyzed the *in vivo* antiviral activity of selected IFITs in zebrafish larvae previously microinjected with expression vectors containing either IFIT12B, 13A or 17A, followed by infection with SVCV. When zebrafish larvae were infected with SVCV (control group), the mortalities reached the maximum level at 36 hours after challenge, and only 10% of the animals survived the infection (Figure 3.9A). At this point, the percentages of survival in animals treated with expression vectors containing IFIT sequences were higher than those obtained in the control group. Animals treated with 12B, 13A and 17A showed a final % survival of 17.5, 22.5 and 40%, respectively. At 36 hours post-infection, significant differences in the survival were observed in animals treated with the three IFITs, whereas at 48 and 72 hours only the larvae treated with IFIT17A showed a significant increase in survival with respect to the control group.

The transcription of the SVCV N gene was also measured through qPCR at 9 h after infection to determine the effect of these IFITs on viral transcription. At this time point, only larvae injected with the IFIT17A plasmid showed a significant lower viral N gene transcription compared with the infected control group (Figure 3.9B).

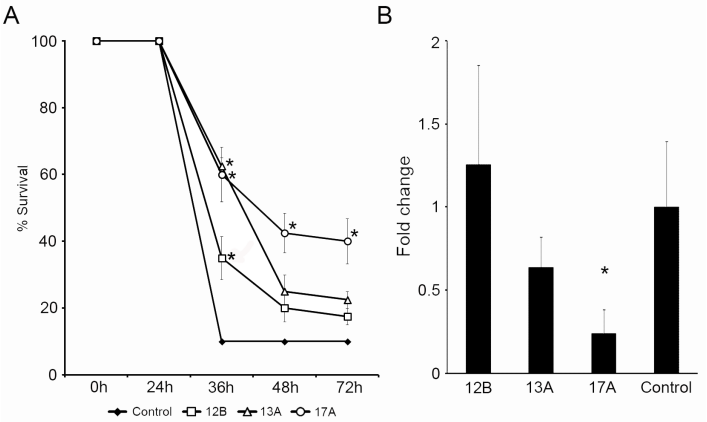

Figure 3.9. Antiviral activity of IFITs 12B, 13A and 17A in larvae infected with SVCV. A. Antiviral activity of selected IFITs was evaluated in zebrafish larvae. One-cell stage zebrafish embryos were microinjected with 100 pg/egg (final volume of 2 nl) of the recombinant plasmids pcDNA 3.1-IFIT12B, pcDNA 3.1-IFIT13A, pcDNA 3.1-IFIT17A as well as pcDNA 3.1-empty. Three days after plasmid administration, the larvae were microinjected in the duct of Cuvier with 2 nL of a SVCV suspension at a final concentration of 10^3 $TCID_{50}$/ml. The data are shown as the percentage of survival observed at 3 days after infection. Significant differences ($P \leq 0.05$) in the percentage of survival between larvae treated with the IFITs and the control group are indicated with asterisks. The results are represented as the mean ± standard error of four independent samples. B. The relative expression level of the viral N gene was analyzed through qPCR at 9 hours post-challenge. The raw data were normalized using the 18 S ribosomal RNA as a housekeeping gene. The results are presented as the mean ± standard error of three biological replicates. Significant differences were displayed as ***(0.0001<p<0.001), **(0.001<p<0.01) or *(0.01<p<0.05).

3.4. Discussion

IFITs are a novel IFN-stimulated gene family with antiviral properties not formally described in fish until a recent published work (Liu et al., 2013). Using genome synteny and sequence

comparison, we identified 10 sequences in the zebrafish genome with homology to human IFIT genes located in chromosome 10 (four genes and one pseudogene). With the exception of *ifit5a*, all zebrafish *ifit* genes presented similar length and conserved domains.

In contrast to humans, most of the *ifit* family genes in zebrafish are located in two chromosomes (12 and 17), similar to the structure observed in dogs (Fensterl and Sen, 2011; Zhou et al., 2013). Five *ifit* genes were clustered on chromosome 12, as previously described (Zhou et al., 2013; Liu et al., 2013), but our analysis also registered the presence of three *ifit* genes on chromosome 17, one gene on chromosome 13 and another additional gene on chromosome 5, in agreement with that recently reported (Liu et al., 2013). The *ifit* genes on chromosomes 5 and 13 did not conserve the synteny with vertebrate chromosomes, likely reflecting genomic translocations (Postlethwait et al., 2000; Woods et al., 2005). Genome duplication events are powerful drivers of evolution (Soukup, 1974; Ravi et al., 2013), as they provide opportunities for the modification or mutation of the gene duplicates, while critical functions are maintained through the other copies. The modified or mutated duplicated genes might acquire new functions or divide the original functions of the ancestral gene among different isoforms. The presence of different members of the *ifit* family genes in fish might facilitate the expansion of innate immune recognition or modulate innate and adaptive immune responses to specific challenges.

The analysis of Darwinian selection was conducted to quantify the selection pressures acting on *ifit* genes (Kimura, 1977; Yang and Bielawski, 2000), and the results showed that the genes located on chromosome 17 underwent positive Darwinian selection. This result, together with the phylogenetic analysis,

reflected the increased accumulation of evolutionary changes in these genes with respect to the other *ifit* genes. The accelerated evolution of the *ifit* genes on chromosome 17 might be associated with the direct interaction of these proteins with pathogenic viruses, as an elevated selective pressure and rapid evolution of immune-related genes, particularly those that directly interact with pathogens, was observed compared with non-immune genes (Sunyer and Lambris, 1998; Zhang et al., 1998; Vilches and Parham, 2002; Bustamante et al., 2005; Viertlboeck et al., 2005; Yu et al., 2006; Stein et al., 2007; Du Pasquier et al., 2009; Fernandes et al., 2010; Boudinot et al., 2011).

Phylogenetic analysis confirmed that mammal IFITs are clustered in a main group comprising the four IFIT genes previously described (Fensterl and Sen, 2011; Zhou et al., 2013). The sequences from other vertebrates constituted different clusters, depending on the class (amphibians, birds or bony fish), as previously reported (Zhou et al., 2013) however, the construction of an internal classification of the *ifit* genes in fish is difficult due to the scarce information available in public databases for other fish species. A deeper analysis of this gene family for organisms belonging to different taxa would help elucidate the evolutionary process involved.

The functional activity of the novel IFIT family described in zebrafish was explored using *in vitro* and *in vivo* experimental models. Most mammalian cell types do not express IFIT genes under basal conditions (Daffis et al., 2007; Diamond and Farzan, 2013); however, we observed a constitutive expression of the *ifits* particularly the genes located on chromosome 12. In addition, the distribution of the ten different *ifit* transcripts in zebrafish displayed distinct patterns of preferential expression at tissue level, and revealed an extremely higher functional complexity than that previously reported in mice (Terenzi et al., 2007; Wacher et

al., 2007; Fensterl et al., 2008; Fensterl and Sen, 2011). Constitutively expressed genes, such as *12c*, *12d* and *12e*, were present in all tissues, but the low expression of other genes, such as *12b*, *13a* and *17a*, might suggest they are inducible genes. Moreover, the high expression levels observed in the intestine might suggest a specific function for *ifit12a*, *17a* and *17b* in this tissue. Indeed, the *ifits* on chromosome 17 are primarily expressed in the liver and intestine. These results suggest that *ifit* genes might have non-redundant antiviral functions, as previously suggested in mice (Terenzi et al., 2007; Wacher et al., 2007), reflecting the differentiation and subsequent specialization of the members, potentially facilitated through the gene expansion observed in fish.

The expression of *ifit* genes was analyzed in kidney primary cell cultures and in ZF4 cells in response to an IFNsΦ treatment. Recombinant zebrafish IFNsΦ (1, 2 and 3) significantly reduced the viral titer in ZF4 cells infected with SVCV, as previously reported (López-Muñoz et al., 2009), and induced a rapid and high expression of the interferon-inducible *mxab* genes in kidney primary cell cultures and ZF4 cells, as described in other fish models. Interestingly, the IFNsΦ from group II (IFNΦ2 and 3) showed higher antiviral activity and induction of the *mxab* genes than that observed for IFNsΦ from group I (IFNΦ1). This differential antiviral activity observed between IFNs from group I (IFNΦ1) and group II (IFNΦ2 and 3) could reflect the induction of several response pathways, as these molecules do not bind the same receptor complexes (Aggad et al., 2009). The treatment of cells with IFNsΦ also induced a rapid increase in *ifit* genes expression in kidney cells (mainly IFIT13A and 17s) consistent with previous studies (Zhou et al., 2013). The modulation of *ifit* genes in ZF4 cells was much lower than that observed in kidney cells most likely because ZF4 is not an immune cell line (Driever and Rangini,

1993), and the effect of IFN stimulation was not comparable with the effect observed in specific immune cells presented in kidney primary cell cultures and the hematopoietic tissues of the fish.

During evolution, some viruses have evolved sophisticated mechanisms to avoid the host innate immune system. In particular, some rhabdoviruses, such as human virus VSV (vesicular stomatitis virus) or RV (rabies virus), have developed counteractions to both IFN induction and IFN signaling (Rieder and Conzelmann, 2009). These viruses have different mechanisms for antagonizing the type I interferon response and blocking the induction of antiviral molecules; however, in both cases, the objective is the evasion of the host immune defense (Faul et al., 2009). In fish, the matrix protein of the novirhabdovirus, IHNV (Infectious hematopoietic necrosis virus), affects host cellular gene expression to inhibit the transcription of immune-related genes (Chiou et al., 2000); however, little is known about how this effect is orchestrated.

ZF4 cells and kidney primary cell cultures infected with SVCV did not show a typical anti-viral response upon *ifn* gene induction and the increased expression of *isgs*, such as *mx* or *ifits* (Randall and Goodbourn, 2008; Sadler and Williams, 2008). The blocking of the interferon system suggests that the virus suppresses the immune response in primary cell cultures.This response was also investigated when kidney cells were forced to mount an antiviral response through the stimulation with recombinant IFNsΦ and also were infected with the virus SVCV. In this case, the *ifits* expression pattern was modulated, as described in human hepatocytes infected with hepatitis C virus (Raychoudhuri et al., 2011). Kidney cells treated with IFNΦ2 and 3 showed the reduced expression of almost all *ifit* genes (*ifit12a* made the difference), whereas cells treated with IFNΦ1 only showed the down modulation of *ifit17c* after viral infection. This result could indicate that the virus avoids the host defense system

and suppresses the expression of a specific subset of *ifit* genes for the establishment of infection. The viral-mediated inhibition of the IFN system has been previously described (Samuel and Diamond, 2006; García-Sastre, 2011; Raychoudhuri et al., 2011). The response pattern observed in cells treated with IFNΦ1 after SVCV infection might reflect different signaling pathways between cells stimulated with IFNsΦ from groups I and II. Importantly, *ifit12a* was the only gene whose expression was synergistically induced through all interferons and in response to virus infection. The different behavior after *in vitro* stimulation together with the tissue-specific expression of *ifits* genes suggests the expansion and differential functions of these genes.

However, when viral infection is conducted *in vivo*, after intraperitoneal infection, a clear up-regulation of the expression of *ifns* and ISGs, including *mxab* and *ifits*, was observed. The overall immunity of the host is required to orchestrate the effective control of viral infections, and the absence of a complete response often results in fatal infections (Samuel and Diamond, 2006). Both ZF4 cells and primary cell head kidney leukocyte cultures exhibited limited defense against viral infections because of the incomplete host machinery and these models are, therefore, easily manipulated by SVCV. These cells respond to IFN stimulus but are unable to mount an effective response against virus.

The most induced *ifits* after *in vivo* infection, *12b*, *13a* and *17a*, were selected to confirm direct antiviral activity. The microinjection of zebrafish eggs at one-cell stage with expression plasmids encoding these genes induced a significant reduction in mortality after SVCV infection, highlighting the antiviral role that these proteins might play in non-mammalian species. In mammals, there is evidence implicating these proteins in the restriction of translation initiation through interactions with the translation initiation factor eIF-3 (Guo et al., 2000a; Guo et al., 2000b; Hui et

al., 2003; Wang et al., 2003; Terenzi et al., 2007). Moreover, IFITs are able to sequester viral proteins, such as human papillomavirus helicase E1 (Terenzi et al., 2008) and inhibit virus replication through the direct binding and sequestering of viral nucleic acids (Daffis et al., 2010; Pichlmair et al., 2010; Yang et al., 2012; Abbas et al., 2013; Katibah et al., 2013) . However, it remains unknown whether the same mechanisms are also present in fish. We can confirm that the present results provide the basis for multiple future research studies concerning not only the protection of fish (particularly aquacultured species) against virus infections but also the investigation of the basic aspects of IFITs biology, which could be studied in zebrafish, an attractive model organism with numerous experimental advantages.

3.5. References

Abbas YM, Pichlmair A, Górna MW, Superti-Furga G, Nagar B (2013) Structural basis for viral 5'-PPP-RNA recognition by human IFIT proteins. Nature 494:60-64.

Aggad D, Mazel M, Boudinot P, Mogensen KE, Hamming OJ, Hartmann R, Kotenko S, Herbomel P, Lutfalla G, Levraud JP (2009) The two groups of zebrafish virus-induced interferons signal via distinct receptors with specific and shared chains. J Immunol 183:3924–3931.

Akaike H (1974) A new look at the statistical model identification. EEE Trans. Automatic Control Ac-19:716-724.

Anisimova M and Gascuel O (2006) Approximate Likelihood-Ratio Test for Branches: A Fast, Accurate, and Powerful Alternative. Syst Biol 55:539–552.

Belanger SE, Balon EK, Rawlings JM (2010) Saltatory ontogeny of fishes and sensitive early life stages for ecotoxicology tests. Aquat. Toxicol 97:88-95.

Berchtold S, Manncke B, Klenk J, Geisel J, Autenrieth IB, Bohn E (2008) Forced IFIT-2 expression represses LPS induced TNF-alpha expression at posttranscriptional levels. BMC Immunol 9:75.

Boudinot P, van der Aa LM, Jouneau L, Du Pasquier L, Pontarotti P, Briolat V, Benmansour A, Levraud JP (2011) Origin and Evolution of TRIM Proteins: New Insights from the Complete TRIM Repertoire of Zebrafish and Pufferfish. PLoS ONE 6:e22022.

Bustamante CD, Fledel-Alon A, Williamson S, Nielsen R, Hubisz MT, Glanowski S, Tanenbaum DM, White TJ, Sninsky JJ, Hernandez RD, Civello D, Adams MD, Cargill M, Clark AG (2005) Natural selection on protein-coding genes in the human genome. Nature 437:1153–1157.

Campanella JJ, Bitincka L, Smalley J (2003) MatGAT: an application that generates similarity/identity matrices using protein or DNA sequences. BMC Bioinform 4:29.

Chiou PP, Kim CH, Ormonde P, Leong JA (2000) Infectious hematopoietic necrosis virus matrix protein inhibits host-directed gene expression and induces morphological changes of apoptosis in cell cultures. J Virol 74:7619-7627.

D'Andrea LD and Regan L (2003) TPR proteins: the versatile helix. Trends Biochem Sci 28:655–662.

Daffis S, Samuel MA, Keller BC, Gale MJ, Diamond MS (2007) Cell-specific IRF-3 responses protect against West Nile virus infection by interferon-dependent and -independent mechanisms. PLoS Pathog 3:e106.

Daffis S, Szretter KJ, Schriewer J, Li J, Youn S, Errett J, Lin TY, Schneller S, Zust R, Dong H, Thiel V, Sen GC, Fensterl V, Klimstra WB, Pierson TC, Buller RM, Gale M Jr, Shi PY, Diamond MS (2010) 2'-O methylation of the viral mRNA cap evades host restriction by IFIT family members. Nature 468:452–456.

Darriba D, Taboada G, Doallo R, Posada D (2011) ProtTest 3: fast selection of best-fit models of protein evolution. Bioinformatics 27:1164-1165.

Diamond MS and Farzan M (2013) The broad-spectrum antiviral functions of IFIT and IFITM proteins. Nat Rev Immunol 13:46-57.

Díaz-Rosales P, Romero A, Balseiro P, Dios S, Novoa B, Figueras A (2012) Microarray-based identification of differentially expressed genes in families of turbot (Scophthalmus maximus) after infection with viral haemorrhagic septicaemia virus (VHSV). Mar Biotechnol 14:515-529.

Driever W and Rangini Z (1993) Characterization of a cell line derived from zebrafish (Brachydanio rerio) embryos. In Vitro Cell Dev Biol Anim 29A:749-754.

Du Pasquier L, Wilson M, Sammut B (2009) The fate of duplicated immunity genes in the dodecaploid Xenopus ruwenzoriensis. Front Biosci 14:177-191.

Faul EJ, Douglas SL, Schnell MJ (2009) Interferon response and viral evasion by members of the family Rhabdoviridae. Viruses 1:832-851.

Fensterl V and Sen GC (2011) The ISG56/IFIT1 gene family. J Interferon Cytokine Res 31:71-78.

Fensterl V, Wetzel JL, Ramachandran S, Ogino T, Stohlman SA, Bergmann CC, Diamond MS, Virgin HW, Sen GC (2012) Interferon-induced Ifit2/ISG54 protects mice from lethal VSV neuropathogenesis. PLoS Pathog 8:e1002712.

Fensterl V, White CL, Yamashita M, Sen GC (2008) Novel characteristics of the function and induction of murine p56 family proteins. J Virol 82:11045–11053.

Fernandes JMO, Ruangsri J, Kiron V (2010) Atlantic cod piscidin and its diversification through positive selection. PloS One 5:e9501.

García MA, Gil J, Ventoso I, Guerra S, Domingo E, Rivas C, Esteban M (2006) Impact of protein kinase PKR in cell biology: from antiviral to antiproliferative action. Microbiol Mol Biol Rev 70:1032–1060.

García-Sastre A (2011) Induction and evasion of type I interferon responses by influenza viruses. Virus Res 162:12-18.

Graham FL, Smiley J, Russell WC, Nairn R (1977) Characteristics of a human cell line transformed by DNA from human adenovirus type 5. J Gen Virol 36:59-74.

Guindon S, Dufayard JF, Lefort V, Anisimova M, Hordijk W, Gascuel O (2010) New algorithms and methods to estimate maximum-likelihood phylogenies: assessing the performance of PhyML 3.0. Syst Biol 59:307–321.

Guo J, Hui DJ, Merrick WC, Sen GC (2000a) A new pathway of translational regulation mediated by eukaryotic initiation factor 3. EMBO J 19:6891–6899.

Guo J, Peters KL, Sen GC (2000b) Induction of the human protein P56 by interferon, double-stranded RNA, or virus infection. Virology 267:209–219.

Haller O, Staeheli P, Kochs G (2007) Interferon-induced Mx proteins in antiviral host defense. Biochimie 89:812–818.

Hui DJ, Bhasker CR, Merrick WC, Sen GC (2003) Viral stress-inducible protein p56 inhibits translation by blocking the interaction of eIF3 with the ternary complex eIF2.GTP.Met-tRNAi. J Biol Chem 278:39477-39482.

Karpenahalli MR, Lupas AN, Söding J (2007) TPRpred: a tool for prediction of TPR-, PPR- and SEL1-like repeats from protein sequences. BMC Bioinformatics 8:2.

Katibah GE, Lee HJ, Huizar JP, Vogan JM, Alber T, Collins K (2013) tRNA binding, structure, and localization of the human interferon-induced protein IFIT5. Mol Cell 49:743-750.

Katoh K, Kuma K, Toh T, Miyata T (2005) MAFFT version 5: improvement in accuracy of multiple sequence alignment. Nucleic Acids Res 33:511-518.

Kawai T and Akira S (2008) Toll-like Receptor and RIG-1-like Receptor Signaling. Ann NY Acad Sci 1143:1–20.

Kimura, M (1977) Preponderance of synonymous changes as evidence for the neutral theory of molecular evolution. Nature 267:275–276.

Kylaniemi MK, Haveri A, Vuola JM, Puolakkainen M, Lahesmaa R (2009) Gene expression signatures characterizing the development of lymphocyte response during experimental Chlamydia pneumoniae infection. Microb Pathog 46:235-242.

Liu Y, Zhang YB, Liu TK, Gui JF (2013) Lineage-specific expansion of IFIT gene family: an insight into coevolution with IFN gene family. PLoS One 8:e66859.

López-Muñoz A, Roca FJ, Meseguer J, Mulero V (2009) New insights into the evolution of IFNs: zebrafish group II IFNs induce a rapid and transient expression of IFN-dependent genes and display powerful antiviral activities. J Immunol 182:3440-3449.

Martens S and Howard J (2006) The interferon-inducible GTPases. Annu Rev Cell Dev Biol 22:559–589.

McCurley AT and Callard GV (2008) Characterization of housekeeping genes in zebrafish: male-female differences and effects of tissue type, developmental stage and chemical treatment. BMC Mol Biol 9:102.

Nusslein-Volhard C and Dahm R (2002) Zebrafish, a practical approach. Oxford University Press, Oxford.

Ovstebo R, Olstad OK, Brusletto B, Moller AS, Aase A, Haug KB, Brandtzaeg P, Kierulf P (2008) Identification of genes particularly sensitive to lipopolysaccharide (LPS) in human monocytes induced by wild-type versus LPS-deficient Neisseria meningitidis strains. Infect Immun 76:2685-2695.

Pfalffl MW (2001) A new mathematical model for relative quantification in real-time RT-PCR. Nucleic Acids Res 29:2002-2007.

Pichlmair A, Lassnig C, Eberle CA, Górna MW, Baumann CL, Burkerd TR, Bürckstümmer T, Stefanovic A, Krieger S, Bennett KL, Tülicke T, Weber F, Colinge J, Müller M, Superti-Furga G (2011) IFIT1 is an antiviral protein that recognizes 5'-triphosphate RNA. Nat Immunol 12:624-630.

Postlethwait JH, Woods IG, Ngo-Hazelett P, Yan YL, Kelly PD, Chu F, Huang H, Hill-Force A, Talbot WS (2000) Zebrafish comparative genomics and the origins of vertebrate chromosomes. Genome Res 10:1890–1902.

Randall RE and Goodbourn S (2008) Interferons and viruses: an interplay between induction, signalling, antiviral responses and virus countermeasures. J Gen Virol 89:1-47.

Rathi AV, Cantalupo PG, Sarkar SN, Pipas JM (2010) Induction of interferon-stimulated genes by Simian virus 40 T antigens. Virol 406:202–211.

Ravi V, Bhatia S, Gautier P, Loosli F, Tay BH, Tay A, Murdoch E, Coutinho P, van Heyningen V, Brenner S, Venkatesh B, Kleinjan DA (2013) Sequencing of Pax6 loci from the elephant shark reveals a family of Pax6 genes in vertebrate genomes, forged by ancient duplications and divergences. PLoS Genet 9:e1003177.

Raychoudhuri A, Shrivastava S, Steele R, Kim H, Ray R, Ray RB (2011) ISG56 and IFITM1 proteins inhibit hepatitis C virus replication. J Virol 85:12881-12889.

Reed LJ and Muench H (1938) A simple method of estimating fifty percent endpoints. Am J Hyg 27:493–497.

Rieder M and Conzelmann KK (2009) Rhabdovirus evasion of the interferon system. J Interferon Cytokine Res 29:499-509.

Robertsen B (2006) The interferon system of teleost fish. Fish Shellfish Immunol 20:172-191.

Roy A, Kucukural A, Zhang Y (2010) I-TASSER: a unified platform for automated protein structure and function prediction. Nat Protoc 5:725-738.

Rozen S and Skaletsky H (2000) Primer3 on the WWW for general users and for biologist programmers. Methods Mol Biol 132:365-386.

Sadler AJ and Williams BR (2008) Interferon-inducible antiviral effectors. Nat Rev Immunol 8:559-568.

Saha S and Rangarajan PN (2003) Common host genes are activated in mouse brain by Japanese encephalitis and rabies viruses. J Gen Virol 84:1729–1735.

Samuel MA and Diamond MS (2006) Pathogenesis of West Nile Virus Infection: a Balance between Virulence, Innate and Adaptive Immunity, and Viral Evasion. J Virol 80:9349-9360.

Schoggins JW and Rice CM (2011) Interferon-stimulated genes and their antiviral effector functions. Curr Opin Virol 6:519-525.

Soukup SW (1974) Evolution by gene duplication. S. Ohno, ed. Springer-Verlag, New York. 160 pp. Teratology, 9:250–251.

Stein C, Caccamo M, Laird G, Leptin M (2007) Conservation and divergence of gene families encoding components of innate immune response system in zebrafish. Genome Biol 8:R251.

Sunyer JO and Lambris JD (1998) Evolution and diversity of the complement system of poikilothermic vertebrates. Immunol Rev 166:39-57.

Talavera G and Castresana J (2007) Improvement of phylogenies after removing divergent and ambiguously aligned blocks from protein sequence alignments. Syst Biol 56:564–577.

Terenzi F, Saikia P, Sen GC (2008) Interferon-inducible protein, P56, inhibits HPV DNA replication by binding to the viral protein E1. EMBO J 27:3311-3321.

Terenzi F, White C, Pal S, Williams BR, Sen GC (2007) Tissue specific and inducer-specific differential induction of ISG56 and ISG54 in mice. J Virol 81:8656–8665.

Verrier ER, Langevin C, Benmansour A, Boudinot P (2011) Early antiviral response and virus-induced genes in fish. Dev Comp Immunol 35:1204–1214.

Viertlboeck BC, Habermann FA, Schmitt R, Groenen MA, Du Pasquier L, Göbel TW (2005) The chicken leukocyte receptor complex: a highly diverse multigene family encoding at least six structurally distinct receptor types. J Immunol 175:385–393.

Vilches C and Parham P (2002) KIR: diverse, rapidly evolving receptors of innate and adaptative immunity. Annu Rev Immunol 20:217-251.

Wacher C, Müller M, Hofer MJ, Getts DR, Zabaras R, Ousman SS, Terenzi F, Sen GC, King NJ, Campbell IL (2007) Coordinated regulation and widespread cellular expression of interferon-stimulated genes (ISG) ISG-49, ISG-54, and ISG-56 in the central nervous system after infection with distinct viruses. J Virol 81:860-871.

Wang C, Pflugheber J, Sumpter RJ, Sodora DL, Hui D, Sen GC, Cale M Jr (2003) Alpha interferon induces distinct translational control programs to suppress hepatitis C virus RNA replication. J Virol 77:3898-3912.

Westerfield M (2000) The zebrafish book. A guide for the laboratory use of zebrafish (Danio rerio), 4th ed. University of Oregon Press, Eugene.

Woods IG, Wilson C, Friedlander B, Chang P, Reyes DK, Nix R, Kelly PD, Chu F, Postlethwait JH, Talbot WS (2005) The zebrafish gene map defines ancestral vertebrate chromosomes. Genome Res 15:1307-1314.

Yang Z (2007) PAML 4: phylogenetic analysis by maximum likelihood. Mol Biol Evol 24:1586-1591.

Yang Z and Bielawski JP (2000) Statistical methods for detecting molecular adaptation. Trends Ecol Evol 15:496–503.

Yang Z, Liang H, Zhou Q, Li Y, Chen H, Ye W, Chen D, Fleming J, Shu H, Liu Y (2012) Crystal structure of ISG54 reveals a novel RNA binding structure and potential functional mechanisms. Cell Res 22:1328-1338.

Yu XJ, Zheng HK, Wang J, Wang W, Su B (2006) Detecting lineage-specific adaptive evolution of brain-expressed genes in human using rhesus macaque as outgroup. Genomic 88:745–751.

Zhang J, Rosenberg HF, Nei M (1998) Positive Darwinian selection after gene duplication in primate ribonuclease genes. Proc Natl Acad Sci USA 95:3708-3713.

Zhou X, Michal JJ, Zhang L, Ding B, Lunney JK, Liu B, Jiang Z (2013) Interferon induced IFIT family genes in host antiviral defense. Int J Biol Sci 9:200–208.

Zhu H, Cong JP, Shenk T (1997) Use of differential display analysis to assess the effect of human cytomegalovirus infection on the accumulation of cellular RNAs: induction of interferon-responsive RNAs. Proc Natl Acad Sci USA 94:13985–13990.

Zou J and Secombes CJ (2011) Teleost fish interferons and their role in immunity. Dev Comp Immunol 35:1376-1387.

Zou J, Tafalla C, Truckle J, Secombes CJ (2007) Identification of a second group of type I IFNs in fish sheds light on IFN evolution in vertebrates. J Immunol 179:3859-3871.

3.6. Supporting information

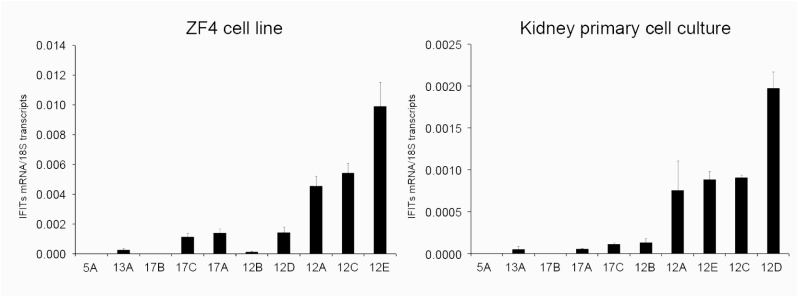

Figure S3.1. Constitutive expression of *ifit* genes in ZF4 cells and in kidney primary cell cultures. The basal expression of the different *ifit* genes was analyzed through real-time PCR in ZF4 cells and in leukocyte primary cell cultures from kidney. The relative expression level of the genes was normalized using the 18 S ribosomal RNA as a housekeeping gene. The graphs represent the mean ± standard error of three independent samples.

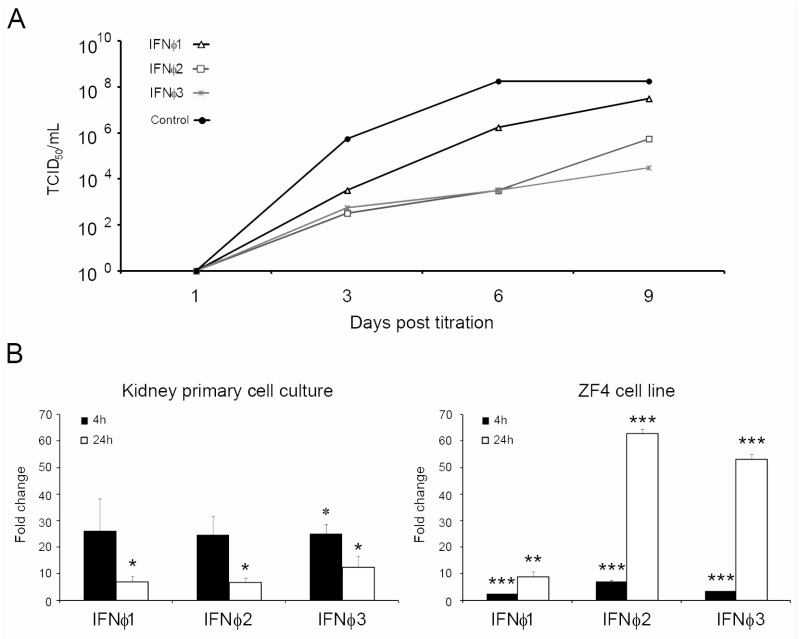

Figure S3.2. Biological activity of recombinant zebrafish IFNs. A. The biological activity of the supernatants from HEK-293 cells transfected with the expression plasmids of zf-IFNΦ1, zf-IFNΦ2 and zf-IFNΦ3 was measured in ZF4 cells dispensed in 96-well plates, treated for 2 h at 26°C with 100 µl of the supernatant containing one of the three different recombinant zf-IFNsΦ. After incubation, the spring viraemia of carp virus (SVCV) was titered. Supernatants obtained from HEK-293 cells transfected with an empty plasmid were used as control. The treatment of ZF4 cells with supernatants containing IFNΦ1, IFNΦ2 or IFNΦ3 induced a significant reduction of the viral titer (the infected cells treated with IFNΦ3 were those that showed the lowest viral titer. B. The treatment with the different zf-IFNsΦ induced a significant increase in *mxab* expression in both cell types at 4 and 24 hours. The results are represented as the mean ± standard error of three independent samples. The asterisk denotes significant differences with respect to the control cells (treated with supernatants obtained from HEK-293 cells transfected with the empty plasmid). Significant differences were displayed as ***(0.0001<p<0.001), **(0.001<p<0.01) or *(0.01<p<0.05).

Table S3.1. Sequence of specific primers designed for ORF confirmation, qPCR experiments and expression vector construction.

ORF confirmation		
Primer Name	**Primer sequence (5´→3´)**	**Amplicon(bp)**
IFIT5aF	ATGAGTCTTGACACCTTAAG	3130
IFIT5aR	TCACTGATTGCCCTTCATTTC	
IFIT12aF	ATGGGAAGTACAGACATGGA	1425
IFIT12aR	TTAAAATTCAAGTCTCTTCG	
IFIT12bF	ATGACTTCAGATGTTTCCAG	1449
IFIT12bR	TTACAGTAAAGACAGTCTGA	
IFIT12cF	ATGTCAGAGCAGAGTTACAG	1452
IFIT12cR	TTATATTTTACAGTTGATCTC	
IFIT12dF	ATGATGTCAGAAATAAGTTT	1406
IFIT12dR	CTAAAAGATTGTGGAGGCAT	
IFIT12eF	ATGAGTTTAATTCAGGCCAG	1416
IFIT12eR	TTACAAAGACATAACCTCAAG	
IFIT13aF	ATGTCAGAGGAAAATCTCAA	1290
IFIT13aR	TCAATCATCTTTGTTTGTTG	
IFIT17aF	ATGGATTCTTTACTGAAAG	1302
IFIT17aR	TTACTCCTCTTTGAGAACAT	
IFIT17bF	ATGAATTCTTTACTGAAAAG	1290
IFIT17bR	TCATTTCTGAGTTGTCTTGA	
IFIT17cF	ATGCAAGACATTGAGCCACA	1329
IFIT17cR	TTAATCAGAACTCACGAGTC	
qPCR		
Primer Name	**Primer sequence (5´→3´)**	**Amplicon(bp)**
IFIT5aF	AGCCGCCCAGTTAAAGGT	106
IFIT5aR	GGCATCATCCTTCTCACCTAAC	
IFIT12aF	ATCTTCAAAAGGCTGAATCAGC	177
IFIT12aR	AGTAAACGGATGAACCCGGT	
IFIT12bF	GCCCGAGGATCAAGAGTTC	79
IFIT12bR	AGGAGGTTGTCAGGCTGGT	
IFIT12cF	GATAGAGCTGTGGAGGCTT	122
IFIT12cR	TCAGTGCGAAATGGATTCAG	
IFIT12dF	GCCTACTATAGATTCACCTGT	80
IFIT12dR	GGACTCTCAGAGCATCATCA	
IFIT12eF	CCCACCACCTTGTACTGTGG	148
IFIT12eR	CAATTGCTCGGACTCGTTC	
IFIT13aF	AGCTCTTCAGCAAGCCTGAC	88
IFIT13aR	GAGCCCAGCCTGTACAATTT	
IFIT17aF	CACTGCAAACTTGGTTGGTC	94
IFIT17aR	TTCCCGAACCCTTTGTACC	
IFIT17bF	GAAGAATTGTCTCCTGACAAGT	123
IFIT17bR	ATCACCTGGGGTTTTCACTC	
IFIT17cF	GGAAATGACAGGTCGCAGA	68
IFIT17cR	GGTCTCGGCCTCTGCTAATA	

Table S3.1 (cont.) Sequence of specific primers designed for ORF confirmation, qPCR experiments and vector expression construction.

qPCR		
Primer Name	**Primer sequence (5´→3´)**	**Amplicon(bp)**
MXabF	CGCTGTCAGGAGTTCCGTTAC	149
MXabR	TTCCGCTGGGTCATCAAAGT	
IFNphi1F	GAGCACATGAACTCGGTGAA	105
IFNphi1R	TGCGTATCTTGCCACACATT	
IFNphi2F	CCTCTTTGCCAACGACAGTT	125
IFNphi2R	CGGTTCCTTGAGCTCTCATC	
IFNphi3F	TTCTGCTTTGTGCAGGTTTG	137
INFphi3R	GGTATACAAACGCGGTCGTC	
N SVCV F	TGAGGTGAGTGCTGAGGATG	101
N SVCV R	ATACCGGACTTTGCTGATGG	
18S F	ACCACCCACAGAATCGAGAAA	97
18S R	GCCTGCGGCTTAATTTGACT	
Expression vector construction		
Primer Name	**Primer sequence (5´→3´)**	**Amplicon (bp)**
IFIT12bF	AGGATGACTTCACATGTTTC	1449
IFIT12bR	CAGTAAAGACAGTCTGA	
IFIT13aF	AAGATGTCAGAGCAAAATCT	1290
IFIT13aR	ATCATCTTTGTTTGTTG	
IFIT17aF	AAGATGCATTCTTTACTGA	1302
IFIT17aR	CTCCTCTTTGAGAACAT	

Table S3.2. Accesion numbers of the IFIT sequences obtained from GenBank, Ensembl and Uniprot databases used to conduct phylogenetic analyses.

	Suffix	Specie	IFIT1	IFIT1B	IFIT2	IFIT3	IFIT5	Other
Mammals	Hs	*Homo sapiens*	NP_001539.3	NP_001010987.1	NP_001538.4	NP_001026853.1	NP_036552.1	-
	Pt	*Pan troglodytes*	NP_001192276.1	XP_003312807.1	XP_507902.2	NP_001182075.1	XP_003312804.1	-
	Mam	*Macaca mulata*	AFE78090.1	XP_001118323.1	NP_001248659.1	XP_001086192.1	XP_001086665.1	-
	Ml	*Myotis lucifugus*	-	-	G1QFX1	G1PV32	G1P5H9	-
	Am	*Atluropoda melanoleuca*	XP_002914452	XP_002914451	XP_002914449	-	XP_001917340	-
	Tt	*Tursiops truncatus*	ENSTTRP00000014611	-	-	-	ENSTTRP00000014612	ENSTTRP00000016138
	Ss	*Sus scrofa*	NP_001231292.1	-	XP_001928706.2	NP_001191324.1	XP_001925987.2	-
	Bt	*Bos taurus*	XP_001787879.1	-	XP_002698402.1	NP_001068882.1	NP_001069166.1	-
	Ec	*Equus caballus*	XP_001498851.1	XP_001496525.2	XR_131523.1	XP_001501453.2	XP_001501427.2	-
	La	*Loxodonta africana*	XP_003409062.1	XP_003409061.1	-	XP_003409063.1	XP_003409060.1	-
	Clf	*Canis lupus familiaris*	XP_848364.1	XP_848342.2	XP_536324.2	XP_848320.2	XP_543917.3	-
	Rn	*Rattus norvegicus*	NP_064481.1	XP_220058.2	NP_001019924.1	NP_001007695.1	-	-
	Mm	*Mus musculus*	NP_032357.2	NP_001095075.1	NP_032358.1	NP_034631.1	-	-
	On	*Ornithorhynchus anatinus*	-	-	-	-	XP_001506422.2	XP_001506725.2
	Dn	*Dasypodidae novemcinctus*	ENSDNOP00000016083	-	ENSDNOP00000016229	-	ENSDNOP00000006827	-
	Me	*Macropus eugenii*	-	-	-	-	ENSMEUP00000002189	-
Birds	Gg	*Gallus gallus*	-	-	-	-	XP_421662.2	-
	Tg	*Taeniopygia guttata*	-	-	-	-	XP_002188588.1	-
Amphibians	Xt	*Xenopus tropicallis*	XP_002937235.1	-	-	-	-	NP_001135660.1
			XP_002937236.1	-	-	-	-	XP_002937238.1
			XP_002944835.1	-	-	-	-	ENSXETP00000035558
Bony fish	Ci	*Ctenopharyngodon idella*	-	-	-	-	ADE73873.1	-
	Ca	*Carassius auratus*		-	-	-	AAP42145.1	-
	Tn	*Tetraodon nigroviridis*	-	-	-	-	CAF89887.1	-
	Om	*Oncorhynchus mykiss*	-	-	-	-	-	AAM18469.1
	Sas	*Salmo salar*	-	-	-	-	ACI34283.1	-
	Lch	*Latimeria chalumnae*	-	-	-	-	-	H3A6B7
	Dl	*Dicentrarchus labrax*	CBK52295.1	-	-	-	-	-
	Lc	*Larimichthys crocea*	ABY55167.1	-	-	-	-	-

Table S3.3. Identities and similarities. Percentages of Identity (grey) and similarity (white) between human/murine IFIT proteins and the 10 IFIT proteins identified in zebrafish.

	HsIFIT1	MmIFIT1	HsIFIT2	MmIFIT2	HsIFIT3	MmIFIT3	HsIFIT5	DrIFIT5A	DrIFIT12A	DrIFIT12B	DrIFIT12C	DrIFIT12D	DrIFIT12E	DrIFIT13A	DrIFIT17A	DrIFIT17B	DrIFIT17C
HsIFIT1		52.1	45.5	39.3	41.2	35.5	55.6	16.2	33.7	33.1	32.5	22.7	31.1	28.0	25.8	25.5	21.7
MmIFIT1	71.3		39.2	34.9	36.1	32.8	46.8	15.9	32.3	32.0	30.0	21.4	30.6	27.0	24.8	24.0	20.1
HsIFIT2	66.3	62.7		61.6	53.4	45.6	44.8	15.4	30.7	31.0	31.1	23.7	31.4	28.1	25.4	26.1	21.0
MmIFIT2	63.6	62.3	78.2		45.6	39.4	39.1	15.6	28.9	27.8	27.6	20.7	28.1	27.6	24.2	22.6	21.4
HsIFIT3	63.5	58.4	69.2	64.9		49.5	41.5	16.1	29.1	31.6	27.9	21.7	28.1	25.8	23.3	24.7	20.6
MmIFIT3	57.5	55.7	60.8	58.1	65.7		33.6	14.2	24.4	28.3	26.1	25.8	27.3	25.9	25.1	24.1	22.8
HsIFIT5	74.9	66.0	64.9	61.6	63.5	54.8		15.8	32.2	36.2	32.4	23.3	31.6	28.8	24.3	23.7	21.9
DrIFIT5A	28.7	27.6	27.6	27.6	28.6	23.8	29.2		15.7	20.6	19.1	12.4	20.1	14.9	14.6	14.1	13.2
DrIFIT12A	54.6	56.1	54.2	53.2	53.3	49.8	56.8	26.6		31.9	30.9	21.4	27.9	29.3	24.2	23.5	20.5
DrIFIT12B	59.1	56.0	55.6	55.2	53.3	48.8	61.8	30.3	56.8		49.9	35.3	49.8	30.1	24.5	25.8	22.0
DrIFIT12C	55.3	52.0	52.8	49.3	54.3	48.4	57.3	29.2	56.3	69.4		43.8	66.4	31.5	22.2	23.2	21.4
DrIFIT12D	36.6	36.5	37.9	35.8	37.3	44.4	39.0	19.6	39.0	45.6	50.7		52.2	23.6	20.2	20.7	17.7
DrIFIT12E	54.6	55.0	53.8	53.4	53.5	48.2	56.8	29.7	54.2	68.9	78.1	56.9		29.6	24.1	24.5	20.6
DrIFIT13A	51.0	50.1	50.8	51.3	49.0	49.0	48.3	24.9	49.8	54.8	51.3	40.6	52.4		25.2	25.6	22.1
DrIFIT17A	48.1	49.2	49.8	46.4	45.9	51.7	49.0	25.0	48.9	45.2	46.2	37.9	46.9	48.7		65.8	57.4
DrIFIT17B	46.7	45.4	47.2	45.8	45.9	48.7	45.6	24.6	46.8	44.6	46.0	37.5	46.9	50.8	79.2		51.8
DrIFIT17C	46.0	45.4	43.9	43.4	42.4	45.5	44.4	23.8	43.9	42.5	41.0	33.3	41.4	46.2	73.8	71.3	

Chapter 4

Characterization of Interleukin-6 in Zebrafish (*Danio rerio*)

Published in:
-Mónica Varela, Sonia Dios, Beatriz Novoa and Antonio Figueras
Developmental and Comparative Immunology 2012; 37(1):97-106

4.1. Introduction

Interleukin-6 (IL6) is one of the most pleiotropic and important cytokines due to its important role mediating the innate and adaptive immune responses (Akira et al., 1990; Naka et al., 2002). This molecule is produced by a wide variety of cell types, including macrophages, endothelial cells, glial cells, keratinocytes and fibroblasts, and participates in hematopoiesis, acute phase responses, metabolic processes and neurogenesis (Spooren et al., 2011).

In mammals, IL6 initially binds to the membrane bound a receptor (IL6R). Subsequently, the IL6/IL6R complex associates with the glycoprotein 130 (gp130), leading to gp130-homodimer formation and signal initiation, which includes activation of the JAK/STAT, ERK and PI3K signal transduction pathways (Scheller et al., 2011). In contrast to the ubiquitous expression of gp130, IL6R exhibits a highly defined pattern of expression and is largely confined to hepatocytes and leukocytes, although the soluble form of this receptor allows other kinds of cells to respond to IL6 (Jones et al., 2001; Heinrich et al., 2003).

Since its characterisation in the eighties, under the name of B-cell differentiation factor (Hirano et al., 1985), IL6 has been under continuous study due to its implication in important diseases. In fish, *il6* was first described in Japanese pufferfish, by exploiting the synteny found between certain regions of the human and Takifugu rubripes versions of the gene (Bird et al., 2005), and afterwards in other fish species as part of (Castellana et al., 2008; Iliev et al., 2007; Nam et al., 2007).

In spite of the importance of zebrafish (*Danio rerio*) as a model organism for fish and mammalian processes such as development, toxicological studies and diseases, the zebrafish *il6* homologue has not been identified in any databases or in any genome projects thus far. For this reason, and in view of the

importance of this cytokine in many biological processes, we sought to identify, characterise and describe the regulation of the expression and ontogeny of zebrafish *il6*. We additionally analysed the expression of genes that form the IL6 receptor complex.

4.2. Material and Methods

Sequence retrieval and analysis

The zebrafish *il6* sequence was initially investigated using the zebrafish genome assembly version Zv8 and Zv9 (www.ensembl.org/Daniorerio/), by exploiting the conservation of synteny between the human, the fugu and the zebrafish genomes. Using the Gnomon prediction tool (http://www.ncbi.nlm.nih.gov/genome/guide/gnomon.shtml), the probable coding regions within the genomic DNA were identified and the amino acid sequences analysed using BLAST (Altschul et al., 1990) and FASTA (Pearson and Lipman, 1988). This analysis identified two contigs of the zebrafish genome assembly, version Zv8, (Accession Nos. NW_00304079.1, NW_003043095.1) which seemed to code for a potential *il6* homologue. The predicted cDNA sequence was further studied by designing primers for obtaining the full-length coding sequence of this gene. Both cDNA and exonic genomic sequences were subcloned into a PCR® 2.1 plasmid vector (Invitrogen) and transformed into One Shot TOP10F' competent cells (Invitrogen) following the manufacturer's instructions. Bacteria were cultured on LB/Ampicillin/IPTG/X-Gal plates for 24 h at 37 °C, and the bacterial colonies were selected using the blue-white screening method. Positive colonies were selected and the insert was amplified using the M13 vector specific primers (M13F: GTAAAACGACGGCCAG, M13R: CAGGAAACAGCTATGA) for sequencing with an automated ABI

3730 DNA Analyser (Applied Biosystems). The resulting full-length *D. rerio il6* cDNA sequence was submitted to GenBank under Accession No. JN698962.

The predicted amino acid sequence was examined for the presence of a signal peptide using the SignalP program (http://www.cbs.dtu.dk/services/SignalP-2.0/) (Nielsen et al., 1997). Known protein domains were defined using Interpro (http://www.ebi.ac.uk/interpro/) and SMART (http://smart.embl-heidelberg.de/). The secondary structure of the protein was predicted using PSIPRED Server (Bryson et al., 2005) and PredictProtein (Rost et al., 2004).

An alignment with the human IL6 was conducted using Modweb and ModBase (Pieper et al., 2011) and Pymol (The PyMOL Molecular Graphics System, Version 1.2r3pre, Schrödinger, LLC). The protein structure modelling was conducted using 3D-JIGSAW (http://bmm.cancerresearchuk.org/~3djigsaw/) and I-TASSER (Zhang, 2007; Roy et al., 2010) selecting the model with the best C-score. The TM-score was used as an indication of structure similarity.

A multiple sequence alignment with other vertebrate IL6 sequences (*Homo sapiens*, NP_000591; *Mus musculus*, NP_112445; *Gallus gallus*, NP_989959; *T. rubripes*, NP_001027894; *Paralichtys olivaceus*, ABJ53333; *Sparus aurata*, ABY76175; *Oncorhynchus mykiss*, NP_001118129) was generated using Clustal W from Bioedit using the Gonnet protein weight matrix. A phylogenetic tree was then constructed based on the amino acid distances of the aligned sequences and other IL6 family molecules by the neighbour-joining method (Saitou and Nei, 1987), bootstrapped 10,000 times, and represented using the MEGA 5 program (Tamura et al., 2011). The IL6 family molecules used were the leukemia inhibitory factor (LIF) (*H. sapiens*, AAA51699; *M. musculus*, AAA37211), the ciliary neurotrophic factor (CNTF) (*H.*

sapiens, CAA43009; *M. musculus*, NP_740756; *G. gallus*, NP_990823), the oncostatin M (ONCM) (*H. sapiens*, AAH11589; *M. musculus*, AAH99866) and the interleukin-11 (IL11) (*H. sapiens*, AAH12506; *M. musculus*, AAI34355; *O. mykiss*, NP_001117854).

The sequences of the IL6 receptors, *il6r* and *gp130*, were obtained from the GenBank databases (NM_001114318 and NM_001113504).

Animals

Adults, embryos and larvae from wild type zebrafish were obtained from our experimental facility, where zebrafish are cultured following established protocols (Westerfield, 2000; Nüsslein-Volhard and Dahm, 2002) (http://zfin.org/zf_info/zfbook/zfbk.html).

Experimental treatments

Fish care and challenge experiments were conducted according the CSIC National Committee on Bioethics.

Naïve adult zebrafish were sacrificed using MS-222 (Tricaine methanesulfonate, Argent Chemical Laboratories, USA) overdose to analyse the basal expression of IL6 and its receptor complex, IL6R and gp130, in several organs. The kidney, liver, spleen and muscle from 12 fish were sampled and pooled, yielding a total of 3 biological replicates of 4 fish each per organ. Total RNA was isolated as described below.

Additionally, 36 adult zebrafish were intraperitoneally injected with 10 µL of 1 mg/mL LPS, and a second group of 36 fish was injected intraperitoneally with the same concentration of poly I:C in PBS solution, mimicking bacterial and viral infection, respectively. Thirty-six fish were injected with PBS and used as

controls. Kidneys were sampled from anesthetized fish at 3, 6 and 24 h post-stimulation (hps), and total RNA was isolated from 3 biological replicates of 4 fish per sampling point. The expression of *il6, il6r* and *gp130* under stressed conditions was measured using real time PCR (qPCR) and compared with the basal expression of these genes. We also analysed the expression of *tnfα* (NM_212859) and *il1β* (NM_212844) to compare the modulation of other pro-inflammatory molecules with the *il6* expression profile.

An additional experiment was conducted to determine the expression of *il6, il6r* and *gp130* during the early development of zebrafish larvae. Several spawnings from the same stock were induced to obtain larvae at different days post-fertilization (dpf), at 3-day intervals from 2 to 29 dpf. Different numbers of embryos or fish were used for each age group due to the differences in size to assure a minimum RNA amount, 1 µg, for cDNA transcription. Two biological replicates with 10–15 animals per group for individuals ranging from 2 to 14 dpf or 6–8 animals per group for individuals ranging from 17 to 29 dpf were used for RNA isolation.

Nucleic acids isolation, cDNA transcription and PCR amplification

Genomic DNA from zebrafish muscle was isolated using the Phenol–Chloroform method (Strauss, 2001). PCR amplification of genomic DNA was performed using 100 ng of DNA with different combinations of specific primers depending on the desired fragment (Table S4.1).

Total RNA isolation was conducted both for adults and larvae using TRIzol reagent (Invitrogen), following the manufacturer's specifications, in combination with a RNeasy mini kit (Qiagen) for RNA purification after DNase I treatment. One

microgram of total RNA was then used to obtain cDNA for qRT-PCR using the SuperScript III first-strand synthesis supermix (Invitrogen).

The expression patterns of *il6* and the genes of the IL6 receptor complex (*il6r* and *gp130*), together with *il1β* and *tnfα* for comparison purposes, were quantified using qPCR under both naïve conditions and after LPS or poly I:C stimulation. Specific PCR primers were designed from the selected sequences (Table S4.1) using the *primer3* program (Rozen and Skaletsky, 2000), according to known qPCR restrictions. The efficiency of the primer pairs was then analysed with seven serial 5-fold dilutions of cDNA and calculated from the slope of the regression line of the cycle thresholds (Cts) versus the relative concentration of cDNA (Pfaffl, 2001). A melting curve analysis was also performed to verify that no primer dimers were amplified. If these conditions were not accomplished, new primer pairs were designed. One microliter of 5-fold diluted cDNA template was mixed with 0.5 µl of each primer (10 µM) and 12.5 µl of SYBR Green PCR master mix (Applied Biosystems) in a final volume of 25 µl. The standard cycling conditions were 95 °C for 10 min, followed by 40 cycles of 95 °C for 15 s and 60 °C for 1 min. All reactions were carried out as technical triplicates. The relative expression levels of the genes were normalized using 18S ribosomal RNA (BX296557) expression as a housekeeping gene control, which was constitutively expressed and not affected by the treatments, following the Pfaffl method (Pfaffl, 2001). Fold change units were calculated by dividing the normalised expression values of stimulated tissues by the normalised expression values of the controls. For basal conditions, the expression units were calculated by dividing the normalised expression values of each organ by the normalised expression value of the liver. In the case of ontogeny, expression units were calculated by dividing the normalised expression values

of each sample point by the normalised expression value at 2 dpf. For the biological replicates, the average relative level of expression from each replicate was considered as a single point and the mean and standard error calculated.

Whole-mount *in situ* hybridisation (ISH)

Sense and antisense RNA-probes were designed to create fragments that were between 713 and 720 bases long. They were produced with the PCR amplification method under standard PCR conditions (35 cycles, 60 °C annealing temperature) using specific primers (Table S4.1). The sense probe had incorporated the promoter sequence necessary for labelling purposes (SP6 promoter, ACGATTTAGGTGACACTATAGAA), while the antisense probe had incorporated the T7 promoter (AGTTAATACGACTCACTATAGGGATT). RNA-probes were prepared using DIG-RNA Labelling Kit (SP6/T7) (Roche) according to the manufacturer's instructions.

The whole-mount *in situ* hybridisation (ISH) was performed on 3 dpf zebrafish embryos, essentially as reported by Thisse and Thisse (2008). Embryos were fixed overnight in 4% paraformaldehyde (PFA, Sigma) in phosphate-buffered saline (PBS). Embryo pigmentation was suppressed by 3% hydrogen peroxide treatment during 30 min. Next, the embryos were washed in PBT (PBS plus 0.1% Tween 20, Sigma), treated with methanol and stored at −20 °C. Methanol-stored embryos were re-hydrated in a methanol/PBS series, permeabilized using proteinase K (10 µg/ml) (Roche), pre-hybridized, and then hybridized overnight at 70 °C with 100 ng of the corresponding probe in 200 µl of hybridisation mix (HM: 50% formamide, 5× SSC, 0.1% Tween 20, 50 mg/ml heparin and 0.5 mg/ml tRNA). After HM/SSC and SSC/PBT washing series, embryos were pre-incubated in blocking solution (2% sheep

serum and 2 mg/ml BSA in PBT) and then incubated overnight at 4 °C with pre-absorbed alkaline phosphatase-conjugated anti-DIG antibodies (Roche) diluted 1:2000 in blocking solution. After PBT washing, embryos were pre-soaked in staining buffer and then incubated in NBT/BCIP (nitro blue tetrazolium/5-bromo-4-chloro-3-indolyl-phosphate) (Roche) for blue staining. Stained embryos were cleared in 100% glycerol, observed under an AZ100 microscope (Nikon) and photographed with a DS-Fi1 digital camera (Nikon).

Statistical analysis

Results are presented as means ± standard error of mean (SEM). The data were analysed using one-way analysis of variance and Tukey's test, and differences were considered significant at $p < 0.05$.

4.3. Results

IL6 gene organization and bioinformatics analysis

A high degree of synteny was found between the human chromosome 7, the fugu scaffold 449 and zebrafish chromosome 19. In both cases, the genes SP4, CDCA7L, TOMM7 and HYCCIN were found in the region of IL6 gene, but they appeared in a different order. The genes SP4 and HYCCIN were in the same contig of the Zv9 assembly version of the zebrafish genome (CU928128.15) with the same orientation, involving a chromosomal inversion that affected the zebrafish *hyccin*, *tomm7* and *il6* genes (Figure 4.1A).

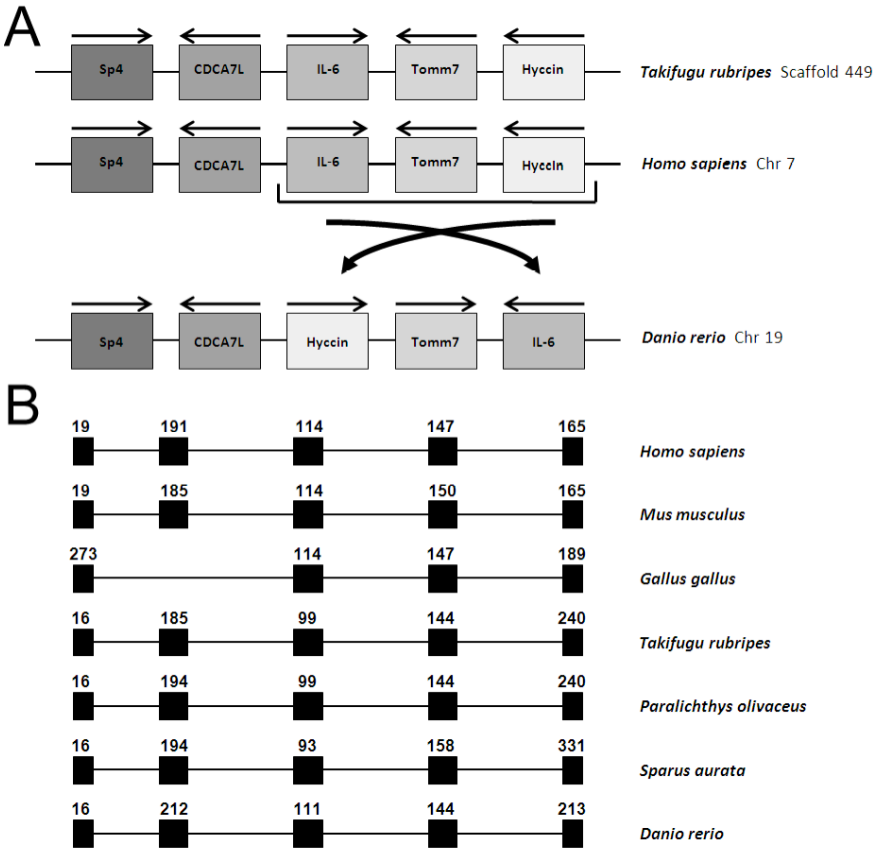

Figure 4.1. Zebrafish *il6* gene organization. A. Comparative gene location diagram among *Takifugu rubripes* (scaffold 449), *Homo sapiens* (chromosome 7) and *Danio rerio* (chromosome 19). Arrows above genes indicate the gene orientation. B. Comparison of the gene organization and exon sizes (bp) among fish *il6* sequences and some higher vertebrates IL6.

The gene organization of *D. rerio il6* was obtained using the predicted zebrafish *il6* ORF sequence and two contigs of the Zv8 assembly version of the zebrafish genome (Accession Nos. NW_00304079.1, NW_003043095.1) that were again amplified and sequenced. The genomic organization of zebrafish *il6* was the same as that observed in the human IL6 gene and other fish *il6* known sequences (Figure 4.1B) and was found to have five exons

and four introns. The intron splicing consensus (GT/CAG) was conserved at the 5′ and 3′ ends of the introns.

Figure 4.2. ORF and predicted amino acid sequence of zebrafish IL6. The start and stop codons are boxed and the predicted signal peptide is underlined. The IL6 domain is in bold. The IL6 family signature (C–X(9)–C–X(6)–G–L–X(2)–Y–X(3)–L) is shaded. Predicted *N*-glycosylation sites appear underlined with a dashed line.

The ORF of the zebrafish *il6* was obtained and confirmed using PCR and specific primers (Table S4.1) that amplified the full-length *il6* cDNA (Figure 4.2). The transcript consisted of a 696 bp sequence that coded for a predicted 231 amino acid protein. Zebrafish IL6 had a predicted signal peptide, an IL6 domain and a four-helical cytokine core. Four possible glycosylation sites were also predicted at amino acids 86, 110, 138 and 195.

Figure 4.3. Amino acid alignment. Multiple alignment of zebrafish IL-6 with other vertebrate IL6 proteins. The location of the four alpha-helices (A–D) is indicated above the sequence for human IL6 and under the sequence for predicted zebrafish IL6 with a dotted line. IL6 family signature is shaded and arrows indicate the cysteine residues involved in disulfide bond formation.

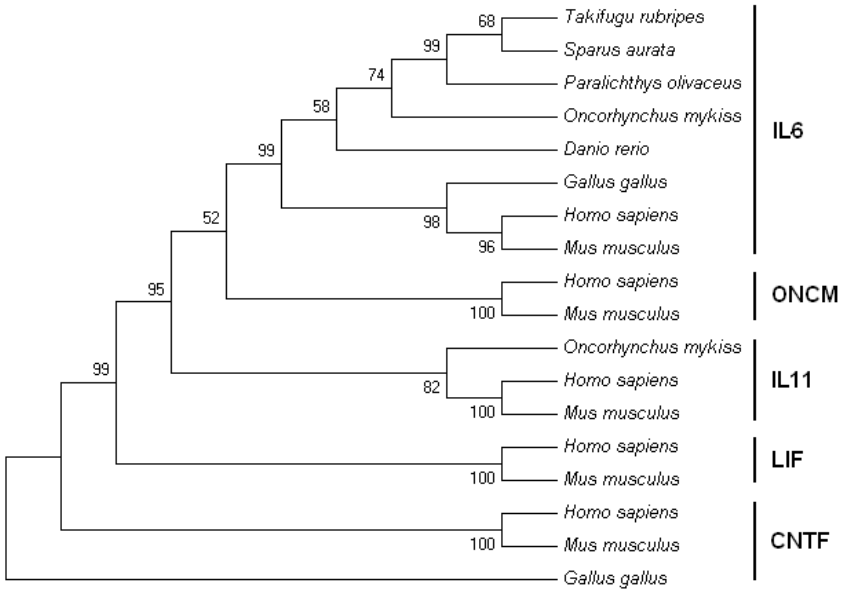

Figure 4.4. **Phylogenetic relationship**. Phylogenetic tree based on deduced amino acid sequences of different vertebrate IL6 family molecules. This unrooted tree was constructed using the neighbour-joining algorithm, bootstrapped 10,000 times.

A multiple alignment with other known IL6 amino acid sequences showed conservation zones among the species (Figure 4.3). The consensus IL6 family signature (C–X(9)–C–X(6)–G–L–X(2)–Y–X(3)–L) showed some changes in the zebrafish IL6 protein, in which the Glycine is replaced by Valine and last Leucine by Tryptophan. Zebrafish IL6, like the other fish IL6, only has two conserved cysteine residues out of the four that are involved in disulfide bond formation. The values of similarity and identity with other IL6 sequences were low, as it happens in other fish species (Table S4.2). Phylogenetic analysis further demonstrated that the zebrafish IL6 was more closely related to other fish IL6 with a bootstrap value of 58%, although it seems to constitute a different clade than the one formed by fugu, gilthead seabream, flounder and trout (Figure 4.4). The tertiary structure of zebrafish IL6 was

modelled with a high confidence (C-score: −0.76), and a TM-score of 0.62 indicated a model of correct topology and an important similarity between the zebrafish and human structures (Figure 4.5).

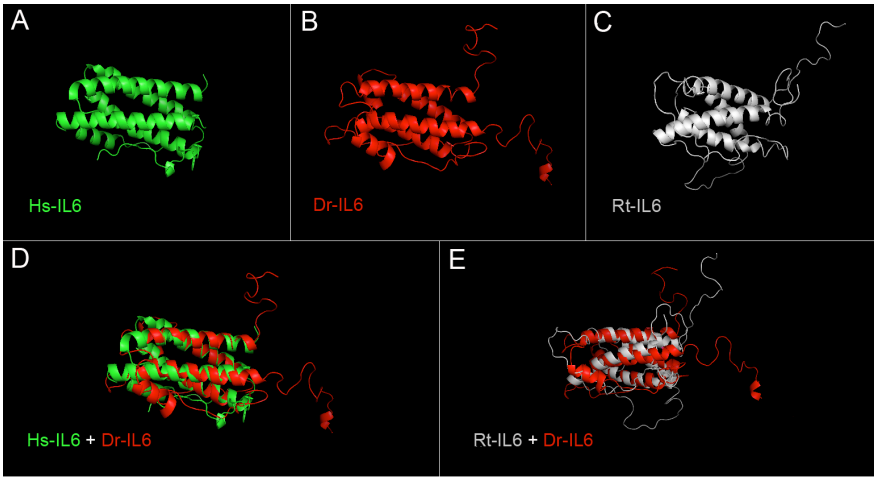

Figure 4.5. Predicted tertiary structure of zebrafish IL6 compared with human and trout IL6. A. *Danio rerio* IL6 predicted tertiary structure. B. *Homo sapiens* IL6 tertiary structure. C. *Rainbow trout* IL6 predicted tertiary structure. D. Comparison of the zebrafish and human IL6 tridimensional structures. E. Comparison of the zebrafish and trout IL6 tridimensional structures.

Tissue-related expression

In adult zebrafish, *il6* was predominantly expressed in the kidney and spleen. The IL6 receptor complex genes *il6r* and *gp130* were detected in all analysed tissues. *il6r* expression was notably higher in the kidney than in the spleen and muscle, where the expression was lower than in any other tissue. The expression level of *gp130* was remarkably similar within all studied tissues and, although it appeared that higher levels of expression occurred in the kidney and spleen, no significant differences were observed (Figure 4.6).

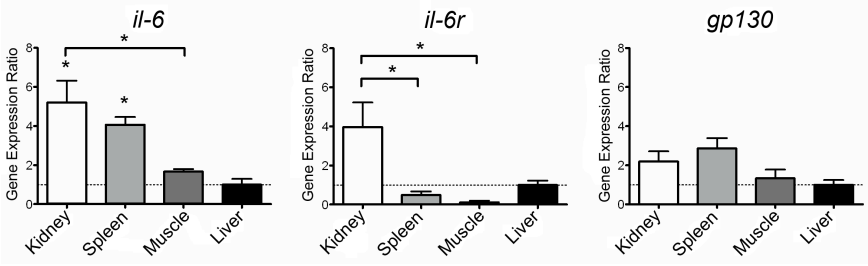

Figure 4.6. Zebrafish *il6, il6r* and *gp130* tissue-related expression. Expression levels of *il6, il6r* and *gp130* genes in organs of non-stimulated adult zebrafish. All qPCRs were carried out as technical triplicates and the expression level of analysed genes was normalized using the 18S rRNA. The expression levels were calculated by dividing the normalized expression values of each organ by the normalized expression values of liver. Each bar represents the mean and standard error of three biological replicates. Significant differences between tissues were displayed as *($0.01 < p < 0.05$).

Inflammatory challenge

The pro-inflammatory cytokines analysed in this study followed a very similar expression pattern to that of *il6*. Kidney expression of *il6, tnfα* and *il1β* increased significantly following exposure to LPS or poly I:C (Figure 4.7). A decrease in the expression of these genes was observed after 3 hps with the exception of *il6*, for which the expression was maintained until 6 h after injection. At 24 hps, the expression levels of the pro-inflammatory cytokines returned to the baseline level.

In contrast, the expression of the IL6 receptor complex genes *il6r* and *gp130* was not significantly regulated at any time after LPS or poly I:C stimulation.

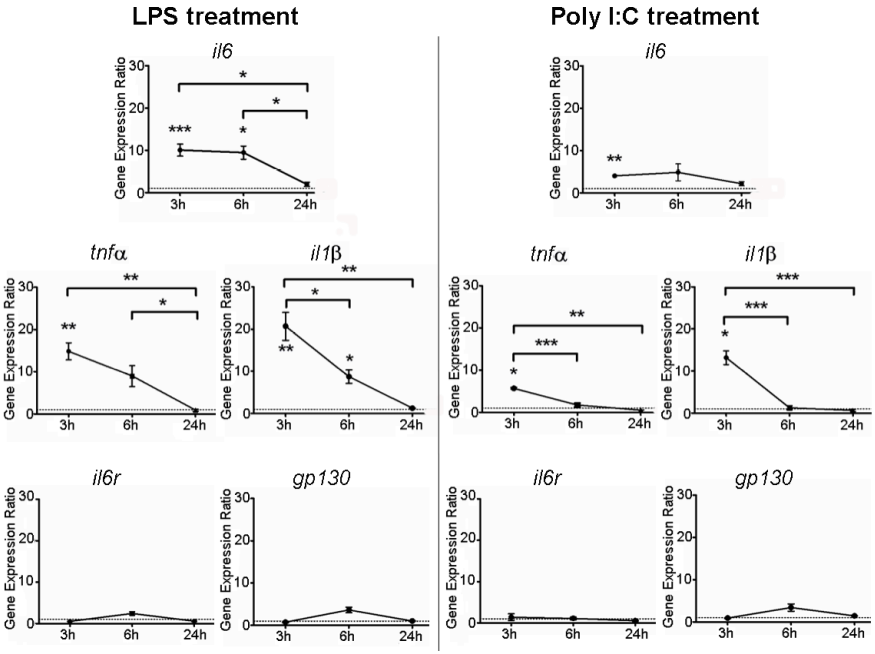

Figure 4.7. Time course of *il6, tnfα, il1β, il6r* and *gp130* expression after stimulation with PAMPs. Expression of *il6, tnfα, il1β, il6r* and *gp130* genes in zebrafish kidney after 1 mg/ml LPS or 1 mg/ml poly I:C intraperitoneal injection at 3, 6 and 24 h post-stimulation. All qPCRs were carried out as technical triplicates and the expression level of analysed genes was normalized using the 18S rRNA. Fold change units were calculated by dividing the normalized expression values of stimulated zebrafish kidneys by the normalized expression values of the controls for each of the time points. Each bar represents the mean and standard error of three biological replicates. Significant differences between samples were displayed as $^{*}(0.01 < p < 0.05)$, $^{**}(0.001 < p < 0.01)$ and $^{***}(.0001 < p < 0.001)$.

Ontogeny and ISH

We also analysed the expression level of *il6, il6r* and *gp130* during zebrafish early development (Figure 4.8). Transcripts of these genes were detected at all sampling points between 2 and 29 dpf. In all cases, we observed that expression gradually increased during the first week post-fertilization. Expression then appeared to reach a steady state with the exception of *il6r*, for

which two peaks were observed at 17 and 23 dpf. In the case of *il6*, the results also suggested a decrease at the end of the larvae's first month of life.

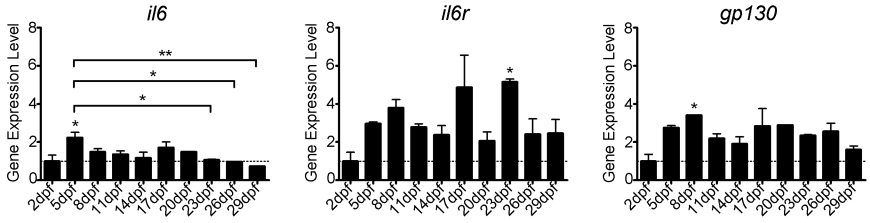

Figure 4.8. Ontogeny of *il6, il6r* and *gp130* genes. Expression levels of *il6, il6r* and *gp130* genes during the zebrafish larvae development. All qPCRs were carried out as technical triplicates and the expression level of analysed genes was normalized using the 18S rRNA. Expression levels were calculated by dividing the normalized expression values of each sample point by the normalized expression values at 2 dpf larvae. Each bar represents the mean and standard error of two biological replicates. Significant differences between development stages were displayed as $^{*}(0.01 < p < 0.05)$ and $^{**}(0.001 < p < 0.01)$.

For whole-mount *in situ* hybridisation, the expression pattern at 3 dpf appeared similar for both *il6* and its receptor complex genes. Our results showed that these three molecules were predominantly expressed in the head, epidermis and neuromasts of the anterior and posterior lateral line system. Moreover, strong expression was observed in the cells surrounding the mouth opening, in the olfactory placodes and in the lateral fins (Figure 4.9).

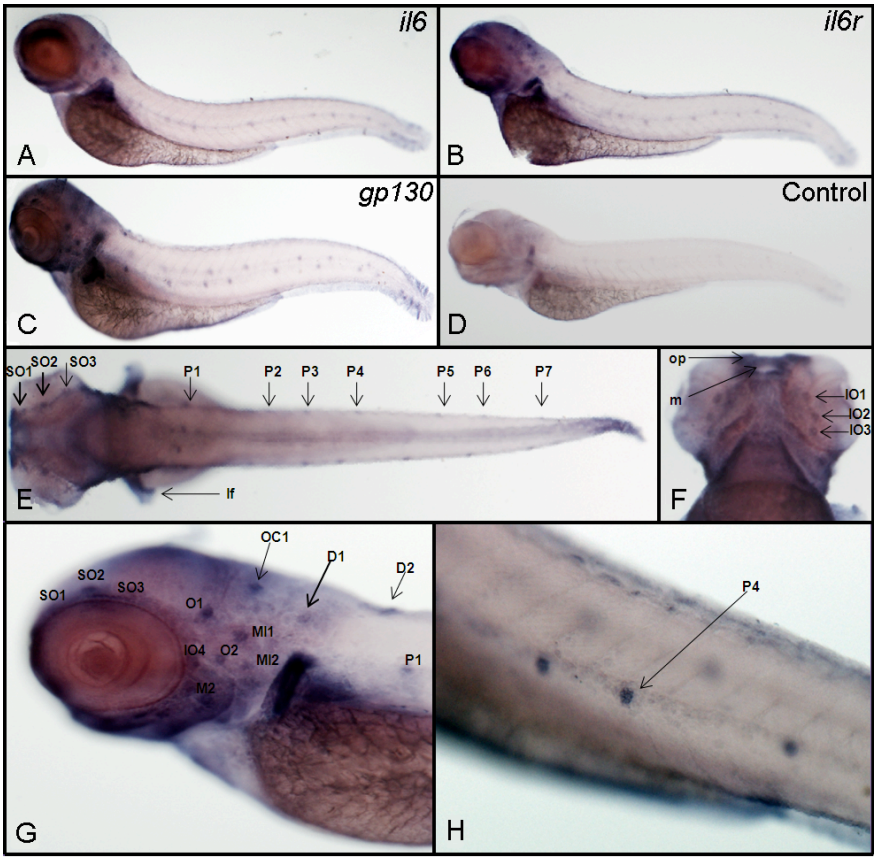

Figure 4.9. *In situ* hybridisation on 3 dpf zebrafish embryos. A–C. Expression pattern of *il6, il6r* and *gp130* genes in embryos hybridized with the antisense probe. D. Control embryos hybridized with the sense probe. E. Dorsal larvae view. F. Infraorbital zone detail. G. Lateral view of a larvae head. H. Detail of neuromasts of the posterior lateral line system. Images from 8e to 8h are representative of the three studied genes. D1–2, dorsal lateral line neuromast; IO1–4, infraorbital lateral line neuromast; lf, lateral fin; M2, mandibular lateral line neuromast; m, mouth opening; MI1–2, middle lateral line neuromast; O1–2, otic lateral line neuromast; OC1, occipital lateral line neuromast; op, olfactory placode; P1–7, posterior lateral line neuromast; SO1–3, supraorbital lateral line neuromast.

4.4. Discussion

In the present work, we identified the zebrafish IL6 by exploiting the synteny between the human, the fugu and the

zebrafish genome. We used several genes situated on human chromosome 7 and fugu scaffold 449, close to the IL6 gene, to find the *D. rerio* IL6 homologue. This gene was identified on the zebrafish chromosome 19, but in a different position with regards to its order within the block of surrounding genes compared to the human chromosome. A chromosomal inversion that affects the IL6, TOMM7 and HYCCIN genes was observed. This is not an isolated event, as many studies show that blocks of conserved synteny between zebrafish and humans are large, but the gene order is frequently inverted and transposed (Postlethwait et al., 2000; Liu et al., 2002). The zebrafish IL6 was predicted to contain 231 amino acids with a 23-amino acid signal peptide. It was also predicted that this molecule possesses a four-helical cytokine core with a conserved IL6/G-CSF/MGF family signature (C–X(9)–C–X(6)–G–L–X(2)–Y–X(3)–L), with the exception of the Glycine and the final Leucine residue. In the zebrafish IL6, the Glycine (GGC) was substituted for Valine (GTC) and Leucine (TTG) for Tryptophan (TGG).

Of all the described IL6 sequences in fish, fugu is the only one for which this characteristic family motif remains unchanged. All other known fish IL6 sequences show some minor modifications. In the case of trout IL6, the first cysteine of the family signature is displaced and there are only 7 amino acids between the first and the second cysteine. In most of the cases, including zebrafish IL6, there are amino acid substitutions. For IL6, only the 3rd and 4th C residues of the 4 important C residues in mammals are conserved in all known IL6 teleosts orthologs, with the exception of seabream IL6, in which only 1 C residue is conserved (Bird et al., 2005, Castellana et al., 2008, Iliev et al., 2007; Nam et al., 2007). Phylogenetically, zebrafish IL6 was grouped with other fish IL6 and, as occurs with other cytokines, the identity and similarity of the zebrafish IL6 are relatively low

compared to their counterparts in other species. The low identity between the zebrafish IL6 and IL6 from higher vertebrates is not an isolated event, as this also happens with other cytokines such as IL1β and IL18 (Huising et al., 2004). In spite of this, there was a high conservation of the three-dimensional structure of zebrafish IL6, which suggests a functional conservation among species.

Tissue-related expression of zebrafish *il6* gene was examined by qPCR in the kidney, spleen, muscle and liver of non-stimulated adult zebrafish. Transcripts of this gene were detected in all analysed tissues. We observed the highest expression in kidney and spleen, in which expression was 5 and 4 times higher, respectively, than in the liver. The lowest expression level was detected in muscle and liver. The results obtained in fugu described the expression of *il6* only in the kidney but not in any other tissue (Bird et al., 2005). Also, Iliev et al. (2007) detected the highest expression in the ovary of trout while Castellana et al. (2008) reported the highest values in the muscle and skin of gilt head seabream. These authors also detected *il6* transcripts in other tissues such as spleen, but in smaller amounts. In flounder, basal expression was not detected in the analysed tissues (Nam et al., 2007). The results reported so far display variable data regarding the basal expression of this gene in fish tissues, probably because the technique used in all cases was RT-PCR, which is less sensitive than the qPCR used in this study. Liongue and Ward (2007) identified the zebrafish *il6r* and *gp130* orthologues. They focused on the phylogenetic analysis of these molecules, therefore their pattern of expression remained unknown until this study. *il6r* transcripts were detected in all analysed tissues, but the highest expression level was found in kidney and liver. To our knowledge, this is the first analysis of tissue-related *il6r* expression in fish and our results agree with the data obtained in mammals, in which IL6R is mainly produced by leukocytes and hepatocytes (Chalaris et

al., 2011; Rose-John et al., 2006), which are especially abundant in kidney and liver, respectively. With regard to the other component of the receptor complex, little is known about *gp130* expression in fish. Santos et al. (2007) described a ubiquitously expressed *gp130*-like molecule in Japanese flounder. In higher vertebrates, this molecule is also ubiquitously expressed (Hibi et al., 1990). GP130 was widely studied during the nineties, due to its relationship with different cytokines such as IL6, LIF, CNTF and IL11 (Hibi et al., 1990, Ip et al., 1992; Nandurkar et al., 1996). GP130 is the common signal transducer for all of these IL6-family cytokines, which could explain its presence in all cell types.

IL6 is one of the most important pro-inflammatory cytokines that, together with TNFα and ILβ, constitutes the first cytokines released after host exposure to pathogens. We compared the expression level of these three genes at different times after intraperitoneal stimulation with LPS and poly I:C. The transcription level increased significantly for all of these cytokines during the first hours after the pathogen-associated molecules (PAMPs) exposure. In mammals, as in another fish species, it is known that IL6 expression can be induced by LPS or poly I:C, as well as by cytokines such TNFα and IL1β. This would explain why *il6* transcript expression was maintained for up to 6 h after injection. These results also suggest that the maximum expression for *il6* took place between 3 and 6 hps for both LPS and poly I:C, probably in response to prior induction of *tnfα* and *il1β*. This was also the case for *Vibrio anguillarum* infected seabream, where an increase in the *il6* expression in head kidney was observed at 4 h post-stimulation (Castellana et al., 2008). A trend of increased expression for the receptor complex could be observed, with a modest transcript increase at 6 hps. This could indicate a peak of expression before or after this sampling point. This would be consistent with the regulation of these complexes demonstrated

in several studies in mammals (Schooltinck et al., 1992, Snyers and Content, 1992; Vallières and Rivest, 1997), where it has been shown that both IL-6R and GP130 are regulated by TNFα, IL1β, IL6 and LPS in different ways depending on the cell type.

IL6 and its receptors are also involved in processes such as hematopoiesis and the growth, differentiation and activation of certain cell types. The expression of IL6 in the ovary of some organisms and some embryonic cellular lines also points to its involvement in reproduction and development (Chung et al., 2000; Iliev et al., 2007). Expression analysis of *il6, il6r* and *gp130* during ontogeny of zebrafish larvae showed that the transcripts were present at all sampled points. Detection took place immediately after the larvae hatched (2–3 dpf) and peaked during the first week of life of the individuals. This suggests that the organism needs these molecules and their biological activities for proper development or early survival. In support of this, GP130-deficient mice are embryonically lethal and conditional deletions of this gene result in hematopoietic, immunological, neurological and hepatic defects (Yoshida et al., 1996; Betz et al., 1998). IL6 or IL6R$^{-}/^{-}$ mice are viable, but they suffer important alterations related to inflammation, organ regeneration and metabolism (Schirmacher et al., 1998; Wallenius et al., 2002).

IL6 also plays a critical role in the nervous system. This system can produce some cytokines, such as IL1β, IL6 and TNFα, and their receptors during both inflammatory responses and normal development. Receptors for a variety of cytokines, including the IL6, have been localized in several brain areas (Mehler and Kessler, 1997; Szelényi, 2001). Under non-pathological conditions, some cytokines of the IL6 family may participate in the development and the function of the central nervous system (Taga and Fukuda, 2005). This would include GP130, as it is the common signal transducer for several members

of this cytokine family. The results of the 3 dpf larvae *in situ* hybridisation suggest that these genes could be involved in the neurogenesis and development of zebrafish. ISH clearly revealed the appearance of *il6, il6r* and *gp130* transcripts in neuromasts. These mechanoreceptor organs of the lateral line system are distributed in the head and along the fish trunk. They are composed of several cell types, among which are mechanosensory hair cells and multipotent progenitors. Although several authors have demonstrated the existence of macrophages around the neuromasts, hybridisation seemed to occur in cells within the neuromasts and the staining appeared specifically in a group of cells at the centre of the cell cluster, including the location where the hair cells will eventually arise. Gallardo et al. (2010) performed a microarray with neuromasts cells, due to its potential as a model of cell migration and differentiation of sensorial cells from multipotent progenitor cells. They catalogued a variety of biological processes and a wide number of signalling pathways involved in neuromasts and lateral line development. Their work has highlighted genes involved in processes related to cellular migration, the immune system and development in which IL-6 was suggested to be involved.

The data reported so far both in mammals and fish point out the important role that IL6 appears to have during both development and the immune response. In our work, we have confirmed that zebrafish IL6 shares structural characteristics with IL6 from other vertebrates. Its expression appears at an early age in zebrafish larvae, and its pattern of expression following immune stimuli shows similarities with other pro-inflammatory cytokines. In summary, our results will facilitate the use of this fish species as a model for the study of various pathologies of increasing interest, such as cancer and chronic inflammation diseases, in which IL6 and its receptors have been associated in recent years.

4.5. References

Akira S, Hirano T, Taga T, Kishimoto T (1990) Biology of multifunctional cytokines: IL 6 and related molecules (IL1 and TNF). FASEB J 4:2860-2867.

Altschul SF, Gish W, W. Miller, Myers EW, Lipman DJ (1990) Basic local alignment search tool. J Mol Biol 215:403–410.

Betz UAK, Bloch W, van den Broek M, Yoshida K, Taga T, Kishimoto T, Addicks K, Rajewsky K, Müller W (1998) Postnatally Induced Inactivation of gp130 in Mice Results in Neurological, Cardiac, Hematopoietic, Immunological, Hepatic, and Pulmonary Defects. J Exp Med 188:1955-1965.

Bird S, Zou J, Savan R, Kono T, Sakai M, Woo J, Secombes CJ (2005) Characterization and expression analysis of an interleukin 6 homologue in the Japanese pufferfish, Fugu rubripes. Dev Comp Immunol 29:775-789.

Bryson K, McGuffin LJ, Marsden RL, Ward JJ, Sodhi JS, Jones DT (2005) Protein structure prediction servers at University College London. Nucleic Acids Res 33:36-38.

Castellana B, Iliev DB, Sepulcre MP, Mackenzie S, Goetz FW, Mulero V, Planas JV, (2008) Molecular characterization of interleukin-6 in the gilthead seabream (Sparus aurata). Mol Immunol 45:3363-3370.

Chalaris A, Garbers C, Rabe B, Rose-Jhon S, Scheller J (2011) The soluble interleukin 6 receptor: Generation and role in inflammation and cancer. Eur J Cell Biol 90:484-494.

Chung KW, Ando M, Adashi EY (2000) Periovulatory and Interleukin (IL)-1-dependent Regulation of IL-6 in the Immature Rat Ovary: A Specific IL-1 Receptor-Mediated Eicosanoid-Dependent Effect. J Soc Gynecol Investig 7:301-308.

Gallardo VE, Liang J, Behra M, Elkahloun A, Villablanca EJ, Russo V, Allende ML, Burgess SM (2010) Molecular dissection of the migrating posterior lateral line primordium during early development in zebrafish. BMC Dev Biol 10:120.

Heinrich PC, Behrmann I, Haan S, Hermanns HM, Müller-Newen G, Schaper F (2003) Principles of interleukin (IL)-6-type cytokine signalling and its regulation. Biochem J 374:1–20.

Hibi M, Murakami M, Saito M, Hirano T, Taga T, Kishimoto T (1990) Molecular cloning and expression of an IL-6 signal transducer, gp130. Cell 63:1149–1157.

Hirano T, Taga T, Nakano N, Yasukawa K, Kashiwamura S, Shimizu K, Nakajima K, Pyun KH, Kishimoto T (1985) Purification to homogeneity and characterization of human B-cell differentiation factor (BCDF or BSFp-2). Proc Natl Acad Sci USA 82:5490-5494.

Huising MO, Stet RJM, Savelkkoul HFJ, Verburg-van Kemenade BM (2004) The molecular evolution of the interleukin-1 family of cytokines; IL-18 in teleost fish. Dev Comp Immunol 28:395-441.

Iliev DB, Castellana B, MacKenzie S, Planas JV, Goetz FW (2007) Cloning and expression analysis of an IL-6 homolog in rainbow trout (Oncorhynchus mykiss). Mol Immunol 44:1803-1807.

Ip NY, Nye SH, Boulton TG, Davis S, Taga T, Li Y, Birren SJ, Yasukawa K, Kishimoto T, Anderson DJ, Stahl N, Yancopoulos GD (1992) CNTF and LIF act on neuronal cells via shared signaling pathways that involve the IL-6 signal transducing receptor component gp130. Cell 69:1121-1132.

Jones SA, Horiuchi S, Topley N, Yamamoto N, Fuller GM (2001) The soluble interleukin 6 receptor: mechanisms of production and implications in disease. FASEB J 15:43-58.

Liongue C and Ward AC (2007) Evolution of Class I cytokines receptors. BMC Evol Biol 7:120.

Liu TX, Zhou Y, Kanki, JP, Deng M, Rhodes J, Yang HW, Sheng XM, Zon LI, Look AT (2002) Evolutionary Conservation of Zebrafish Linkage Group 14 with Frequently Deleted Regions of Human Chromosome 5 in Myeloid Malignancies. Proc Natl Acad Sci USA 99:6136-6141.

Mehler MF and Kessler JA (1997) Hematolymphopoietic and inflammatory cytokines in neural development. Trends Neurosci 20:357-365.

Naka T, Nishimoto N, Kishimoto T (2002) The paradigm of IL-6: from basic science to medicine. Arthritis Res 4:S233-S242.

Nam BH, Byon JY, Kim YO, Park EM, Cho YC, Cheong JH (2007) Molecular cloning and characterization of the flounder (Paralichthys olivaceus) interleukin-6 gene. Fish Shellfish Immunol 23:231-236.

Nandurkar HH, Hilton DJ, Nathan P, Willson T, Nicola N, Begley CG (1996) The human IL-11 receptor requires gp130 for signalling: demonstration by molecular cloning of the receptor. Oncogene 12:585-93.

Nielsen H, Engelbrecht J, Brunak S, von Heijne G (1997) Identification of prokaryotic and eukaryotic signal peptides and prediction of their cleavage sites. Protein Eng 10:1–6.

Nüsslein-Volhard C and Dahm R (2002) Zebrafish: a practical approach. New York: Oxford University Press.

Pearson WR and Lipman DJ (1988) Improved tools for biological sequence comparison. Proc Natl Acad Sci USA 85:2444-2448.

Pfaffl MW (2001) A new mathematical model for relative quantification in real-time RT-PCR. Nucleic Acids Res 29:e45.

Pieper U, Webb BM, Barkan DT, Schneidman-Duhovny D, Schelessinger A, Braberg H, Yang Z, Meng EC, Pettersen EF, Huang CC, Datta RS Sampathkumar P, Madhusudhan MS, Sjölander K, Ferrin TE, Burley SK, Sali A (2011) ModBase, a database of annotated comparative protein structure models, and associated resources. Nucleic Acids Res 39:D465-D474.

Postlethwait JH, Woods IG, Ngo-Hazelett P, Yan YL, Kelly PD, Chu F, Huang H, Hill-Force A, Talbot WS, (2000) Zebrafish comparative genomics and the origins of vertebrate chromosomes. Genome Res 10:1890-1902.

Rose-John S, Scheller J, Elson G, Jones SA (2006) Interleukin-6 biology is coordinated by membrane-bound and soluble receptors: role in inflammation and cancer. J Leuk Biol 80,:227-236.

Rost B, Yachdav G, Liu J (2004) The PredictProtein Server. Nucleic Acids Res 32:321-326.

Roy A, Kucukural A, Zhang Y (2010) I-TASSER: a unified platform for automated protein structure and function prediction. Nat Protocol 5:725-738.

Rozen S, Skaletsky H (2000) Primer3 on the WWW for general users and for biologist programmers. Methods Mol Biol 132:365-386.

Saitou N and Nei M (1987) The neighbor-joining method: a new method for reconstructing phylogenetic trees. Mol Biol Evol 4:406-425.

Santos MD, Yasuike M, Kondo H, Hirono I, Aoki T (2007) A novel type-1 cytokine receptor from fish involved in the Janus kinase/Signal transducers and activators of transcription (Jak/STAT) signal pathway. Mol Immunol 44:3355-3363.

Scheller J, Chalaris A, Schmidt-Arras D, Rose-John S (2011) The pro- and anti-inflammatory properties of the cytokine interleukin-6. Biochim Biophys Acta 1813:878-888.

Schirmacher P, Peters M, Ciliberto G, Blessing M, Lotz J, zum Büschenfelde KM, Rose-John S (1998) Hepatocellular hyperplasia, plasmacytoma formation, and extramedullary hematopoiesis in interleukin (IL)-6/soluble IL-6 receptor double-transgenic mice. Am J Pathol 153:639–648.

Schooltinck H, Schmitz-Van de Leur H, Heinrich PC Rose-John S (1992) Up-regulation of the interleukin-6-signal transducing protein (gp130) by interleukin-6 and dexamethasone in HepG2 cells. FEBS Lett 297:263–265.

Snyers L and Content J (1992) Enhancement of IL-6 receptor β chain (gp130) expression by IL-6, IL-1 and TNF in human epithelial cells. Biochem Biophys Res Commun 185:902-908.

Spooren A, Kolmus K, Laureys G, Clinckers R, De Keyser J, Haegeman G, Gerlo S (2011) Interleukin-6, a mental cytokine. Branin Res Rev 67:157-183.

Strauss WM (2001) Preparation of genomic DNA from mammalian tissue. In: Coligan JE, Bieres B, Margulies DH, Schevach EM, Strober W, Coico R (Eds), Protoc Immunol.

Szelényi J (2001) Cytokines and the central nervous system. Brain Res Bull:54, 329-338.

Taga T, Fukuda S (2005) Role of IL-6 in the neural stem cell differentiation. Clin Rev Allergy Immunol 28:249-256.

Tamura K, Peterson D, Peterson N, Stecher G, Nei M, Kumar S (2011) MEGA5: Molecular Evolutionary Genetics Analysis using Maximum Likelihood, Evolutionary Distance, and Maximum Parsimony Methods. Mol. Biol. Evol 28:2731-2739.

Thisse C and Thisse B (2008) High-resolution in situ hybridization to whole-mount zebrafish embryos. Nat Protoc 3:59-69.

Vallières L and Rivest S (1997) Regulation of the Genes Encoding Interleukin-6, Its Receptor, and gpl3O in the Rat Brain in Response to the Immune Activator Lipopolysaccharide and the Proinflammatory Cytokine Interleukin-1ß. J Neurochem 69:1668-1683.

Wallenius V, Wallenius K, Ahrén B, Rudling M, Carlsten H, Dickson SL, Ohlsson C, Jansson J (2002) Interleukin-6-deficient mice develop mature-onset obesity. Nat Med 8:75-79.

Westerfield M (2000) The Zebrafish Book; A Guide for the Laboratory Use of Zebrafish (Danio rerio). Eugene, OR: University of Oregon Press.

Yoshida K, Taga T, Saito M, Suematsu S, Kumanogoh A, Tanaka T, Fujiwara H, Hirata M, Yamagami T, Nakahata T, Hirabayashi T, Yoneda Y, Tanaka K, Wang WZ, Mori C, Shiota K, Yoshida N, Kishimoto T (1996) Targeted disruption of gp130, a common signal transducer for the interleukin 6 family of cytokines, leads to myocardial and hematological disorders. Proc Natl Acad Sci USA 93:407-411.

Zhang Y (2007) Template-based modeling and free modeling by I-TASSER in CASP7. Proteins 69:108-117.

4.6. Supporting Information

Table S4.1. Oligonucleotide sequences.

IL6 characterisation		
Primer Name	**Primer sequence (5´→3´)**	**Amplicon (bp)**
IL6 ORFF	ATGCCATCCGCTCAGAGT	696
IL6 ORFR	TTAGTTCTTGTCAGCGCTGC	
IL6 gen1F	ATGCCATCCGCTCAGAGT	713
IL6 gen1R	GCGTCAGGTTTACTCACTT	
IL6 gen2F	TTTGCTTACAGAAGATTCAAG	1104
IL6 gen2R	ATATGGACAAACACAAACTGT	
IL6 gen3F	TCTTTATCAAATACGCAACAG	968
IL6 gen3R	CTTCCCTTTTTCCAGCATTT	
IL6 gen4F	GCTGAATCAACGCAATTCTT	379
IL6 gen4R	CTGTTAGTTCTTGTCAGCG	
qPCR		
Primer Name	**Primer sequence (5´→3´)**	**Amplicon (bp)**
IL6 F	TCAACTTCTCCAGCGTGATG	73
IL6 R	TCTTTCCCTCTTTTCCTCCTG	
IL6R F	GCCAACTGCAACATACCAAA	136
IL6R R	ACTGACAGCACGCAAAACTC	
gp130 F	TTCCTGTTCCTGAGCGTCTT	120
gp130 R	AGGTGACCAGTGGGCAATAG	
TNFα F	ACCAGGCCTTTTCTTCAGGT	148
TNFα R	GCATGGCTCATAAGCACTTGTT	
IL1β F	TTCCCCAAGTGCTGCTTATT	149
IL1βR	AAGTTAAAACCGCTGTGGTCA	
18S F	ACCACCCACAGAATCGAGAAA	97
18S R	GCCTGCGGCTTAATTTGACT	
***in situ* hybridisation**		
Primer Name	**Primer sequence (5´→3´)**	**Amplicon (bp)**
IL6 senseF	ACGATTAGGTGACACTATAGAAATGCCATCCGCTCAAGAAAAC	718
IL6 senseR	TTAGTTCTTGTCAGCGCTGC	
IL6 antisenseF	ATGCCATCCGCTCAGAAAAC	720
IL6 antisenseR	AGTTAATACGACTCACTATAGGGATTAGTTCTTGTCAGCGCTGC	
IL6R senseF	ACGATTTAGGTGACACTATAGAATGTGCCAACTGCAACATACC	717
IL6R senseR	AGTTGAGTACAGGGCTCATC	
IL6R antisenseF	TGTGCCAACTGCAACATACC	719
IL6R antisenseR	AGTTAATACGACTCACTATAGGGAAGTTGAGTACAGGGCTCATC	
gp130 senseF	ACGATTTAGGTGACACTATAGAACAGCACCTGTAAACAGAGTC	713
gp130 senseR	TTCTTCTGGTGGCACTTCCA	
gp130 antisenseF	CAGCACCTGTAAACAGAGTC	715
gp130 antisenseR	AGTTAATACGACTCACTATAGGGATTCTTCTGGTGGCACTTCCA	

Table S4.2. Protein sequences comparison among IL6 molecules.

Identities (%)								
	H. sapiens	*M. musculus*	*G. gallus*	*T. rubripes*	*P. olivaceus*	*S. aurata*	*O. mykiss*	***D. rerio***
H. sapiens	100	40.8	29	16.9	17.4	14.1	16.8	**15.1**
M. musculus		100	21.9	12.6	11.8	15.8	14.4	**12.5**
G. gallus			100	16.9	15.9	14.8	14.5	**17.7**
T. rubripes				100	45.2	49.6	23.6	**16.5**
P. olivaceus					100	47	23.4	**17.5**
S. aurata						100	21.4	**17.1**
O. mykiss							100	**21.5**

Similarities (%)								
	H. sapiens	*M. musculus*	*G. gallus*	*T. rubripes*	*P. olivaceus*	*S. aurata*	*O. mykiss*	***D. rerio***
H. sapiens	100	71.4	51	38.1	40.2	36	41.8	**33.6**
M. musculus		100	47.5	34.6	36.3	37.2	40.3	**31.4**
G. gallus			100	33.9	33.8	31.6	35.3	**34.6**
T. rubripes				100	64.2	66	46	**40**
P. olivaceus					100	62.6	47.2	**37.9**
S. aurata						100	42.3	**34.7**
O. mykiss							100	**43**

Chapter 5

Characterisation of 6 perforin genes in zebrafish (*Danio rerio*)

Published in:
Mónica Varela, Gabriel Forn-Cuní, Sonia Dios, Antonio Figueras and Beatriz Novoa
Journal of Innate Immunity 2015; DOI:10.1159/000431287

5.1. Introduction

Cytotoxic lymphocytes (CLs) comprise natural killer (NK) T cells and cytotoxic T lymphocytes (CTLs), which are cells that use their cytoplasmic granules to promote the cytolysis and apoptosis of target cells. Perforin plays a key role in secretory granule-dependent cell death, in defense against virus-infected and neoplastic cells (Thiery and Lieberman, 2014) and also in killing of other cells that are recognized as non-self by the immune system (Trapani and Smyth, 2002).

Perforin is expressed by CTLs and NK cells and forms pores in the membrane of target cells in the presence of calcium (Voskoboinik et al., 2002). These pores cause not only the osmotic lysis of target cells but also the entry of molecules such as granzymes. Effective induction of apoptosis by CLs requires both granzymes and perforin, although high concentrations of perforin alone can kill cells by necrosis (Keefe et al., 2005). Pore formation depends on the two characteristic domains of perforin: MACPF and CaLB (Lopez et al., 2012). The MACPF domain is also found in other molecules involved in the immune system, such as MPEG1 and complement components C6-C9. Furthermore, MPEG1, a protein produced exclusively by macrophages (Spilsbury et al., 1995), has recently been identified as the precursor of perforin (D´Angelo et al., 2012).

Knowledge about fish perforin genes is scarce, and these genes have only been characterized in 4 species (Hwang et al., 2004; Praveen et al., 2006; Athanasopoulou et al., 2009; Toda et al., 2011). Contrary to what occurs in higher vertebrates, fish species have more than one perforin gene in their genomes. As suggested by D'Angelo and collaborators (D´Angelo et al., 2012), this fact could imply the existence of multiple or different functions for fish perforin genes.

In the present study, we confirmed the existence of 6

perforin genes in zebrafish by sequencing and characterized these genes. We studied the evolution of these perforin genes, and we also determined their differential constitutive expression and response to different stimuli in different organs and cell types. Moreover, we studied the changes in these genes' expression throughout the first month of zebrafish development and their response to a systemic viral infection at 3 days post-fertilization (dpf). Our results could open doors to the study of possible new roles for fish perforins.

5.2. Material and Methods

Sequence retrieval and analysis

Zebrafish perforin sequences were searched by MACPF domain using the zebrafish genome assembly version Zv9 (www.ensembl.org/Danio_rerio/). Nine perforin genes were identified in the zebrafish genome using this method, but only 6 were selected for further analysis. The sequences were confirmed through PCR amplification using specific primers (Table S5.1) to obtain the full-length open reading frame (ORF) of each gene. The PCR products were subcloned into the pCR® 2.1 vector (Invitrogen) and transformed into One Shot TOP10F competent cells (Invitrogen) for subsequent sequencing and ORF confirmation. The confirmed sequences were submitted to GenBank under accession numbers KP099718-KP099723.

Identity and similarity analyses of the zebrafish perforin proteins were performed using MatGAT (Campanella et al., 2003). The domain distribution and signal peptide prediction were obtained using InterProScan 5 (Jones et al., 2014) and Phobius (Käll et al., 2004), respectively. The 3D structure of the zebrafish perforin proteins was predicted using the I-TASSER server (Roy et

al., 2010), selecting the model with the best C-score, and was viewed using PyMOL (http://www.pymol.org). The template modeling score (TM-score), a measure of structural similarity between two proteins, was also analyzed to identify structural analogs with known crystal architecture in the Protein Data Bank (PDB; http://www.rcsb.org/pdb/).

Phylogenetic tree and analysis of Darwinian selection

MPEG1, C6-C9 and PRF1 sequences were retrieved from the available published genomes in the Ensembl Genome Browser, version 75 (Flicek et al., 2012), and their phylogeny was studied as previously described by Forn-Cuní et al. (2014).

To identify gene duplications and loss events during the evolution of the PRF1 family, a reconciliation (Maddison, 1997; Page and Charleston, 1997) of the obtained gene tree with their species phylogeny was performed, in which divergence times among fish species were retrieved from the TimeTree database when possible and from other published studies when data were missing (Hedges et al., 2006; Sjostrand et al., 2012). The species tree was drawn with neighbor joining of the distance matrix using the R package APE v3.1-1 (Paradis et al., 2004). Finally, the most parsimonious reconciliation of the estimated gene tree and the species tree was performed with PrimeTV (Sennblad et al., 2007) and was manually represented using Adobe Illustrator CS6.

Animals

Adult RAG1$^{+/+}$ and RAG1$^{-/-}$ zebrafish and their larvae were obtained from our experimental facility, where the fish were cultured using established protocols (Westerfield, 2000; Nusslein-Volhard and Dahm, 2002). Eggs were obtained according to

protocols described in The Zebrafish Book (Westerfield, 2000) and maintained at 28.5°C in egg water (5 mM NaCl, 0.17 mM KCl, 0.33 mM $CaCl_2$, 0.33 mM $MgSO_4$, and 0.00005% methylene blue). Fish care and the challenge experiments were conducted according to the guidelines of the CSIC National Committee on Bioethics under approval number 07_09032012.

Fish challenge experiments

Adult zebrafish were intraperitoneally injected with 10 µL of 1 mg/mL LPS, 10 µL of 1 mg/mL poly I:C or 10 µL of PBS. Kidneys were sampled from anesthetized fish at 3, 6 and 24 hours post-stimulation (hps) and processed for gene expression analysis.

The Spring Viraemia of Carp Virus (SVCV) isolate 56/70 was propagated on EPC cells (ATCC CRL-2872) and titrated in 96-well plates. The TCID50/mL was calculated according to the protocol of Reed and Muench (1938). Adult zebrafish were intraperitoneally injected with 10 µL of $3 \cdot 10^6$ TCID50/mL. Zebrafish larvae were infected with SVCV through microinjection into the duct of Cuvier, as described in Benard et al. (2012), at 3 dpf. A total of 2 nL of a 1:20 dilution of the $3 \cdot 10^6$ TCID50/mL SVCV stock was microinjected per larva. PBS microinjection was used as a control in the experiments with larvae. To monitor the progression of the infection in larvae we checked by qPCR the SVCV N gene transcription and thhe *mx* gene (a and b paralogs) transcription (Figure S5.1.).

Kidney cell population sorting

Kidney leukocytes from adult fish were prepared for analysis and sorting based on forward and side scatter using a FACSCalibur flow cytometer (Becton Dickinson) equipped for cell

sorting, as described Traver et al. (2003). A total of 100,000 events were sorted from the regions corresponding to the myeloid (R2), lymphoid (R3) and precursor (R4) populations, pelleted by centrifugation at 4000*g* for 5 minutes at 4°C and processed for gene expression analysis. The cells from the total population (non-sorted) were also processed for RNA isolation. To confirm the identity of the 3 leukocyte fractions sorted by flow cytometry, specific cell markers (*marco* for macrophages, *mpx* for neutrophils, *cd4* and *cd8a* for T lymphocytes) were amplified by qPCR (Figure S5.2).

RNA isolation and gene expression

Total RNA was isolated using the Maxwell® 16 LEV simplyRNA Tissue Kit (Promega) and the automated Maxwell® 16 Instrument according to the manufacturer's instructions. cDNA synthesis using random primers and qPCR were performed as previously described (Varela et al., 2012). Pfaffl method was used to evaluate the efficiency of the primer pairs using serial 5-fold dilutions of cDNA and calculating the slope of the regression line of the cycle thresholds (Cts) versus the relative concentration of cDNA. The 18S gene was used as a housekeeping gene to normalize the expression values (primers specified in Table S5.1). Fold-change units were calculated by dividing the normalized expression values of infected larvae by the normalized expression values of the controls.

Statistical analysis

The results are expressed as the mean ± standard error. Significant differences were determined using one-way analysis of variance (ANOVA) followed by Tukey's multiple comparison test.

The differences were considered statistically significant when $p \leq 0.05$.

5.3. Results

Defining the complete repertoire of perforin genes in zebrafish

Using the zebrafish Ensembl Genome version Zv9, we identified 9 annotated perforin genes: *prf1.9p* (ENSDARG00000093777), *prf1.5* (ENSDARG00000037598), *prf1.3* (ENSDARG00000001572), *prf1.6* (ENSDARG00000024522), *prf1.2* (ENSDARG00000021444), *prf1.8* (ENSDARG00000089259), *prf1.7* (ENSDARG00000073969), *prf1* (ENSDARG00000060662) and *prf1.1* (ENSDARG00000030394). Of these, *prf1* and *prf1.1* were located on chromosome 3, *prf1.5* and *prf1.6* were located on chromosome 8, and the other 5 perforins were located on chromosome 19 (Figure 5.1). Of the perforin genes situated on chromosome 19, *prf1.9p* was identified in the database as a pseudogene, so we decided to remove it from the characterization. Furthermore, amplifications obtained for the *prf1.8* gene did not produce a complete protein, and therefore, this gene was also discarded from the characterization. In addition, *prf1.7* was 100% identical (CDS and UTRs) to *prf1.2* and indistinguishable by PCR. Although this finding could have been due to gene duplication, we could not rule out a certain type of error during the assembly of this region of the genome. We only considered *prf1.2*. In summary, after confirming all of the perforin sequences, we performed our study on 6 perforin genes, which were renamed according to their chromosomal positions: *prf3a* and *prf3b* (on chromosome 3), *prf8a* and *prf8b* (on chromosome 8), and *prf19a* and *prf19b* (on chromosome 19) (Figure 5.1).

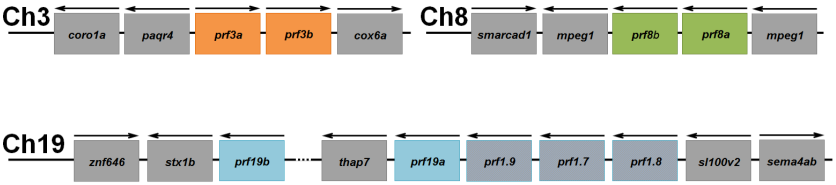

Figure 5.1. Perforin sequences location. Gene location of perforin sequences on zebrafish chromosomes 3, 8 and 19.

Sequence analysis and structural domains

The study of the domain structure of the 6 perforin genes revealed the presence of the two characteristic domains: MACPF and CaLB (Figure 5.2). The zebrafish perforin genes had an amino acid number between 516 and 588, with the perforins on chromosome 8 being the shortest and the perforins on chromosome 3 being the longest. The variation in length sequences was mainly observable after the CaLB domain. Regarding the identity and similarity between the zebrafish perforins (Figure 5.2), the high values observed between Prf8a and Prf8b should be noted (85.9% and 74.7%, respectively). The perforin genes on chromosome 3 were also relatively similar, with 69.4% identity and 51.5% similarity. Prf19b showed identity values ranging between 59.2% and 54.1% with all perforin genes (similarity ranging between 38.7% and 33.2%), with Prf3a being the nearest perforin. We also examined the tridimensional predicted structure of the perforin proteins (Figure 5.3). The TM-scores observed for the zebrafish perforins revealed that the X-ray crystal structure of *Mus musculus* lymphocyte perforin was the best template for all of the proteins (TM-scores ranging between 0.92 and 0.98).

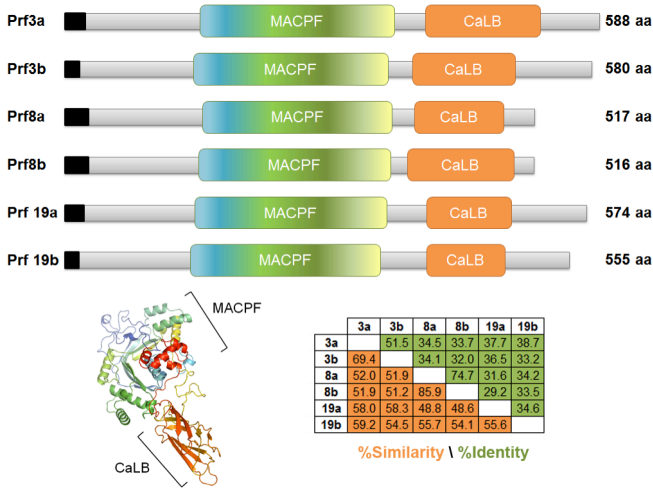

	3a	3b	8a	8b	19a	19b
3a		51.5	34.5	33.7	37.7	38.7
3b	69.4		34.1	32.0	36.5	33.2
8a	52.0	51.9		74.7	31.6	34.2
8b	51.9	51.2	85.9		29.2	33.5
19a	58.0	58.3	48.8	48.6		34.6
19b	59.2	54.5	55.7	54.1	55.6	

Figure 5.2. Zebrafish perforins structure and similarity/identity percentages. Domain structure of 6 perforin genes showing the signal peptide (black) and the MACPF and CaLB characteristic domains. The figure shows the position of these domains in a 3D reconstruction of a perforin molecule. The percentages of similarity (orange) and identity (green) between the zebrafish perforin genes are displayed in the chart.

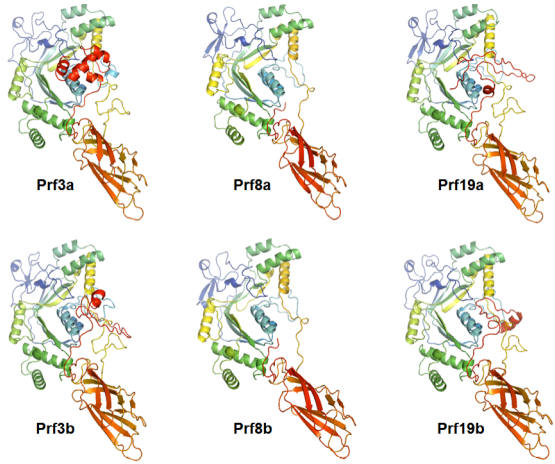

Figure 5.3. 3D reconstruction. 3D structure of zebrafish perforins predicted using the I-TASSER server, with selection of the model with the best C-score, and viewed using PyMOL.

Analysis of Darwinian selection and phylogenetic tree

We estimated the dN/dS ratios (ω) among the zebrafish perforin sequences to quantify the evolutionary pressure acting on the perforin genes and determined that there was no positive selection pressure (ω=0.35) (Figure 5.4A). The unreconciled gene tree (Figure S5.3) was not completely resolved, as one clade was found to be ambiguous: the *Latimeria chalumnae prf1.1* gene was found both on the vertebrate *PRF1* and grouped with the rest of the perforin genes in its genome. In subsequent analysis, we represented the topology concurrent with the vertebrate *PRF1* evolution. Phylogenetic reconciliation of the perforin gene tree with the fish species' evolution confirmed that this is a very dynamic gene family, with as many as 20 predicted gene duplications only in the fish lineage (Figure 5.4B). An invertebrate *MPEG1*-like gene (represented by *Crassostrea gigas* MPEG1 in this study) seems to be the most likely ancestral gene from which both the final components of the complement cascade and perforins evolved. Presumably, the C6-C9/PRF precursor originated in the chordate lineage, based on the presence of many C6-like genes in the *Ciona intestinalis* genome. No MACPF domain-containing genes were found in the European or Japanese lamprey's current genome. The earliest branching species with a *prf1* sequence was *Callorhinchus milii*, which suggests that perforins appeared during or after the 1R and 2R whole-genome duplications. It is important to note that based on similarity, zebrafish *prf19b* seems to be the 1-to-1 ortholog to both mammalian and shark *PRF1*. The analysis suggests that the ancestor of the zebrafish genes *prf19a/3a/3b* and *prf8a/8b* arose in this time frame from a duplication of the *prf19b* gene (Figure 5.5). Later, the Fish Genome Duplication (3R) differentiated *prf19a* and *prf3b*, whereas it was not until the *Danio rerio* and *Astyanax mexicanus* common ancestor that *prf3a* and

prf3b were duplicated. Finally, the duplication between *prf8a* and *prf8b* appears to be zebrafish specific.

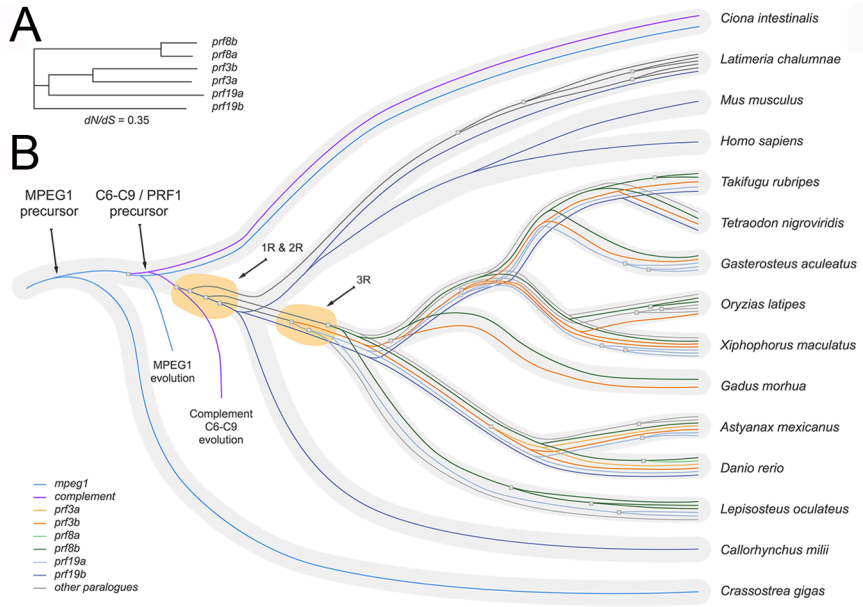

Figure 5.4. Darwinian selection and phylogenetic tree. A. The dN/dS ratio among the zebrafish perforin sequences was calculated to quantify the evolutionary pressure acting on these genes. B. Reconciliation of the PRF family within vertebrate evolution, focusing on the fish with sequenced genomes. The reconciliation suggests that the most probable time frame for the origination of the perforin gene was during or after the 1R and 2R genome duplication time frames. 3R indicates the fish-specific genome duplication.

Constitutive and tissue-specific expression of perforin genes

The presence of 6 perforin genes led us to investigate whether there was differential constitutive expression in 6 adult zebrafish tissues. The perforin genes on chromosome 8 (*prf8a* and *prf8b*) showed high basal expression in all analyzed tissues (Figure 5.6A). In contrast, the perforin genes on chromosomes 3 and 19 had differential expression between the compared tissues, with

prf3a and *prf19b* being the perforins with lower expression. When we compared the levels of perforins between the analyzed tissues, the gill and spleen were the tissues with higher perforin gene expression (Figure 5.6B).

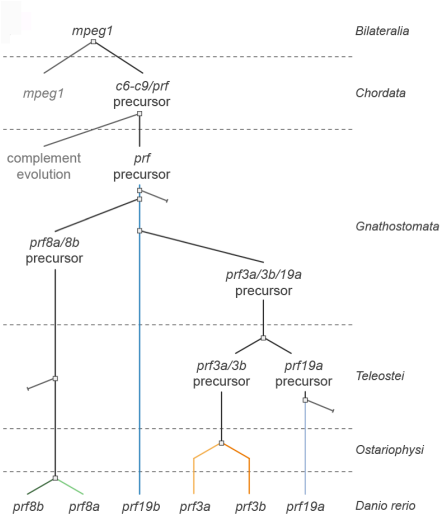

Figure 5.5. Schematic gene evolution. Schematic representation of the gene evolution of the studied zebrafish *prf* genes. The time frames represent the most recent taxonomic classification, in which the duplications (shown as squares) are predicted and the truncated lines represent other PRF paralogs not found in the zebrafish genome.

Regarding the relative proportions of the perforin genes' expression in the analyzed tissues, *prf8a* predominated in all analyzed tissues, with the exception of the muscle, in which *prf8b* expression was more present (Figure 5.6C). The presence of *prf19a* expression in the kidney and spleen was remarkable, representing 13% and 20%, respectively, of the total perforin gene expression. The expression of *prf19b* and *prf3a* was minimal in the kidney and gill.

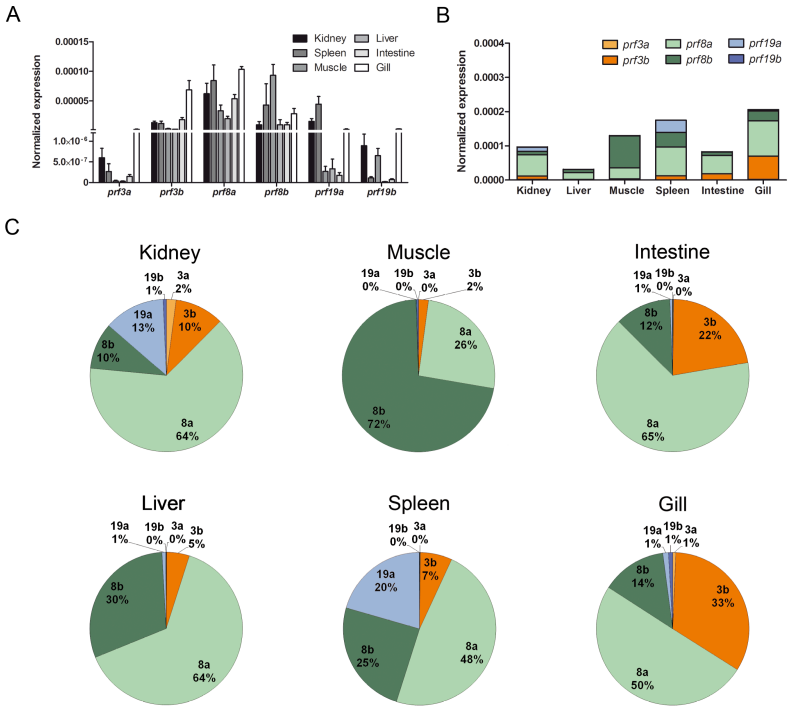

Figure 5.6. Constitutive tissue-specific expression. A. Normalized expression of zebrafish perforin genes in the kidney, spleen, muscle, liver, intestine and gill. The graphs represent the mean ± standard error of 4 independent biological replicates. B. Cumulative normalized expression of zebrafish perforin genes in different tissues. The relative expression of each perforin gene was normalized to the expression level of the 18S ribosomal RNA gene in the same tissue. C. Relative proportion (%) of the perforin transcripts in different zebrafish tissues.

Ontogeny of perforin genes in zebrafish larvae

We also analyzed the constitutive expression of the perforin genes during the ontogeny of larvae from 1 dpf to 29 dpf. We observed different expression patterns along the development of zebrafish larvae for different perforin genes (Figure 5.7A). The gene *prf3a* showed two peaks of expression throughout larval development, with the first at 1 dpf and the second at 23 dpf. The

gene *prf3b* showed the highest expression at 23 dpf, which was also observed for *prf19b*. It must be noted that *prf19b* also exhibited a great increase in expression between days 5 and 8. Moreover, in the case of *prf19a*, a peak of expression was evident at 5 dpf. Regarding the perforin genes located on chromosome 8, *prf8a* expression peaked at 2 dpf, and a considerable increase in expression was detected at 29 dpf in the case of *prf8b*. Considering the expression of all of the perforin genes over time, we found that the prevailing perforin was by far *prf8a* (Figure 5.7B).

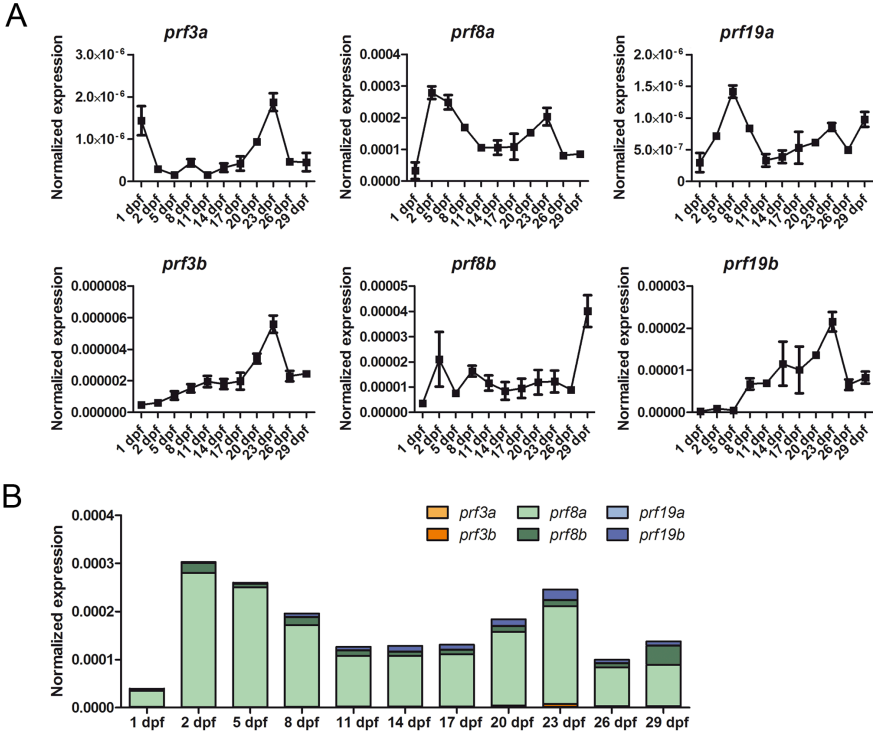

Figure 5.7. Perforin gene expression during zebrafish larvae ontogeny. A. Normalized expression of zebrafish perforin genes during the development of zebrafish larvae between 1 and 29 dpf. The graphs represent the mean ± standard error of 3 independent biological replicates. B. Cumulative normalized expression of perforin genes during the first month of larval life. The relative expression of each perforin gene was normalized to the expression level of the 18S ribosomal RNA gene in the same sample.

Perforin genes in adult kidney cell populations

Given the heterogeneous response observed among the 6 zebrafish perforin genes, we wanted to check the expression of these genes in different cell populations in the adult kidney. We separated the 3 principal cell populations in the kidney, the lymphoid, myeloid and precursor populations, by FACS (Figure 5.8A). The lymphoid population showed the highest perforin expression, highlighting in particular the presence of *prf8a* and *prf3b* (Figure 5.8B). Expression of the *prf3b* gene accounted for 1% and 2% of total perforin expression in the myeloid and precursor populations, respectively, in contrast to the 23% observed in the lymphoid population (Figure 5.8C). We also noted that *prf19b* was most represented in the myeloid and precursor populations, accounting for 18% and 15%, respectively, of total perforin expression. The *prf19b* was poorly represented in the lymphoid population, accounting for 1% of total perforin expression. This finding led us to suspect that there might be a functional difference between the 6 perforins.

RAG1$^{-/-}$ fish showed a different perforin expression pattern

Because the lymphoid population showed the highest perforin expression, we used mutant RAG1$^{-/-}$ fish, a line that has no mature T or B lymphocytes (Wienholds et al., 2002), to determine the existence of differential cellular expression among the 6 perforin genes within these mutants relative to RAG1$^{+/+}$ fish. Analyzing the amount of perforins in the kidney of RAG1$^{-/-}$ fish, we observed that the mutant expressed more perforin transcripts than the control fish did, with *prf3a* and *prf19a* expression being predominant (Figure 5.9A). The gene *prf3a* showed a 11-fold

change in expression in RAG1$^{-/-}$ compared with RAG1$^{+/+}$ fish, and *prf19a* expression increased nearly 60-fold (Figure 5.9B). Another gene that showed significantly higher expression in the mutant fish was *prf19b*. Only *prf8a* showed significantly lower expression in RAG1$^{-/-}$ fish.

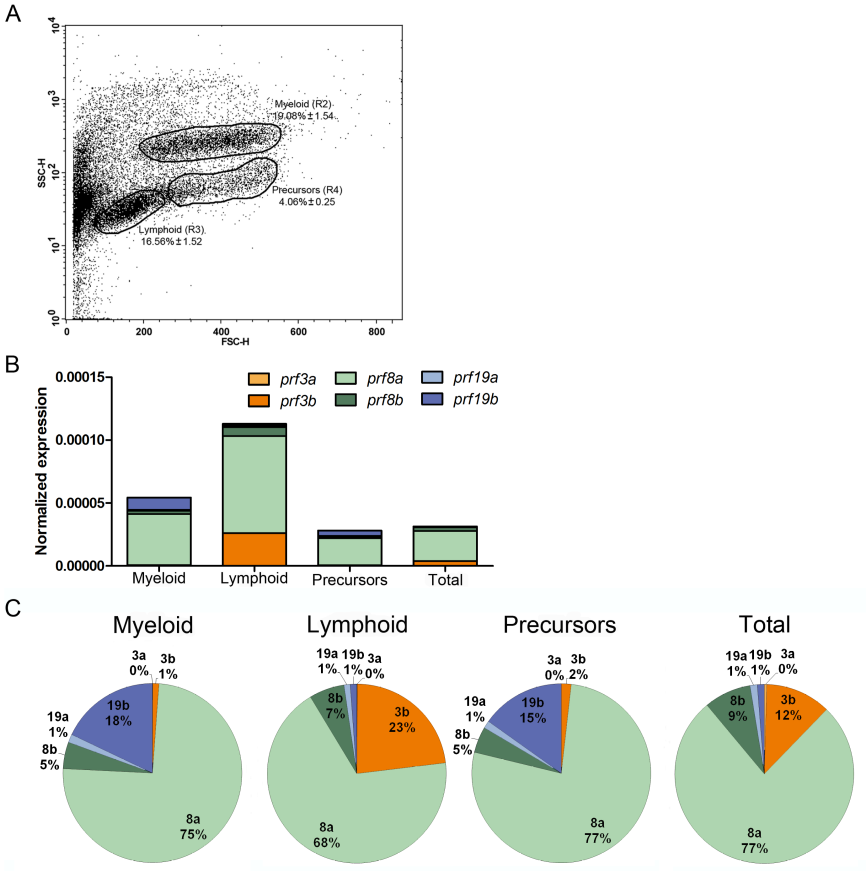

Figure 5.8. Perforin expression in adult kidney cell populations. A. Flow cytometry analysis of cell populations from the zebrafish kidney based on cell size (forward scatter; FSC-H: voltage E00/mode Lin) and granularity (side scatter; SSC-H: voltage 350/mode Log). R2, R3 and R4 represent the myeloid, lymphoid and precursor populations, respectively. B. Cumulative normalized expression of zebrafish perforin genes in the sorted cell populations from the kidney and in total (non-sorted) cells. The expression of each perforin was normalized to the expression of the 18S ribosomal RNA gene. C. Relative proportion (%) of the perforin transcripts in each population and in total cells.

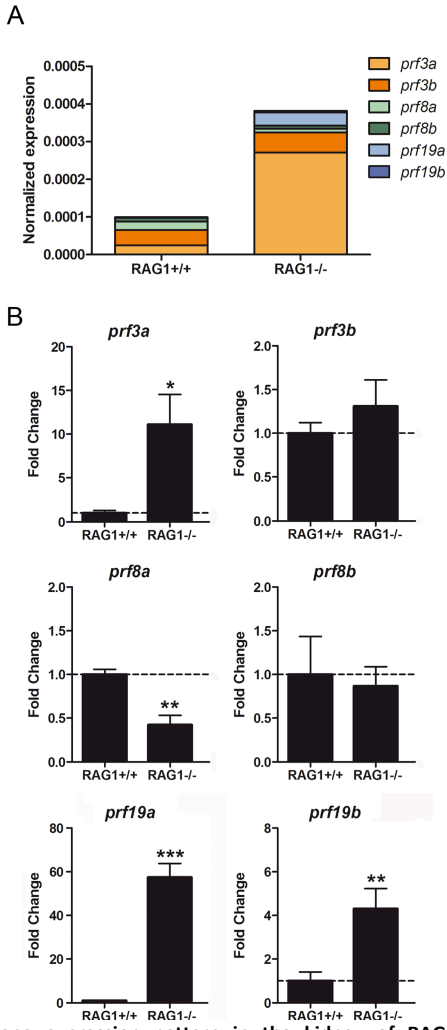

Figure 5.9. Perforin gene expression pattern in the kidney of RAG1$^{-/-}$ fish. A. Cumulative normalized expression of zebrafish perforin genes in RAG1$^{+/+}$ and RAG1$^{-/-}$ fish. The relative expression of each perforin gene was normalized to the expression level of the 18S ribosomal RNA gene in the same sample. B. Expression of each perforin gene in RAG1$^{+/+}$ and RAG1$^{-/-}$ fish. The fold change was calculated by dividing the normalized expression values in RAG1$^{-/-}$ zebrafish by the normalized expression values obtained in RAG1$^{+/+}$ zebrafish. The graphs represent the mean ± standard error of 4 independent biological replicates. The asterisks denote statistically significant differences with respect to the RAG1$^{+/+}$ group. Significant differences are displayed as ***(0.0001<p<0.001), **(0.001<p<0.01) or *(0.01<p<0.05).

Modulation of perforin genes upon a challenge in the adult kidney

Once we determined that the zebrafish perforins showed different tissue/cell expression profiles, we evaluated the *in vivo* effect of LPS, poly I:C and SVCV in the adult kidney at 3, 6 and 24 hours post-injection (hpi) (Figure 5.10). Again, *prf8a* and *prf8b* showed a similar response with all the stimuli used (Figure 5.10). The gene *prf3b* was up-regulated at 6 and 24 hpi with SVCV and LPS. *prf3a* was also up-regulated after SVCV and LPS injection, but at 3 and 6 hpi. Regarding *prf19a*, the inhibition induced after poly I:C administration and the up-regulation at 24 hpi induced by LPS were remarkable. The gene *prf19b* showed a curious pattern of expression, with a strong inhibition at 3 hours with any of the stimuli administered to the fish. Considering that the injection was intraperitoneal, this could be related with the migration of certain cell type in the kidney to the peritoneal cavity. Interestingly, the expression of *prf19b* increased to a 3-fold change with SVCV at 6 hours.

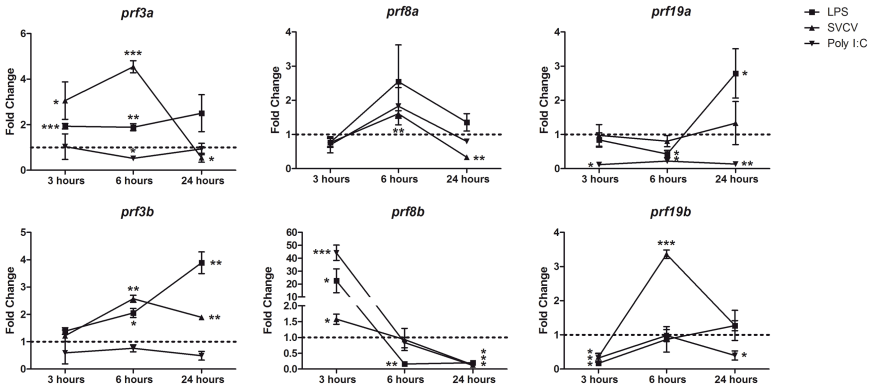

Figure 5.10. *In vivo* effect of LPS, poly I:C and SVCV in the adult kidney. Expression of perforin genes in the zebrafish adult kidney 3, 6 and 24 hours after challenge. The expression level of each gene was expressed as the fold change with respect to the levels detected in the control group (injected with PBS). The graphs represent the mean ± standard error of 4 independent biological replicates. The asterisks denote statistically significant differences with respect to the control group. Significant differences are displayed as ***(0.0001<p<0.001), **(0.001<p<0.01) or *(0.01<p<0.05).

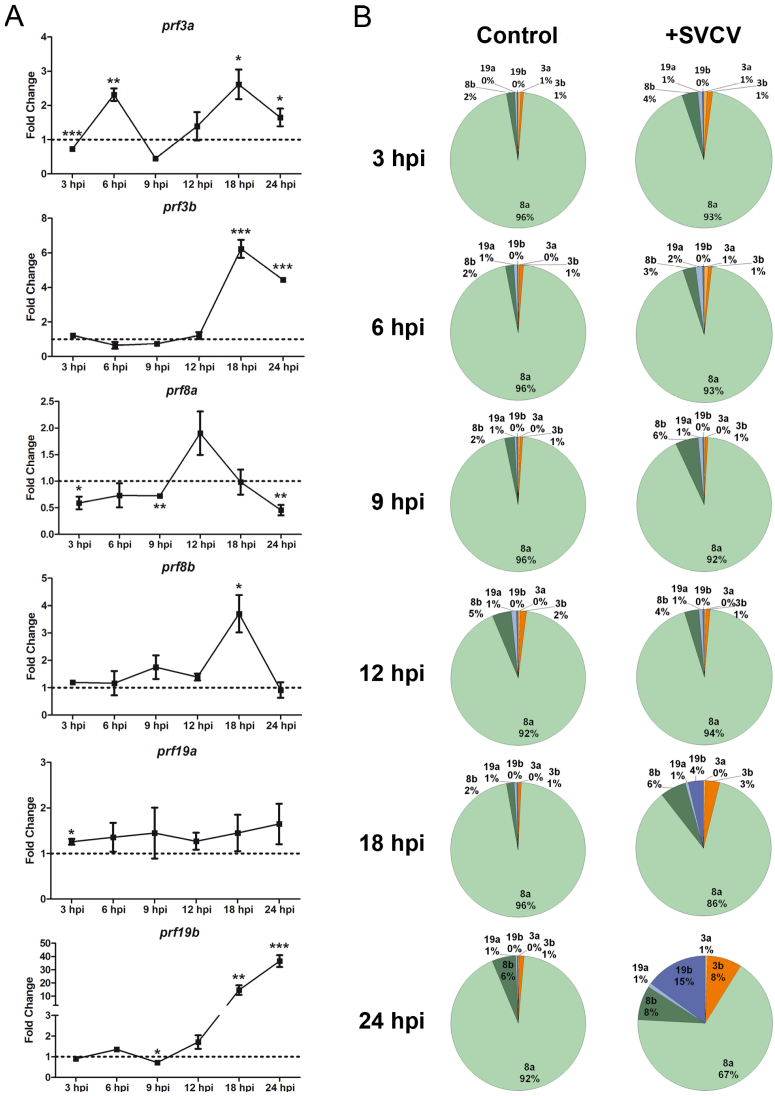

Figure 5.11. Perforin response in SVCV-infected larvae. A. Expression of perforin genes between 3 and 24 hpi with SVCV. The fold change was calculated by dividing the normalized expression values in infected larvae by the normalized expression values obtained in control individuals (injected with PBS). The graphs represent the mean ± standard error of 3 independent biological replicates. The asterisks denote statistically significant differences with respect to the control group. Significant differences are displayed as ***(0.0001<p<0.001), **(0.001<p<0.01) or *(0.01<p<0.05). B. Relative proportion (%) of perforin transcripts in zebrafish larvae during the SVCV challenge.

Perforin response in SVCV-infected larvae

We next investigated the role of perforin genes in the response against SVCV in zebrafish larvae with a time course infection experiment from 3 to 24 hpi comparing infected and non-infected fish. The expression profiles over time showed different perforin genes behavior during SVCV infection (Figure 5.11A). In general, perforin genes response against SVCV was not high, with the exception of *prf3b* and *prf19b* that showed a more robust response to the virus from 12 hpi. The gene *prf19a* was the only one that does not seem to respond to the virus. By plotting the percentage of each perforin over time during infection compared to uninfected fish, we observed the largest differences at 24 hpi (Figure 5.11B). At this point, *prf3b* and *prf19b* expression was higher (8% and 15% of the total, respectively) compared with expression in uninfected fish.

5.4. Discussion

In contrast to mammals, fish species possess more than one perforin gene in their genomes. We were able to confirm the existence of 6 perforin genes in zebrafish, located on chromosomes 3, 8 and 19. These genes possess the characteristic MACPF and CaLB domains, which are needed for pore formation in the plasma membrane of target cells (Law et al., 2010).

The phylogenetic analysis of the perforin gene family evolution in fish confirmed previous published results (D´Angelo et al., 2012): the perforin ancestor gene differentiated from MPEG1 via a common precursor of C6-C9 and PRF in the chordate lineage. Furthermore, the presence of C6-like genes and the absence of PRF in the *C. intestinalis* and *Ciona savignyi* genomes suggest that the complement gene family probably evolved first. As an update

to the referenced study, we found a partial *PRF1* sequence in the elephant shark genome, confirming the presence of *PRF1* in the Chondrichthyes lineage and its origin prior to the jawed vertebrates' evolution. However, the notable absence of any MACPF domain-containing gene in the sequenced lamprey genomes does not allow more precision in the analysis.

Our results suggest that *prf19b* probably evolved first from the common precursor of C6-C9 and PRF, corresponding to a 1-to-1 ortholog of mammalian *PRF1* and possibly being the ancestor gene. Undoubtedly, improvement in the currently published genomes and new species genome sequencing projects will help to support the conclusions drawn by the present study. Until then, it is advisable to be cautious when suggesting similar functions and inferring orthologous relationships with distant fish species, especially in such a highly dynamic and active gene family as perforins. Furthermore, deeper study of evolutionary events such as concerted evolution or site-specific selection pressure may help to explain the variability and evolution of this gene family**.**

As D'Angelo et al. (2012) wondered, the question is why fish require so many perforins in contrast to mammals, in which a single gene is enough for correct CL function. Our results indicate that the 6 zebrafish perforin genes were expressed under basal conditions in all analyzed tissues, contrary to what was reported in Japanese flounder and trout, in which perforin mRNA was not detected in liver samples (Hwang et al., 2004; Praveen et al., 2006). However, the tissue distribution was different for each perforin gene. Whereas certain genes, such as *prf8a*, showed broad expression across different tissues, other perforins were more tissue specific, such as *prf8b* in the muscle or *prf19a* in the spleen and kidney. These differential expression profiles were also detected to be constitutive during the first month of zebrafish larval development, suggesting possible functional differences or

different cellular locations. Cellular ontogeny in zebrafish is a well-characterized process (Zapata et al., 2006), and it is known that larvae do not acquire a completely functional immune system until the 4th to 6th week of development (Lam et al., 2004). This phenomenon may be related to the expression peaks observed around the fourth week of development in several of the zebrafish perforin genes.

When we analyzed the expression of the 6 perforin genes at the cellular level in the main hematopoietic tissue of fish, we confirmed that the perforins were expressed in the kidney lymphoid and myeloid cell populations. In mammals, perforin is primarily produced by NK cells and CTLs, but it is also expressed by human alveolar macrophages (Burnham et al., 2011). In zebrafish, as expected, the lymphoid population showed the highest perforin expression, with *prf3b* expression being the most remarkable, accounting for 23% of the total perforin expression in this population. In the myeloid population, *prf19b* expression was high, accounting for 18% of the total. This finding could be related to *prf19b* possible role as an ancestral perforin. This perforin might therefore be similar to *mpeg1*, which is expressed mainly in macrophages (Ellet et al., 2011). Interestingly, rainbow trout perforin is also induced in the monocyte/macrophage-like RTS-11 cell line after VHSV infection (Ordás et al., 2011), suggesting that teleost perforins are commonly expressed in the myeloid cell population. These results also agreed with our results obtained in $RAG1^{-/-}$ mutant zebrafish, which have a reduced lymphocyte-like cell population (Hohn and Petrie-Hanson, 2012). $RAG1^{-/-}$ fish have more perforin mRNAs in the kidney than $RAG1^{+/+}$ fish do, including more expression of *prf19b*, which is probably related to their increased myelomonocyte population compared with that of $RAG1^{+/+}$ fish (Petrie-Hanson et al., 2009). This finding again

suggests that *prf19b* could be more specific to the myeloid population.

The evaluation of the *in vivo* effects of LPS, poly I:C and SVCV in kidney cells showed us different response patterns among the zebrafish perforin genes. Several of the perforin genes seemed to respond in the same way, independently of the stimuli used, but the *prf19b* response appeared to be more stimulus specific because there was a significant increase in its expression after infection with a viral pathogen. After systemic infection with the rhabdovirus SVCV, zebrafish larvae modulated their perforin gene expression, with a particular increase in *prf3b* and *prf19b* expression toward the end of the infection.

From our results, we can conclude that *prf19b*, which appeared to be differentially expressed in the myeloid cell population, is probably the perforin gene that is closest to the macrophage *MPEG1* gene and is therefore the putative perforin ancestor. Interestingly, this gene was the main one that responded to viral infection both in adult kidney and after systemic infection of zebrafish larvae.

The perforin identified as a perforin precursor in our study, *prf19b*, retained an expression pattern similar to that of *MPEG1*, the gene from which the perforin family evolved. Perforin genes arising subsequently showed different expression patterns which, as in the case of *prf3b*, were more similar to the results expected based on the data available for humans. It seems that the diversification that occurred during the evolution of this family probably affected the functionality and cellular localization among species.

5.5. References

Athanasopoulou S, Marioli D, Mikrou A, Papanastasiou AD, Zarkadis IK (2009) Cloning and characterization of the trout perforin. Fish Shellfish Immunol 26:908-912.

Benard EL, van der Sar AM, Ellett F, Lieschke GJ, Spaink HP, Meijer AH (2012) Infection of zebrafish embryos with intracellular bacterial pathogens. J Vis Exp 61:e3781.

Burnham EL, Phang TL, House R, Vandivier RW, Moss M, Gaydos J (2011) Alveolar macrophage gene expression is altered in the setting of alcohol use disorders. Alcohol Clin Exp Res 35:284-294.

Campanella JJ, Bitincka L, Smalley J (2003) MatGAT: an application that generates similarity/identity matrices using protein or DNA sequences. BMC Bioinformatics 4:29.

D´Angelo ME, Dunstone MA, Whisstock JC, Trapani JA, Bird PI (2012) Perforin evolved from a gene duplication of MPEG1, followed by a complex patern of gene gain and loss within Euteleostomi. BMC Evol Biol 12:59.

Ellett F, Pase L, Hayman JW, Andrianopoulos A, Lieschke GJ (2011) mpeg1 promoter transgenes direct macrophage-lineage expression in zebrafish. Blood 117:e49-56.

Flicek P, Amode MR, Barrell D, Beal K, Brent S, Carvalho-Silva D, Clapham P, Coates G, Fairley S, Fitzgerald S, Gil L, Gordon L, Hendrix M, Hourlier T, Johnson N, Kahari AK, Keefe D, Keenan S, Kinsella R, Komorowska M, Koscielny G, Kulesha E, Larsson P, Longden I, McLaren W, Muffato M, Overduin B, Pignatelli M, Pritchard B, Riat HS, Ritchie GRS, Ruffier M, Schuster M, Sobral D, Tang YA, Taylor K, Trevanion S, Vandrovcova J, White S, Wilson M, Wilder SP, Aken BL, Birney E, Cunningham F, Dunham I, Durbin R, Fernandez-Suarez XM, Harrow J, Herrero J, Hubbard TJP, Parker A, Proctor G, Spudich G, Vogel J, Yates A, Zadissa A, Searle SMJ (2012) Ensembl 2012. Nucleic Acids Res 40:D84–D90.

Forn-Cuní G, Reis ES, Dios S, Posada D, Lambris JD, Figueras A, Novoa B (2014) The evolution and appearance of C3 duplications in fish originate an exclusive teleost c3 gene form with anti-inflammatory activity. PLoS One 9:e99673.

Hedges SB, Dudley J, Kumar S (2006) TimeTree: a public knowledge-base of divergence times among organisms. Bioinformatics 22:2971–2972.

Hohn C and Petrie-Hanson L (2012) Rag1−/− Mutant Zebrafish Demonstrate Specific Protection following Bacterial Re-Exposure. PLoS One 7:e44451.

Hwang JY, Ohira T, Hirono I, Aoki T (2004) A pore-forming protein, perforin, from a non-mammalian organism, Japanese flounder, Paralichtys olivaceus. Immunogenetics 56:360-367.

Jones P, Binns D, Chang HY, Fraser M, Li W, McAnulla C, McWilliam H, Maslen J, Mitchell A, Nuka G, Pesseat S, Quinn AF, Sangrador-Vegas A, Scheremetjew M, Yong SY, Lopez R, and Hunter S (2014) InterProScan 5: genome-scale protein function classification. Bioinformatics 30:1236-1240.

Käll L, Krogh A, Sonnhammer EL (2004) A Combined Transmembrane Topology and Signal Peptide Prediction Method. J Mol Biol 338:1027-1036.

Keefe D, Shi L, Feske S, Massol R, Navarro F, Kirchhausen T, Lieberman J (2005) Perforin Triggers a Plasma Membrane-Repair Response that Facilitates CTL Induction of Apoptosis. Immunity 23:249-262.

Lam SH, Chua HL, Gong Z, Lam TJ, Sin YM (2004) Development and maturation of the immune system in zebrafish, Danio rerio: a gene expression profiling, in situ hybridization and immunological study. Dev Comp Immunol 28:9-28.

Law RH, Lukoyanova N, Voskoboinik I, Caradoc-Davies TT, Baran K, Dunstone MA, D´Angelo ME, Orlova EV, Coulibaly F, Verschoor S, Browne KA, Ciccone A, Kuiper MJ, Bird PI, Trapani JA, Saibil HR, Whisstock JC (2010) The structural basis for membrane binding and pore formation by lymphocyte perforin. Nature 468:447-451.

Lopez JA, Brennan AJ, Whisstock JC, Voskoboinik I, Trapani JA (2012) Protecting a serial killer: pathways for perforin trafficking and self-defence ensure sequential target cell death. Trends Immunol 33:406-412.

Maddison WP (1997) Gene trees in species trees. Systematic Biology 46:523–536.

Nusslein-Volhard C and Dahm R (2002) Zebrafish, a practical approach, ed 1. Oxford University Press, Oxford.

Ordás MC, Cuesta A, Mercado L, Bols NC, Tafalla C (2011) Viral hemorrhagic septicaemia virus (VHSV) up-regulates the cytotoxic activity and the perforin/granzyme pathway in the rainbow trout RTS11 cell line. Fish Shellfish Immunol 31:252-259.

Page RD, and Charleston MA (1997) From gene to organismal phylogeny: reconciled trees and the gene tree/species tree problem. Molecular phylogenetics and evolution 7:231–240.

Paradis E, Claude J, Strimmer K (2004) APE: Analyses of Phylogenetics and Evolution in R language. Bioinformatics 20:289–290.

Petrie-Hanson L, Hohn C, Hanson L (2009) Characterization of rag1 mutant zebrafish leukocytes. BMC Immunol 10:8.

Praveen K, Leary JH 3rd, Evand DL, Jaso-Friedmann L (2006) Nonspecific cytotoxic cells of teleosts are armed with multiple granzymes and other components of the granule exocytosis pathway. Mol Immunol 43:1152-1162.

Reed LJ and Muench H (1938) A simple method for estimating fifty percent endpoints. Am J Epidemiol 27:493-497.

Roy A, Kucukural A, Zhang Y (2010) I-TASSER: a unified platform for automated protein structure and function prediction. Nat Protoc 5:725–738.

Sennblad B, Schreil E, Berglund Sonnhammer, AC, Lagergren J, Arvestad L (2007) primetv: a viewer for reconciled trees. BMC Bioinformatics 8:148.

Sjostrand J, Sennblad B, Arvestad L, Lagergren J (2012) DLRS: Gene tree evolution in light of a species tree. Bioinformatics 28:2994–2995.

Spilsbury K, O´Mara MA, Wu WM, Rowe PB, Symonds G, Takayama Y (1995) Isolation of a novel macrophage-specific gene by differential cDNA analysis. Blood 85:1620-1629.

Thiery J and Lieberman J (2014) Perforin: A Key Pore-Forming Protein for Immune Control of Viruses and Cancer. Subcell Biochem 80:197-220.

Toda H, Araki K, Moritomo T, Nakanishi T (2011) Perforin-dependent cytotoxic mechanism in killing by CD8 positive T cells in ginbuna crucian carp, Carassius auratus langsdorfii. Dev Comp Immunol 35:88-93.

Trapani JA and Smyth MJ (2002) Functional significance of the perforin/granzyme cell death pathway. Nat Rev Immunol 2:735-747.

Traver D, Paw BH, Poss KD, Penberthy WT, Lin S, Zon LI (2003) Transplantation and in vivo imaging of multilineage engraftment in zebrafish bloodless mutants. Nat Immunol 4:1238-1246.

Varela M, Dios S, Novoa B, Figueras A (2012) Characterisation, expression and ontogeny of interleukin-6 and its receptors in zebrafish (*Danio rerio*). Dev Comp Immunol 37:97-106.

Voskoboinik I, Smyth MJ, Trapani JA (2002) Perforin-mediated target-cell death and immune homeostasis. Nat Rev Immunol 6:940-952.

Westerfield M (2000) The zebrafish book. A guide for the laboratory use of zebrafish (Danio rerio), ed 4. University of Oregon Press, Eugene.

Wienholds E, Merker SS, Walderich B, Plasterk RHA (2002) Target-Selected inactivation of the Zebrafish rag1 Gene. Science 297:99–101.

Zapata A, Diez B, Cejalvo T, Gutiérrez-de Frías C, Cortés A (2006) Ontogeny of the immune system of fish. Fish Shellfish Immunol 20:126-136.

5.6. Supporting Information

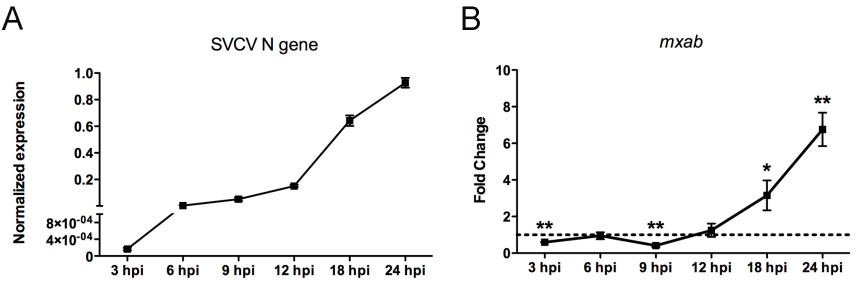

Figure S5.1. SVCV systemic infection course in zebrafish larvae. A. Relative quantification of SVCV N gene transcripts as a measure of the viral load in the larvae during the course of infection. Three biological replicates were used to calculate the means ± standard error of the mean. B. Relative quantification of *mxab* gene expression as a measure of the IFN response induced by the virus during the course of infection. Samples were obtained from infected larvae at different times post-infection. To avoid differences due to the larval development stage. The samples were standardized with respect to an uninfected control of the same age. Three biological replicates were used to calculate the means ± standard error of the mean. Significant differences were displayed as ** ($0.001<p<0.01$) or * ($0.01<p<0.05$).

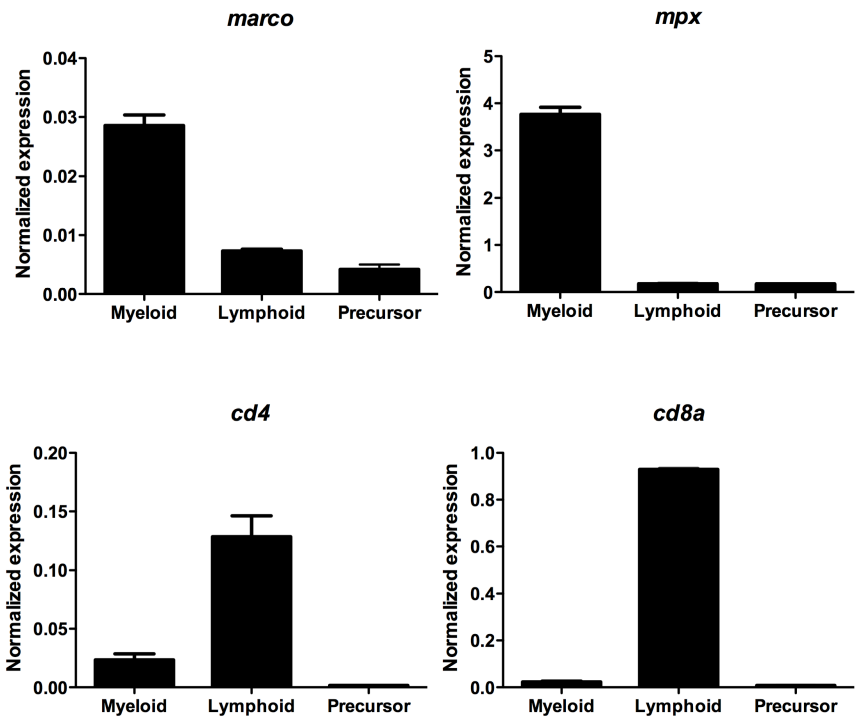

Figure S5.2. Cell markers analysis of zebrafish kidney populations. Expression level of *marco* (macrophages), *mpx* (neutrophils), *cd4* and *cd8a* (T lymphocytes). Three biological replicates were used to calculate the means ± standard error of the mean.

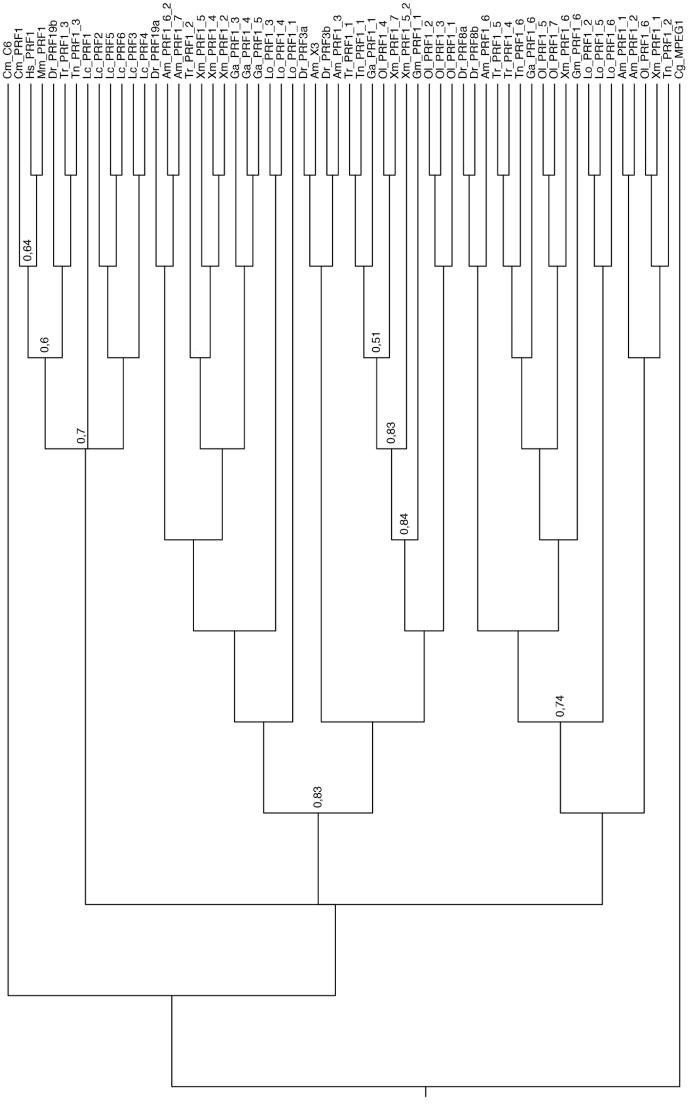

Figure S5.3. Unreconciled tree

Table S5.1. Oligonucleotide sequences.

Perforin genes characterisation		
Primer Name	**Primer sequence (5´→3´)**	**Amplicon (bp)**
PRF3a F	ATGGTTCCTGTAGCTCTA	1797
PRF3a R	AGATTTACGAGAGACTAGCA	
PRF3b F	ATGAGGGCTGGATTGTTTTT	1743
PRF3b R	CTACAAAACTGTATTATTGTAAT	
PRF8a F	ATGGACACCAATAAATGTGT	1554
PRF8a R	GATATTCACCAAAACTGTGA	
PRF8b F	GCATACTCAGTGTGGACATG	1631
PRF8b R	TCAATGCTACACAACCACACC	
PRF19a F	ATGAGGCACGTACCAGTTT	1725
PRF19a R	TTACAGCATCAAGAGCTTTC	
PRF19b F	GTGAGCTACTGAGCAAACTG	1752
PRF19b R	TTAAAGGAAGGACATATCTCTTT	
qPCR		
Primer Name	**Primer sequence (5´→3´)**	**Amplicon (bp)**
PRF3a F	GGTTCCTGTAGCTCTACTGT	257
PRF3a R	GCTTCTGCTTTTCGTTCTGC	
PRF3b F	ACCTTCTCTTGCCTGTTGTG	211
PRF3b R	AAAGCTCCGTCCATATAGGG	
PRF8a F	GTTTCCCTCACATTCCTTTG	202
PRF8a R	TACCGTTGTCTATGTGTGAC	
PRF8b F	CTTTGTGTTTGGTGCTCTGG	280
PRF8b R	GTAGAAGGCTGTGCTGTAGT	
PRF19a F	TGAGGCACGTACCAGTTTAC	177
PRF19a R	TCACGTAAGTACCTTTGCGC	
PRF19b F	ATGGCTCTCCTTCTGTTGCT	164
PRF19b R	ACACCACCACAAAGCGTCC	
IL1β F	TTCCCCAAGTGCTGCTTATT	205
IL1β R	AAGTTAAAACCGCTGTGGTCA	
CASPa F	AAAAGGAGCGGCTCAGAGAA	149
CASPa R	CACCCATAATGGCGTCTCTT	
18S F	ACCACCCACAGAATCGAGAAA	97
18S R	GCCTGCGGCTTAATTTGACT	

Chapter 6

SVCV Systemic Infection in Zebrafish Larvae as a Model of Hemorrhagic Disease

Published in:
-Mónica Varela, Alejandro Romero, Sonia Dios, Michiel van der Vaart, Antonio Figueras, Annemarie H. Meijer, Beatriz Novoa
Journal of Virology 2014; 88(20):12026-12040

6.1. Introduction

Endothelial cells and leukocytes are at the front line of defense against pathogens. Most infectious pathogens have some relationship with the endothelium, although not all pathogens are true endothelial invading organisms (Valbuena and Walker, 2006). Infections can produce large changes in endothelial cells function, particularly in relation to inflammation. Inflammatory stimuli can activate endothelial cells, which secrete cytokines and chemokines. Moreover, the importance of endothelial cells in the regulation of leukocyte transmigration to the site of inflammation has given these cells a major role in immunity (Muller, 2003).

Host-pathogen interactions are essential for the modulation of immunity (Lupfer and Kanneganti, 2012). The presence of a pathogen alters the immune balance prevailing in a host under normal conditions causing the appearance of diseases, which lead to the death of the host if it is not able to control the infection. Clear examples of these effects are evident in viral hemorrhagic fevers, in which an understanding of the relative pathogenic roles of the viral agent and the host response to the infection is crucial (Paessler and Walker, 2013). Hemorrhagic manifestations are characteristic of these fevers, which have historically been associated with endothelium infections. Currently, many pathogens causing hemorrhagic diseases do not infect endothelial cells as the primary target (Valbuena and Walker, 2006). Indeed, macrophages and dendritic cells are targets for some hemorrhagic viruses, such as Ebola Virus (Bray and Geisbert, 2005) or Dengue Virus (Halstead et al., 1977; Aye et al., 2014).

Most of the research regarding interactions between viruses and host cells has been performed in cell lines that might not be major targets during natural infections (Mercer and Greber, 2013), making it difficult to characterize the behavior of pathogens in individuals and reducing the likelihood of discovering an

effective therapeutic target. The lack of a good animal model in which the infection can be followed from the beginning and in the context of the whole organism has contributed to these difficulties. Zebrafish (*Danio rerio*) provide advantages, as these organisms exhibit rapid development, transparency and a high homology between its genome and the human one (Howe et al., 2013). Furthermore, the existence of mutant and transgenic fish lines and the potential use of reverse genetics techniques, such as the injection of antisense morpholino oligonucleotides or synthetic mRNA, make zebrafish a useful tool for the study of host-pathogen interactions.

No naturally occurring viral infections have been characterized for zebrafish (Crim and Riley, 2012). Moreover, the experimental susceptibility of zebrafish to viral infections has been demonstrated with other fish viruses (Encinas et al., 2010; López-Muñoz et al., 2010; Ludwig et al., 2011) and also with mammalian viruses (Burgos et al., 2008; Hubbard et al., 2010; Palha et al., 2013).

We used the rhabdovirus Spring Viraemia of Carp Virus (SVCV) as a viral model to show the potential of the zebrafish in host-pathogen interaction studies. SVCV predominantly affects cyprinid fish and causes important economical losses and mortalities worldwide (Ahne et al., 2002; Taylor et al., 2013). Affected fish exhibit destruction of tissues, such as kidney or spleen, leading to hemorrhage and death. However, little is known about the infection mechanism of this enveloped RNA virus.

Thus, the main objective of the present study was to improve the knowledge of the pathology generated by SVCV, as an example of hemorrhagic virus, focusing on interactions between the virus and host cells at early stages of the infection in zebrafish larvae.

6.2. Material and Methods

Ethics statement

The protocols for fish care and the challenge experiments were reviewed and approved by the CSIC National Committee on Bioethics under approval number 07_09032012. Experiments were conducted in fish larvae before independently feeding and therefore, before an ethical approval is required (EU directive 2010_63).

Animals

Homozygous embryos and larvae from wild-type zebrafish and transgenic line Tg(Fli1a:eGFP)y1, that labels endothelial cells, were obtained from our experimental facility, where the zebrafish were cultured using established protocols (Westerfield, 2000; Nüsslein-Volhard and Dahm, 2002). The eggs were obtained according to protocols described in The Zebrafish Book (Westerfield, 2000) and maintained at 28.5˚C in egg water (5 mM NaCl, 0.17 mM KCl, 0.33 mM CaCl2, 0.33 mM MgSO4, and 0.00005% methylene blue), and 0.2 mM N-phenylthiourea (PTU; Sigma) was used to prevent pigment formation from 1 days post-fertilization (dpf).

Virus and infection

The SVCV isolate 56/70 was propagated on epithelioma papulosum cyprini (EPC) carp cells (ATCC CRL-2872) and titrated in 96-well plates. The plates were incubated at 15°C for 7 days and examined for cytophathic effects each day. After the observation of the cells under the microscope, the virus dilution causing

infection of 50% of the inoculated cell line (TCID50) was determined using the Reed-Müench method (Reed and Muench, 1938).

The fish larvae were infected through microinjection into the duct of Cuvier as described in Benard et al. (2012) at 2 or 3 dpf. SVCV was diluted to the appropriate concentration in PBS with 0.1% phenol red (as a visible marker to the injection of the solution into the embryo) just before the microinjection of 2 nl of viral suspension per larvae. The infections were conducted at 23˚C. SVCV was heat-killed at 65ºC during 20 minutes.

Imaging

Images of the signs and videos of the blood flow were obtained using an AZ100 microscope (Nikon) coupled to a DS-Fi1 digital camera (Nikon). Confocal images of live or fixed larvae were captured using a TSC SPE confocal microscope (Leica). The images were processed using the LAS-AF (Leica) and ImageJ software. The 3D reconstructions and the volume clipping were performed using Image Surfer (http://imagesurfer.cs.unc.edu/) and LAS-AF (Leica), respectively.

Immunohistochemistry

Whole-mount immunohistochemistry was performed as previously described (Cui et al., 2011). The following primary antibodies and dilutions were used: L-plastin (rabbit anti-zebrafish, 1:500, kindly provided by Dr. Paul Martin); SVCV (mouse anti-SVCV, 1:500; BioX Diagnostics). The secondary antibodies used were Alexa 488 anti-rabbit, Alexa 546 anti-rabbit or Alexa 635 anti-mouse (Life Technologies), all diluted 1:1000.

Real-Time PCR

Total RNA was isolated from snap-frozen larvae using the Maxwell® 16 LEV simply RNA Tissue kit (Promega) with the automated Maxwell® 16 Instrument according to the manufacturer's instructions. cDNA synthesis using random primers and qPCR were performed as previously described (Varela et al., 2012). 18S was used as a housekeeping to normalize the expression values. Gene expression ratio was calculated by dividing the normalized expression values of infected larvae by the normalized expression values of the controls. Table S6.1 in supplemental material shows the sequences of the primer pairs used. Two independent experiments, of 3 biological replicates each, were performed.

Microangiography

Tetramethylrhodamine dextran ($2x10^6$ MW, Life Technologies) was injected into the caudal vein of anesthetized zebrafish Tg(Fli1a-GFP) embryos at 24 hours post-infection (hpi). The images were acquired within 30 min after injection.

TUNEL assay

The TUNEL assay was performed using the In Situ Cell Death Detection Kit, TMR red or POD (Roche) as previously described (Espín et al., 2013).

In vivo acridine orange staining

For acridine orange staining, larvae were incubated for 2 hours in 10 µg/ml acridine orange solution followed by washing for 30 min.

Statistical analysis

Kaplan-Meier survival curves were analyzed with a Log-rank (Mantel Cox) test. The neutrophil count and qPCR data were analyzed using one-way analysis of variance and Tukey's test, and differences were considered significant at $p<0.05$. The results are presented as the means ± standard error of mean (SEM).

6.3. Results

Course of the SVCV infection in zebrafish larvae

Zebrafish larvae are susceptible to SVCV through bath infection, but typically the results show high interindividual variations (Levraud et al., 2007; López-Muñoz et al., 2010). Moreover, the long infection times required exclude the use of temporal knockdown techniques, such as morpholino microinjection. As with caudal vein injection (Levraud et al., 2007), we found that SVCV injection into the duct of Cuvier was efficient, thereby providing a reproducible route of infection with fast kinetics. We injected 2 nl of a SVCV stock solution ($3x10^6$ $TCID_{50}$/ml) per larva. Mortality began at 22-24 hpi, consistently reaching nearly 100% between 48 and 50 hpi (Figure 6.1A). There were no differences in the development of the infection between the use of 2 or 3 dpf larvae (data not shown). To assess viral transcription, the expression of the SVCV nucleoprotein (N gene)

was measured through quantitative RT-PCR (Figure 6.1B). The samples were collected between 3 and 24 hpi (just prior to mortality). Efficient viral transcription was observed from 6 hpi, with an important increment between 12 and 18 hpi. Moreover, we found that viral N gene transcription began quickly in the fish as significant differences were found between heat-killed SVCV (HK-SVCV) and SVCV infected fish at 3 hpi (Figure 6.1B).

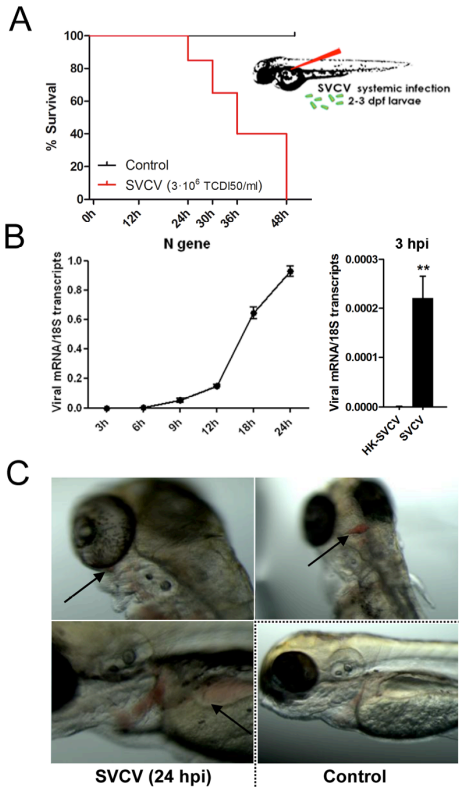

Figure 6.1. Infection course. A. Kaplan-Meier survival curve after infection with 2 nl of a SVCV solution of $3x10^6$ TCID50/ml ($p<0.001$). B. Quantification of SVCV N gene transcripts as a measure of the viral amount in the larvae over time. Heat-killed SVCV was injected in order to separate immune response against the initial viral load. C. The common macroscopic symptoms observed at 24 hpi were hemorrhages and blood accumulation around the eyes and head (arrows). **($0.001<p<0.01$).

With regard to macroscopic signs, the first ones were visible after 18 hours (Figure 6.1C). A progressive decrease in the blood flow rate was observed, particularly in the tail. The circulation in the tail was completely stopped after 20-22 hpi, although it remained visible at the anterior part of the fish. The circulation in the head lasted longer but also eventually stopped. At this point, blood was clearly visible inside the veins, with exception of the hemorrhage areas (Figure 6.1C). Hemorrhages appeared in the anterior part of the larvae, mostly in areas with a huge amount of microvessels but, a great heterogeneity was observed in the occurrence of these hemorrhages varying in terms of location and time post-infection. The heartbeat was clearly less powerful over time until it completely stopped, moment in which the larvae were considered dead. The observed signs and times are consistent with those previously described for this virus using a similar infection model (Levraud et al., 2007). Consistency in the infection results reaffirms the idea that SVCV and zebrafish larvae are an appropriate duo for an in-depth study of the innate immune response against that intracellular pathogen.

SVCV does not affect the integrity of the endothelium

The loss of circulation in the trunk and hemorrhages in larvae head were the most characteristic symptoms of infection. Therefore, we characterized the effect of the virus in the vascular system of the fish, as previously determined for another rhabdovirus, IHNV (Ludwig et al., 2011). Using the transgenic line Tg(Fli1a-GFP) (Lawson and Weinstein., 2002), which facilitates the visualization of the vascular system, we clearly observed a loss of GFP fluorescence in infected fish at 24 hpi (Figures 6.2A, 6.2B). This effect was particularly visible in the main veins of the head (Figure 6.2A) and in the tail (Figure 6.2B). In addition, we used this transgenic line in combination with a whole-mount fluorescent

immunohistochemistry for L-plastin (leukocyte-plastin) (Mathias et al., 2009). The anti-L-plastin antibody was a useful tool for the detection of macrophages and neutrophils in the larvae. In addition to the loss of Fli1a-GFP fluorescence in the trunk, a decrease in the number of L-plastin-positive cells in the area corresponding to the caudal hematopoietic tissue was also observed at 24 hpi (Figure 6.2B). Moreover, a shape change in L-plastin-positive cells was clearly visible in infected fish. The morphology of the cells in infected fish changed from thin and elongated (with prolonged extensions) to rounded and lobulated (Figure 6.2C). The morphological changes might be associated with alterations in cell motility or the infection of the leukocytes themselves (Herbomel et al., 1999; Brannon et al., 2009).

To confirm the integrity of the endothelium in the tail at 24 hpi, we injected tetramethylrhodamine dextran into the caudal vein of the larvae. This fluorescent dye remained inside the vessels, even when Fli1a-GFP fluorescence was absent (Figure 6.3A). Shadows in tetramethylrhodamine dextran fluorescence correspond with blood cells that remain inside vessels even when circulation was stopped (Figure 6.3A, 6.3B). Moreover, the results of the TUNEL assay and the acridine orange staining revealed no DNA damage neither necrosis, respectively, in the endothelial cells of infected fish (Figure 6.4A), suggesting that the cells were apparently healthy and the loss of fluorescence likely reflected a transcriptional regulation of the Fli1a gene and not cell death. This was verified by combining Fli1a-GFP fish with DIC microscopy (Figure 6.4B). Further, TUNEL-positive cells in the caudal hematopoietic tissue of infected larvae were observed, and the localization of these cells was consistent with the position of L-plastin-positive hematopoietic precursor cells in control fish (Figure 6.4C). This observation was not surprising as blood flow is essential for hematopoietic stem cell development (Wang et al.,

2011). In addition, several studies have shown the relationship between blood circulation and Fli1, as Fli1-deficient mice exhibit impaired hematopoiesis (Spyropoulos et al., 2000). Indeed, previous studies in mice described that both morphants and knockouts of Fli1 showed normal vessel development, with impaired circulation and hemorrhaging (Spyropoulos et al., 2000; Pham et al., 2007). This might suggest that the simple transcriptional regulation of *fli1a* could be sufficient to cause the symptoms observed in SVCV-infected larvae.

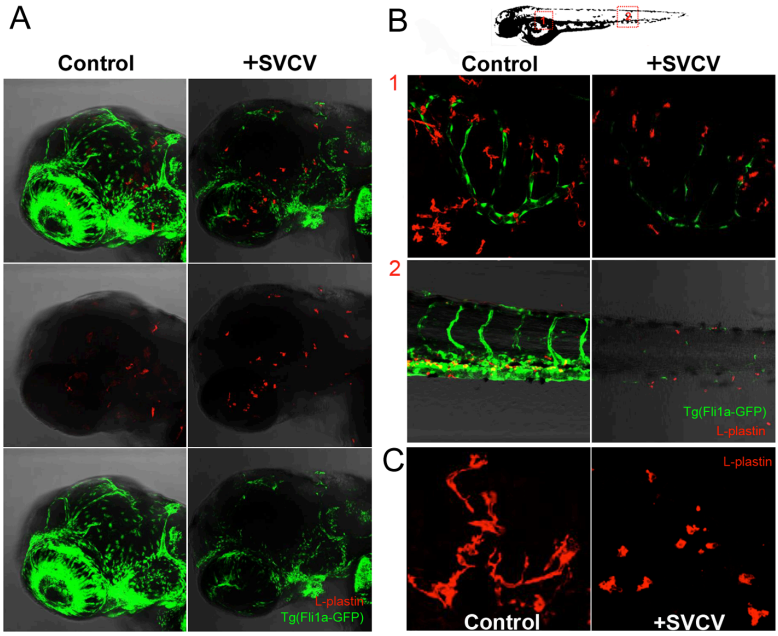

Figure 6.2. Loss of endothelium fluorescence in infected larvae. A. Zebrafish larvae head confocal images (maximal projections from multiple z-stacks) of infected 3 dpf Tg(Fli1a-GFP) larvae immunostained with L-plastin antibody at 24 hpi (20x magnification) showing the loss of GFP fluorescence in infected fish. B. Confocal images (maximal projections from multiple z-stacks) of infected 3 dpf Tg(Fli1a-GFP) larvae immunostained with L-plastin antibody at 24 hpi (20x magnification) of vessels in the yolk sac and trunk showing the loss of GFP fluorescence in infected fish. C. Higher magnification images are shown morphological changes in L-plastin-positive cells in SVCV-infected fish.

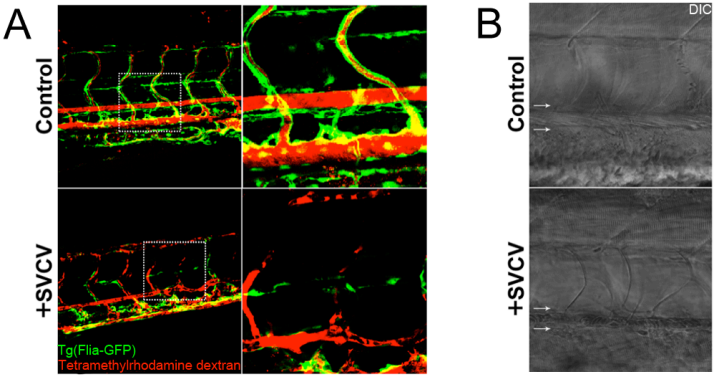

Figure 6.3. Endothelium integrity (I). A. Microangiography performed at 24 hpi injecting tetramethylrhodamine into the caudal vein of 3 dpf infected and control larvae. Higher magnification images are shown in the right panels. B. DIC images showed the dorsal aorta morphological integrity (arrows) in 24 hpi and control larvae. Note that blood cells were visible inside dorsal aorta.

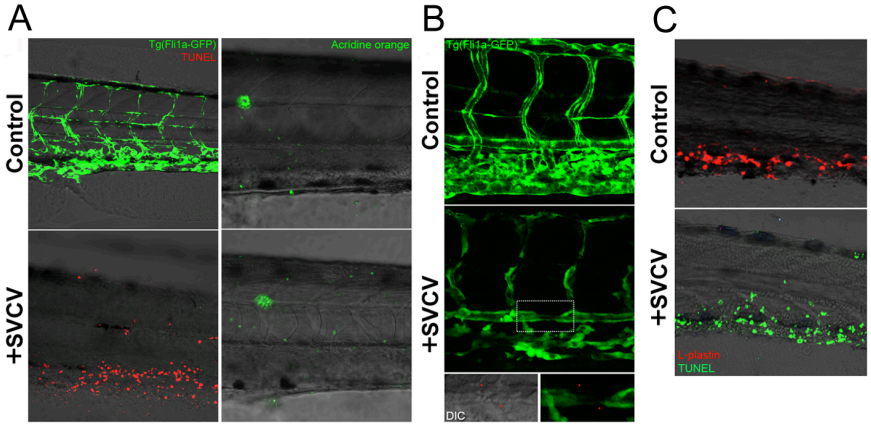

Figure 6.4. Endothelium integrity (II). A. TUNEL assay and acridine orange staining were performed in 24 hpi and control larvae to detect cells with DNA damage and necrotic dead cells, respectively. B. Fluorescent images of Fli1a-GFP of 3dpf SVCV-infected and control larvae showing the loss of fluorescence in endothelial cells after 22 hours of infection. Higher magnification images showed the intact morphology of the dorsal aorta in infected larvae even when the fluorescence was lost (arrow head). C. The localization of L-plastin positive cells in caudal hematopoietic tissue is consistent with that of TUNEL positive cells at 24 hours post-infection. TUNEL assay was performed in 24 hours SVCV-infected and control larvae to detect cells with DNA damage.

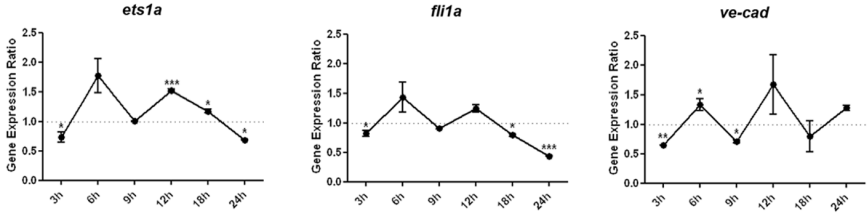

Figure 6.5. Expression qPCR measurements of vascular endothelium-related genes. The samples were obtained from infected larvae at different times post-infection. Each sample (technical triplicates) was normalized to the 18S gene. To avoid differences due to the larval development stage, the samples were standardized with respect to an uninfected control of the same age. Three biological replicates were used to calculate the means ± standard error of mean. Significant differences between infected and non-infected larvae at the same time point were displayed as *** ($0.0001<p<0.001$), ** ($0.001<p<0.01$) or * ($0.01<p<0.05$).

To determine the mechanism underlying *fli1a* mRNA transcription and to associate it with the loss of blood flow in the larvae, we performed a time course during SVCV infection. Based on the signs of their morphants and on their implication in the maintenance of vessel integrity, we also selected the v-ets erythroblastosis virus E26 oncogene homolog 1a (*ets1a*) and the vascular endothelial cadherin (*ve-cad*) genes for qPCR analysis (Figure 6.5). Fli1a and Ets1a are both transcription factors involved in the regulation of hematopoiesis and vasculogenesis (Sumanas and Lin, 2006). A statistically significant decrease in the level of *fli1a* gene transcripts was observed from 12 hpi. Similar results were observed for *ets1a*, as the time course profile for this transcription factor was identical to that for *fli1a*. The interindividual variations in *ve-cad*, a key regulator of endothelial intercellular junctions (Vestweber, 2008), made it difficult to observe a clear expression pattern, particularly at the late stages of the infection. This effect might be associated with the observed heterogeneity in the appearance of hemorrhages, in terms of time, area or larvae. Notably, the downregulation of *ve-cad* at 9 hpi suggests an increase in the permeability of the endothelium at

that infection point. Interestingly, *fli1a* downregulation clearly occurred before the onset of hemorrhages and the loss of circulation, suggesting that hemorrhages were a consequence of this downregulation.

Zebrafish antiviral response to SVCV

To further study the mechanisms involved in the defense against SVCV, we analyzed the expression of some important genes associated with viral detection. Pattern recognition receptors, such as Toll-like receptors (TLRs) and RIG-1-like receptors (RLRs), are membrane-bound and cytosolic sensors, respectively (Kawai and Akira, 2006). We observed a significant downregulation of *tlr7*, *tlr22*, *tlr8a* and *mda5* at 3 hpi (Figure 6.6A). As occurred with Dengue virus (Chang et al., 2012) or Influenza (Keynan et al., 2011), this downmodulation could correspond to an immune evasion strategy. *rig-1* was not regulated during the first 24 hours of the infection. Regarding *tlr3*, we also saw a slight, but significant, regulation at 12 hpi.

Pattern recognition receptors initiate antimicrobial defense mechanisms through several conserved signaling pathways (Broz and Monack, 2013). The activation of interferon-regulatory factors induces the production of several antiviral response-related genes. We observed that SVCV elicited a response in all the analyzed genes (Figure 6.6B). *ifnφ1* and *ifnφ2* showed different response profiles. *ifnφ1* remained downregulated between 3 and 9 hpi, the time in which *ifnφ2* was regulated. *ifnφ1* was upregulated from 12 hpi, similar to *mx* (a and b paralogues), which increased from 12 hours and reached a maximum at 24 hours. *rarres3* showed a biphasic response, with higher expression at 9 and 24 hpi. The recently characterized *ifit* gene family in zebrafish (Liu et al., 2013;

Varela et al., 2014) was also present in the response, highlighting the response of *ifit17a*, which reached a 20-fold change.

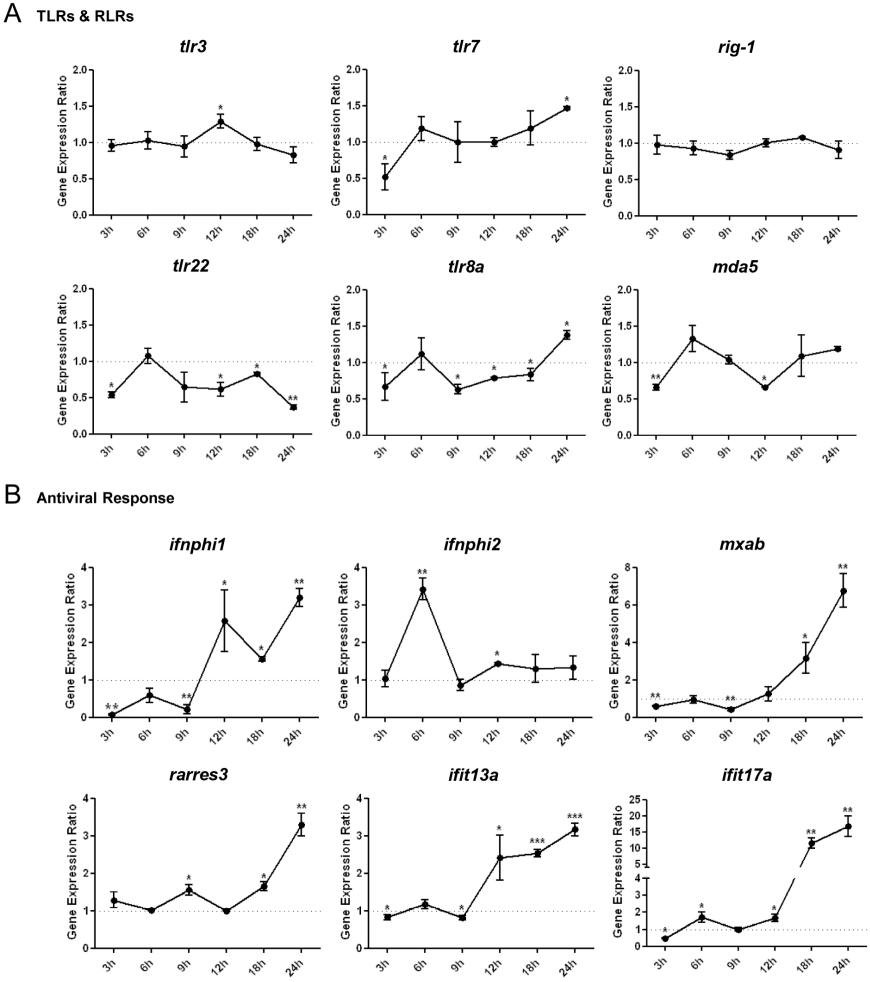

Figure 6.6. Viral detection and antiviral response measure over time. A. Expression qPCR measurements of TLRs and RLRs associated with viral detection. B. Expression qPCR measurements of antiviral response-related genes. Samples were obtained from infected larvae at different times post-infection. Each sample (technical triplicates) was normalized to the 18S gene. To avoid differences due to the larval development stage, the samples were standardized with respect to an uninfected control of the same age. Three biological replicates were used to calculate the means ± standard error of mean. Significant differences were displayed as *** ($0.0001<p<0.001$), ** ($0.001<p<0.01$) or * ($0.01<p<0.05$).

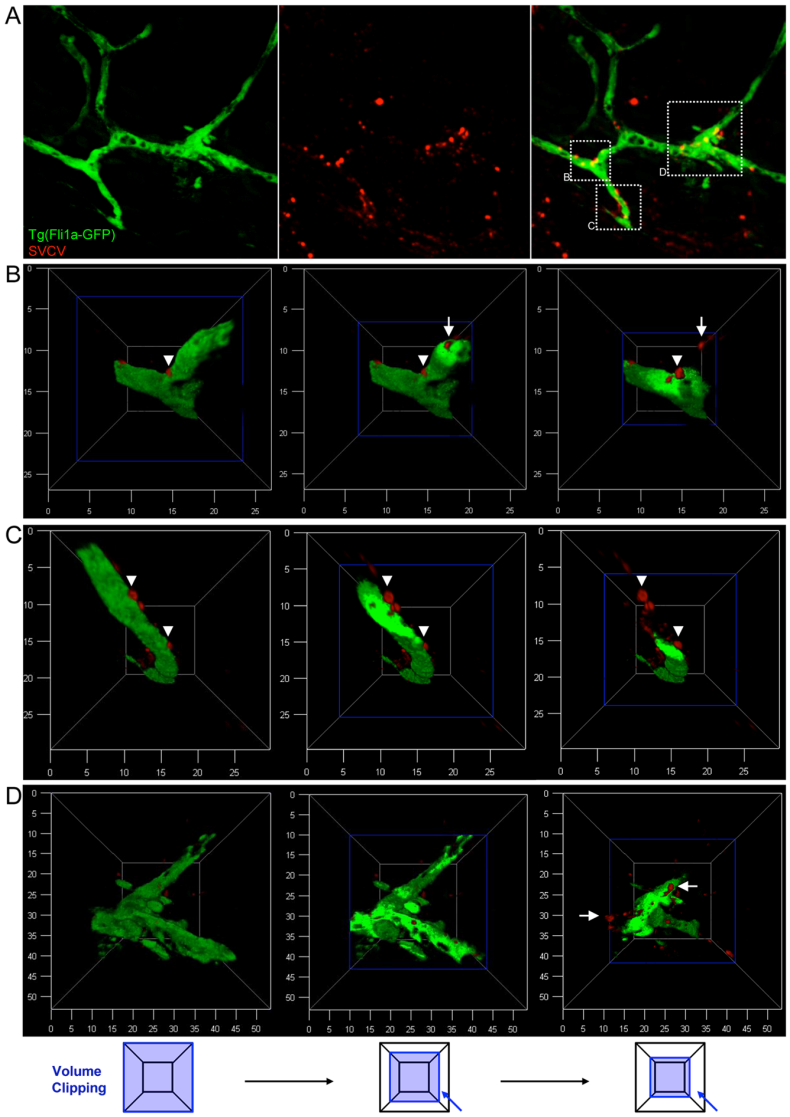

Figure 6.7. SVCV positive cells are distinct from endothelial cells. A. Confocal images (maximal projections from multiple z-stacks) of 3 dpf infected Tg(Fli1a-GFP) larvae immunostained with SVCV antibody at 20 hpi (60x magnification). B, C, D. 3D reconstructions of the different zones shown in A. Sequential steps of volume clipping of the Fli1a channel are shown from left to right. We classified SVCV-positive cells as circulating- (white arrows) and interacting- (white head arrows) cells. The axis numbers correspond to µm.

SVCV positive cells are not endothelial cells

To determine whether endothelial cells were the primary targets of SVCV in this *in vivo* model of infection we performed an immunohistochemistry using an antibody against SVCV (Figure 6.7). Using Fli1a-GFP infected larvae, SVCV was clearly visible in areas surrounding vessels (Figure 6.7A). The 3D reconstruction and volume clipping of the Fli1a channel showed that the SVCV positive cells were not endothelial cells (Figure 6.7B, 6.7C, 6.7D). We observed crossing and circulating SVCV-positive cells, suggesting that these cells might be leukocytes interacting with the endothelium.

Our hypothesis was confirmed by performing L-plastin labelling (Figure 6.8). L-plastin positive cells were observed surrounding vessels and many of these cells co-localized with SVCV. Again, the 3D reconstruction of the confocal images conferred information about the cells and their position relative to the vessels (Figure 6.8A). In addition, we observed that SVCV-infected cells showed viral antigen positive signal inside and on their surface (Figure 6.8A). The signal detected on the cell surface might be associated with viral assembly, antigen presentation by infected cells or both (Halstead et al., 1977). We observed cells labeled with only L-plastin (interacting or not with the endothelium), double-positive cells (interacting or not with the endothelium) and cellular debris positive for one or both markers. Large amounts of cellular debris were observed, always with L-plastin-positive cells phagocytising SVCV-positive particles in the same area (Figure 6.8B). This cellular debris might play a role in the first line of defense against SVCV, as observed with other pathogens (Norling and Perretti, 2013). Furthermore, defective debris clearance has been associated with persistent inflammatory diseases (Nathan and Ding, 2010).

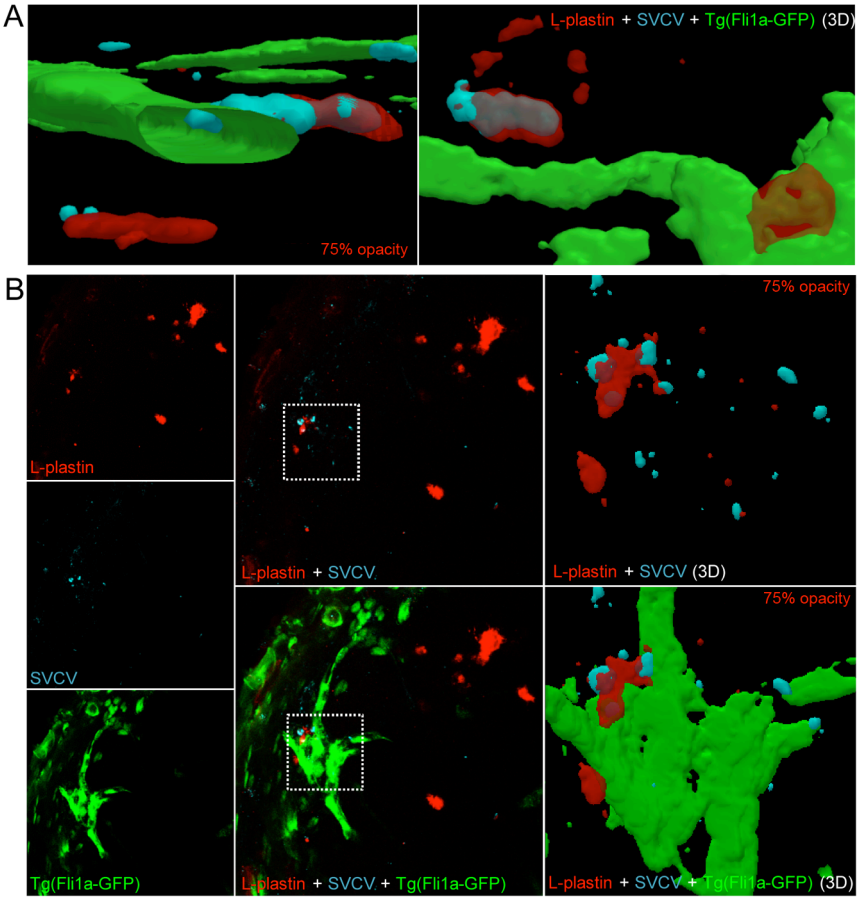

Figure 6.8. SVCV positive cells are L-plastin positive and Fli1a negative. A. Confocal images 3D reconstruction of different scenes observed during the infection of 3 dpf larvae. Double positive cells are observed around vessels, interacting or not with the endothelium. B. Confocal images (maximal projections from multiple z-stacks) of infected Tg(Fli1a-GFP) larvae double-immunostained with SVCV and L-plastin antibodies at 20 hpi (60x magnification). Panels on the right show 3D reconstructions of the areas identified in the central panels.

6.4. Discussion

Hemorrhagic viral diseases are globally observed with important pathogens, such as Dengue Virus or Hantaviruses (Zapata et al., 2014). Although hemorrhages have been associated with the infection of endothelial cells (Valbuena and Walker, 2006), other cellular types could be the main targets for viral infection (Paessler and Walker, 2013). The lack of adequate *in vivo* infection models has limited the research on viral pathogenesis. In SVCV-infected zebrafish larvae, we observed a loss of fluorescence of the endothelial marker Fli1a. However, this was not due to infection of endothelial cells or cytopathic effects, and vascular integrity remained intact, at least in the tail. The fact that haemorrhages always occur in the head of the larva suggests the possibility that these occur as a result of damage or permeability regulation in a particular kind of vessel, as it is known that the control of the permeability may be different in different vessel types (Dejana and Orsenigo, 2013). The dysregulation of the vascular endothelium, observed as a loss of Fli1a fluorescence, could reflect strong immune activation during infection. In addition, the response induced in the rest of the organism should also be considered. The downregulation of important transcription factors, such as Fli1a and Ets1a, in endothelial cells shows the importance of a response of the organism as a whole. It has been shown that the downregulation of Fli1 in response to LPS is mediated through TLRs (Ho and Ivashkiv, 2010). Endothelial cells express different receptors, such as Tlr3, Rig-1 and Mda5, among others. Based on this fact and the qPCR results obtained in the present study, the activation of endothelial cells through the Tlr3 might the cause of the loss of Fli1a expression, thereby inducing loss of circulation, hemorrhages and inhibition in the development of hematopoietic precursors.

Recent studies have shown a relationship between Fli1 and glycosphingolipids metabolism (Richard et al., 2013). Thus, we could consider Fli1a downregulation as a mechanism for protection against viral infection in endothelial cells. Although, similar to other hemorrhagic viral infections, we cannot rule out the possibility that endothelial cells could be infected during the final stages of infection (Paessler and Walker, 2013). However, this situation would not be decisive for the pathogenesis of the disease.

Altogether, the qPCR results provide interesting data regarding the dynamics of the response. The viral transcription began to emerge from 9 hpi, time from which we observed the regulation of antiviral genes as *ifnφ1*, *mxab*, *ifit13a* and *ifit17a*. It has been recently published that *ifit17a* confers protection against SVCV in zebrafish larvae (Varela et al., 2014). Here, even being the antiviral gene with the highest expression increment, such heightening was not enough to avoid the larvae death.

The role of leukocytes during the infection was also explored. We determined that endothelial cells were not the primary target of SVCV in this *in vivo* model, but positive SVCV cells were also positive for leukocyte-plastin. The transendothelial migration of leukocytes during inflammation has been well characterized (Muller et al., 2009), but future studies are needed to assess such process during SVCV infection in zebrafish larvae.

Our results rekindle the controversy concerning hemorrhagic viruses and the importance of using an appropriate model of infection. Furthermore, the application of these techniques and studies to other pathogens will improve the current knowledge of host-pathogen interactions and increase the potential for the discovery of new therapeutic targets.

6.5. References

Ahne W, Bjorklund HV, Essbauer S, Fijan N, Kurath G, Winton JR (2002) Spring viraemia of carp (SVC). Dis Aquat Organ 52:261–272.

Aye KS, Charngkaew K, Win N, Wai KZ, Moe K, Punyadee N, Thiemmeca S, Suttitheptumrong A, Sukpanichnant S, Prida M, Halstead SB (2014) Pathologic highlights of dengue hemorrhagic fever in 13 autopsy cases from Myanmar. Hum Pathol 45:1221-33.

Benard EL, van der Sar AM, Ellett F, Lieschke GJ, Spaink HP, Meijer AH (2012) Infection of zebrafish embryos with intracellular bacterial pathogens. J Vis Exp 61:e3781.

Brannon MK, Davis JM, Mathias JR, Hall CJ, Emerson JC, Crosier PS, Huttenlocher A, Ramakrishnan L, and Moskowitz SM (2009) *Pseudomonas aeruginosa* Type III secretion system interacts with phagocytes to modulate systemic infection of zebrafish embryos. Cell Microbiol 11:755-768.

Bray M and Geisbert TW (2005) Ebola virus: the role of macrophages and dendritic cells in the pathogenesis of Ebola hemorrhagic fever. Int J Biochem Cell Biol 37:1560–1566.

Broz P and Monack DM (2013) Newly described pattern recognition receptors team up against intracellular pathogens. Nat Immunol Rev 13:551-565.

Burgos JS, Ripoll-Gomez J, Alfaro JM, Sastre I, Valdivieso F (2008) Zebrafish as a new model for herpes simplex virus type 1 infection. Zebrafish 5:323-333.

Chang TH, Chen SR, Yu CY, Lin YS, Chen YS, Kubota T, Matsuoka M, Lin YL (2012) Dengue Virus Serotype 2 Blocks Extracellular Signal-Regulated Kinase and Nuclear Factor-κB Activation to Downregulate Cytokine Production. PLoS One 7:e41635.

Crim MJ and Riley LK (2012) Viral diseases in zebrafish: what is known and unknown. ILAR J 53:135-143.

Cui C, Benard EL, Kanwal Z, Stockhammer OW, van der Vaart M, Zakrzewska A, Spaink HP, Meijer AH (2011) Infectious disease modeling and innate immune function in zebrafish embryos. Methods Cell Biol 105:273-308.

Dejana E and Orsenigo F (2013) Endothelial adherens junctions at a glance. J Cell Sci 126:2545-2549.

Encinas P, Rodriguez-Milla MA, Novoa B, Estepa A, Figueras A, Coll, J (2010) Zebrafish fin immune responses during high mortality infections with viral haemorrhagic septicemia rhabdovirus. A proteomic and transcriptomic approach. BMC Genomics 11:518.

Espín R, Roca FJ, Candel S, Sepulcre, MP, González-Rosa, JM (2013) TNF receptors regulate vascular homeostasis in zebrafish through a caspase-8, caspase-2 and P53 apoptotic program that bypasses caspase-3. Dis Model Mech 6:383-396.

Halstead SB, O´Rourke EJ, Allison AC (1977) Dengue viruses and mononuclear phagocytes. II. Identity of blood and tissue leukocytes supporting in vitro infection. J Exp Med 146: 218-228.

Herbomel P, Thisse B, Thisse C (1999) Ontogeny and behaviour of early macrophages in the zebrafish embryo. Development 126:3735-3745.

Ho HH and Ivashkiv LB (2010) Downregulation of friend leukemia virus integration 1 as a feedback mechanism that restrains lipopolysaccharide induction of matrix metalloproteases and interleukin-10 in human macrophages. J. Interferon Cytokine Res 30:893-900.

Howe K, Clark MD, Torroja CF, Torrance J, Berthelot C, Muffato M, Collins JE, Humphray S, McLaren K, Matthews L, McLaren S, Sealy I, Caccamo M, Churcher C, Scott C, Barrett JC, Koch R, Rauch GJ, White S, Chow W, Kilian B, Quintais LT, Guerra-Assunção JA, Zhou Y, Gu Y, Yen J, Vogel JH, Eyre T, Redmond S, Banerjee R, Chi J, Fu B, Langley E, Maguire SF, Laird GK, Lloyd D, Kenyon E, Donaldson S, Sehra H, Almeida-King J, Loveland J, Trevanion S, Jones M, Quail M, Willey D, Hunt A, Burton J, Sims S, McLay K, Plumb B, Davis J, Clee C, Oliver K, Clark R, Riddle C, Elliot D, Threadgold G, Harden G, Ware D, Begum S, Mortimore B, Kerry G, Heath P, Phillimore B, Tracey A, Corby N, Dunn M, Johnson C, Wood J, Clark S, Pelan S, Griffiths G, Smith M, Glithero R, Howden P, Barker N, Lloyd C,

Stevens C, Harley J, Holt K, Panagiotidis G, Lovell J, Beasley H, Henderson C, Gordon D, Auger K, Wright D, Collins J, Raisen C, Dyer L, Leung K, Robertson L, Ambridge K, Leongamornlert D, McGuire S, Gilderthorp R, Griffiths C, Manthravadi D, Nichol S, Barker G, Whitehead S, Kay M, Brown J, Murnane C, Gray E, Humphries M, Sycamore N, Barker D, Saunders D, Wallis J, Babbage A, Hammond S, Mashreghi-Mohammadi M, Barr L, Martin S, Wray P, Ellington A, Matthews N, Ellwood M, Woodmansey R, Clark G, Cooper J, Tromans A, Grafham D, Skuce C, Pandian R, Andrews R, Harrison E, Kimberley A, Garnett J, Fosker N, Hall R, Garner P, Kelly D, Bird C, Palmer S, Gehring I, Berger A, Dooley CM, Ersan-Ürün Z, Eser C, Geiger H, Geisler M, Karotki L, Kirn A, Konantz J, Konantz M, Oberländer M, Rudolph-Geiger S, Teucke M, Lanz C, Raddatz G, Osoegawa K, Zhu B, Rapp A, Widaa S, Langford C, Yang F, Schuster SC, Carter NP, Harrow J, Ning Z, Herrero J, Searle SM, Enright A, Geisler R, Plasterk RH, Lee C, Westerfield M, de Jong PJ, Zon LI, Postlethwait JH, Nüsslein-Volhard C, Hubbard TJ, Roest Crollius H, Rogers J, Stemple DL (2013) The zebrafish reference genome sequence and its relationship to the human genome. Nature 496:498-503.

Hubbard S, Darmani NA, Thrush GR, Dey D, Burnham L, Thompson JM, Jones K, Tiwari V (2010) Zebrafish-encoded 3-O-sulfotransferase-3 isoform mediates herpes simplex virus type 1 entry and spread. Zebrafish 7:181-187.

Kawai T and Akira S (2006) Innate immune recognition of viral infection. Nat immunol 7:131-137.

Keynan Y, Fowke KR, Ball TB, Meyers, AFA (2011) Toll-Like Receptors Dysregulation after Influenza Virus Infection: Insights into Pathogenesis of Subsequent Bacterial Pneumonia. ISRN Pulmonology 2011:142518.

Lawson ND and Weinstein BM (2002) *In vivo* imaging of embryonic vascular development using transgenic zebrafish. Dev Biol 248:307-318.

Levraud JP, Boudinot P, Colin I, Benmansour A, Peyrieras N, Herbomel P, Lutfalla G (2007) Identification of the zebrafish IFN receptor: implications for the origin of the vertebrate IFN system. J Immunol 178:4385-4394.

Liu Y, Zhang YB, Liu TK, Gui JF (2013) Lineage-Specific Expansion of IFIT Gene Family: An Insight into Coevolution with IFN Gene Family. PLoS One 8:e66859.

López-Muñoz A, Roca FJ, Sepulcre MP, Meseguer J, Mulero V (2010) Zebrafish larvae are unable to mount a protective antiviral response against waterborne infection by spring viremia of carp virus. Dev Comp Immunol 34:546–552.

Ludwig M, Palha N, Torhy C, Briolat V, Colucci-Guyon E, Brémont M, Herbomel P, Boudinot P, Levraud, JP (2011) Whole-body analysis of a viral infection: vascular endothelium is a primary target of infectious hematopoietic necrosis virus in zebrafish. PLoS Pathog 7:e1001269.

Lupfer CR, Kanneganti TD (2012) The role of inflammasome modulation in virulence. Virulence 3:262-270.

Mathias JR, Dodd ME, Walters KB, Yoo SK, Ranheim EA, Huttenlocher A (2009) Characterization of zebrafish larval inflammatory macrophages. Dev Comp Immunol 33:1212-1217.

Mercer J and Greber UF (2013) Virus interactions with endocytic pathways in macrophages and dendritic cells. Trends Microbiol 21:380-388.

Muller WA (2003) Leukocyte-endothelial cell interactions in leukocyte transmigration and the inflammatory response. Trends Immunol 24:327-334.

Muller WA. (2009) Mechanisms of Transendothelial Migration of Leukocytes. Circ Res 105:223-230.

Nathan C and Ding A (2010) Nonresolving Inflammation. Cell 140:871–882.

Norling LV and Perretti M (2013) Control of Myeloid Cell Trafficking in Resolution. J Innate Immun 5:367-376.

Nüsslein-Volhard C and Dahm R (2002) *Zebrafish: a practical approach*. New York: Oxford University Press. 303 pp.

Paessler S and Walker DH (2013) Pathogenesis of the viral Hemorrhagic Fevers. Annu Rev Pathol 8:411-440.

Palha N, Guivel-Benhassine F, Briolat V, Lutfalla G, Sourisseau M, Ellett F, Wang CH, Lieschke GJ, Herbomel P, Schwartz O, Levraud JP (2013) Real-time whole-

body visualization of Chikungunya Virus infection and host interferon response in zebrafish. PLoS Pathog 9:e1003619.

Pham VN, Lawson ND, Mugford JW, Dye L, Castranova D, Lo B, Weinstein, BM (2007) Combinatorial function of ETS transcription factors in the developing vasculature. Dev Biol 303:772–783.

Richard EM, Thiyagarajan T, Bunni MA, Basher F, Roddy PO, Siskind LJ, Nietert PJ, Nowling TK. (2013) Reducing FLI1 Levels in the MRL/lpr Lupus Mouse Model Impacts T Cell Function by Modulating Glycosphingolipid Metabolism. PLoS One 8:e75175.

Spyropoulos DD, Pharr PN, Lavenburg KR, Jackers P, Papas TS, Ogawa M, Watson DK (2000) Hemorrhage, impaired hematopoiesis, and lethality in mouse embryos carrying a targeted disruption of the Fli1 transcription factor. Mol Cell Biol 20:5643–5652.

Sumanas S, Lin S (2006) Ets1-Related Protein Is a Key Regulator of Vasculogenesis in Zebrafish. PLoS Biol 4:e10.

Taylor NG, Peeler EJ, Denham KL, Crane CN, Thrush MA, Dixon PF, Stone DM, Way K, Oidtman, BC (2013) Spring viraemia of carp (SVC) in the UK: The road to freedom. Prev Vet Med 111:156-164.

Valbuena G and Walker DH (2006) The endothelium as a target for infections. Annu Rev Pathol 1:171-198.

Varela M, Dios S, Novoa B, Figueras A (2012) Characterisation, expression and ontogeny of interleukin-6 and its receptors in zebrafish (*Danio rerio*). Dev Comp Immunol 37:97-106.

Varela M, Díaz-Rosales P, Pereiro P, Forn-Cuní G, Costa MM, Dios S, Romero A, Figueras A, Novoa B (2014) Interferon-induced genes of the expanded IFIT family show conserved antiviral activities in non-mammalian species. PLoS One 9(6):e100015.

Vestweber D (2008) VE-cadherin: the major endothelial adhesion molecule controlling cellular junctions and blood vessel formation. Arterioscler Thromb Vasc Biol 28:223-232.

Wang L, Zhang P, We, Y, Gao Y, Patient R, Liu F (2011) A blood flow–dependent klf2a-NO signaling cascade is required for stabilization of hematopoietic stem cell programming in zebrafish embryos. Blood 118:4102-4110.

Westerfield M (2000) The zebrafish book. *A guide for the laboratory use of zebrafish (Danio rerio)*. Eugene: University of Oregon Press.

Zapata JC, Cox D, Salvato MS (2014) The role of platelets in viral hemorrhagic fevers. PLoS Negl Trop Dis 8:e2858.

6.6. Supporting Information

Table S6.1. Oligonucleotide sequences.

Primer Name	Primer sequence (5´→3´)	Amplicon (bp)
18SF	ACCACCCACAGAATCGAGAAA	97
18SR	GCCTGCGGCTTAATTTGACT	
SVCVNF	TGAGGTGAGTGCTGAGGATG	101
SVCVNR	ATACCGGACTTTGCTGATGG	
TLR3F	AAGCCCATCATGCTCTTCAT	150
TLR3R	AAGGCCAGTAGAGGACACATTT	
TLR22F	TGGGCCAAGAAGAATGAATC	181
TLR22R	ATGACAACAGGAGGGTGAGG	
TLR7F	GCCCAACTCAGCATCCTAAA	131
TLR7R	ATTGGGGAACCGTAATAGGC	
TLR8aF	CGGTGTGACTTGTACCATGC	146
TLR8aR	TGATGGCTGCGAAAGTAGTG	
RIG-IF	TTGAGGAGCTGCATGAACAC	135
RIG-IR	CCGCTTGAATCTCCTCAGAC	
MDA5F	GAATCAGAATGTTCGCGTGTGT	149
MDA5R	CCTCGTCAGGGCTAGATTTGG	
IFNΦ1F	GAGCACATGAACTCGGTGAA	105
IFNΦ1R	TGCGTATCTTGCCACACATT	
IFNΦ2F	CCTCTTTGCCAACGACAGTT	125
IFNΦ2R	CGGTTCCTTGAGCTCTCATC	
MXabF	CGCTGTCAGGAGTTCCGTTAC	149
MXabR	TTCCGCTGGGTCATCAAAGT	
RARRES3F	TCCTTACGTGGCTCATCTGA	141
RARRES3R	ATGCTTGTCGTCCAGGTAGT	
IFIT13aF	AGCTCTTCAGCAAGCCTGAC	88
IFIT13aR	GAGCCCAGCCTGTACAATTT	
IFIT17aF	CACTGCAAACTTGGTTGGTC	94
IFIT17aR	TTCCCGAACCCTTTGTACC	
FLI1aF	GGAAAAGGCTCTCCAACAGT	100
FLI1aR	TGCTGGTGGGTCCTAATATC	
ETS1aF	AGACTCTCCATCCCCAAAGA	165
ETS1aR	GACCTCCAGAAATCTCTCCT	
VECADF	TGCGACAATTGTGCTGAAGC	198
VECADR	GCACTGACACTCATTCCAGT	

Chapter 7

Leukocyte Response and Inflammation During SVCV Infection in Zebrafish Larvae

Published in:
-Mónica Varela, Alejandro Romero, Sonia Dios, Michiel van der Vaart, Antonio Figueras, Annemarie H. Meijer, Beatriz Novoa
Journal of Virology 2014; 88(20):12026-12040
-Mónica Varela, Gabriel Forn-Cuní, Sonia Dios, Antonio Figueras and Beatriz Novoa. Journal of Innate Immunity 2015; DOI: 10.1159/000431287

7.1. Introduction

Endothelial cells and leukocytes are at the front line of defense against pathogens, but little is known about how leukocytes participate in the innate immune response. Macrophages and neutrophils are indispensable to innate immunity in higher vertebrates and presumably play a similar role in zebrafish (Sullivan and Kim, 2008). The identification of the cellular producers and the targets of the molecules that control host responses to infection, and the elucidation of the mechanisms that pathogens can use to manipulate these and other signalling pathways of the innate immune system are important challenges where the zebrafish model can contribute (Meijer et al., 2014).

Over the recent years the number of zebrafish infection models for bacterial and viral pathogens has rapidly increased (van der Sar et al., 2003; Prajsnar et al., 2008; Palha et al., 2013; Ramakrishnam, 2013; Nguyen-Chi et al., 2014; Varela et al., 2014). The context of the zebrafish embryo's developing immune system makes it possible to study the contribution of different immune cell types to host-pathogen interaction (Meijer and Spaink, 2011). Moreover, the transparency of early life stages is another advantage that allows useful real-time visualization (Novoa and Figueras, 2012).To facilitate *in vivo* imaging, fluorescent reporter lines that mark different immune cell types have been developed (Renshaw et al., 2006, Ellet et al, 2011, Gray et al., 2011).

Most of the studies about host-pathogen interactions in zebrafish have been made using bacteria. Regarding viral pathogenesis, host-pathogen interaction studies are a step behind. In the previous chapter, we used the rhabdovirus Spring Viraemia of Carp Virus (SVCV) as a viral model to show the potential of the zebrafish in host-pathogen interaction studies. After the visualization of the virus in leukocytes located sorrounding the

endothelium in zebrafish larvae, we wanted to deepening in the role of leukocytes during the infection. Also we focused on the posible effects that the virus might have on the regulation of the host inflammatory response.

Thus, the main objective of the present study was to improve the knowledge of the pathology generated by SVCV, as an example of hemorrhagic virus, focusing on interactions between the virus and leukocytes at early stages of the infection in zebrafish larvae. Taking advantage of zebrafish transgenic lines, imaging techniques and, using morpholino-induced cell depletion, viral-induced pyroptosis and IL1β release were observed in macrophages at the single cell level.

7.2. Material and Methods

Ethics statement

The protocols for fish care and the challenge experiments were reviewed and approved by the CSIC National Committee on Bioethics under approval number 07_09032012. Experiments were conducted in fish larvae before independently feeding and therefore, before an ethical approval is required (EU directive 2010_63).

Animals

Homozygous embryos and larvae from wild-type zebrafish, transgenic line Tg(Mpx:GFP)i114 that labels neutrophils, transgenic line Tg(Mpeg1:eGFP)gl22 that labels macrophages and transgenic line Tg(Cd41:GFP)la2 that labels thrombocytes were obtained from our experimental facility, where the zebrafish were cultured using established protocols (Westerfield, 2000; Nüsslein-

Volhard and Dahm, 2002). The eggs were obtained according to protocols described in The Zebrafish Book (Westerfield, 2000) and maintained at 28.5˚C in egg water (5 mM NaCl, 0.17 mM KCl, 0.33 mM CaCl2, 0.33 mM MgSO4, and 0.00005% methylene blue), and 0.2 mM N-phenylthiourea (PTU; Sigma) was used to prevent pigment formation from 1 days post-fertilization (dpf).

Virus and infection

The SVCV isolate 56/70 was propagated on epithelioma papulosum cyprini (EPC) carp cells (ATCC CRL-2872) and titrated in 96-well plates. The plates were incubated at 15°C for 7 days and examined for cytophathic effects each day. After the observation of the cells under the microscope, the virus dilution causing infection of 50% of the inoculated cell line (TCID50) was determined using the Reed-Müench method (Reed and Muench, 1938).

The fish larvae were infected through microinjection into the duct of Cuvier as described in Benard et al. (2012) at 2 or 3 dpf. SVCV was diluted to the appropriate concentration in PBS with 0.1% phenol red (as a visible marker to the injection of the solution into the embryo) just before the microinjection of 2 nl of viral suspension per larvae. The infections were conducted at 23˚C. SVCV was heat-killed at 65ºC during 20 minutes.

Imaging

Images of the signs and videos of the blood flow were obtained using an AZ100 microscope (Nikon) coupled to a DS-Fi1 digital camera (Nikon). Confocal images of live or fixed larvae were captured using a TSC SPE confocal microscope (Leica). The images were processed using the LAS-AF (Leica) and ImageJ software. The

3D reconstructions and the volume clipping were performed using Image Surfer (http://imagesurfer.cs.unc.edu/) and LAS-AF (Leica), respectively.

Immunohistochemistry

Whole-mount immunohistochemistry was performed as previously described (Cui et al., 2011). The following primary antibodies and dilutions were used: L-plastin (rabbit anti-zebrafish, 1:500, kindly provided by Dr. Paul Martin); Caspase a (rabbit anti-zebrafish, 1:500; Anaspec); SVCV (mouse anti-SVCV, 1:500; BioX Diagnostics) and Il1β (rabbit anti-zebrafish, 1:500, kindly provided by Dr. John Hansen). The secondary antibodies used were Alexa 488 anti-rabbit, Alexa 546 anti-rabbit or Alexa 635 anti-mouse (Life Technologies), all diluted 1:1000.

Real-Time PCR

Total RNA was isolated from snap-frozen larvae using the Maxwell® 16 LEV simply RNA Tissue kit (Promega) with the automated Maxwell® 16 Instrument according to the manufacturer's instructions. cDNA synthesis using random primers and qPCR were performed as previously described (Varela et al., 2012). 18S was used as a housekeeping to normalize the expression values. Gene expression ratio was calculated by dividing the normalized expression values of infected larvae by the normalized expression values of the controls. Table S7.1 in supplemental material shows the sequences of the primer pairs used. Two independent experiments, of 3 biological replicates each, were performed.

TUNEL assay

The TUNEL assay was performed using the In Situ Cell Death Detection Kit, TMR red or POD (Roche) as previously described (Espín et al., 2013).

In vivo acridine orange staining

For acridine orange staining, larvae were incubated for 2 hours in 10 µg/ml acridine orange solution followed by washing for 30 min.

Macrophages depletion with PU.1-MO

For the PU.1 knockdown, the morpholino was injected into the yolk at the one-cell stage at 1 mM to block macrophages development as previously described (Rhodes et al., 2005). Macrophage-depleted fish were infected at 2 dpf to ensure morpholino effectiveness until the end of the infection.

In vivo propidium iodide staining

For propidium iodide (PI) staining, larvae were incubated for 2 hours in 10 µg/ml propidium iodide solution followed by washing for 30 min.

Caspase-1 activity measurement

Total protein was obtained from 25 larvae/biological replicate after their homogenization in lysis buffer (25 mM HEPES,

5 mM EGTA, 5 mM DTT, and protease inhibitor). Caspase-1 activity in 75 μg of total protein/technical replicate was determined using Ac-YVAD-AFC (Calbiochem, 688225) as a substrate. A total of 1 μL of the substrate was added per well, and after an incubation of 90 minutes at 25°C, the fluorescence was measured (exc. 405, emi. 492). The experiment was repeated twice, with two biological replicates and three technical replicates per group and experiment.

Plasmid construction

A selected zebrafish perforin (*prf19b*) was amplified by PCR (primers in Table S7.1), and the PCR product was cloned using the pcDNA 3.1/V5-His TOPO TA Expression Kit (Invitrogen). One Shot TOP10F competent cells (Invitrogen) were transformed to generate the plasmid constructs. Plasmid purifications were conducted using the PureLink HiPure Plasmid Midiprep Kit (Invitrogen). The recombinant plasmids were microinjected into one-cell stage zebrafish embryos with a glass microneedle using a Narishige MN-151 micromanipulator and a Narishige IM-30 microinjector. Each egg was microinjected with 100 pg of the corresponding plasmid in a final volume of 2 nL. An additional untreated group was included to control for egg quality and survival. Three days after plasmid administration, the larvae were microinjected with 2 nL of a SVCV suspension at a final concentration of $1.5 \cdot 10^5$ $TCID_{50}$/mL into the duct of Cuvier. The fish culture conditions were controlled three times per day. Three days after plasmid administration, samples were taken to measure caspase-1 activity and to perform RNA isolation.

Statistical analysis

Kaplan-Meier survival curves were analyzed with a Log-rank (Mantel Cox) test. The neutrophil count and qPCR data were analyzed using one-way analysis of variance and Tukey's test, and differences were considered significant at $p<0.05$. The results are presented as the means ± standard error of mean (SEM).

7.3. Results

Cellular response to SVCV infection

The transendothelial migration of leukocytes during inflammation has been well characterized (Muller et al., 2009). In the present study, the role of leukocytes during infection was explored using the Mpx-GFP zebrafish transgenic line combined with L-plastin immunohistochemistry (Figure 7.1). Using this system, we were able to differentiate between macrophages (L-plastin^{+}, Mpx^{-}) and neutrophils (L-plastin^{+}, Mpx^{+}). After 24 hours of infection, practically all macrophages were undetectable (Figure 7.1A) and a statistically significant migration of neutrophils to the head was observed (Figure 7.1A, 7.1B, 7.1C, S7.1). The loss of leukocytes in the caudal hematopoietic region was also confirmed (Figure 7.1B). Using markers for both cellular types, *marco* for macrophages and *mpx* for neutrophils, we could determine by qPCR the dynamics of that leukocytes population (Figure 7.1D). The analysis of *marco* gene expression suggested an initial decrease in the macrophage population between 3 and 6 hpi and then, macrophages remained stable until 18 hpi. Thereafter, the macrophage population markedly reduced to nearly 0 at 24 hpi (Figure 7.1D).

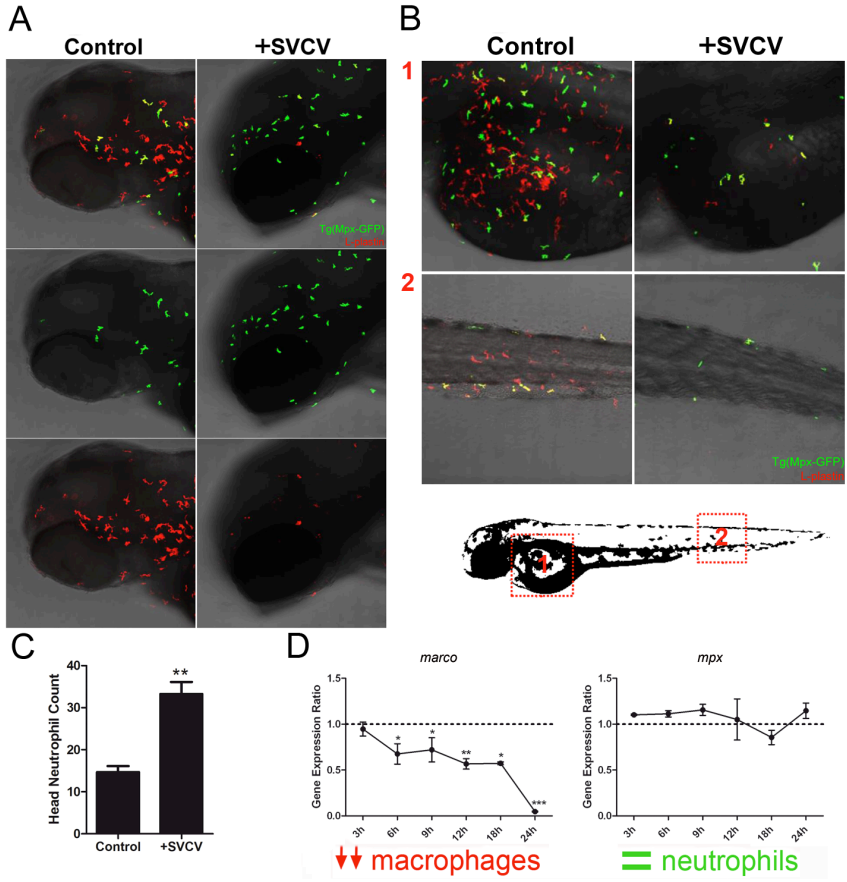

Figure 7.1. Neutrophils and macrophages respond to SVCV. A. Confocal images (maximal projections from multiple z-stacks) of infected 3 dpf Tg(Mpx-GFP) larvae immunostained with L-plastin antibody 24 hpi (20x magnification). Head showing the loss of L-plastin-positive cells in infected fish. MPX-positive cells increase in the same area as a consequence of the migratory wave from the yolk sac population. B. View of yolk sac and tail of infected and control larvae. A yolk sac neutrophil population was observed in the control larvae. Macrophages are missing in infected larvae. C. Neutrophil count in the head of control and 24 hours SVCV-infected larvae (n=4). D. qPCR results of the dynamics of macrophages and neutrophils population during SVCV infection. Significant differences were displayed as *** ($0.0001<p<0.001$), ** ($0.001<p<0.01$) or * ($0.01<p<0.05$).

Regarding neutrophils, *mpx* revealed no differences in the number of cells, thus confirming the migration observed in confocal images of these cells during the infection (Figure 7.1D). Complementary experiments using other transgenic lines possessing fluorescent macrophages (Mpeg1-GFP), neutrophils (Mpx-GFP) or thrombocytes (Cd41-GFP) showed that only macrophages were SVCV positive at 18 hpi (data not shown). Moreover, given the importance of platelets and coagulation system in hemorrhagic infections (Zapata et al., 2014) we used the transgenic line with fluorescent thrombocytes (fish equivalent to mammalian platelets) to detect a possible thrombocytopenia or coagulopathy after SVCV infection. As no differences in platelet behavior or count between control and SVCV-infected larvae were found (data not shown), we decided to focus our attention in macrophages.

To further confirm macrophage role as preferred target for this hemorrhagic virus, at least during the first hours of the infection, we took advantage of the morpholino-mediated gene knockdown technique. We injected the morpholino (MO) PU.1 at a concentration of 1 mM to prevent the formation of macrophages in embryos (He et al., 2012). A comparison of the normal fish and macrophage-depleted fish in these experimental infections showed a delay in the mortality of morphants (Figure 7.2), although eventually the mortality reached 100% in both groups. The duration of the MO effect was analyzed at an equivalent time of 48 hpi in non-infected fish. Marco expression was completely inhibited, as demonstrated using qPCR analysis (Figure 7.2). In contrast, the population of neutrophils was not affected by the morpholino, as demonstrated by the *mpx* gene expression after 48 hpi (Figure 7.2). The approximate 9-hour delay in the mortality between both groups, suggested that macrophage presence is crucial for SVCV pathogenesis during the first hours of infection.

Therefore, we analyzed the transcription levels of the SVCV N gene at 9 hpi (Figure 7.2). At this time, fish without macrophages had lower viral transcription levels compared with normal fish. Macrophage depletion delays the kinetics of viral transcription but is not enough to prevent the death of morphant fish. This effect likely reflects the high virulence of the infection. As an obligate intracellular pathogen, SVCV infects to survive and even if the primary target is not present, the virus could still infect other cells. However, the efficiency of infection is reduced in the first hours, resulting in a different timing of mortality. This, plus the fact that the only SVCV-positive cells detected at 18 hpi are macrophages, suggested that these cells could be the primary target of the virus.

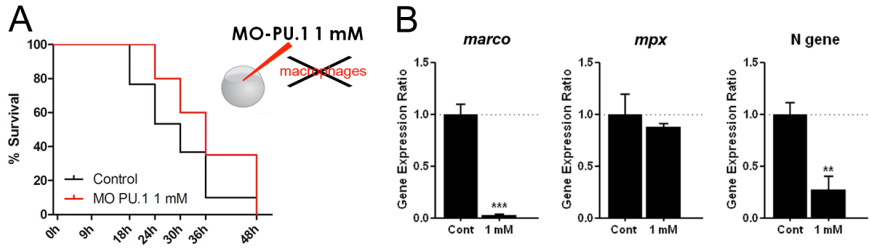

Figure 7.2. Macrophage depletion in zebrafish larvae. PU.1 MO was used to block macrophages development. Macrophages-depleted fish showed a delay in mortality of 9 hours after SVCV infection at 2 dpf compared to controls. The results are representative of 3 independent experiments of 2 or 3 biological replicates each. qPCR of *marco* and *mpx* facilitated an assessment of the efficiency of PU.1 MO at 48 hpi. Regarding SVCV N gene, the morphants showed less viral transcription during first hours of infection, suggesting that macrophages are the main target of SVCV during the first hours of infection. Significant differences were displayed as *** ($0.0001<p<0.001$), ** ($0.001<p<0.01$) or * ($0.01<p<0.05$).

SVCV elicits an inflammatory response that induces macrophages pyroptosis and IL1β release

The fact that macrophages were primarily infected with SVCV prompted us to examine the “disappearance” of these cells and determine whether pyroptosis is involved. Pyroptosis might

play a role in pathogen clearance, leading to inflammatory pathology, which is detrimental to the host but positively affects the spread of the pathogen (Lupfer and Kanneganti, 2012). This programmed cell death depends on inflammasome activation and consequent Caspase-1 action (Miao et al., 2011). In zebrafish, Caspa associates with ASC, an inflammasome adaptor (Masumoto et al., 2003). Moreover, it has recently been demonstrated that this caspase is able to cleave Il1β in zebrafish (Vojtech et al., 2012).

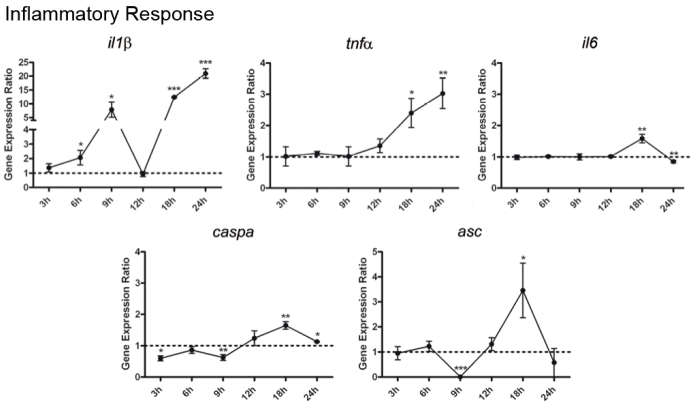

Figure 7.3. SVCV elicits an inflammatory response. Expression qPCR measurements of some important inflammatory response genes. Three biological replicates were used to calculate the means ± standard error of mean. Significant differences between infected and non-infected larvae at the same time point were displayed as *** (0.0001<p<0.001), ** (0.001<p<0.01) or * (0.01<p<0.05).

Using qPCR, we characterized the regulation of some important genes involved in the inflammatory response (Figure 7.3). Three typical pro-inflammatory cytokines, *il1β*, *tnfα* and *il6*, were regulated during infection. *Il1β* was the first responder, and a clear biphasic profile was observed. The initial up-regulation of cytokine expression might be associated with the recognition of SVCV by TLRs, followed by a second up-regulation of cytokine with a consequent inflammatory response (Negash et al., 2013). This

inflammatory response also triggered the response of Tnfα and Il6. Tnfα was induced from 12 to 24 hpi. In addition, *il6* showed a subtle expression peak at 18 hpi. Strikingly, the response of this cytokine was delayed and weak. Similar results were observed in the *caspa* time course. A complete inhibition of *asc* was observed at 9 hpi, then, the expression of *asc* reached a maximum at 18 hpi (Figure 7.3).

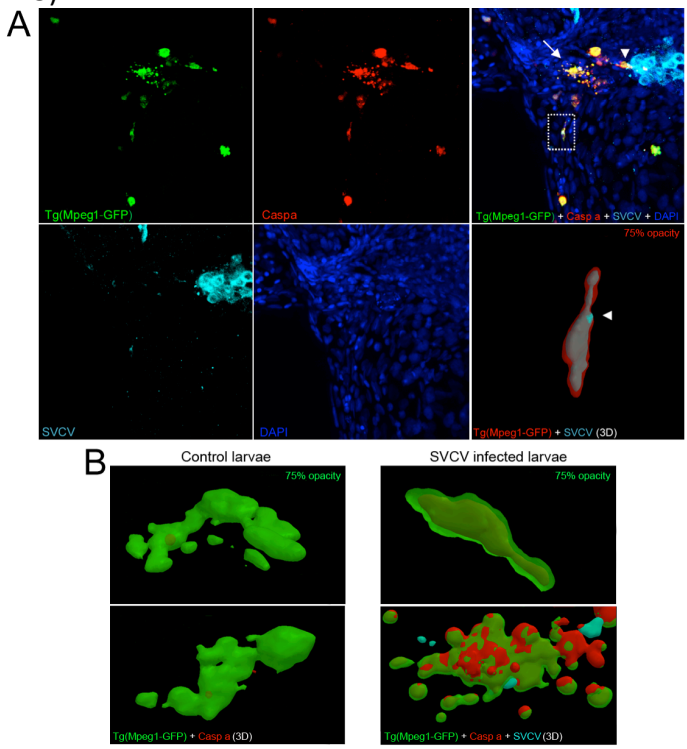

Figure 7.4. SVCV induces macrophages pyroptosis. A. Confocal images (maximal projections from multiple z-stacks) of 3 dpf infected Tg(Mpeg1-GFP) larvae immunostained with SVCV and Caspa antibodies at 22 hpi (60x magnification). The last macrophages in the larvae were Caspa positive. Some of these cells were infected (boxed area) and the other cells were interacting with a group of infected cells (arrowhead). The arrow shows potential macrophage pyroptosis, observed as visible membrane vesicle shedding. The last panel shows a 3D reconstruction of the infected macrophage in the boxed area, with a viral antigen positive area on its surface (arrowhead). B. Resting macrophages shown Caspa signal inside the cell. The level of Caspa was significantly less in resting macrophages than that in the macrophages of infected larvae.

Immunohistochemistry against Caspa and SVCV showed that the macrophages remaining at 20 hpi were positive for Caspa (Figure 7.4A). These macrophages showed interactions with infected cells (Figure 7.4A, S7.2). In addition, Mpeg1-positive and Caspa-positive vesicles, presumably from macrophages, were observed in the same area near SVCV-positive cells. Consistently with previus experiments, the 3D reconstruction revealed that infected macrophages had external SVCV-positive signals (Figure 7.4A). Significant differences were found in Caspa levels between control and infected fish (Figure 7.4B) showing the participation of that protein in the infection.

Il1β regulation is essential for a proper acute inflammatory response to an infectious challenge. The implication of Caspa in Il1β secretion prompted us to investigate the presence of that pro-inflammatory cytokine in infected larvae. An antibody against zebrafish Il1β in combination with the Mpeg1-GFP transgenic line allowed us the detection of this cytokine in macrophages (Figure 7.5A). A 3D reconstruction of the confocal images was generated to amplify the details, and two types of Il1β-positive macrophages were observed in SVCV-infected larvae. The first type was SVCV-positive macrophages (Figure 7.5B). The second type of macrophages localized near zones with SVCV signal, was Il1β positive but was not positive for the virus (Figure 7.5B). The difference between these two macrophages types was the amount of Il1β detected. Non-permissive macrophages in areas with SVCV-positive signal contained a higher amount of Il1β. Furthermore, the Mpeg1 signal was lost in favor of Il1β signal, which could lead to the release of this cytokine.

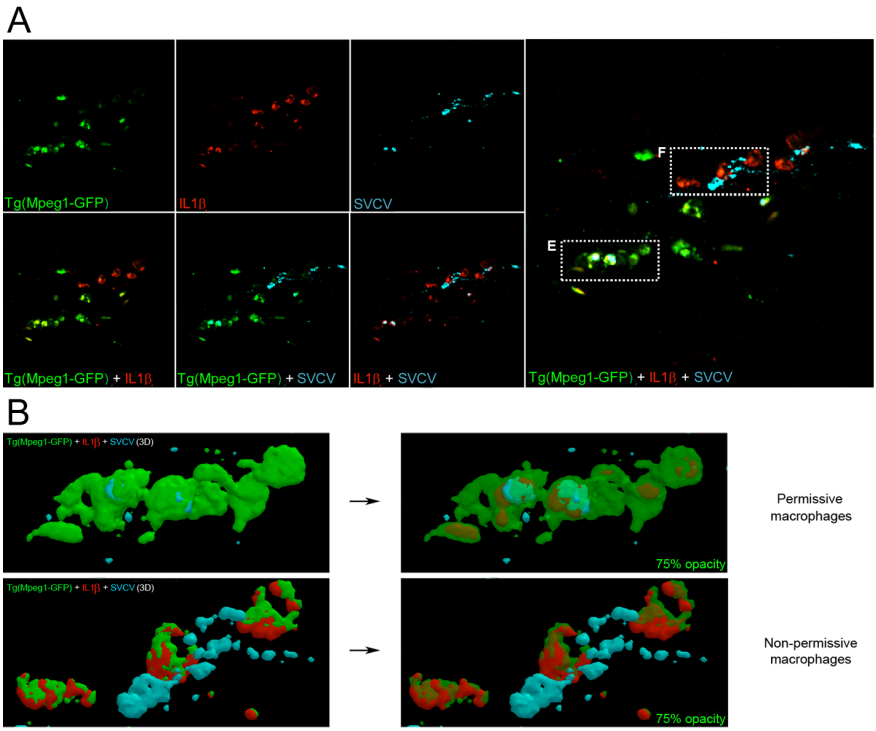

Figure 7.5. **Interleukin 1β detection during SVCV infection.** A. Confocal images (maximal projections from multiple z-stacks) of infected Tg(Mpeg1-GFP) larvae immunostained with SVCV and Il1β antibodies at 20 hpi (60x magnification). Regarding the proportion of Il1β and SVCV fluorescence observed, we distinguished two types of macrophages. B. 3D reconstruction of infected macrophages in the boxed area is displayed. Il1β signal is visible inside cells, as the SVCV signal. SVCV antigens are also visible on the cell surface. C. 3D reconstruction of non-infected macrophages positive for Il1β in boxed is displayed. Mpeg1 fluorescence is lost in favor of the Il1b signal. Cellular debris positive for SVCV is visible around these macrophages.

Il1β was detected in the macrophages of non-infected fish, but the signal in these resting macrophages was clearly different that observed in stimulated cells (Figure 7.6A). Macrophages from infected fish showed a higher amount of Il1β and what could be the release of this cytokine by microvesicle shedding (Figure 7.6B) or directly through the cell membrane (Figure 7.6C) were observed. To assess the membrane disruption produced during pyroptosis

we used a cell membrane-impermeant dye, PI. This dye was used *in vivo* and the uptake of PI by macrophages during SVCV infection was confirmed (Figure 7.7A). Furthermore, TUNEL assay showed IL1β releasing cells dying during infection (Figure 7.7B).

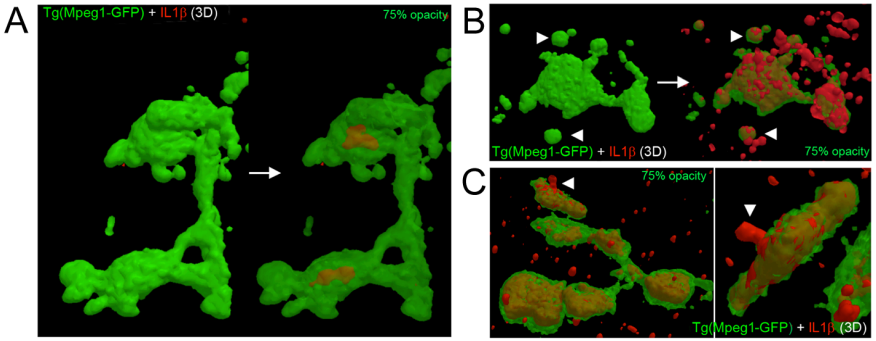

Figure 7.6. Interleukin 1β release is induced by SVCV infection. A. Resting macrophages shown Il1β signal inside the cell. The level of il1β was significantly less in resting macrophages than that in the macrophages of infected larvae. B. The macrophages in 3 dpf infected larvae showed shedding of Il1β-positive vesicles. C. Il1β also could be released directly through membrane pores in the macrophages of infected larvae.

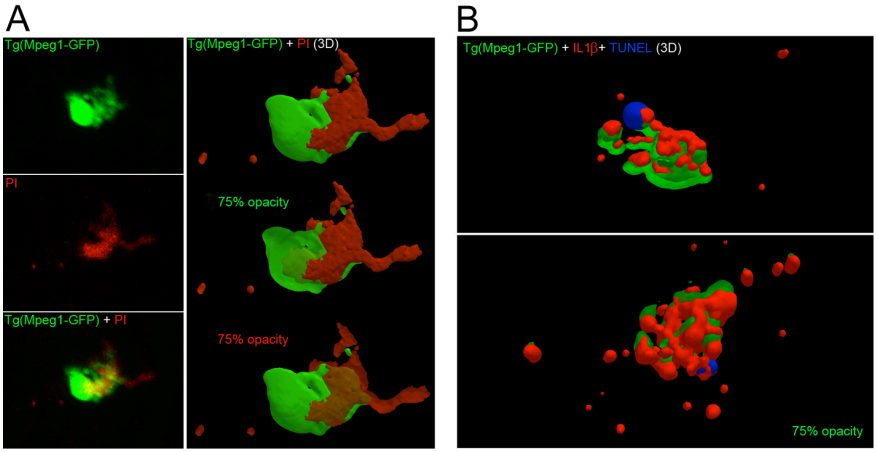

Figure 7.7. Pyroptosis induced by SVCV infection. A. *In vivo* PI staining of infected larvae showing macrophages PI uptake through membrane pores. B. 3D reconstruction of macrophages in an SVCV infected larvae positive for IL1β and TUNEL are displayed.

Pro-inflammatory Caspase-a activation and antiviral state induced by a zebrafish perforin

Because *prf19b* was the most expressed perforin in the myeloid population and considering its response to SVCV in zebrafish larvae (Varela et al., 2015), we wanted to analyze its importance in the resolution of the infection. In the antiviral response to this virus, macrophages are particularly important. As we described previously, these cells may be the primary target of the virus, dying due to pyroptosis after Caspase-a activation and IL1β release (Varela et al., 2014).

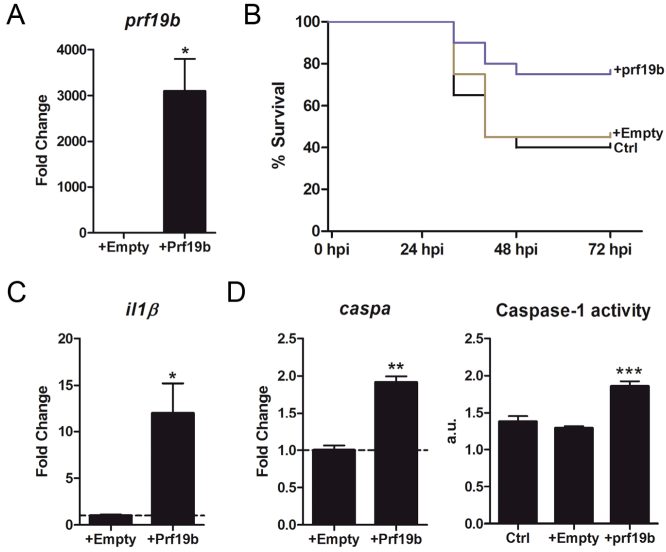

Figure 7.8. *prf19b* over-expression and inflammatory response in zebrafish larvae. A. Expression of *prf19b* in zebrafish larvae injected with Prf19b expression plasmid at 3 dpf. B. Kaplan-Meier survival curve after infection with SVCV ($p<0.001$). C. Expression of *il1β* in zebrafish larvae injected with Prf19b expression plasmid at 3 dpf. D. Expression of *caspase a* and caspase a activity (arbitrary units) in zebrafish larvae injected with Prf19b expression plasmid at 3 dpf. The fold change was calculated by dividing the normalized expression values in larvae injected with Prf19b plasmid by the normalized expression values obtained in larvae injected with empty plasmid. The graphs represent the mean ± standard error of 3 independent biological replicates. The asterisks denote statistically significant differences with respect to the empty plasmid group. Significant differences are displayed as ***($0.0001<p<0.001$), **($0.001<p<0.01$) or *($0.01<p<0.05$).

With the aim of inducing overexpression of Prf19b in zebrafish larvae, we microinjected an expression plasmid into one-cell-stage zebrafish eggs. The expression of *prf19b* in these larvae was 3000 times higher than in control larvae at 3 dpf (Figure 7.8A). No mortalities of defects in development in *prf19b* over-expressing larvae were observed. After a challenge with SVCV at 3 dpf, these prf19b over-expressing larvae showed enhanced survival compared with control larvae at 72 hpi (80% versus 45%, respectively) (Figure 7.8B). Since inflammation and pyroptosis after Caspase-a activation have been shown to play an important role during SVCV infection in zebrafish larvae (Varela et al., 2014), we checked whether *prf19b* overexpression could affect these processes, by a qPCR analysis of *il1β*. This pro-inflammatory cytokine appeared to be up-regulated 12-fold as a consequence of Prf19b overexpression at 3 dpf (Figure 7.8C). Recent publications have described the cleavage of zebrafish Il1β by the caspase-1 homolog Caspase a (Vojtech et al., 2012). We observed that *prf19b* over-expression triggers the activation of Caspase-a at 3 dpf at the transcriptional and translational levels, as observed based on increases in *caspase a* expression and caspase-1 activity, respectively (Figure 7.8D).

7.4. Discussion

In the present work we obtained images of the infection at the single cell level using a zebrafish model, identifying macrophages as the preferred target of SVCV. We were able to demonstrate for the first time that pyroptosis and Il1β release were involved in the viral-induced cell dead in a whole organism. The direct observation of such processes in individual cells provided a deeper knowledge of the inflammatory mechanisms implicated in this viral disease.

Altogether, the qPCR results provide interesting data regarding the dynamics of the response. We observed the first increase in *il1β* transcription and the strong downregulation of *asc* at 9 hpi. With regard to the complete inhibition of *asc* transcription observed at 9 hpi, we cannot rule out the involvement of the virus. Pathogens have developed diverse strategies to block some of the components of the inflammasome (Taxman et al., 2011). It has been shown that ASC transcription is downregulated during the infection of keratinocytes with some types of human papillomavirus (Karim et al., 2011). The host might also control this response (Bedoya et al., 2007); thus, it is likely that, in this case, the host could control macrophage loss through the inhibition of asc transcription. However, the potential blockade by the virus to favor viral spread cannot be excluded. Furthermore, the accumulation of Caspa as an unprocessed protein (pro-caspase) into the cells (Fernandes-Alnemri et al., 2007) would explain the weak transcriptional regulation observed for this gene during the infection.

Recent studies have demonstrated the importance of the inflammasome in Il1β generation upon infection with RNA viruses (Poeck et al., 2010) and showed that a biphasic response might be associated with the two signals necessary for Il1β release from macrophages (Netea et al., 2010). If we take into account of the results obtained also at protein level, the second upregulation observed at 12 hpi might be related with inflammasome activation. Inflammasome activation could be induced directly by the virus or cellular debris, but further investigation is necessary to confirm the type or types of inflammasomes implicated in this process.

The zebrafish model facilitated the capture of images showing Il1β release from single macrophages during SVCV infection. The shedding of microvesicles containing fully processed Il1β from the plasma membrane represents a major secretory

pathway for the rapid release of this cytokine (Piccioli and Rubartelli, 2013). We observed vesicles presumably derived from macrophages in areas with cellular debris or SVCV-positive cells. However, we also observed the possible direct release of Il1β through the cellular membrane.

The transcriptional regulation of some of the genes associated with pyroptosis and the complete disappearance of macrophages before the onset of mortality, being positive for Caspa and Il1β, suggested that pyroptosis is involved in SVCV infection. In recent years, there have been many advances in research concerning this type of cell death, particularly with regard to bacteria (Richard et al., 2010). In the case of viruses, our understanding remains a step behind. It is known that some viruses cause pyroptosis of macrophages in vitro, but so far, it is less clear whether this process occurs in vivo (Aachoui et al., 2013; Tan and Chu, 2013). Using the zebrafish model, we have provided the first description of viral-induced pyroptosis in the context of a whole organism. The fact that a hemorrhagic viral infection was able to induce macrophage pyroptosis in zebrafish, *in vivo* and in the whole larvae, promotes the use of this model organism for studying host-pathogen interactions.

As we described the importance of the inflammatory response mediated by macrophages during an infection with SVCV in zebrafish larvae, we further investigated the role of *prf19b* in this viral infection. *prf19b* has been characterised as the possible ancestral perforin, mainly expressed in macrophages and whose expression was modulated upon a SVCV systemic infection in zebrafish larvae (Varela et al., 2015). Over-expression of *prf19b* in zebrafish larvae before the infection with SVCV induced protection against the virus. Although further research is needed to fully understand the mechanism involved, the increased caspase-1 activity and the expression of caspa and il1b could have a role in

relation to inflammasome activation and pyroptotic cell death. The inflammasome platform is conserved across vertebrate phylogeny therefore zebrafish present all the components of this mechanism (Vojtech et al., 2012). The appearance of pores in the membrane of cells is one of the hallmarks of pyroptotic cell death (Fink and Cookson, 2005), and membrane permeability and channel formation have been shown to trigger inflammasome activation (Ichinohe et al., 2010). In fact, it has been recently reported that the membrane attack complex (MAC) of complement pores trigger inflammasome activation in the cytosol (Triantafilou et al., 2013). Whether the potassium and calcium mobilization induced by perforin (Stewart et al., 2014) is associated with inflammasome activation and pyroptosis (Dagenais et al., 2012; Murakami et al., 2012) and, eventually, with antiviral activity is a topic that deserves further study.

Future studies will be particularly important for an in deep study of the role of the endothelium, the inflammasome and pyroptosis in defense against the infection. Indeed, without losing sight of the possible effects that the virus might have on the regulation of the host response, the results obtained in the present study could be the starting point to understand the antiviral immune response as a whole. Furthermore, the application of these techniques and studies to other pathogens will improve the current knowledge of host-pathogen interactions and increase the potential for the discovery of new therapeutic targets.

7.5. References

Aachoui Y, Sagulenko V, Miao EA, Stacey KJ (2013) Inflammasome-mediated pyroptotic and apoptotic cell death, and defense against infection. Curr Opin Microbiol 16:319-326.

Bedoya F, Sandler LL, Harton JA (2007) Pyrin-only protein 2 modulates NF-kappaB and disrupts ASC:CLR interactions. J Immunol 178:3837–3845.

Benard EL, van der Sar AM, Ellett F, Lieschke GJ, Spaink HP, Meijer AH (2012) Infection of zebrafish embryos with intracellular bacterial pathogens. J Vis Exp 61:e3781.

Cui C, Benard EL, Kanwal Z, Stockhammer OW, van der Vaart M, Zakrzewska A, Spaink HP, Meijer AH (2011) Infectious disease modeling and innate immune function in zebrafish embryos. Methods Cell Biol 105:273-308.

Dagenais M, Skeldon A, Saleh M (2012) The inflammasome: in memory of Dr. Jurg Tschopp. Cell Death Differ 19:5-12.

Dejana E and Orsenigo F (2013) Endothelial adherens junctions at a glance. J Cell Sci 126:2545-2549.

Ellet F, Pase L, Hayman JW, Andrianopoulos A, Lieschke GJ (2011) mpeg1 promoter transgenes direct macrophage-lineage expression in zebrafish. Blood 117:e49-e56.

Espín R, Roca FJ, Candel S, Sepulcre, MP, González-Rosa, JM (2013) TNF receptors regulate vascular homeostasis in zebrafish through a caspase-8, caspase-2 and P53 apoptotic program that bypasses caspase-3. Dis Model Mech 6:383-396.

Fernandes-Alnemri T, Wu J, Yu JW, Datta P, Miller B, Jankowski W, Rosenberg S, Zhang J, Alnemri ES (2007) The pyroptosome: a supramolecular assembly of ASC dimers mediating inflammatory cell death via caspase-1 activation. Cell Death Differ 14:1590-1604.

Fink SL and Cookson BT (2005) Mechanistic description of dead and dying eukaryotic cells. Infect Immun 73:1907-1916.

Gray C, Loynes CA, Whyte MK, Crossman DC, Renshaw SA, Chico TJ (2011) Simultaneous intravital imaging of macrophage and neutrophil behavior during inflammation using a novel transgenic zebrafish. Thromb Haemost 105:811-819.

He S, Lamers GE, Beenakker JW, Cui C, Ghotra VP, Danen EH, Meijer AH, Spaink HP, Snaar-Jagalska BE (2012) Neutrophil-mediated experimental metastasis is enhanced by VEGFR inhibition in a zebrafish xenograft model. J Pathol 227:431-445.

Ichinohe T, Pang IK, Iwasaki A (2010) Influenza virus activates inflammasomes via its intracellular M2 ion channel. Nat Immunol 11:404-410.

Karim R, Meyers C, Backendorf C, Ludigs K, Offringa R, van Ommen GJ, Melief CJ, van der Burg SH, Boer, JM (2011) Human Papillomavirus Deregulates the Response of a Cellular Network Comprising of Chemotactic and Proinflammatory Genes. PLoS One 6:e17848.

Lupfer CR and Kanneganti TD (2012) The role of inflammasome modulation in virulence. Virulence 3:262-270.

Masumoto J, Zhou W, Chen FF, Su F, Kuwada JY (2003) Caspy, a Zebrafish Caspase, Activated by ASC Oligomerization Is Required for Pharyngeal Arch Development. J Biol Chem 278:4268-4276.

Meijer AH and Spaink HP (2011) Host-pathogen interactions made transparent with the zebrafish model. Curr Drug Targets 12:1000-1017.

Meijer AH, van der Vaart M, Spaink HP (2014) Real-time imaging and genetic dissection of hos-microbe interactions in zebrafish. Cell microbiol 16:39-49.

Miao EA, Rajan JV, Aderem A (2011) Caspase-1-induced Pyroptotic cell death. Immunol Rev 243:206-214.

Muller WA (2009) Mechanisms of Transendothelial Migration of Leukocytes. Circ Res 105:223-230.

Murakami T, Ockinger J, Yu J, Byles V, McCol A, Hofer AM, Horng T (2012) Critical role for calcium mobilization in activation of the NLRP3 inflammasome. Proc Natl Acad Sci USA 109:11282-11287.

Negash AA, Ramos HJ, Crochet N, Lau DT, Doehle B, Papic N, Delker DA, Jo J, Bertoletti A, Hagedorn CH, Gale MJ 2013 IL-1β Production through the NLRP3 Inflammasome by Hepatic Macrophages Links Hepatitis C Virus Infection with Liver Inflammation and Disease. PLoS Pathog 9:e1003330.

Netea MG, Simon A, van de Veerdonk F, Kullberg BJ, van der Meer JW, Joosten LA (2010) IL-1β processing in host defense: beyond the inflammasomes. PLoS Pathog 6:e1000661.

Nguyen-Chi M, Phan QT, Gonzalez C, Dubremetz JF, Levraud JP, Lutfalla G (2014) Transient infection of the zebrafish notochord with *E. coli* induces chronic inflammation. Dis Model Mech 7:871-882.

Novoa B and Figueras A (2012) Zebrafish: model for the study of inflammation and the innate immune response to infectious diseases. Adv Exp Med Biol 946:253-275.

Nüsslein-Volhard C and Dahm R (2002) *Zebrafish: a practical approach*. New York: Oxford University Press. 303 pp.

Palha N, Guivel-Benhassine F, Briolat V, Lutfalla G, Sourisseau M, Ellett F, Wang CH, Lieschke GJ, Herbomel P, Schwartz O, Levraud JP (2013) Real-time whole-body visualization of Chikungunya Virus infection and host interferon response in zebrafish. PLoS Pathog 9:e1003619.

Piccioli P and Rubartelli A (2013) The secretion of IL-1β and options for release. Semin Immunol 25:425-9.

Poeck H, Bscheider M, Gross O, Finger K, Roth S, Rebsamen M, Hannesschläger N, Schlee M, Rothenfusser S, Barchet W, Kato H, Akira S, Inoue S, Endres S, Peschel C, Hartmann G, Hornung V, Ruland J (2010) Recognition of RNA virus by RIG-I results in activation of CARD9 and inflammasome signaling for interleukin 1 beta production. Nat Immunol 11:63-69.

Prajsnar TK, Cunliffe VT, Foster SJ, Renshaw SA (2008) A novel vertebrate model of *Staphylococcus aureus* infection reveals phagocyte-dependent resistance of zebrafish to non-host specialized pathogens. Cell Microbiol 10:2312-2325.

Ramakrishnan L (2013) Looking within the zebrafish to understand the tuberculous granuloma. Adv Exp Med Biol 783:251-266.

Reed JL and Muench H (1938) A simple method of estimating fifty per cent end point. Am J Hyg 27:493-497.

Renshaw SA, Loynes CA, Trushell DM, Elworthy S, Ingham PW, Whyte MK (2006) A transgenic zebrafish model of neutrophilic inflammation. Blood 108:3976-3978.

Rhodes J, Hagen A, Hsu K, Deng M, Liu TX, Look AT, Kanki JP (2005) Interplay of pu.1 and gata1 determines myelo-erythroid progenitor cell fate in zebrafish. Dev Cell 8:97–108.

Richard EM, Thiyagarajan T, Bunni MA, Basher F, Roddy PO, Sarkar A, Warren SE, Wewers MD, Aderem A (2010) Caspase-1-induced pyroptosis is an innate immune effector mechanism against intracellular bacteria. Nat Immunol 11:1136-1142.

Stewart SE, Kondos SC, Matthews AY, D´Angelo ME, Dunstone MA, Whisstock JC, Trapani JA, Bird PI (2014) The perforin pore facilitates the delivery of cationic cargos. J Biol Chem 289:9172-9181.

Sullivan C and Kim CH (2008) Zebrafish as a model for infectious disease and immune function. Fish. Shellfish Immunol 25:341-350.

Tan TY and Chu JJ (2013) Dengue virus-infected human monocytes trigger late activation of caspase-1, which mediates pro-inflammatory IL-1β secretion and pyroptosis. J Gen Virol 94:1215-1220.

Taxman DJ, Huang MT, Ting JP (2011) Inflammasome Inhibition as a Pathogenic Stealth Mechanism. Cell Host Microbe 8:7-11.

Triantafilou K, Hughes TR, Triantafilou M, Morgan BP (2013) The complement membrane attack complex triggers intracellular Ca^{2+} fluxes leading to NLRP3 inflammasome activation. J Cell Sci 126:2903-2913.

van der Sar AM, Musters RJ, van Eeden FJ, Appelmelk BJ, Vandenbroucke-Grauls CM, Bitter W (2003) Zebrafish embryos as a model host for the real time analysis of *Salmonella typhimurium* infections. Cell Microbiol 5:601-611.

Varela M, Dios S, Novoa B, Figueras A (2012) Characterisation, expression and ontogeny of interleukin-6 and its receptors in zebrafish (*Danio rerio*). Dev Comp Immunol 37:97-106.

Varela M, Romero A, Dios S, van der Vaart M, Figueras A, Meijer AH, Novoa B (2014) Cellular visualization of macrophage pyroptosis and interleukin-1β release in a viral hemorrhagic infection in zebrafish larvae. J Virol 88:12026-12040.

Varela M, Forn-Cuní G, Dios S, Figueras A, Novoa B (2015) Proinflammatory Caspase-a activation and antiviral state induced by a zebrafish perforin after posible celular and functional diversification from a myeloid ancestor. J Innate Immun. DOI:10.1159/000431287.

Vojtech LN, Scharping N, Woodson JC, Hansen JD (2012) Roles of inflammatory caspases during processing of zebrafish interleukin-1β in Francisella noatunensis infection. Infect Immun 80:2878-85.

Westerfield M (2000) The zebrafish book. *A guide for the laboratory use of zebrafish (Danio rerio)*. Eugene: University of Oregon Press.

Zapata JC, Cox D, Salvato MS (2014) The role of platelets in viral hemorrhagic fevers. PLoS Negl Trop Dis 8:e2858.

7.6. Supporting Information

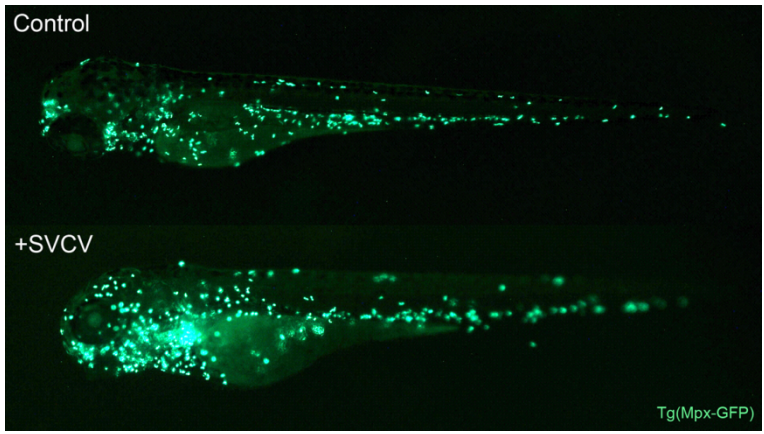

Figure S7.1. Neutrophil population changes in SVCV-infected larvae at 24 hours post-infection.

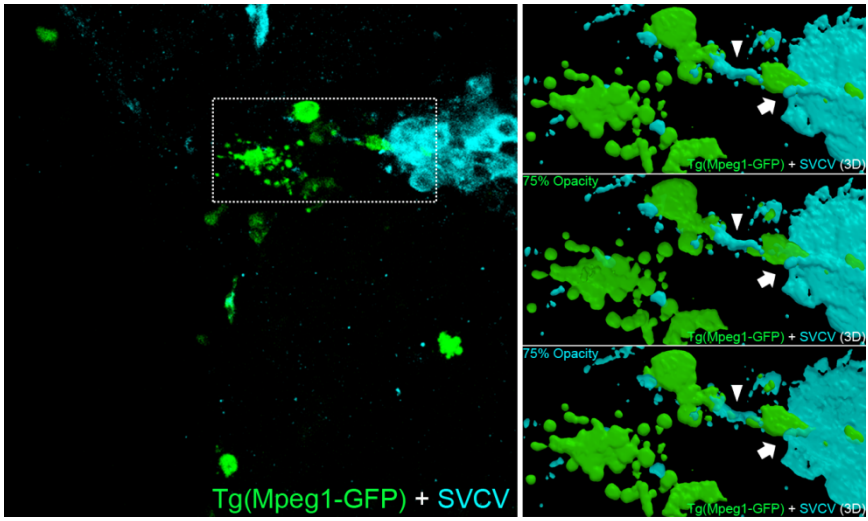

Figure S7.2. Macrophages interact with infected cells. Z-stack confocal images 3D reconstruction showing macrophage-macrophage interaction (arrowhead) and macrophage-infected cells interaction (arrow).

Table S7.1. Oligonucleotide sequences.

Primer Name	Primer sequence (5´→3´)	Amplicon (bp)
18SF	ACCACCCACAGAATCGAGAAA	97
18SR	GCCTGCGGCTTAATTTGACT	
MARCOF	AAGGACCCACAGGACAACAG	184
MARCOR	ATGTGGTGATGCTCCTCCTC	
IL1B	TTCCCCAAGTGCTGCTTATT	149
IL1BR	AAGTTAAAACCGCTGTGGTCA	
TNFaF	ACCAGGCCTTTTCTTCAGGT	148
TNFaR	GCATGGCTCATAAGCACTTGTT	
IL6F	TCAACTTCTCCAGCGTGATG	73
IL6R	TCTTTCCCTCTTTTCCTCCTG	
CASPaF	AAAAGGAGCGGCTCAGAGAA	205
CASpaR	CACCCATAATGGCGTCTCTT	
ASCF	CGGAATCTTTCAAGGAGCAG	222
ASCR	TGATCGCCCTCAAAATCTCC	
PRF19b-plasmid F	AGAATGGCTCTCCTTCTGTTGCT	1671
PRF19b-plasmid R	AAGGAAGGACATATCTCTTT	

Chapter 8

General Discussion

As it has been described in this work, although fish immunology has moved forward in recent years, there is still much research to be done. As reviewed in **Chapter 1,** the innate immune system relies on the detection of pathogens and consequent cellular and molecular response. Zebrafish possesses a highly developed immune system (Novoa and Figueras, 2012) that exhibits a remarkable similarity to the human one (Howe et al., 2013). Therefore, it is expected that the majority of the signalling pathways and molecules involved in the immune response of mammals, exist and behave similarly in fish.

Innate antiviral response depends on recognition of viral components by host cells. Pattern recognition receptors initiate antimicrobial defence mechanisms through several well-conserved signalling pathways (Broz and Monack, 2013). The detection of viral pathogens by the host leads to the activation of transcription factors such as interferon regulatory factors (IRFs) and nuclear factor kappa beta (NFκβ), to induce the antiviral interferon and inflammatory immune responses (Wu and Chen, 2014).

In order to improve or complete the knowledge about these signalling pathways in zebrafish, we characterised different genes that participate in the innate antiviral response. In **Chapter 3**, we described the complete repertoire of *ifit* genes in zebrafish. IFITs compose a novel expanded IFN-stimulated gene family with antiviral properties. We found 10 *ifit* genes in zebrafish, all expressed in basal conditions contrary to what occurs in mammals (Daffis et al., 2007; Diamond and Farzan, 2013). Even so, we found differences between genes that can be grouped into high and low constitutive expressed genes. These results suggest a certain grade of specialization and also that lower expressed genes could be inducible genes. The expression of *ifit* genes in response to zebrafish IFNsΦ was analysed using kidney primary cell cultures resulting in a rapid increase of IFIT genes expression. We have

found that not all the IFIT genes responded in the same way or to the same stimulus, which could suggest a complex regulation of the IFN signalling pathway in zebrafish. This also became clear when we studied the antiviral activity of selected IFIT genes in zebrafish larvae previously microinjected with expression vectors and infected with SVCV. Despite confirming that the antiviral activity of these genes is also present in non-mammalian species, differences among genes were again visible.

In **Chapter 4**, we characterised one of the most important cytokines of the inflammatory pathway, the IL6. Together with the IL1β and the TNFα, the IL6 is promptly and transiently produced in response to infections and tissue injuries (Tanaka et al., 2014). IL6 contributes to host defence through the stimulation of acute phase responses, hematopoiesis and immune reactions. We detected the presence of *il6* in several tissues of non-stimulated adult zebrafish, being the kidney the tissue with the higher presence of this cytokine. Also in kidney we analysed the regulation of *il6* after the stimulation with LPS and poly I:C. In mammals, it is know that IL6 expression can be induced by LPS or poly I:C as occurred in zebrafish.

The complete understanding of fish immune system and its response to pathogens could be useful for the development of new therapeutic targets, applicable to both biomedical research and aquaculture. The sequencing of the genome of several fish species such as zebrafish (Howe et al., 2013), fugu (Aparicio et al., 2012) and tetraodon (Roest, 2006) has helped to the breakthrough that occurred in the characterisation of fish immune genes in recent years. The evolution of teleost fish, marked by several phases of duplication and gene losses, made arose paralogs pairs in their genomes (Kassahn et al., 2009). This makes the characterisation of genes and its functionally comparison with their human orthologs difficult. Despite of this, zebrafish have

become a popular organism for the study of vertebrate gene function (Driever et al., 1996; Haffter et al., 1996). Zebrafish has a relatively large genome with many highly expanded gene families, compared to other fish model species (Glasauer and Neuhauss, 2014). As we described in **Chapter 5**, in contrast to human genome, zebrafish posses al least 6 functional perforin genes in its genome. Our phylogenetic analysis confirmed that the perforin ancestor gene differentiated from MPEG1 via a common precursor of complement C6-C9 and PRF in the chordate lineage. We found that zebrafish *prf19b* probably evolved first from the common precursor and, according to our results, with a similar functionality to that of MPEG1 more to the human PRF. Differences in spatiotemporal expression observed during embryogenesis, suggest significant changes in gene regulatory control after whole-genome duplication (Kassahn et al., 2009). It seems that the diversification that occurred during the evolution of this family probably affected the functionality and cellular localization of this expanded gene family among species. This gene expansion requires further characterisation work and makes difficult the functional comparison between fish and human orthologous.

The continuing development of genetic and molecular tools for the zebrafish has produced a multitude of ways to study host-pathogen responses. The use of morpholino oligonucleotides to obtain efficient targeted gene 'knockdown', chemical and insertional mutagenesis, or RNAi has been crucial in recent years to carry out studies with zebrafish (Mullins et al., 1994; Nasevicius and Ekker, 2000; Chen et al., 2002; Kelly and Hurlstone, 2011). Other techniques as microarrays and next-generation sequencing methods (Stockhammer et al., 2009; Ordas et al., 2011; van der Vaart et al., 2013) and the improvement of imaging techniques (Bassi et al., 2011; Palha et al., 2013; Hosseini et al., 2014; Varela et al., 2014) allowed detailed comparative studies that are directly

relevant for the knowledge of diseases. In the last decade the zebrafish has proven to be a versatile model for studying host-microbe interactions (Meeker and Trede, 2008; Kanther and Rawls, 2010; Meijer and Spaink, 2011; Berg and Ramakrishnan, 2012; Palha et al., 2013; Varela et al., 2014). In **Chapters 6 and 7** we described the SVCV systemic infection model in zebrafish larvae. We took advantage of the techniques developed in zebrafish to study the hemorrhagic disease caused by the virus and to observe its consequences, even at a cellular level. Although future studies will be particularly important for an in deep study of the role of the endothelium, the inflammasome and pyroptosis in the defence against SVCV infection, the results obtained in the present study could be the starting point to understand the antiviral immune response as a whole. Furthermore, as we saw in **Chapter 7**, the SVCV infection model could also be useful for the discovery of new gene functions, as it has been shown with the zebrafish perforin gene family.

Zebrafish present several features that make them optimal for disease modelling, but still lack several resources and functional information about specific gene functions known to other animal models. The analysis of the zebrafish immune system is still in its infancy, which means that tools for analysis, such as marker antibodies, are almost completely lacking. The difficulty of establishing zebrafish cell cultures has also been a handicap to the complete establishment of zebrafish as a vertebrate model. Despite this, zebrafish has proven to present a unique combination of characteristics for its complete development as a vertebrate model. It is expected that in the coming years the use of zebrafish as a model will be well established, providing new insights into immune system development, function and disease.

References

Aparicio S, Chapman J, Stupka E, Putnam N, Chia JM, Dehal P, Christoffels A, Rash S, Hoon S, Smit A, Gelpke MD, Roach J, Oh T, Ho IY, Wong M, Detter C, Verhoef F, Predki P, Tay A, Lucas S, Richardson P, Smith SF, Clark MS, Edwards YJ, Doggett N, Zharkikh A, Tavtigian SV, Pruss D, Barnstead M, Evans C, Baden H, Powell J, Glusman G, Rowen L, Hood L, Tan YH, Elgar G, Hawkins T, Venkatesh B, Rokhsar D, Brenner S (2012) Whole-genome shotgun assembly and analysis of the genome of Fugu rubripes. Science 297:1301-1310.

Bassi A, Fieramonti L, D´Andrea C, Mione M, Valentini G (2011) In vivo labez-free three-dimensional imaging of zebrafish vasculature with optical projection tomography. J Biomed Opt 16:100502.

Berg RD and Ramakrishnan L (2012) Insights into tuberculosis from the zebrafish model. Trends Mol Med 18:689-690.

Broz P and Monack DM (2013) Newly described pattern recognition receptors team up against intracellular pathogens. Nat Rev Immunol 13:551-565.

Chen W, Burgess S, Golling G, Amsterdam A, Hopkins N (2002) High-throughput selection of retrovirus producer cell lines leads to markedly improved efficiency of germ line-transmissible insertions in zebrafish. J Virol 76:2192-2198.

Daffis S, Samuel MA, Keller BC, Gale MJ, Diamond MS (2007) Cell-specific IRF-3 responses protect against West Nile virus infection by interferon-dependent and -independent mechanisms. PLoS Pathog 3:e106.

Diamond MS and Farzan M (2013) The broad-spectrum antiviral functions of IFIT and IFITM proteins. Nat Rev Immunol 13:46-57.

Driever W, Solnica-Krezel L, Schier AF, Neuhauss SC, Malicki J, Stemple DL, Stainier DY, Zwartkruis F, Abdelilah S, Rangini Z, Belak J, Boggs C (1996) A genetic screen for mutations affecting embryogenesis in zebrafish. Development 123:37-46.

Glasauer SMK and Neuhauss SCF (2014) Whole-genome duplication in teleost fishes and its evolutionary consequences. Mol Genet Genomics 289:1045-1060.

Haffter P, Granato M, Brand M, Mullins MC, Hammerschmidt M, Kane DA, Odenthal J, van Eeden FJ, Jiang YJ, Heisenberg CP, Kelsh RN, Furutani-Seiki M, Vogelsang E, Beuchle D, Schach U, Fabian C, Nüsslein-Volhard C (1996) The identification of genes with unique and essential functions in the development of the zebrafish, Danio rerio. Development 123:1-36.

Hosseini R, Lamers GEM, Hodzic Z, Meijer AH, Schaaf MJM, Spaink HP (2014) Correlative light and electron microscopy imaging of autophagy in a zebrafish infection model. Autophagy 10:1844-1857.

Howe K, Clark MD, Torroja CF, Torrance J, Berthelot C, Muffato M, Collins JE, Humphray S, McLaren K, Matthews L, McLaren S, Sealy I, Caccamo M, Churcher C, Scott C, Barrett JC, Koch R, Rauch GJ, White S, Chow W, Kilian B, Quintais LT, Guerra-Assunção JA, Zhou Y, Gu Y, Yen J, Vogel JH, Eyre T, Redmond S, Banerjee R, Chi J, Fu B, Langley E, Maguire SF, Laird GK, Lloyd D, Kenyon E, Donaldson S, Sehra H, Almeida-King J, Loveland J, Trevanion S, Jones M, Quail M, Willey D, Hunt A, Burton J, Sims S, McLay K, Plumb B, Davis J, Clee C, Oliver K, Clark R, Riddle C, Elliot D, Threadgold G, Harden G, Ware D, Begum S, Mortimore B, Kerry G, Heath P, Phillimore B, Tracey A, Corby N, Dunn M, Johnson C, Wood J, Clark S, Pelan S, Griffiths G, Smith M, Glithero R, Howden P, Barker N, Lloyd C, Stevens C, Harley J, Holt K, Panagiotidis G, Lovell J, Beasley H, Henderson C, Gordon D, Auger K, Wright D, Collins J, Raisen C, Dyer L, Leung K, Robertson L, Ambridge K, Leongamornlert D, McGuire S, Gilderthorp R, Griffiths C, Manthravadi D, Nichol S, Barker G, Whitehead S, Kay M, Brown J, Murnane C, Gray E, Humphries M, Sycamore N, Barker D, Saunders D, Wallis J, Babbage A, Hammond S, Mashreghi-Mohammadi M, Barr L, Martin S, Wray P, Ellington A, Matthews N, Ellwood M, Woodmansey R, Clark G, Cooper J, Tromans A, Grafham D, Skuce C, Pandian R, Andrews R, Harrison E, Kimberley A, Garnett J, Fosker N, Hall R, Garner P, Kelly D, Bird C, Palmer S, Gehring I, Berger A, Dooley CM, Ersan-Ürün Z, Eser C, Geiger H, Geisler M, Karotki L, Kirn A, Konantz J, Konantz M, Oberländer M, Rudolph-Geiger S, Teucke M, Lanz C, Raddatz G, Osoegawa K, Zhu B, Rapp A, Widaa S, Langford C, Yang F, Schuster SC, Carter NP, Harrow J, Ning Z, Herrero J, Searle SM, Enright A, Geisler R, Plasterk RH, Lee C, Westerfield M, de Jong PJ, Zon LI, Postlethwait JH, Nüsslein-Volhard C, Hubbard TJ, Roest Crollius H, Rogers J, Stemple DL (2013) The zebrafish reference genome sequence and its relationship to the human genome. Nature 496:498-503.

Kanther M and Rawls J (2010) Host-microbe interactions in the developing zebrafish. Curr Opin Immunol 22:10-19.

Kassahn KS, Dang VT, Wilkins SJ, Perkins AC, Ragan MA (2009) Evolution of gene function and regulatory control after whole-genome duplication: comparative analyses in vertebrates.

Kassahn KS, Dang VT, Wilkins SJ, Perkins AC, Ragan MA (2009) Evolution of gene function and regulatory control after whole-genome duplication: comparative analyses in vertebrates. Genome Res 19:1404-1418.

Kelly A and Hurlstone AF (2011) The use of RNAi technologies for gene knockdown in zebrafish. Brief Funct Genomics 10:189-196.

Meeker ND and Trede NS (2008) Immunology and zebrafish: spawning new models of human disease. Dev Comp Immunol 32:745-757.

Meijer AH and Spaink HP (2011) Host-pathogen interactions made transparent with the zebrafish model. Curr Drug Targets 12:1000-1017.

Mullins MC, Hammerschnidt M, Haffer P, Nusslein-Volhard C (1994) Large-scale mutagenesis in the zebrafish: in search of genes controlling development in a vertebrate. Curr Biol 4:189-202.

Nasevicius A and Ekker SC (2000) Effective targeted gene 'knockdown' in zebrafish. Nat Genet 26:216-220.

Novoa B and Figueras A (2012) Zebrafish: model for the study of inflammation and the innate immune response to infectious diseases. Adv Exp Med Biol 946:253-275.

Ordas A, Hegedus Z, Henkel CV, Stockhammer OW, Butler D, Jansen HJ, Racz P, Mink M, Spaink HP, Meijer AH (2011) Deep sequencing of the innate immune transcriptomic response of zebrafish embryos to Salmonella infection. Fish Shellfish Immunol 31:716-724.

Palha N, Guivel-Benhassine F, Briolat V, Lutfalla G, Sourisseau M, Ellett F, Wang CH, Lieschke GJ, Herbomel P, Schwartz O, Levraud JP (2013) Real-time whole-

body visualization of Chikungunya Virus infection and host interferon response in zebrafish. PLoS Pathog 9:e1003619.

Roest Crollius H (2006) The tetraodon genome. Genome Dyn 2:154-164.

Stockhemmer OW, Zakrzewska A, Hegedus Z, Spaink HP, Meijer AH (2009) Transcriptome profiling and functional analyses of the zebrafish embryonic innate immune response to Salmonella infection. J Immunol 182:5641-5653.

Tanaka T, Narazaki M, Kishimoto T (2014) IL-6 in inflammation, immunity and disease. Cold Spring Harb Perspect Biol 6:a016295.

van der Vaart M, van Soest JJ, Spaink HP, Meijer AH (2013) Functional analysis of a zebrafish myd88 mutant identifies key transcriptional components of the innate immune system. Dis Model Mech 6:841-854.

Varela M, Romero A, Dios S, van der Vaart M, Figueras A, Meijer AH, Novoa B (2014) Cellular visualization of macrophage pyroptosis and interleukin-1β release in a viral hemorrhagic infection in zebrafish larvae. J Virol 88:12026-12040.

Wu J and Chen ZJ (2014) Innate immune sensing and signaling of cytosolic nucleic acids. Annu Rev Immunol 32:461–488.

Conclusions

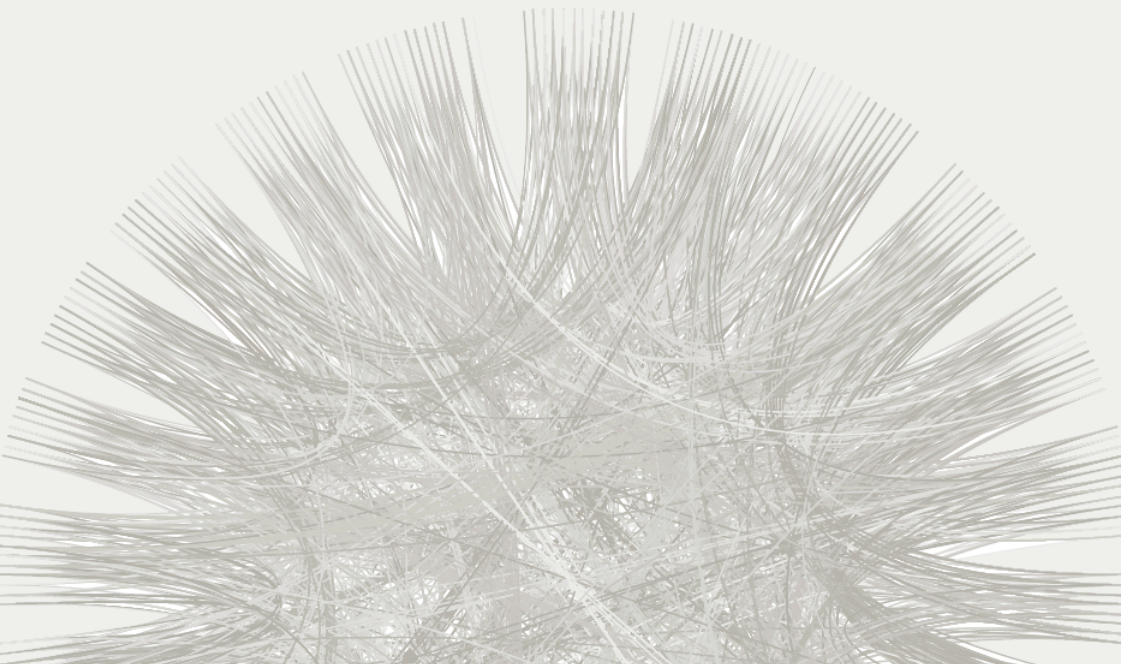

1. Zebrafish can be a valuable tool to increase our knowledge of antiviral innate immune response and the regulation of inflammation.

2. The interferon-induced genes of the IFIT gene family is expanded in zebrafish genome and, as occurs in mammals, presents antiviral properties.

3. Zebrafish interleukin-6 played an important role both during development and immune response. This could facilitate the use of zebrafish as a model for the study of various pathologies of increasing interest with which IL6 has been associated in recent years.

4. Zebrafish posses six perforin genes in its genome compared to humans that have only one. The diversification occurred during the evolution of this family probably has affected the functionality of these genes.

5. The gene duplication events occurred in zebrafish during evolution can complicate the comparison of genes function among species, so a deeper characterisation is required.

6. Despite of being a hemorrhagic virus, SVCV does not infect endothelial cells as a primary target in the zebrafish larvae systemic infection model.

7. SVCV modulates the inflammatory response inducing the death of macrophages by pyroptosis with the consequent release of interleukin-1β.

8. New gene functions, as the antiviral activity of *perforin 19b*, can be easily studied using SVCV infection model in zebrafish.

9. The results obtained during this work confirm the advantages of zebrafish as a model to understand the antiviral immune response as a whole, to visualize host-pathogen interactions and to increase the potential for the discovery of new antiviral therapeutic targets.

Resumen

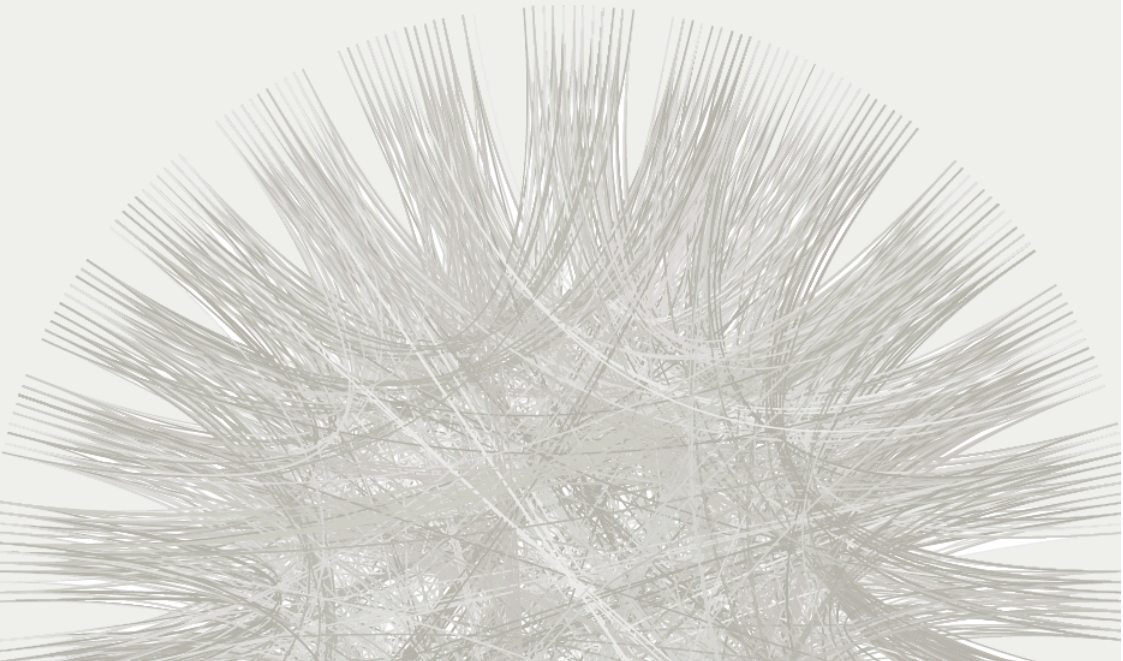

Estudio de la Respuesta Inmune Antiviral del Pez Cebra (*Danio rerio*) frente al Virus Hemorrágico SVCV

Respuesta Inmune Innata Antiviral en Pez Cebra (*Danio rerio*)

El pez cebra (*Danio rerio*) se ha utilizado como modelo en investigación durante más de 100 años. Este pez ciprínido es una herramienta excepcional en diferentes campos de investigación debido a su pequeño tamaño, su ciclo de vida rápido, la facilidad de cría y de modificación genética, y la transparencia de sus embriones. En los últimos años el uso del pez cebra como modelo de enfermedades humanas ha despuntado, con ejemplos tan importantes como el cáncer, la obesidad o enfermedades cardíacas, entre otros.

El creciente uso del pez cebra como modelo de vertebrado, ha facilitado el desarrollo de herramientas genómicas. La disponibilidad del genoma del pez cebra ha llevado a la identificación y caracterización de sus genes. Además, el progreso producido últimamente en el conocimiento del genoma del pez cebra se ha visto facilitado por el alto grado de conservación observado entre el genoma de este organismo modelo y otros genomas como el del humano. Esta es una de las ventajas que fomenta el uso del pez cebra como organismo modelo, pero también lo son la facilidad de crear líneas de peces mutantes, líneas de peces transgénicas y ensayos transitorios *in vivo*.

El pez cebra está siendo ampliamente utilizado como una herramienta para el estudio de enfermedades infecciosas y estudios sobre la interacción del hospedador y el patógeno. En los últimos años se han publicado numerosos modelos de infección con bacterias, virus y hongos utilizando el pez cebra como hospedador. El pez cebra posee un sistema inmunológico muy

desarrollado, lo que permite el estudio en profundidad tanto de los aspectos básicos de la respuesta inmune como su interacción con diferentes organismos y agentes patógenos.

Los principales componentes celulares del sistema inmune innato del pez cebra son los macrófagos y los neutrófilos. La existencia de líneas de peces transgénicos con células innatas fluorescentes y la facilidad de visualización de las mismas, hacen que el pez cebra posea un alto potencial para ser utilizado en el estudio de las interacciones entre las células del hospedador y el patógeno.

Por otra parte, el sistema inmune innato del pez cebra muestra un fuerte grado de conservación de las secuencias en muchos genes del sistema inmune de mamíferos. Genes determinantes implicados en la respuesta innata, como lo son las citoquinas o los receptores de tipo Toll, presentan una elevada homología en su secuencia genética con las de mamíferos, y los estudios actuales se centran en comprobar si esta equivalencia genética también puede trasladarse a una equivalencia funcional.

El objetivo de esta Tesis es la caracterización de la respuesta antiviral del pez cebra frente al virus hemorrágico SVCV, con el fin de conocer las moléculas implicadas y profundizar en el conocimiento de la respuesta inflamatoria causada por el patógeno (células implicadas, migración celular, y genes y circuitos génicos implicados en la respuesta).

Teniendo esto en cuenta, podemos dividir esta tesis doctoral en dos secciones diferenciadas, la sección I (Capítulos 3, 4 y 5), cuyo objetivo consiste en la caracterización de la expresión y función de diferentes genes implicados en la respuesta inmune antiviral del pez cebra. Por otro lado, la sección II (Capítulos 6 y 7) se centra en el establecimiento del modelo de infección sistémica con SVCV en larvas de pez cebra y en el estudio de la respuesta inflamatoria generada por el patógeno en los peces.

Capítulo 3: Caracterización de los Genes Inducidos por Interferón de la Familia IFIT en el Pez Cebra

La respuesta inmune antiviral comienza con la detección del virus, lo que activa la inducción de efectores celulares y moleculares con poder antiviral, como es el caso del interferón (IFN) tipo I y cientos de genes estimulados por IFN (ISGs).

El conocimiento acerca de las propiedades antivirales de los ISGs se limita a unos pocos genes que han sido exhaustivamente estudiados como PKR o MX. Incluso en humanos, a pesar de que la importancia del sistema del IFN es clara, no existe suficiente información acerca de los mecanismos que participan en la inhibición de la replicación viral mediada por IFN.

Dentro de los ISGs, la familia de proteínas denominadas IFIT (proteínas inducidas por IFN con repeticiones de tetratricopépticos) ha sido estudiada en vertebrados superiores. Estudios recientes han demostrado que la familia IFIT está conservada en mamíferos, anfibios y pájaros, pero no está presente en levaduras, plantas o animales inferiores como la mosca de la fruta o los nematodos. Las proteínas pertenecientes a esta familia participan en muchos procesos de la respuesta antiviral y en otras funciones como las interacciones proteína-proteína o proteína-ARN, y en la migración y proliferación celular.

En peces, y hasta este estudio en el que hemos caracterizado 10 genes de la familia *ifit* en pez cebra, la información relacionada con estas moléculas era prácticamente inexistente. Nuestro trabajo reveló que esta familia de proteínas surgió a partir de eventos de duplicación génica antiguos. Analizamos su expresión basal en 8 tejidos diferentes de pez cebra adulto y en la línea celular ZF4, observando los diferentes patrones de expresión entre los genes *ifit*. Las diferencias encontradas entre ellos reflejan la diferenciación y subsecuente especialización de los

miembros de esta familia durante su evolución, potencialmente facilitadas por la expansión génica que se produce en los peces.

Además, para explorar a fondo las propiedades antivirales de estos ISGs, realizamos experimentos *in vitro* e *in vivo* en pez cebra después del tratamiento con IFNs recombinantes y después de una infección viral con SVCV, observando diferentes respuestas entre las células de riñón y la línea celular ZF4, posiblemente debido a que estas últimas no son células inmunes. Observamos también un posible mecanismo de bloqueo de la vía de señalización del IFN por parte del virus ya que ni las células ZF4 ni los cultivos primarios de células de riñón respondieron de la manera esperada a la infección con SVCV. En cambio, cuando la infección se realizó *in vivo*, mediante una inyección intraperitoneal en peces adultos, se observó una respuesta antiviral típica caracterizada por la inducción de IFNs e ISGs.

Por otro lado, la protección generada ante una infección viral por 3 genes de *ifit* seleccionados fue examinada también *in vivo* utilizando larvas de pez cebra microinyectadas con plásmidos de expresión. Los resultados obtenidos proporcionan la base para futuras investigaciones, no solo en cuanto a la protección que estas moléculas confieren en peces ante una infección viral, sino también para la investigación de los aspectos básicos de la biología de la familia de IFITs y de la vía de señalización del IFN.

Capítulo 4: Caracterización de la Interleuquina-6 en el Pez Cebra

La interleuquina-6 (IL6) es una de las citoquinas pro-inflamatorias más importantes, junto al TNFα y a la IL1β, debido a su participación tanto en la respuesta inmune innata como en la respuesta inmune adaptativa. Esta molécula es producida por una gran variedad de células, incluyendo macrófagos, células endoteliales, queratinocitos y fibroblastos, y participa en procesos

como la hematopoyesis, las respuestas de fase aguda, procesos metabólicos y la neurogénesis.

A pesar de la importancia del pez cebra como organismo modelo en estudios sobre desarrollo, estudios toxicológicos y en el estudio de diversas enfermedades, el homólogo de la IL6 en pez cebra no había sido identificado en ninguna base de datos ni en ningún proyecto genoma hasta el momento. En vista de la importancia que esta molécula tiene en muchos procesos biológicos, y utilizando la conservación de genes que existe entre el genoma del humano y del pez cebra como herramienta, hemos localizado y caracterizado la IL6 en pez cebra. A lo largo de este trabajo, hemos descrito la regulación de la expresión de esta molécula en condiciones basales y en diferentes órganos, así como frente a diferentes moléculas asociadas a patógenos (PAMPs) estímulos como el LPS o el poly I:C. Hemos observado una respuesta de la IL6 durante las primeras horas después de la estimulación con ambos PAMPs, al igual que ocurre con el TNFα y a la IL1β. Además, se analizó adicionalmente la expresión de los genes que forman el complejo receptor de la IL6, *il6r* y *gp130*.

El análisis de la expresión de *il6* durante el primer mes de desarrollo de las larvas de pez cebra resultó en su detección desde una muy temprana edad, sugiriendo la necesidad de esta molécula y su actividad biológica para un correcto desarrollo y supervivencia. Utilizando la hibridación *in situ* de sondas de ARN en larvas completas hemos podido visualizar la expresión de la *il6* en la cabeza, la epidermis y los neuromastos de la línea lateral de los peces, denotando su importancia durante la neurogénesis y el desarrollo de estos peces.

Con nuestros resultados remarcamos la importancia que esta molécula tiene tanto en procesos relacionados con el sistema inmunitario como durante el desarrollo. Esto podría facilitar el uso del pez cebra como modelo para el estudio de varias patologías de

creciente interés, como el cáncer o las enfermedades inflamatorias crónicas, a las que la IL6 ha sido vinculada en los últimos años.

Capítulo 5: Caracterización de 6 Genes de Perforina en el Pez Cebra

En mamíferos, la perforina se expresa en linfocitos T citotóxicos (CTLs) y células NK, que son células que utilizan sus gránulos citoplasmáticos para promover la citolisis y la apoptosis de las células diana. La perforina juega un papel clave en la muerte dependiente de gránulos secretores, en la defensa frente a células infectadas por virus y también en la muerte de otras células no reconocidas como propias por el sistema inmunitario.

La perforina forma poros en las membranas de las células diana en presencia de calcio. Estos poros no solo causan la lisis por choque osmótico de las células, sino que también provocan la entrada de otras moléculas como las granzimas. La formación de poros depende de los dos dominios característicos de esta molécula, el MACPF y el dominio de unión al calcio CaLB. Dominios que también encontramos en otras moléculas inmunes como MPEG1, una proteína exclusivamente producida por macrófagos y posible precursora de la perforina, y los componentes C6-C9 del complemento.

Al contrario de lo que ocurre en vertebrados superiores, los peces cuentan con más de un gen que codifica para perforina en sus genomas. Este hecho podría implicar la existencia de múltiples o diferentes funciones en estos genes entre las diferentes especies.

A lo largo de este trabajo, hemos confirmado la existencia de 6 genes de perforina en el genoma del pez cebra. Hemos estudiado la evolución de estos genes y determinado la expresión diferencial constitutiva y la respuesta de los mismos frente a

diferentes estímulos, en diferentes órganos y tipos celulares. Esto nos ha permitido comprobar que los 6 genes se comportan de maneras diferentes antes los estímulos y que su expresión puede ser asociada a diferentes tipos celulares, lo que confirmaría la sospecha de la posible evolución funcional y/o de localización celular sufrida por esta familia de genes durante su evolución.

Además, hemos estudiado los cambios que se producen en la expresión de las 6 perforinas de pez cebra durante el primer mes de desarrollo de las larvas, y su respuesta frente a una infección sistémica viral a los 3 días post-fertilización. La *perforina 19b* se mostró como la más inducible por el virus SVCV tanto en la infección intraperitoneal en adultos, como en la infección sistémica en larvas.

Nuestros análisis filogenéticos han arrojado luz sobre la evolución de estos genes. Hemos visto que la perforina de pez cebra identificada como precursora en nuestro estudio, la *perforina 19b*, se asemeja más en cuanto a su patrón de expresión al gen a partir del cual evolucionó la familia de las perforinas, MPEG1, que a la perforina de humanos, ya que ambos se expresarían en células mieloides. Los análisis evolutivos combinados con los análisis de expresión dejan entrever la posibilidad de que existan diferencias funcionales y de localización celular entre las distintas perforinas del pez cebra.

Capítulo 6: Infección Sistémica con SVCV en Larvas de Pez Cebra como Modelo de una Enfermedad Hemorrágica Viral

Las células endoteliales y los leucocitos constituyen la primera línea de defensa contra los patógenos. De hecho, la mayoría de los patógenos tienen alguna relación con el endotelio, aunque no todos ellos llegan a infectar sus células. La infecciones pueden provocar grandes cambios en la funcionalidad de las

células endoteliales, particularmente en relación con la inflamación. Los estímulos inflamatorios pueden activar las células endoteliales, las cuales pueden secretar citoquinas y quimioquinas. Además, la importancia de las células endoteliales en la regulación de la transmigración de leucocitos al lugar de la inflamación ha supuesto otorgarle a estas células un papel principal en la inmunidad.

Las interacciones entre el hospedador y el patógeno son esenciales para la modulación de la respuesta inmunitaria. La presencia de un patógeno altera el equilibrio inmune prevalente en un hospedador bajo condiciones normales, causando la aparición de enfermedades que en muchos casos conllevan la muerte del hospedador si este no es capaz de controlar la infección. Encontramos claros ejemplos de este efecto en las fiebres hemorrágicas virales, en las que entender el papel relativo que juegan el patógeno y la propia respuesta del hospedador es esencial. Las hemorragias son un síntoma característico de estas fiebres, y es por ello que históricamente han estado siempre asociadas a la infección de las células endoteliales. Actualmente se conoce que muchos patógenos causantes de fiebres hemorrágicas no infectan las células endoteliales. De hecho, los macrófagos y las células dendríticas son las células diana de algunos virus hemorrágicos como el virus del Ébola o el virus del dengue.

La mayor parte de las investigaciones llevadas a cabo para estudiar las interacciones hospedador-patógeno se han realizado en líneas celulares que podrían no ser las dianas principales durante una infección natural, haciendo difícil la caracterización del comportamiento del patógeno dentro del hospedador y reduciendo así las posibilidades de descubrir una diana terapéutica efectiva. La falta de un buen modelo animal en el que la infección pueda ser seguida de principio a fin y en el contexto del individuo completo también ha contribuido a estas dificultades.

Por todo esto, el principal objetivo de este trabajo es mejorar el conocimiento de la patología generada por el virus SVCV, como ejemplo de virus hemorrágico, centrándonos sobre todo en las interacciones entre el virus y las células del hospedador durante los estadíos más tempranos de la infección. Hemos puesto a punto un modelo de infección sistémica microinyectando el virus en el sistema circulatorio de larvas de pez cebra. Utilizando este modelo hemos podido visualizar las primeras consecuencias de la infección en el pez. A pesar de las hemorragias observadas en los peces, las células endoteliales no son infectadas por el virus, al menos durante los primeros momentos de la infección, siendo los leucocitos las células marcadas como positivas para el virus durante esta etapa de la infección. La aplicación de las técnicas empleadas durante este estudio a otros patógenos podrá mejorar el conocimiento de las interacciones entre patógenos y hospedadores e incrementar el potencial para el posible descubrimiento de nuevas dianas terapéuticas.

Capítulo 7: Respuesta Leucocitaria e Inflamatoria durante la Infección con SVCV en Larvas de Pez Cebra

Los macrófagos y los neutrófilos son indispensables para la respuesta inmune innata en vertebrados superiores y presumiblemente jueguen un papel similar en el caso del pez cebra. La identificación de las células que producen las quimioquinas y de las células diana de estas, y la elucidación de los mecanismos que los patógenos utilizan para manipular estas y otras vías de señalización de la respuesta inmune innata son retos importantes en los que el pez cebra puede contribuir.

En los últimos años, el número de modelos de infecciones utilizando el pez cebra como hospedador se ha visto incrementado.

La mayoría de los estudios sobre la interacción entre el hospedador y el patógeno se han llevado a cabo utilizando bacterias, tales como Mycobacterium tuberculosis o Salmonella typhimurium. En cuanto a las investigaciones relativas a enfermedades virales, estas han ido siempre un paso por detrás. En el capítulo anterior utilizamos el virus SVCV como modelo para mostrar el potencial del pez cebra en estudios sobre la interacción entre el hospedador y el patógeno. Después de la visualización del virus en los leucocitos localizados alrededor de las células endoteliales en larvas de pez cebra, nuestro siguiente objetivo fue profundizar en el papel de los leucocitos durante la infección. Por otro lado, también nos propusimos estudiar los posibles efectos que el virus pudiese tener en la regulación de la respuesta inflamatoria del hospedador.

Utilizando diferentes líneas de peces transgénicos, técnicas de imagen y la microinyección de morfolinos para generar peces sin macrófagos, hemos obtenido imágenes de la infección a nivel celular y hemos demostrado por primera vez que la piroptosis y la liberación de IL1β están relacionadas con la muerte celular inducida por un virus en un organismo completo. Hasta ahora, aunque ha habido en los últimos años numerosos avances en la investigación sobre este tipo de muerte celular, la piroptosis solo se había demostrado en infecciones virales mediante estudios realizados *in vitro*. El hecho de que una infección hemorrágica viral sea capaz de inducir la piroptosis de los macrófagos del pez cebra, *in vivo* y en el contexto de un individuo completo, es un punto a favor del uso de este organismo modelo para este tipo de estudios. También analizamos la expresión a lo largo del tiempo de numerosos genes que participan en la respuesta inflamatoria, lo que nos ha aportado datos de la dinámica de la respuesta. Teniendo en cuenta la importancia de los macrófagos y de la respuesta inflamatoria durante la infección con SVCV, hemos

investigado también el papel que desempeña una de las perforinas caracterizadas en el capítulo anterior. La *perforina 19b*, se expresa mayoritariamente en macrófagos y su expresión es modulada por SVCV. Aunque se necesita más investigación en este aspecto, hemos comprobado que la sobreexpresión de la *perforina 19b* de pez cebra tiene propiedades antivirales ya que confiere protección a los peces, y que estas propiedades antivirales podrían estar relacionadas con la muerte por piroptosis de los macrófagos, y por tanto, con la regulación de la inflamación.

Conclusiones

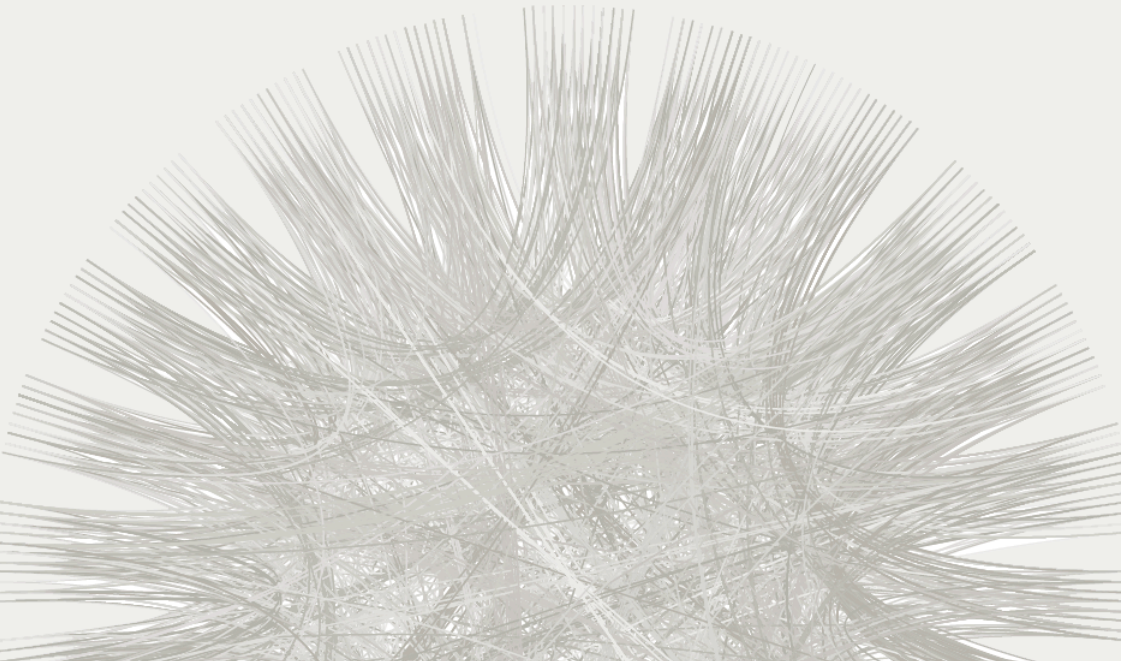

1. El pez cebra puede ser una herramienta muy útil para incrementar el conocimiento relativo a la respuesta inmune innata antiviral y la regulación de la inflamación.

2. Los genes inducidos por interferón pertenecientes a la familia de las IFITs se han expandido en el genoma del pez cebra y, al igual que ocurre en mamíferos, poseen propiedades antivirales.

3. La interleuquina-6 (IL6) del pez cebra mostró un papel importante tanto durante el desarrollo de las larvas como en la respuesta inmunitaria. Esto podría facilitar el uso del pez cebra como modelo para el estudio de varias patologías de creciente interés a las que ha sido asociada la IL6 en los últimos años.

4. El pez cebra posee seis genes de perforinas en su genoma, en contraposición al genoma humano que posee un único gen. La diversificación ocurrida durante la evolución de esta familia de genes probablemente ha afectado a la funcionalidad de los mismos.

5. Los eventos de duplicación génica ocurridos durante la evolución en el pez cebra complican la comparación funcional de los genes entre las especias, y por tanto, se requiere una caracterización en mayor profundidad.

6. A pesar de ser un virus hemorrágico, las células endoteliales no son la diana principal de SVCV en el modelo de infección sistémica en larvas de pez cebra.

7. SVCV modula la respuesta inflamatoria y produce la muerte de los macrófagos por piroptosis, con la consecuente liberación de la interleuquina-1β.

8. Nuevas funciones de los genes, como la actividad antiviral de la *perforina 19b*, pueden ser fácilmente estudiadas utilizando el modelo de infección de SVCV en pez cebra.

9. Los resultados obtenidos en esta tesis confirman las ventajas del pez cebra como modelo para el estudio de la respuesta inmune antiviral en todo su conjunto, para la visualización de las interacciones patógeno-hospedador y para el posible descubrimiento de nuevas dianas terapéuticas.

LIST OF PUBLICATIONS

Publications derived from this doctoral thesis:

- **Varela M**, Dios S, Novoa B, Figueras A (2012) Characterisation, expression and ontogeny of interleukin-6 and its receptors in zebrafish (*Danio rerio*). Dev Comp Immunol 37:97-106.
- **Varela M***, Díaz-Rosales P*, Pereiro P, Forn-Cuní G, Costa MM, Dios S, Romero A, Figueras A, Novoa B (2014) Interferon-induced genes of the expanded IFIT family show conserved antiviral activities in non-mammalian species. PLoS one 9:e100015.
- **Varela M**, Romero A, Dios S, van der Vaart M, Figueras A, Meijer AH, Novoa B (2014) Cellular visualization of macrophage pyroptosis and interleukin-1β release in a viral hemorrhagic infection in zebrafish larvae. J Virol 88:12026-12040.
- **Varela M**, Forn-Cuní G, Dios S, Figueras A, Novoa B (2015) Proinflammatory Caspase-a activation and antiviral state induced by a zebrafish perforin after possible cellular and functional diversification from a myeloid ancestor. J Innate Immun. DOI: 10.1159/000431287.
- **Varela M**, Figueras A, Novoa B. Antiviral innate immune response in zebrafish (*Danio rerio*). Manuscript in preparation.

Other publications:

- Leiro JM, **Varela M**, Piazzon MC, Arranz JA, Noya M, Lamas J (2010) The anti-inflammatory activity of the polyphenol resveratrol may be partially related to inhibition of tumour necrosis factor-alpha (TNF-alpha) pre-mRNA splicing. Mol Immunol 47:1114-1120.

- Forn-Cuní G, **Varela M**, Fernández-Rodríguez CM, Figueras A, Novoa B (2015) Liver immune responses to inflammatory stimuli in a diet-induced obesity model of zebrafish. J Endocrinol 224:159-170.
- Pereiro P*, **Varela M***, Díaz-Rosales P, Romero A, Dios S, Figueras A, Novoa B (2015) Zebrafish Nk-lysins: First insights about their cellular and functional diversification. Dev Comp Immunol 51:148-159.
- Forn-Cuní G, **Varela M**, Novoa B, Figueras A. Do genomic responses in zebrafish model mimic human inflammatory diseases? Submitted for publication.